The Dissertation Committee for Clint Aaroen Boyd Certifies that this is the approved version of the following dissertation:

TAXONOMIC REVISION OF LATEST CRETACEOUS NORTH AMERICAN BASAL NEORNITHISCHIAN TAXA AND A PHYLOGENETIC ANALYSIS OF BASAL ORNITHISCHIAN RELATIONSHIPS

Committee:

Julia A. Clarke, Supervisor

Christopher J. Bell

Timothy B. Rowe

David C. Cannatella

Peter J. Makovicky

TAXONOMIC REVISION OF LATEST CRETACEOUS NORTH AMERICAN BASAL NEORNITHISCHIAN TAXA AND A PHYLOGENETIC ANALYSIS OF BASAL ORNITHISCHIAN RELATIONSHIPS

by

Clint Aaroen Boyd, B.S.

Dissertation

Presented to the Faculty of the Graduate School of

The University of Texas at Austin

in Partial Fulfillment

of the Requirements

for the Degree of

Doctor of Philosophy

The University of Texas at Austin

May 2012

Dedication

To my grandfather, James Boyd, for teaching me how to hold history in my hands and be filled with its wonder.

Acknowledgements

Thank you first and foremost to my advisor, Julia Clarke, for giving me the opportunity to pursue a career in the field that I enjoy so much and for dedicating so much of her time and effort towards my professional development. The remaining members of my committee, C. Bell, D. Cannatella, P. Makovicky, and T. Rowe, provided me with valuable guidance during the course of my graduate studies that greatly improved the quality of my research. I would also like to thank the former members of my committee at North Carolina State University (J. Hibbard, M. Schweitzer, and B. Wiegmann) for their guidance and efforts on my behalf during my time at NCSU, which was very much appreciated.

Access to collections and specimens was generously provided by C. Mehling and M. Norell (AMNH), X. Xing (IVPP), J. Horner and B. Baziak (MOR), V. Schneider and D. Russell (NCSM), K. Q. Gao (Peking University), S. Shelton and M. Greenwald (SDSM), J. Nelson (TLAM), M. Carrano and M. Brett-Surman (USNM), S. Sampson, M. Getty, and R. Irmis (UMNH), and D. Brinkman and C. Norris (YPM). P. Brinkman (NCSM) collaborated in the preparation of NCSM 15728 and M. Brown (VPL) provided instruction in the preparation of several new specimens of *Scutellosaurus*. D. Evans (ROM) provided information on the anatomy of ROM 804. D.A. Winkler provided anatomical information about the 'Proctor Lake ornithopod.' D. Varricchio provided additional information on the anatomy of MOR 1636a. C.M. Brown provided photographs of several specimens referred to *Thescelosaurus*, information regarding

orodromine material from the Dinosaur Park Formation, and details regarding the anatomy of *Parksosaurus.* P. M. Galton provided encouragement and enlightening conversations over the years regarding basal ornithischian taxa. T. P. Cleland provided select photographs of NCSM 15728 and USNM 7758. S. Nesbitt provided access to photographs of several basal ornithischian taxa from South Africa. E. L. Schmidt provided illustrations of NCSM 15728 and USNM 7758.

I am indebted to S. Masters for bringing the basal neornithischian material from the Kaiparowits Formation of Utah to my attention and A. Titus of the Utah Bureau of Land Management for assistance in locating additional specimens referable to this new taxon. A. DeBee and S. Nesbitt assisted in identifying material from the holotype of *Skaladromeus goldenii* gen. et sp. nov. and A.D.B. Behlke assisted in constructing the name of this taxon. T. P. Cleland and N. Marrero assisted in the design of the ASCC program suite and E.B. Cleland, N. Marrero, and S.J. Nesbitt helped troubleshoot early versions of the ASCC program suite. A. Molineux provided generous access to the photographic equipment at the Nonvertebrate Paleontology Laboratory at the University of Texas at Austin. The Willi Hennig Society provided free access to the phylogenetic program TNT. The Polyglot Paleontologist website provided access to multiple translations of important scientific research papers on ornithischian dinosaurs.

This research was funded via the American Museum of Natural History Collection Study Grant, an Ernest L. and Judith W. Lundelius Scholarship in Vertebrate Paleontology, a Francis L. Whitney Endowed Presidential Scholarship from the University of Texas, a Geological Society of America Graduate Student Research Grant,

the National Science Foundation's East Asia and Pacific Summer Institutes for U.S. Graduates Students program, the North Carolina Fossil Club, and financial support from the Jackson School of Geosciences at the University of Texas at Austin and the Department of Marine, Earth, and Atmospheric Sciences at North Carolina State University. A. D. B. Behlke, T. P. Cleland, A. DeBee, D. R. Eddy, T. Gates, J. L. Green, M. L. Householder, J. Hutchinson, E. A. Johnson, D. Ksepka, K. Lamm, S. Nesbitt, K. Pickett, D. Pol, R. Scheetz, N. A. Smith, and H. D. Sues provided thoughtful comments on previous drafts of this dissertation that greatly improved its quality.

I thank my father, Gerald Kenneth, Boyd, for constantly reminding me that I can learn more by going out and experiencing the world around me than I can by reading about it, and for cultivating my love for the outdoors. My deepest thanks to my mother, Coralee Boyd, for always being the friend I needed at all the right moments. Thank you to my children, Alexis Marie Boyd and William Shaw Boyd, for brightening all of my days and constantly reminding me what is truly important in this world. Special thanks to Mindy Lynn Householder, my love, for being the steady hand I needed at the wheel when I found myself lost in the stormy seas of life.

Preface

This dissertation combines a variety of data and analytical methods to explore the taxonomy, systematics relationships, and biogeography of basal ornithischian dinosaurs (Archosauromorpha, Archosauria). Because the chapters following the introduction are formatted to be published as independent works, there is some repetition with respect to introductory statements and materials and methods sections. Although figures and tables are imbedded throughout the text of the dissertation, the reader is frequently referred to a wealth of information contained in the appendices that follow directly after the text of the final chapter. References included in each chapter and the appendices are combined into a single references section found at the end of the dissertation. All photographs were taken by the author unless otherwise noted.

TAXONOMIC REVISION OF LATEST CRETACEOUS NORTH AMERICAN BASAL NEORNITHISCHIAN TAXA AND A PHYLOGENETIC ANALYSIS OF BASAL ORNITHISCHIAN RELATIONSHIPS

Clint Aaroen Boyd, PhD

The University of Texas at Austin, 2012

Supervisor: Julia A. Clarke

The systematic relationships of basal ornithischian dinosaurs remain contentious, especially the position of basal neornithischians (i.e., 'hypsilophodontids'). Prior analyses of basal ornithischian relationships have been hampered by the fact that the hypodigm material of many basal neornithischian taxa is fragmentary, denying access to character data crucial to resolving their relationships. The recent discovery of several new basal neornithischian taxa and the referral of more complete specimens to known taxa provide important new data pertinent to resolving these relationships. The results of this study supplement those recent advances by improving our understanding of the anatomy and systematic relationships of basal neornithischian taxa from the Late Cretaceous of North America. These new insights are accomplished through a taxonomic revision of the Maastrichtian taxa *Bugenasaura* and *Thescelosaurus*, a detailed anatomical description of the cranial anatomy of *Thescelosaurus neglectus* based on the referral of a specimen that includes a nearly complete skull (NCSM 15728), and description of a new basal

neornithischian taxon from the Kaiparowits Formation (Campanian) of Utah. All of these new data are compiled into a dataset composed of 255 characters for 65 terminal taxa (all species exemplars) focused on assessing basal ornithischian relationships. The recovered strict consensus topology is the most highly resolved, stratigraphically congruent phylogenetic hypothesis of basal ornithischian relationships yet proposed. This analysis places all basal neornithischians except *Hypsilophodon foxii* outside of Cerapoda, substantially reducing the taxonomic contents of Ornithopoda. A new clade containing fourteen basal neornithischian taxa is recovered as the sister taxon to Cerapoda and includes all North American basal neornithischians from the Cretaceous. The historical biogeography of Ornithischia is also reconstructed using a method that incorporates time calibrated branch lengths that represent the implied missing fossil record of each taxon. The results of this analysis support two dispersals of neornithischian taxa into South America during the Cretaceous: one consisting of basal iguanodontians dispersing from Australia (possibly via Antarctica) and a second consisting of basal neornithischians dispersing from Asia through North America.

Table of Contents

List of Tables

List of Figures

INTRODUCTION

Early phylogenetic analyses of Ornithischia focused on assessing the relationships of large ornithischian subclades (e.g., Ornithopoda, Ceratopsia, and Pachycephalosauria: Norman, 1984; Cooper, 1985; Sereno, 1986; Maryańska and Osmólska, 1985). Although there was disagreement among the results of those early hypotheses, a general consensus was gradually reached concerning the relationships of most ornithischian subclades (Buchholz, 2002; Liu, 2004; Spencer, 2007; Butler et al., 2008a). Ceratopsia and Pachycephalosauria together form the node-based clade Marginocephalia, and that clade along with Ornithopoda form the node-based clade Cerapoda. Ankylosauria and Stegosauria together form the stem-based clade Thyreophora, and that clade and Cerapoda form the node-based clade Genasauria. The clade Neornithischia (sensu Sereno, 2005) often is considered to be synonymous with Cerapoda; however, the former clade is phylogenetically defined as a stem-based clade while the latter is a node-based clade (see Appendix 7 for internal and external specifiers) allowing each clade to include slightly different sets of taxa. Traditionally, this distinction was of little importance, because no non-thyreophoran genasaurian taxa were recovered outside of Cerapoda (e.g., Sereno, 1999; Buchholz, 2002).

The broader relationships within Ornithischia gradually stabilized, but the systematic relationships of the traditional taxonomic contents of the ornithischian subclade Ornithopoda have become increasingly uncertain. Under the traditional stem-

based definition, Ornithopoda is composed of three subclades: Heterodontosauridae, Hypsilophodontidae, and Iguanodontia (Sereno, 1998, 2005). Beginning at the turn of the latest century, the recovered position of Heterodontosauridae varied between analyses, with most analyses recovering this clade outside of Ornithopoda either as the sister taxon to Marginocephalia (e.g., Buchholz, 2002; Xu et al., 2006), as a basal neornithischian clade outside of Cerapoda (e.g., Liu, 2004; Spencer, 2007), or outside of Genasauria near the base of Ornithischia (e.g., Butler et al., 2008a; Makovicky et al., 2011). In all of those analyses, the placement of Heterodontosauridae outside of Cerapoda resulted in Ornithopoda (sensu Sereno, 2005) being paraphyletic with respect to Marginocephalia. As a result, a new phylogenetic definition for Ornithopoda was proposed that removed heterodontosaurids as internal specifiers (Butler et al., 2008a).

Around that same time, phylogenetic analyses of neornithischian taxa began to lose support for the monophyly of Hypsilophodontidae (Scheetz, 1998, 1999; Winkler et al., 1998). Since that time, in no phylogenetic analysis that included large numbers of 'hypsilophodontid' taxa were they all recovered within a monophyletic group exclusive of all other ornithischian taxa (e.g., Scheetz, 1999; Boyd et al., 2009; Brown et al., 2011), though in some analyses a more restricted Hypsilophodontidae was recovered (e.g., Butler, 2005; Spencer, 2007). Given the uncertainty surrounding the relationships of these 'hypsilophodontids,' many authors now refer to these taxa as basal ornithopods. However, the latter term also does not take into account the full range of uncertainty surrounding their systematic relationships. Beginning with the analyses by Liu (2004) and Butler (2005) and continuing with the more recent analyses by Butler et al. (2008a)

and Makovicky et al. (2011), several taxa traditionally referred to as basal ornithopods were placed outside of Cerapoda as basal neornithischians (e.g., *Agilisaurus*, *Hexinlusaurus*). In the most extreme example, Liu (2004) recovered all traditional 'hypsilophodontids' placed outside of Cerapoda as basal neornithischians. Given the high level of uncertainty regarding the systematic positions of traditional 'hypsilophodontid,' or basal ornithopod, taxa, I refer to all non-iguanodontian, non-marginocephalian neornithischian taxa as basal neornithischians.

Over the last few years there was also an increasing trend of reduced resolution of relationships among basal neornithischians. This situation reached an extreme in the most inclusive analysis of basal ornithischian relationships yet conducted (Butler et al., 2008a), in which the positions of eleven of the fourteen basal neornithischian taxa included were unresolved in the strict consensus tree. Recovery of a fully dichotomous topology required the removal of six of the fourteen basal neornithischian taxa (and two heterodontosaurids) from the analysis (Butler et al., 2008a:fig. 3). Those difficulties led those authors to note that, "Considerable future work is required to determine exactly which taxa can be referred to [Ornithopoda], what characters diagnose this clade, and how basal taxa are related to one another" (Butler et al., 2008a:p. 23).

Over the last five years, substantial improvement into our understanding of basal neornithischian anatomy and diversity was achieved. Several new taxa were named from Asia (Huh et al., 2010; Zheng et al., 2012), North America (Varricchio et al., 2007; Brown et al., 2011), and South America (Calvo et al., 2007). Thorough anatomical descriptions of known taxa were also published based either on redescription of the type

material (e.g., Boyd et al. 2009; Jin et al., 2010; Butler et al., 2011) or description of additional referred specimens (e.g., Barrett and Han, 2009). In addition, undescribed specimens of basal neornithischian taxa exist that provide previously unknown morphological character data that is crucial to resolving the systematic relationships of all basal neornithischian taxa (i.e., *Jeholosaurus*; *Orodromeus*; *Othnielosaurus*; *Thescelosaurus*; and *Zephyrosaurus*).

The purpose of this study is to bring all of these new data to bear on assessing the problematic relationships of basal neornithischian dinosaurs. The dissertation is divided into five chapters, each with a different taxonomic and/or methodological focus. The first chapter consists of an evaluation of the taxonomic affinities of nine specimens previously referred to the problematic basal neornithischian taxon *Thescelosaurus*, which includes a revision of the existing taxonomy of those specimens and the identification of a phylogenetically assessed set of apomorphic traits that diagnose *Thescelosaurus*. Description of the cranial anatomy of *Thescelosaurus neglectus* (the name bearing species) based on the nearly complete, three dimensionally preserved skull from NCSM 15728 constitutes the second chapter. Recently collected specimens from the Kaiparowits Formation (Campanian) of Utah represent a previously undescribed basal neornithischian taxon, and its anatomy and systematic relationships are detailed in the third chapter. In the fourth chapter I evaluate possible methods for incorporating systematic uncertainty into the calculation of stratigraphic consistency metrics, select a preferred method that describes the full range of variation that systematic uncertainty imparts on these metrics, and present a new program that incorporates those methods and simplifies the calculation

of stratigraphic consistency metrics. The final chapter presents an exhaustive analysis of basal ornithischian relationships that utilizes only species exemplars as terminal taxa. That analysis incorporates the new data presented herein, as well as additional morphological data gleaned from examination of several newly discovered, but mostly undescribed, specimens referable to basal ornithischian taxa that were previously poorly understood.

The first chapter focuses on resolving the taxonomic diversity of *Thescelosaurus* via a phylogenetic analysis of nine specimens previously referred to that taxon from Maastrichtian sediments within the Western Interior Basin of North America. These nine specimens previously were proposed to represent as many as five different species, but the validity of those species and their interrelationships were never thoroughly assessed. Inclusion of these nine specimens in a dataset along with terminals representing eighteen other basal ornithischian taxa assessed the character support for, and contents of, a monophyletic *Thescelosaurus* clade. Also included in this chapter is a description of newly recognized cranial material preserved in the paratype of *Thescelosaurus neglectus*. The results of this analysis were used to determine the treatment of *Thescelosaurus* and other closely related taxa (i.e., *Bugenasaura* and *Parksosaurus*) in subsequent chapters.

A basal neornithischian specimen collected from the Hell Creek Formation of South Dakota, NCSM 15728, includes the best-preserved skull yet discovered for any basal neornithischian taxon. The specimen is clearly referable to *Thescelosaurus neglectus* based on characters shared only with the paratype specimen of that taxon. Prior to this referral, only three fragmentary cranial bones were known from specimens

confidently referred to *T. neglectus*. The second chapter of this dissertation consists of a detailed description of the cranial anatomy of *T. neglectus*, based on NCSM 15728. This was facilitated through extensive preparation of the skull that revealed important morphological features, and through the use of CT data that allowed description of the anatomy of internal portions of the skull that could not be exposed via traditional preparation techniques.

The third chapter is an anatomical description of a new basal neornithischian taxon from the Kaiparowits Formation of Utah. The systematic relationships of the new taxon were assessed using a slightly modified version of the dataset from chapter one. A new clade of basal neornithischian dinosaurs is recognized and named based on the presence of several synapomorphies. Additionally, the distribution of several characters previously proposed to be linked to fossorial behavior in the basal neornithischian taxon *Oryctodromeus cubicularis* is traced across basal Ornithischia to determine if those characters are restricted to a small group of possibly fossorial taxa, or if they are more broadly distributed across the Ornithischia.

A final goal of this dissertation is to robustly assess the relationships of basal ornithischian dinosaurs. However, before conducting such an investigation, a method was needed to facilitate comparison of the new phylogenetic hypothesis to previously proposed hypotheses. Because all fossils provide two independent sources of data, the morphological features preserved on the fossil and the stratigraphic data regarding where the fossil was collected, stratigraphic consistency metrics are useful tools for comparing alternative phylogenetic hypotheses. Two difficulties presented themselves in using these

metrics in this study. First, there was no standardized method for incorporating phylogenetic uncertainty (i.e., polytomies) into stratigraphic consistency calculations. Second, no automated program was available for calculating these complicated metrics. Therefore, in chapter four I present an investigation into the differential impact that alternative methods for incorporating phylogenetic uncertainty into stratigraphic consistency calculations have on the resulting scores. Based on these result, I select a preferred method for describing the full range of variation that phylogenetic uncertainty imparts on these metrics. Additionally, a new program is introduced that simplifies the calculation of stratigraphic consistency metrics.

The final chapter presents an analysis of basal ornithischian relationships that utilizes a dataset composed entirely of species exemplars (no supraspecific terminal taxa). All diagnosably distinct basal neornithischian taxa were included in the analysis regardless of completeness, except for a few taxa that were not available for study. The resulting phylogenetic hypothesis is compared to all recent hypotheses of basal ornithischian relationships using the modified stratigraphic consistency methods and program presented in chapter four. A biogeographic reconstruction is also conducted using the resulting phylogenetic hypothesis and a method that impliments time calibrated branch lengths set equal to the implied missing fossil record for each taxon, allowing older taxa having a larger impact on ancestral area reconstructions than younger taxa.

Via the work presented in this dissertation, I strive to advance our knowledge of basal neornithischian anatomy and systematic relationships and to provide a solid foundation for future studies of the clade. The recovery of a well-resolved,

stratigraphically congruent phylogenetic hypothesis of basal ornithischian relationships will provide future researchers with a robust framework within which to assess a wide range of hypotheses regarding trends in ornithischian evolution and patterns of biogeographic dispersal, among other topics. Additionally, recovery of a well-resolved hypothesis of basal ornithischian relationships is the first crucial step towards facilitating the first analysis of the relationships of all ornithischian taxa using a single dataset composed only of species exemplars, which will provide a depth of knowledge concerning evolutionary patterns and processes present in the evolutionary history of Ornithischia that remain incompletely understood. Finally, the novel methods employed herein and detailed in portions of chapters four and five have broad applicability beyond any single clade and are intended to provide valuable tools to advance the entire field of paleontology.

CHAPTER 1.

Reassesing the Taxonomic Status of the Basal Neornithischian Taxa *Thescelosaurus* and *Bugenasaura*

INTRODUCTION

The taxonomic diversity of basal neornithischians (stem based definition of Sereno, 1998) in North America during the Maastrichtian (70.6 to 65.5 Ma; Weishampel et al., 2004; Gradstein et al., 2005) remains controversial despite recent attempts to provide clarity to this issue (Galton, 1995, 1997, 1999). An array of species have been named and repeatedly revised as parts of three taxa (*Bugenasaura*, *Parksosaurus*, and *Thescelosaurus*), and the referral of individual specimens to these species remains fluid (Gilmore, 1913; Parks, 1926; Sternberg, 1937, 1940; Morris, 1976; Galton, 1995). Currently, no consensus exists on the systematic positions of these taxa. For instance, *Thescelosaurus* has been placed within a monophyletic Hypsilophodontidae (sensu Sereno, 1998; Figs. 1.1A, B, F) or basal to Iguanodontia (sensu Sereno, 2005; Figs. 1.1C, D, E). New information from previously unreported cranial material from the paratype specimen of *Thescelosaurus neglectus* (USNM 7758), the name bearing species of the taxon *Thescelosaurus*, and two new specimens allow identification of previously unrecognized cranial characters that facilitate a taxonomic revision of previously described *Bugenasaura*, *Parksosaurus*, and *Thescelosaurus* species.

The type series of *Thescelosaurus neglectus* (Gilmore, 1913) consists of a nearly-complete postcranial skeleton named as the holotype specimen (USNM 7757) and a second, fragmentary postcranial skeleton (USNM 7758) assigned as the paratype. Both specimens were collected from the Lance Formation of Wyoming (Maastrichtian; 70.6 to 65.5 Ma; Weishampel et al., 2004; Gradstein et al., 2005) and between these two

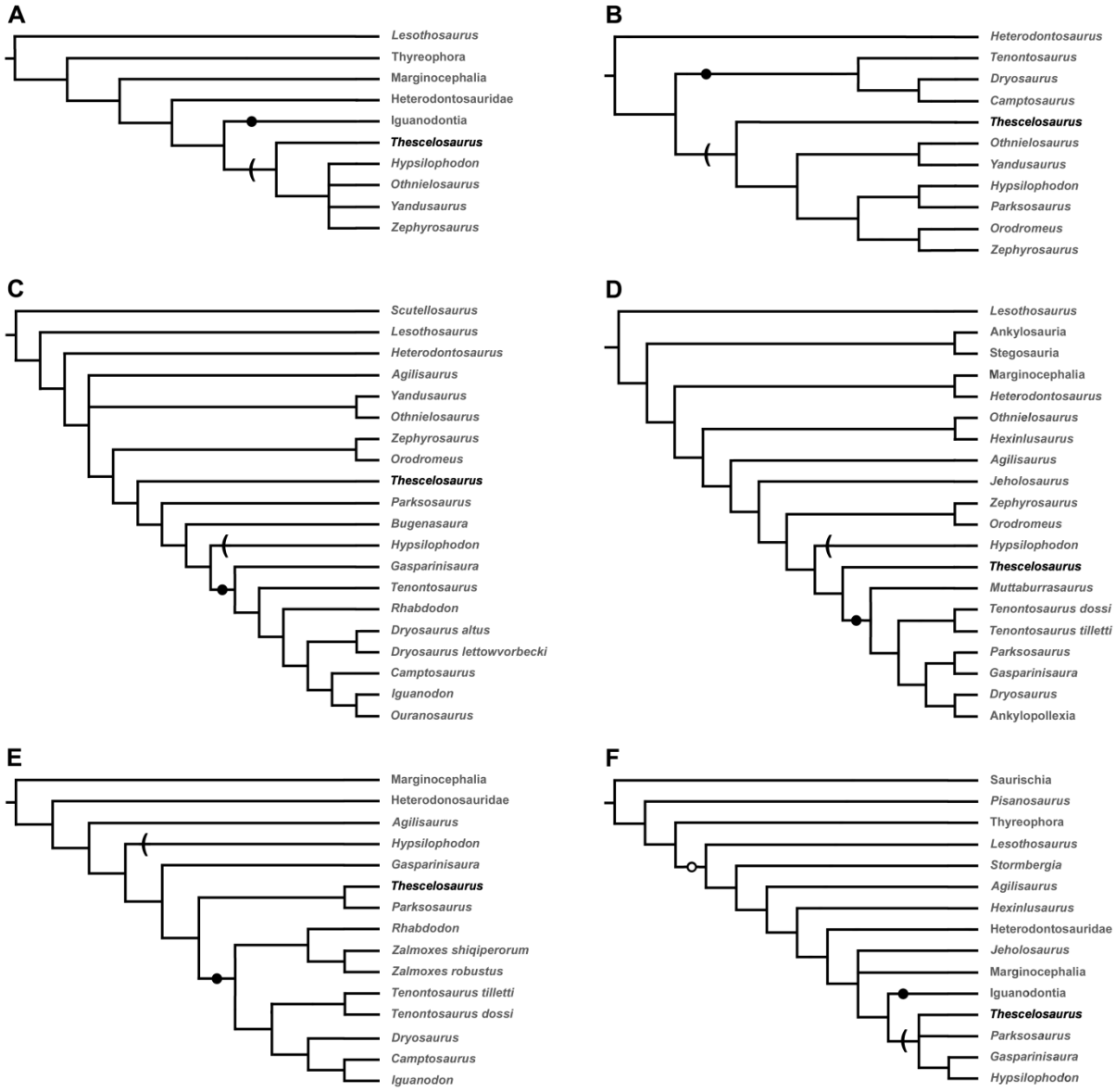

Figure 1.1: Overview of the position of *Thescelosaurus* in previously published phylogenetic analyses. **A**. phylogeny from Sereno (1986) modified to focus on the position of 'hypsilophodontid' taxa; **B**. single most parsimonious tree (MPT) from Weishampel and Heinrich (1992); **C**. majority rule consensus tree of three MPTs from Scheetz (1999); **D**. majority rule consensus tree of ten MPTs from Buchholz (2002); **E**. strict consensus of two MPTs from Weishampel et al. (2003); **F**. majority rule consensus of twenty–three MPTs from Butler (2005). The empty circle indicates the position of the stem-based clade Neornithischia (sensu Sereno, 1998) in Butler (2005). Black circles indicate the position of the stem–based clade Iguanodontia (sensu Sereno, 2005) and the curved lines denote the position of the stem–based clade Hypsilophodontidae (sensu Sereno, 1998). Modified from Boyd et al. (2009).

specimens all postcranial elements are represented with the exception of the anterior cervical vertebrae and coracoids. However, no cranial material was identified from either specimen (Gilmore, 1913; Gilmore, 1915). An array of additional specimens have since been referred to this species from the Lance (Gilmore, 1915), Hell Creek (Gilmore, 1915; Morris, 1976; Galton, 1997; Fisher et al., 2000), Scollard (Sternberg, 1940; Galton, 1974b), and Frenchman (Galton, 1974b, 1989) formations of North America.

Three additional species of *Thescelosaurus* have been described: *Thescelosaurus warreni*, Parks, 1926, *Thescelosaurus edmontonensis*, Sternberg, 1940, and *?Thescelosaurus garbanii*, Morris, 1976. Sternberg (1937) designated the holotype specimen of *Thescelosaurus warreni*, ROM 804, the type of a new taxon, *Parksosaurus*, because he considered the differences present between it and *T. neglectus* greater than those he identified between *T. edmontonensis* and *T. neglectus*. Galton (1974b, 1995) argued that the differences noted by Sternberg (1940) between *T. edmontonensis* and *T. neglectus* fell within the range of individual variation exhibited by other closely related taxa (e.g., *Dryosaurus altus*, *D. lettowvorbecki*, and *Hypsilophodon foxii*; Galton, 1974a, 1981); therefore, he considered *T. edmontonensis* to be a subjective junior synonym of *T. neglectus.*

Morris (1976) described a partial left hind limb and associated cervical and dorsal vertebrae (LACM 33542) from the Hell Creek Formation as a new species, *?Thescelosaurus garbanii*, which was tentatively referred to *Thescelosaurus* based on general similarity with the hind limb. Morris (1976) also described a partial skull with fragmentary mandibles and associated postcrania (SDSM 7210) from the Hell Creek

Formation, which he proposed may represent a previously undescribed species. This specimen lacks material that can be directly compared to the type series of *T. neglectus* and the holotype of *T. garbanii* and the only cranial material known from *Thescelosaurus* at that time was the fragmentary material preserved with the holotype of *T. edmontonensis* (CMN 8537). For these reasons he referred SDSM 7210 to *Thescelosaurus* sp. rather than erect a new species. Sues (1980) concurred and stated that this specimen should remain unnamed until new material was discovered that facilitated its comparison with the type series of *T. neglectus*. Galton (1995) made SDSM 7210 the holotype of *Bugenasaura infernalis* and tentatively referred the holotype of ?*Thescelosaurus garbanii* (LACM 33542) to this new species, despite the lack of comparable material between these specimens.

The taxonomy of *Bugenasaura*, *Parksosaurus,* and *Thescelosaurus* has not been revised since Galton (1995). Since then, two important specimens have been discovered that preserve nearly complete skulls and mandibles (NCSM 15728 referred to *T. neglectus* and MOR 979 referred to *B. infernalis*; Fisher et al., 2000; Horner, 2001), enhancing our knowledge of the anatomy of these taxa. These new specimens, combined with data obtained from the newly recognized skull material from USNM 7758, allow for a new phylogenetic analysis and taxonomic revision of eight specimens previously referred to these taxa (Fig. 1.2) that preserve material from the skull and/or tarsus (Parks, 1926; Sternberg, 1940; Galton, 1974b, 1989, 1997, 1999; Morris, 1976; Fisher et al., 2000; Horner, 2001). Two partial dentaries (AMNH 5020 and CMN 9534) that were

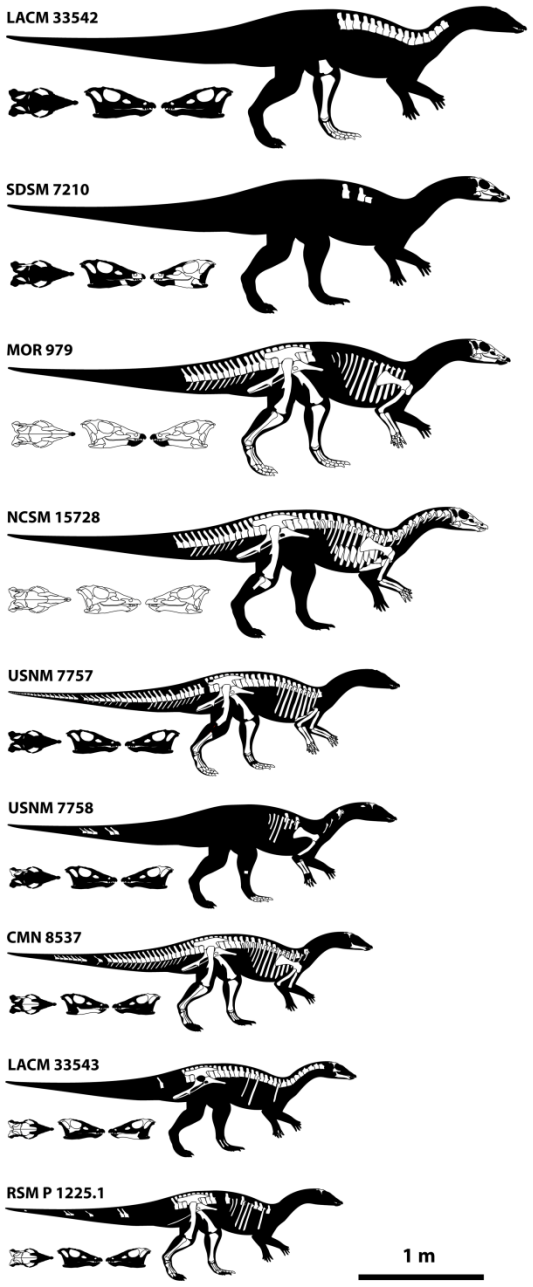

Figure 1.2: Diagram illustrating the relative size and completeness of all specimens referred to *Thescelosaurus* by this study. Bones present in each specimen are colored white. Skeletons are scaled isometrically based on femur and tibia length when available. Skeletons lacking both tibiae and femora were scaled using the following elements: anteroposterior width of orbit for SDSM 7210; length of the dentary for LACM 33543; and length of the humerus for USNM 7758. Proportions for each specimen represent those of USNM 7757 and do not illustrate proportion changes that would be effected due to allometric scaling. Modified from Boyd et al. (2009).

referred to *T. neglectus* by Galton (1974b, 1997) will not be considered because no dentary characters were found to be diagnostic of a *Thescelosaurus* clade in this analysis. The postcranial anatomy of these taxa will only be briefly discussed as reexamination of the postcrania of these and other referred specimens is ongoing. For institutional abbreviations see Appendix 1.

CLADISTIC METHODOLOGY

A new phylogenetic analysis was conducted that evaluated: (1) character support for a monophyletic *Thescelosaurus* clade; (2) removal of ROM 804 from *Thescelosaurus*; and (3) the relationships of LACM 33542, the holotype of *Thescelosaurus garbanii* (Appendix 3–4, Fig. 1.3, Table 1.1). This analysis used the Varricchio et al. (2007) dataset, which is based on that of Scheetz (1999). The following modifications were made to this dataset: included six characters originally proposed by Galton (1997, 1999) to diagnose *Thescelosaurus*, added two new characters, and incorporated character scorings based on personal observations (see Appendix 3-4). The terminal taxa "*Bugenasaura"* and *"Thescelosaurus"* (Fig. 1.3A) from Scheetz (1999) were removed from this analysis because they were scored from both the type series and referred specimens and the current analysis aims to reassess these referrals. *Parksosaurus* was also completely rescored from ROM 804. The holotype material of *Bugenasaura infernalis* and *Parksosaurus warreni*, the type series of *Thescelosaurus neglectus*, and six specimens previously referred to these taxa were included as terminals in this analysis

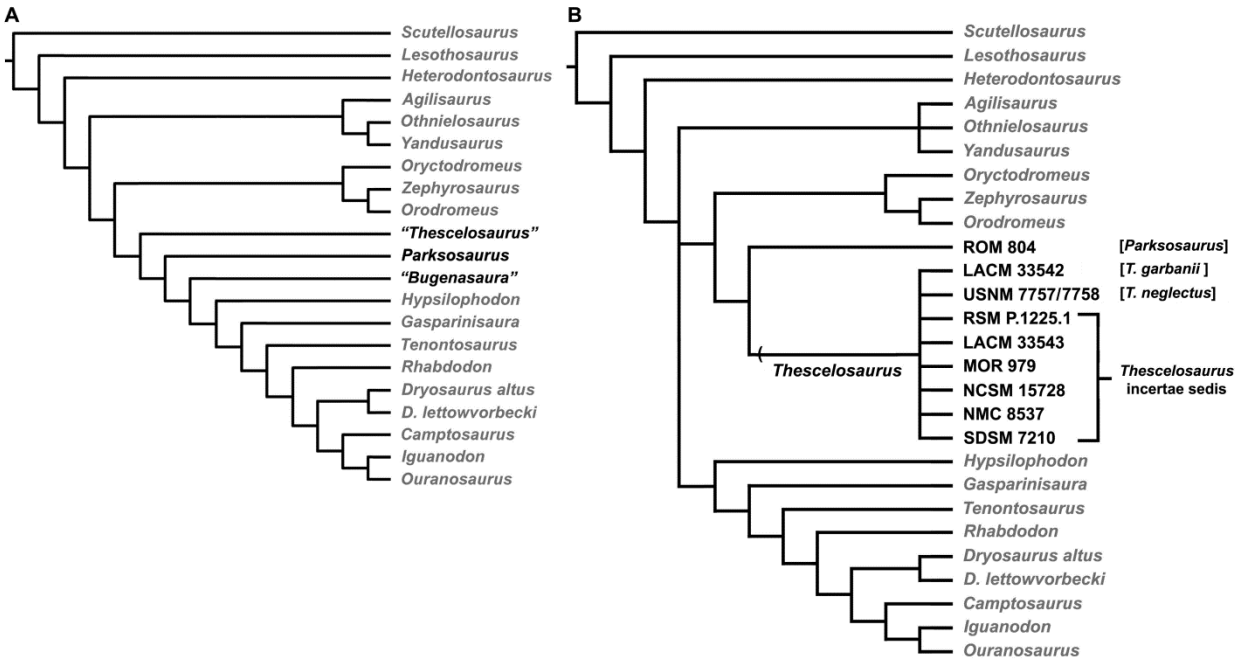

Figure 1.3: Phylogenetic analysis supporting the monophyly of a *Thescelosaurus* clade, synonymization of *Bugenasaura* with *Thescelosaurus*, and the placement of *Thescelosaurus garbanii* within a *Thescelosaurus* clade. **A**. single MPT from Varricchio et al. (2007); **B**. strict consensus of 748 MPTs with a length of 366, retention index (RI) of 0.67, and a consistency index (CI) of 0.50 resulting from analysis of the new dataset constructed for this investigation. On the second tree, Bremer support values are positioned above the nodes and bootstrap values are below the nodes. Quotations were added to *Thescelosaurus* and *Bugenasaura* in the Varricchio et al. (2007) tree to indicate that those terminal taxa were scored from both the type series and referred material. The taxonomic referrals of the nine terminals under investigation are listed to the right of their respective specimen numbers. Modified from Boyd et al. (2009).

(see Table 1.1 and Appendix 4 for the list of specimens and their respective scorings and Figure 1.2 for material preserved in each specimen). All characters were run unordered, but additional analysis demonstrated that alternative ordering of characters did not affect the placement of the nine terminals under investigation here (unpub. data). *Scutellosaurus* was selected as the outgroup taxon for this analysis because it has been consistently placed outside the Neornithischia by prior analyses (e.g., Sereno, 1986, Butler, 2005). The analysis was run in the program TNT (Goloboff et al., 2008) using the implicit

Table 1.1: Review of character data supporting synonymization of *Bugenasaura* with *Thescelosaurus* and for removing ROM 804, the holotype of *Parksosaurus warreni*, from *Thescelosaurus*. The presence or absence of nine characters was traced: Seven proposed by Galton (1997, 1999; characters 125-131) and two new characters (132-133) identified in this analysis. Each character is described in Appendix 3 and listed by its respective number in Appendix 4. Abbreviations: (**0**) character state zero is present (see Appendix 3); (**1**) character state one is present (see Appendix 3); (-) character state not preserved or unable to be scored.

Specimen	Original Taxonomic Assignment	Current Taxonomic Assignments	Characters from Appendix 4								
			125	126	127	128	129	130	131	132	133
USNM 7757	*Thescelosaurus neglectus*	*Thescelosaurus neglectus*	-	-	-	-	-	1	-	-	-
USNM 7758	*Thescelosaurus neglectus*	*Thescelosaurus neglectus*	-	1	-	-	-	-	-	-	-
NCMS 15728	*Thescelosaurus neglectus*	*Thescelosaurus* sp.	1	1	1	1	1	-	1	1	1
MOR 979	*Bugenasaura infernalis*	*Thescelosaurus* sp.	1	-	-	-	1	1	1	1	1
SDSM 7210	*Bugenasaura infernalis*	*Thescelosaurus* sp.	1	-	-	-	-	-	1	1	-
CMN 8537	*Thescelosaurus edmontonensis*	*Thescelosaurus* sp.	1	1	-	-	1	1	-	-	-
LACM 33543	*Thescelosaurus neglectus*	*Thescelosaurus* sp.	-	-	1	-	1	-	-	1	-
RSM P.1225.1	*Thescelosaurus neglectus*	*Thescelosaurus* sp.	1	1	1	1	-	1	-	-	-
LACM 33542	*?Thescelosaurus garbanii*	*Thescelosaurus garbanii*	-	-	-	-	-	-	-	-	-

enumeration search option that recovers all most parsimonious trees (MPTs). Seven hundred forty-eight MPTs (tree length = 366) were recovered and the resulting strict consensus tree is presented in Figure 1.3B. A bootstrap analysis (1000 replicates) was run and Bremer support values were calculated using PAUP*v.4.0b10 (Swofford, 2002). The results of this analysis are used to support the taxonomic referrals given in the Systematic Paleontology section below.

SYSTEMATIC PALEONTOLOGY

DINOSAURIA Owen, 1842

ORNITHISCHIA Seeley, 1887

NEORNITHISCHIA Cooper, 1985

Thescelosaurus Gilmore, 1913

Bugenasaura Galton, 1995:308.

Type Species

Thescelosaurus neglectus Gilmore, 1913.

Distribution

Frenchman Formation, Saskatchewan; Hell Creek Formation, Montana and South Dakota; Lance Formation, Wyoming; Scollard Formation, Alberta (all Maastrichtian age [70.6–65.5 Ma]; Weishampel et al., 2004; Gradstein et al., 2005).

Emended Diagnosis

Each of the characters proposed below is followed by (character number:state present) from Appendix 2 and illustrated in Figure 1.4. The following proposed autapomorphies comprise characters optimized as unique to a *Thescelosaurus* clade relative to all other analyzed taxa: frontals wider at midorbital level than across posterior end (126:1); dorsolaterally directed process on surangular (129:1); prominent, horizontal ridge on

maxilla with at least the posterior portion covered by a series of coarse, rounded, obliquely inclined ridges (131:1); depressed posterior half of ventral edge of jugal covered laterally with obliquely inclined ridges (132:1); foramen in dorsal surface of prefrontal dorsomedial to articulation surface for palpebral that opens into the orbit (133:1). Two additional characters are currently uniquely known for parts of the *Thescelosaurus* clade, but are unable to be evaluated for its sister taxon *Parksosaurus*: dorsal edge of opisthotic indented by deep, 'Y-shaped' excavation in dorsal view (127:1); palpebral dorsoventrally flattened and rugose along the medial and distal edges (125:1). The latter character is also present in an otherwise distinct basal neornithischian specimen from China housed at IVPP (CAB pers. obs.) whose relationships have not yet been evaluated. Only NCSM 15728 displays all proposed autapomorphies for *Thescelosaurus* (See Figure 1.4 and Table 1.1), but subsets are preserved in all other referred specimens.

Two additional characters are optimized as local apomorphies of the *Thescelosaurus* clade, but occur convergently within major neornithischian subclades: angle between ventral margin of braincase (occipital condyle, basal tubera, and basipterygoid processes) and a line drawn through center of the trigeminal foramen and posterodorsal hypoglossal foramen less than fifteen degrees (128:1); and femur longer than tibia (130:1). The former is found in Iguanodontia and the latter occurs in both Iguanodontia and Marginocephalia.

Comments

As shown in Table 1.1, the proposed diagnostic sets of characters identified by

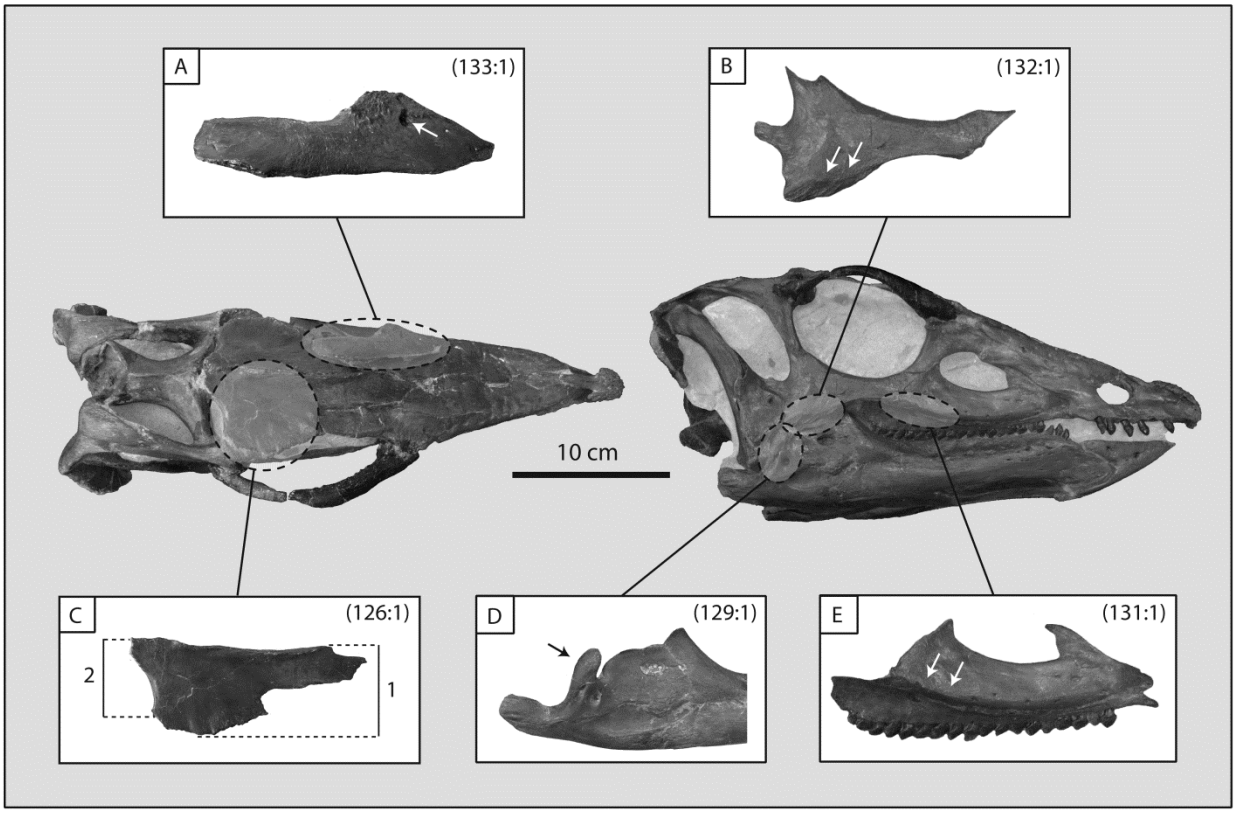

Figure 1.4: The five autapomorphies of *Thescelosaurus* as seen on the skull of NCSM 15728 in dorsal (left) and lateral (right) views. **A**. foramen in dorsal surface of prefrontal dorsomedial to articulation surface for palpebral that opens into the orbit (133:1); **B**. depressed posterior half of ventral edge of jugal covered laterally with obliquely inclined ridges (132:1); **C**. frontals wider at midorbital level (1) than across posterior end (2) (126:1); **D**. dorsolaterally directed process on surangular (129:1); **E**. prominent, horizontal ridge on maxilla with at least the posterior portion covered by a series of coarse, rounded, obliquely inclined ridges (131:1). Modified from Boyd et al.(2009).

previous authors (Galton, 1997, 1999) from the type series of *Thescelosaurus* (USNM 7757, 7758) and the holotype of *Bugenasaura* (SDSM 7210) represent morphologies observed on distinct, non-comparable cranial elements preserved in these specimens. None of these previously proposed characters can be assessed in both the type series of *Thescelosaurus* and the holotype of *Bugenasaura*. No character conflict exists between

these specimens or among any of the seven referred specimens examined here aside from ROM 804, which is placed outside of a *Thescelosaurus* clade (Fig. 1.3B). Thus, *Bugenasaura* is proposed to be a subjective junior synonym of *Thescelosaurus*, a conclusion that is also supported by the placement of the holotype specimen of *Bugenasaura* in a *Thescelosaurus* clade (Fig. 1.3B).

Three characters proposed by Galton (1997, 1999) to diagnose either *Thescelosaurus neglectus* or *Bugenasaura infernalis* were not found to diagnose a *Thescelosaurus* clade nor presently support species differentiation within that clade. These characters were not included in the analysis for the reasons described below. The presence of "numerous secondary ridges that form two converging crescentic patterns" on the maxillary and dentary teeth (buccal and lingual surfaces, respectively) was proposed by Galton (1997:253) to diagnose *T. neglectus*. This character was excluded because this morphology was found to vary across the maxillary and dentary dentition of individual specimens of *Thescelosaurus* (e.g., NCSM 15728). The degree of development of a prominent ridge on the dentary (proposed to diagnose *B. infernalis*; Galton, 1999) varies continuously between evaluated specimens. This variation, without discernibly distinct cut-offs, may be due to ontogenetic differences, but this hypothesis remains to be tested (see Discussion).

The degree of participation of the supraoccipital in the dorsal margin of the foramen magnum (proposed to diagnose *T. neglectus*; Galton, 1997) may be a useful character for analyzing the relationships of basal neornithischians and deserves further investigation. However, its distribution is complex and it does not appear to diagnose a

Thescelosaurus clade or *T. neglectus*. For example, in SMNS P.1225.1, the supraoccipital barely participates in the dorsal margin of the foramen magnum, but in LACM 33543 there is a notch in the dorsal border of the foramen magnum and the supraoccipital just touches the dorsal-most extent of this notch. The presence of this notch, along with other differences in the braincase of these specimens not discussed here, may later prove to be of diagnostic value at the species level within *Thescelosaurus*, but at this time sufficient data regarding the morphology of this region is not available from most specimens due to preservational issues and incomplete preparation.

***Thescelosaurus neglectus* Gilmore, 1913:1.**

Holotype

USNM 7757: nearly complete postcranial skeleton.

Paratype

USNM 7758: fragmentary skeleton including parts of skull (Figs. 1.4–1.5).

Locality

USNM 7757: Collected by J. B. Hatcher and W. H. Utterback in 1891 from Doegie Creek, Niobrara County, Wyoming. USNM 7758: Collected by O. A. Peterson in 1889 from Lance Creek, Niobrara County, Wyoming.

Distribution

Lance Formation of Wyoming (Maastrichtian age [70.6–65.5 Ma]; Weishampel et al., 2004; Gradstein et al., 2005).

Referred Specimens

None

Emended Differentia

This species differs from *Thescelosaurus garbanii* in: retention of calcaneum participation in midtarsal joint.

Emended description of type series

Three previously unrecognized cranial bones were identified in material from paratype specimen USNM 7758. These consist of a partial left squamosal, partial left postorbital, and a fragmentary piece of frontal (Figs. 1.5–1.6). Although all three of these bones are incomplete, sufficient morphological detail is preserved to provide important insights into the cranial anatomy of *Thescelosaurus neglectus*.

The dorsal surface of the squamosal is slightly inclined medially. The facet for the posterior ramus of the postorbital is dorsally directed (Fig. 1.5B) and the midpoint of the posterior edge of this facet is raised into a narrow flange that would have overlapped the midsection of the articulated postorbital (Fig. 1.5A, B). The postorbital would have been visible medial and lateral to this flange in dorsal view. In dorsal view, the posterior edge of the squamosal is deeply concave (Fig. 1.5A). The lateral half of the postorbital-

squamosal facet extends to the edge of this concavity as a broad, shallow groove. Ventral to this concavity the articulation surface for the paroccipital process (opisthotic) faces posterolaterally and consists of a raised, rugose surface. The quadrate facet is a deep socket dorsolaterally enclosed by a small wall of bone that would have covered the tip of the quadrate head in lateral view. The origin of the m. adductor externus superficialis (sensu Galton, 1974a) is developed as a conspicuous facet dorsal to the remains of the quadratic process and the edge of the lateral temporal fenestra (Fig. 1.5B). The ventrally directed quadratic process is not preserved, and the medial portion of the squamosal is also missing.

The postorbital is triradiate, but only the anterior ramus is completely preserved (Fig. 1.6A). The posterodorsal margin of the orbit is arcuate and marked with numerous small bosses that extend into the orbit (Fig. 1.6B). Near the base of the anterior ramus the edge of the orbital margin bears an anteroventrally directed projection (Fig. 1.6B). An irregular, rugose, 'C-shaped' ridge of bone extends onto the lateral surface of this projection, possibly indicating a point of attachment for the palpebral or a secondary palpebral (if present). The ventrolateral surface of the postorbital is covered with a series of small ridges that vary in orientation and extend dorsally to a short horizontal ridge (Fig. 1.6B). The postorbital excludes the frontal from the anterolateral corner of the supratemporal fenestra (Fig. 1.6A). The articular surface for the frontal is complex, marked with a set of interlocking anteroposteriorly-oriented ridges and grooves.

A small piece of the frontal is preserved that articulates with the preserved section of the postorbital. As noted, the surfaces of the postorbitofrontal contact bear interlocking

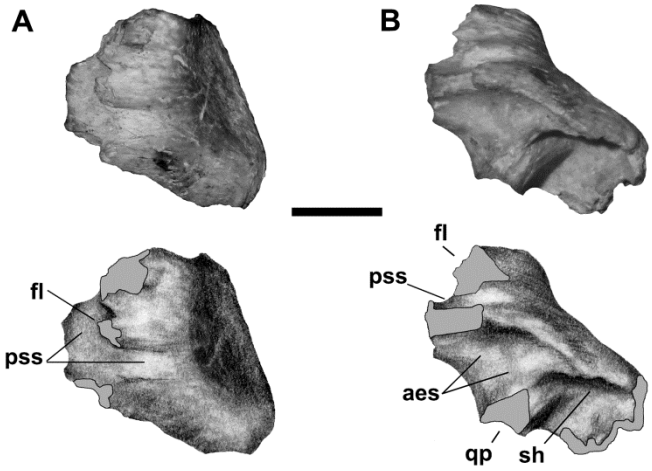

Figure 1.5: Squamosal from USNM 7758. **A**. photograph (top) and illustration (bottom) in dorsal view; **B**. photograph (top) and illustration (bottom) in lateral view. Areas shaded in grey indicate damaged regions of the bone. Scale bar equals 1 cm. Modified from Boyd et al. (2009). See Appendix 2 for anatomical abbreviations.

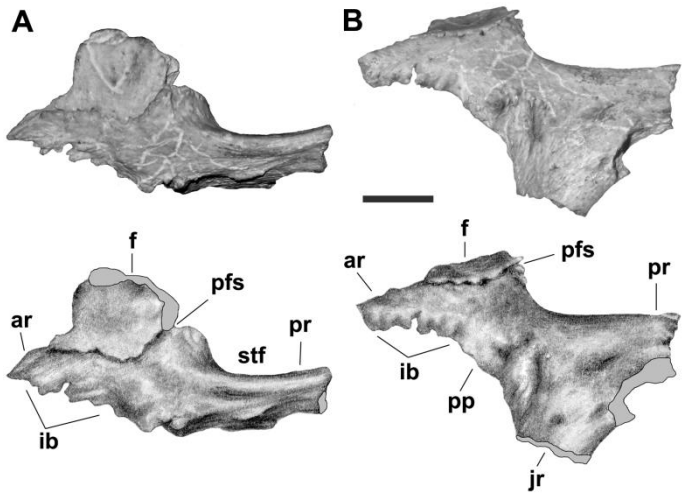

Figure 1.6: Postorbital and frontal from USNM 7758. **A**. photograph (top) and illustration (bottom) in dorsal view; **B**. photograph (top) and illustration (bottom) in lateral view. Areas shaded in grey indicate damaged regions of the bone. Scale bar equals 1 cm. Modified from Boyd et al. (2009) See Appendix 2 for anatomical abbreviations..

anteroposteriorly-oriented ridges and grooves. The shape of the postorbitofrontal suture, specifically the lateral flaring of the anterior tip of the postorbital, indicates that the frontals would have been transversely wider at midorbit level than across their posterior end (Fig. 1.6A).

Comments

All characters previously proposed to differentiate the species *T. neglectus* by Galton (1997) are here found either to be synapomorphies of a clade *Thescelosaurus* (see above) or are broadly distributed within neornithischian taxa. Due to the fragmentary nature of the holotype of *T. garbanii*, the only other species of *Thescelosaurus* found to be valid by this analysis (see below), the anatomy of the hind limb and anterior vertebral column alone can be used to differentiate these two species. While *T. neglectus* is currently based on a differential diagnosis including a single character, further examination of the postcranial anatomy of this species and future referral of more complete specimens to *T. garbanii* may illuminate additional traits that will further differentiate these two species, or, ideally, diagnose *T. neglectus*.

***Thescelosaurus garbanii* Morris, 1976**

?*Thescelosaurus garbanii* Morris, 1976:100, figs. 3a–c, 5d–f.

Holotype

LACM 33542: Five posterior cervical and eleven anterior dorsal vertebrae, left pes, tarsus, tibia, fibula, and distal end of femur (Morris, 1976:figs. 3a–c, 5d–f; Galton, 1995:figs. 2e–f).

Locality

Discovered by Harli Garbani from LACM Locality v3152; T. 21N, R.42E, NE/2, NW/4, Sec. 22, Garfield County, Montana.

Distribution

Hell Creek Formation of Montana (Maastrichtian [70.6–65.5 Ma]; Weishampel et al., 2004; Gradstein et al., 2005).

Diagnosis

Autapomorphy of species: calcaneum excluded from midtarsal joint by laterally expanded astragalus.

Comments

Morris (1976) designated LACM 33542 the holotype of *?Thescelosaurus garbanii* based upon its general similarity to the hind limb of *T. neglectus*, but noted that the fragmentary nature of this specimen prevents the recognition of autapomorphies of any known basal neornithischian taxon. It was later tentatively referred to *Bugenasaura infernalis* by Galton (1995, 1999); however, LACM 33542 contains no elements directly

comparable to the holotype of *B. infernalis*. The synonymization of *Bugenasaura* with *Thescelosaurus* places this species back within the latter taxon.

The exclusion of the calcaneum from the surface of the midtarsal joint is unique to LACM 33542, as indicated by comparisons to the structure of the tarsal region in CMN 8537, MOR 979, RSM P.1225.1, and USNM 7757. The analysis shown in Figure 1.3B places this specimen within a *Thescelosaurus* clade, supporting the prior tentative referral of this species to this taxon (Morris, 1976). These results support the recognition of *T. garbanii* as a valid species, though much of its anatomy remains poorly understood.

Thescelosaurus incertae sedis

Referred Specimens

CMN 8537, LACM 33543, MOR 979, NCSM 15728, SDSM 7210, RSM P.1225.1

Comments

The six referred specimens listed above each preserve multiple autapomorphies of *Thescelosaurus* (see Emended Diagnosis of *Thescelosaurus* and Table 1.1), but cannot be referred with certainty to one of the two species described above for reasons given below.

The holotype of *B. infernalis*, SDSM 7210, consists of an incomplete skull including premaxillae, maxillae, palpebral, prefrontal, lacrimal, jugal, quadratojugal, postorbital, ectopterygoid, pterygoid, dentary, surangular, coronoid, splenial, and prearticular as well as four dorsal vertebrae and two manual phalanges (see Fig. 1.2)

collected from the Hell Creek Formation of South Dakota (Morris, 1976:figs. 5a–c; Galton, 1999:figs. 1–2, pl. 1). SDSM 7210 preserves neither the squamosal nor the tarsal region (Fig. 1.2), preventing direct comparison to the type series of *T. neglectus* and the holotype of *T. garbanii*. However, the discovery of specimens MOR 979 and NCSM 15728, which are indistinguishable from SDSM 7210, allow the morphology of SDSM 7210 to be indirectly compared to the holotype of *T. garbanii* and the type series of *T. neglectus*. The analysis in Figure 1.3B places this specimen within a monophyletic *Thescelosaurus* clade, supporting the synonymization *Bugenasaura* with *Thescelosaurus*.

The synonymization of *Bugenasaura* with *Thescelosaurus* results in a new taxonomic combination: *Thescelosaurus infernalis*. This raises the question of whether the holotype specimen (SDSM 7210) is sufficiently diagnostic or if this species should be considered a nomen dubium. Galton (1999) described two features of the premaxillae of SDSM 7210, which are damaged anteriorly, dorsally, posteriorly, and along much of the oral margin, that may distinguish this species from *T. neglectus*. Five alveoli are preserved on each side and extend to the anterior-most tip of the preserved portion of the premaxilla. Galton (1999) suggested that the close spacing of the anterior-most left and right alveoli (~ 5 mm) and their anterolateral orientation indicate this specimen only had five premaxillary teeth and may have lacked an anterior edentulous region. The only other specimen referred to *Thescelosaurus* that preserves a significant portion of the premaxillae is NCSM 15728. This specimen possesses elongate premaxillae that contain six alveoli and an anterior edentulous region that is approximately three tooth positions long. Computed Tomography (CT) scans of NCSM 15728 (CAB unpub. data) show that

the three anterior-most alveoli on each side arise within one millimeter of the premaxillary suture and extend anterolaterally from the midline. Therefore, the close spacing and orientation of the anterior-most alveoli in SDSM 7210 does not necessitate the presence of only five premaxillary teeth or the lack of an anterior edentulous region in this specimen; instead, it may indicate a significant loss of bone from the lateral and anterior portions of this element due to postmortem damage. No other unique features are recognized in this specimen. As a result, *T. infernalis* is considered a nomen dubium.

RSM P.1225.1 consists of a partial skull including a palpebral, frontals, parietal, a complete left squamosal (Fig. 1.7), a partial right squamosal, postorbital, pterygoid, dentary, and partial braincase as well as portions of the postcranial skeleton (Fig. 1.2) collected from the Frenchman Formation of Saskatchewan (Galton, 1989:figs. 3g–l, 4k, pl. 4 [figs. 1–8]; Galton, 1997:figs. 3a–e, 4, pl. 1–2). The majority of the anterior ramus of the postorbital is not preserved, but enough of the orbital margin is present to determine a lack of irregular bosses seen in *T. neglectus*. The postorbital-squamosal suture on the squamosal is more anteriorly positioned than in *T. neglectus* (Fig. 1.7A). On the floor of this suture several anteroposteriorly-oriented ridges and grooves are present (Fig. 1.7A), unlike in *T. neglectus* where the floor of this facet is smooth. A portion of the posterior edge of this suture is raised into a narrow flange that would have slightly overlapped the midsection of the articulated postorbital (Fig. 1.7A). In dorsal view (Fig. 1.7A), the posterior edge of the squamosal is transversely wide and broadly convex, as opposed to the deep, dorsomedially directed concavity present in *T. neglectus*. In lateral view (Fig. 1.7B), the posterodorsal corner of the squamosal is broadly rounded as

opposed to the angular condition observed in *T. neglectus* (Fig. 1.5B). This specimen differs from *Thescelosaurus garbanii* in that the calcaneum participates in the midtarsal joint.

Specimen RSM P.1225.1 appears to be distinctly different from *T. neglectus* (based on the squamosal and postorbital) and *T. garbanii* (based on the midtarsal joint). Despite these differences, we feel that erecting a new species for receipt of this specimen would be premature until the postcranial anatomy of this specimen is compared in more detail to *T. neglectus* and other specimens here referred to *Thescelosaurus*, in order to determine if additional differences exist. Also, this specimen displays some similarities to CMN 8537 (e.g., shape of the frontal), the holotype of *Thescelosaurus edmontonensis* (currently referred to *Thescelosaurus* incertae sedis), that may unite these two specimens as a single species. If this is the case, then *T. edmontonensis* would have taxonomic priority over a newer species based on RSM P.1225.1. Thus, until the anatomy of this specimen is examined in more detail and its relationship to CMN 8537 is clarified, this specimen should remain unnamed.

LACM 33543 consists of a partial skull including frontals, parietal, squamosal, partial braincase, ectopterygoids, jugals, and incomplete mandibles as well as a partial postcranial skeleton (see Fig. 1.2) collected from the Hell Creek Formation of Montana (Morris, 1976:figs. 1–2, 4; Galton, 1989:fig. 4k; Galton, 1997:figs. 3f, 5–7). The presence of two right jugals indicates that this specimen comprises material from two differently sized individuals (Morris, 1976). The squamosal was not described by Morris (1976) and only figured in lateral view by Galton (1997). The tarsal region is lacking and the

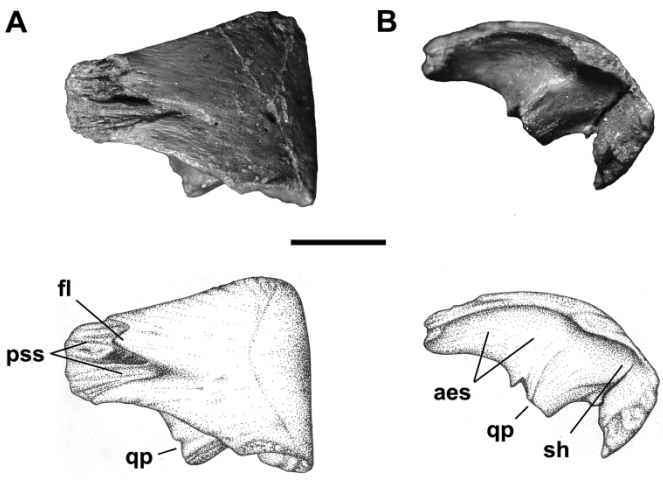

Figure 1.7: Squamosal from RSM P.1225.1. **A**. photograph (top) and illustration (bottom) in dorsal view; **B**. photograph (top) and illustration (bottom) in lateral view. Scale bar equals 1 cm. Modified from Boyd et al. (2009).

squamosal has not been examined by the authors, preventing comparison to the holotype material of *T. garbanii* and *T. neglectus* as well as RSM P.1225.1.

CMN 8537, the holotype of *Thescelosaurus edmontonensis*, consists of a partial skull including frontals, parietal, postorbital, partial braincase, a mandible containing only replacement teeth, and associated premaxillary, maxillary, and dentary teeth along with a relatively complete postcranial skeleton (see Fig. 1.2) collected from the Scollard Formation of Alberta, Canada (Sternberg, 1940:figs. 1–18; Galton, 1974b:figs. 1a–i, pl. 1 [figs. 3–6, 9–12]; Morris, 1976:fig. 3e; Galton, 1995:figs. 1b–c, 2b–d, 3; Galton, 1997:figs. 1–2). The calcaneum of CMN 8537 participates in the midtarsal joint, contrasting with the structure of the holotype specimen of *T. garbanii*. The squamosals are not preserved and the postorbital is fragmentary, preventing detailed comparison to *T. neglectus*.

MOR 979 consists of a nearly complete skull, mandibles, and postcranial skeleton collected from the Hell Creek Formation of Montana (Horner, 2001:unnumbered figure on p. 129). The postorbital differs from *T. neglectus* in lacking the irregular bosses extending into the orbit and from both *T. neglectus* and RSM P.1225.1 in lacking the anterior inflation into the orbit (Fig. 1.3B). The squamosals are damaged and incompletely prepared, preventing comparison to *T. neglectus* and RSM P.1225.1. The tarsal region of MOR 979 is intact and visible in lateral view on the right hind limb. The calcaneum is not excluded from the midtarsal joint, contrasting with the autapomorphic condition seen in *T. garbanii*. This specimen facilitated the indirect comparison of SDSM 7210 to the type series of *T. neglectus* and the holotype of *T. garbanii* as its cranial morphology is indistinguishable from that of SDSM 7210.

NCSM 15728, which preserves a complete skull, mandibles, and partial postcranial skeleton (see Fig. 1.2), was collected from the Hell Creek Formation of South Dakota (Fisher et al., 2000:figs. 1–2). This is the only specimen that preserves all five autapomorphies proposed here to diagnose a *Thescelosaurus* clade (Table 1.1). The postorbital differs from *T. neglectus* in lacking the irregular bosses along the orbital margin and the anterolaterally directed bend at the tip of the anterior ramus of the postorbital. The general structure of the postorbital-squamosal suture more closely resembles that of *T. neglectus* than RSM P.1225.1. A prominent lateral expansion on the posterior edge of the squamosal is present, but this area is damaged in both *T. neglectus* and RSM P.1225.1. A large, anteriorly projecting sheet of bone on the squamosal arises from the posterior edge of the postorbital-squamosal facet and overlaps the medial two-

thirds of the postorbital-squamosal suture, obscuring much of the medial and dorsal surfaces of the posterior ramus of the postorbital. This contrasts with the small, centrally placed flange of bone seen in *T. neglectus*. The structure of the squamosal distinguishes NCSM 15728 from both *T. neglectus* and RSM P.1225.1, but it lacks the necessary material to compare to *T. garbanii*. This specimen facilitated the indirect comparison of SDSM 7210 to the type series of *T. neglectus* as its cranial morphology is indistinguishable from that of SDSM 7210.

Parksosaurus **Sternberg, 1937**

Type Species

Thescelosaurus warreni Parks, 1926.

Distribution

Horseshoe Canyon Formation, Alberta (Maastrichtian [70.6–65.5 Ma]; Weishampel et al., 2004; Gradstein et al., 2005).

Diagnosis

As for type and only known species.

Parksosaurus warreni **(Parks, 1926)**

Thescelosaurus warreni Parks, 1926:figs. 1–18, pl. 1–2.

Parksosaurus warreni (Parks, 1926): Sternberg, 1937.

Holotype

ROM 804: partial skull and partial postcranial skeleton.

Locality

One half mile from the Red Deer River, on the east side, immediately south of the road to Rumsey ferry, 100 feet above the level of the water (Parks, 1926).

Distribution

Horseshoe Canyon Formation, Alberta (Maastrichtian [70.6–65.5 Ma]; Weishampel et al., 2004; Gradstein et al., 2005).

Referred Specimens

None.

Diagnosis

This species was diagnosed by Galton (1995) as follows: deep posterior process of premaxilla; extensive sutural contact between maxilla and nasal; small, oval antorbital fenestra; squamosal transversely wide; well-enameled surface of cheek teeth has numerous low, rounded ridges. Further preparation and study of ROM 804 is currently underway by other authors (D. Evans pers. comm.) that will provide more information about the anatomy of this species.

Comments

Parksosaurus warreni was originally described by Parks (1926) as *Thescelosaurus warreni*, but was removed from *Thescelosaurus* by Sternberg (1937). One prior analysis (Fig. 1.1E) and the analysis presented in Figure 3B place *Parksosaurus* and *Thescelosaurus* as sister taxa, but this conflicts with the placement of these taxa in three other analyses (Figs. 1.1B–D). The holotype and only known specimen of *P. warreni*, ROM 804, lacks all of the proposed autapomorphies of *Thescelosaurus* described above (Table 1.1; characters 126, 129, 131, 132, and 133) and the presence or absence of two other characters (Table 1.1; characters 125 and 127) cannot be determined due to the preservation of this specimen. Based upon this evidence and the placement of ROM 804 outside of a *Thescelosaurus* clade (Fig. 1.3B), the removal of this species from *Thescelosaurus* is supported.

DISCUSSION

Newly recognized material from the paratype specimen of *Thescelosaurus neglectus* (USNM 7758) facilitated a taxonomic revision of all specimens that preserve cranial material previously referred to *Thescelosaurus*. For the first time six specimens (not including the type series of *T. neglectus* and the hypodigm of *T. garbanii*) are confidently referred to this taxon based upon the presence of shared apomorphies. These results shape future directions for the evaluation of basal neornithischian taxa and provide insight into the diversity of latest Cretaceous dinosaurian ecosystems in North America.

They also raise questions about ontogenetic issues effecting further taxonomic revision of these and other basal neornithischian species.

This phylogenetic analysis is the first to recover a clade containing all known Cretaceous basal neornithischian taxa from North America, exclusive of all other taxa (Fig. 1.3B). The basal-most divergence within this clade is between two morphologically distinct subclades, one comprised of taxa proposed to be adapted to a fossorial mode of life (Varricchio et al., 2007) and the other that includes the relatively large-bodied *Thescelosaurus* clade. These two subclades are both morphologically and temporally distinct. The proposed fossorial *Orodromeus*, *Oryctodromeus*, and *Zephyrosaurus* have been recovered exclusively from sediments of Campanian age or older (70.6 Ma and older; Norman et al., 2004c; Weishampel et al., 2004; Gradstein et al., 2005), while definitive fossil material referred to *Parksosaurus* and *Thescelosaurus* based on shared apomorphies is currently known only from the Maastrichtian (65.5-70.6 Ma; Weishampel et al., 2004; Gradstein et al., 2005), a fact that has been largely overlooked in the published literature. This temporal segregation may signify an important environmental change during the latest Cretaceous, as proposed by Lehman (2001 and references therein), that favored the larger-bodied forms such as *Parksosaurus* and *Thescelosaurus* over potentially fossorial taxa. Alternatively, this apparent temporal disparity may simply be a byproduct of the incompleteness of the fossil record. While this issue deserves detailed consideration by future investigations, the answer is beyond the scope of this discussion.

The specimens here evaluated and found to be part of a *Thescelosaurus* clade represent a marked range in size (approximately 2.5 to 4 meters; Fig. 1.2). Given this size range, the possibility that these individuals represent different ontogenetic stages of development must be taken into consideration in any taxonomic evaluation of these specimens. Differences noted between the type series of *T. neglectus* and RSM P.1225.1, which may represent a new species of *Thescelosaurus*, are considered potentially taxonomically informative because the similar size of these two specimens reduces the probability that they represent two distinct ontogenetic stages of the same species. By contrast, differences noted between the specimens here referred to *Thescelosaurus* incertae sedis must be examined with caution, as these specimens exhibit a much more disparate variation in size. Until either the ontogenetic stage of each of these specimens is determined or osteological changes that correlate with ontogenetic stage of development are identified, morphological differences noted between these specimens (e.g., shape of posterior margin of the frontals) should only be considered of diagnostic value when observed in specimens of similar size.

This investigation is a crucial step in a thorough reevaluation of the anatomy, ontogeny, and systematic position of the taxon *Thescelosaurus*. These results emphasize: (1) the need to base specimen referrals on shared apomorphies; (2) that erecting species based on specimens that lack material directly comparable to the hypodigm or type series material of known species should be avoided; and (3) that caution must be exercised when comparing specimens of differing size due to the possible effects of ontogeny. The next step in this process will be the thorough anatomical description of RSM P.1225.1

and NCSM 15728 that will seek to: (1) clarify the taxonomic relationships of these specimens; and (2) identify postcranial autapomorphies of the taxon *Thescelosaurus* to supplement the cranial characters identified above.

CHAPTER 2.

Cranial Anatomy of the Large-Bodied Basal Neornithischian Taxon *Thescelosaurus neglectus* from the Late Maastrichtian of North America

INTRODUCTION

Thescelosaurus neglectus is a relatively large-bodied taxon (adult size > four meters according to Fisher et al., 2000 and C. Boyd. pers. obs.) known only from the Late Maastrichtian of North America (Norman et al., 2004c; Boyd et al., 2009). The holotype specimen of *T. neglectus* (USNM 7757) was collected in 1891 in then Converse County (now Niobrara County) Wyoming (Gilmore, 1913, 1915) and consists of a nearly complete skeleton missing the entire skull, the cervical vertebrae, and portions of the humeri, scapulae, and coracoids (Gilmore, 1915). USNM 7757 remained unexamined for twenty years before preparation work began on the specimen (Gilmore, 1913). The specimen was quickly recognized as representing a new species of ornithischian dinosaur, and a preliminary description was published by Gilmore in 1913 based on the holotype and a paratype specimen (USNM 7758), consisting of a fragmentary postcranial skeleton, from Converse County (now Niobrara County), Wyoming that was already within the collections of the United States National Museum. A full description of *T. neglectus* was published by Gilmore in 1915 and although the anatomy of nearly the entire postcranial skeleton was described, no portion of the skull was known.

Subsequently, additional specimens were referred to the taxon *Thescelosaurus* from the Frenchman (Galton, 1989), Hell Creek (Morris, 1976; Fisher, 2000), Horseshoe Canyon (Parks, 1926), and Scollard (Sternberg, 1937, 1940) formations of North America. However, the most compete specimens are either undescribed museum specimens (e.g., MOR 979; NCSM 15728) or remain in private collections. In total, four

species were referred to the taxon *Thescelosaurus* at one time or another: the name bearing species *Thescelosaurus neglectus* (Gilmore, 1913); *Thescelosaurus warreni* (Parks, 1926); *Thescelosaurus edmontonensis* (Sternberg, 1940); and, *Thescelosaurus garbanii* (Morris, 1976). A fifth contemporaneous species was placed in its own taxon: *Bugenasaura infernalis* (Galton, 1995). However, the interrelationships, taxonomic validity, and systematic placement of these species remained poorly understood owing largely to a poor understanding of the cranial anatomy of *Thescelosaurus* in general, a lack of recognized postcranial apomorphies, and the fact that the best preserved specimens referred to the taxon remained undescribed.

As a result of these alphataxonomic issues, the broader systematic position of the taxon *Thescelosaurus* within Ornithischia remain uncertain. The taxon was originally tentatively referred to the Camptosauridae within Ornithopoda based on a preliminary examination of the anatomy of the type series (Gilmore, 1913), but was soon after referred to the Hypsilophodontidae (Gilmore, 1915). This referral was upheld by most subsequent authors for more than sixty years (e.g., Parks, 1926; Swinton, 1936; Janensch, 1955; Romer, 1956, 1966; Thulborn, 1970, 1972), with a few notable exceptions. Sternberg (1940) placed *Thescelosaurus* in its own clade within Hypsilophodontidae, which he named Thescelosaurinae (=Thescelosauridae of Sternberg [1937]), a referral that was followed by some authors (e.g., Kuhn, 1966; Morris, 1976). Galton (1971a, b, 1972, 1973, 1974b) argued against the placement of *Thescelosaurus* within Thescelosaurinae and even Hypsilophodontidae, instead referring the taxon to Iguanodontidae. Galton (1995, 1997, and 1999) later reassessed this referral and instead

assigned *Thescelosaurus* to the Hypsilophodontidae. Despite these taxonomic disagreements, the placement of *Thescelosaurus* within Ornithopoda was uncontested by all these authors.

Inclusion of *Thescelosaurus* in phylogenetic analyses of ornithischian relationships brought into question the monophyly of Hypsilophodontidae and the placement of *Thescelosaurus* within Ornithopoda. Aside from a single analysis (i.e., Butler, 2005), a monophyletic Hypsilophodontidae has not been recovered in a strict consensus cladogram generated using a single data set designed to analyze basal ornithischian relationships since the analysis by Weishampel and Heinrich (1992). Several analyses that included *Thescelosaurus* did not include marginocephalian taxa, making it impossible to assess if *Thescelosaurus* is placed within, or basal, to Ornithopoda (e.g., Weishampel and Heinrich, 1992; Scheetz, 1999; Varricchio et al., 2007; Boyd et al., 2009). In the strict consensus trees published by Butler (2005), Spencer (2007), and Butler et al. (2008), *Thescelosaurus* is in an unresolved position that precludes its definitive referral to Ornithopoda. Another analysis (Buchholz, 2002) did not calculate the strict consensus tree of the recovered set of ten most parsimonious trees, nor did they publish the dataset used in the analysis, making it impossible to determine if all of the character data support placing *Thescelosaurus* within Ornithopoda as shown in the published tree. Finally, Weishampel et al. (2003) set their supraspecific terminal taxon Marginocephalia as an outgroup, making their unambiguous recovery of *Thescelosaurus* within Ornithopoda a certainty. Thus, in no previous cladistic analysis of ornithischian relationships was *Thescelosaurus* definitively recovered within

Ornithopoda (sensu Butler et al., 2008a) unless such a placement was part of the a priori assumptions.

In an effort to improve our understanding of the anatomy, taxonomic diversity, and systematic relationships of the taxon *Thescelosaurus*, a multi-step research plan was undertaken. The first step of that research plan was a reappraisal of all specimens referred to *Thescelosaurus* to assess the validity of previously described species and the taxonomic relationships of additional specimens (Boyd et al., 2009). Reexamination of the paratype specimen during the course of that study resulted in the recognition of three partial cranial bones, the left frontal, postorbital, and squamosal (Boyd et al., 2009), that provided important insights into the anatomy and relationships of *T. neglectus*. In the end, the study by Boyd et al. (2009) resulted in the synonymization of the taxon *Bugenasaura* with *Thescelosaurus*, supported the prior removal by Sternberg (1937, 1940) of *T. warreni* into a new taxon (*Parksosaurus*), and recognized *T. neglectus* (the name bearing species), *T. garbanii*, and an undescribed species from the Frenchman Formation of Saskatchewan, Canada (based on RSM P1225.1) as three diagnosably distinct species. The second step of the research plan was the description of the new species represented by RSM P.1225.1: *Thescelosaurus assiniboiensis* (Brown et al., 2011).

The third step in the research plan, and the focus of this study, is the description of the cranial anatomy of *Thescelosaurus neglectus* based upon a previously undescribed specimen, NCSM 15728. That specimen was collected in 1999 from the Hell Creek Formation in Harding County, South Dakota. The specimen includes much of the axial skeleton, part of the appendicular skeleton (largely from the right side), and a complete,

three-dimensionally preserved skull (Fig. 2.1). Despite the excellent preservation of the skeleton and the poor understanding of the cranial anatomy of *Thescelosaurus*, prior research on NCSM 15728 focused on the possible preservation of soft tissue structures in the specimen (Fisher et al., 2000; Rowe et al., 2001; Russell et al., 2001; Cleland et al., 2011) and the histology, morphology, and osteogenesis of de novo ossifications associated with the anterior dorsal ribs in the specimen (Boyd et al., 2011b). The specimen was originally referred to *Thescelosaurus neglectus* by Fisher et al. (2000) based on general similarity. Reassessment of the anatomy of all species and specimens previously referred to *Thescelosaurus* found that the anatomy of NCSM 15728 was consistent with *T. neglectus* and distinct from RSM P.1225.1 (now the holotype of *T. assiniboiensis*), but because it could not be sufficiently compared to the holotype of *T. garbanii* owing to the preservation of non-overlapping elements in the type material, NCSM 15728 was conservatively referred to *Thescelosaurus* incertae sedis until such comparisons could be made (Boyd et al., 2009).

Subsequent examination of additional specimens (outlined below) allows for the confident referral of this specimen to *T. neglectus* and differentiation from *T. garbanii*. The excellent preservation of the skull of NCSM 15728 not only allows the cranial anatomy of *T. neglectus* to be fully described for the first time, but it also provides insights into portions of the cranial anatomy of basal ornithischians that previously were unknown or poorly understood. Here, I present a detailed anatomical description and comparative discussion of the cranial anatomy of *T. neglectus*. The data collected during this study will be crucial for gaining a clearer understanding of the systematic

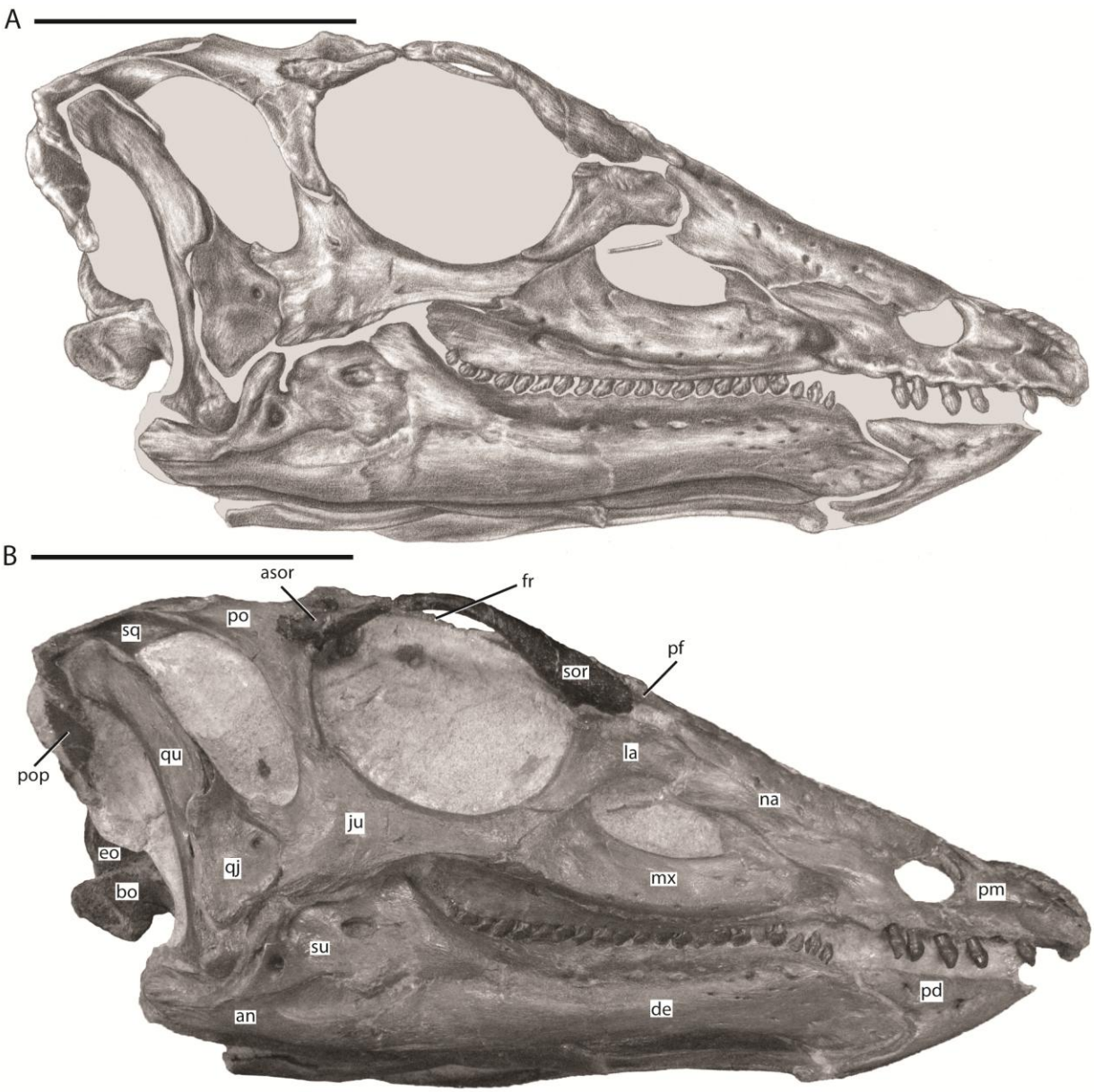

Figure 2.1: Skull of NCSM 15728 in right lateral view. **A**. Illustration of right side of skull. **B**. Photograph of right side of skull. In **A**, grey regions indicate the presence of matrix on the specimen. Scale bars equal 10 cm. See Appendix 2 for anatomical abbreviations.

relationships not only of *Thescelosaurus*, but for basal ornithischians more generally.

MATERIALS AND METHODS

The anatomy of NCSM 15728 was studied using a combination of methodologies that provided maximum insight into the cranial morphology of *Thescelosaurus neglectus*. Extensive preparation work was conducted on the skull of NCSM 15728 under the direction and with the assistance of Dr. Paul Brinkman (NCSM). Preparation focused on removing matrix from the dorsal surface of the parietal, from inside the supratemporal fenestrae, the entire posterior surface of the skull, within the left orbit and antorbital fenestra, within the nares, ventrally between the lower jaws, and between the oral margins of the premaxillae and predentary. The left quadratojugal, the posterior three-quarters of the jugal, and the left quadrate (not including the proximal head) were removed, exposing the lateral surfaces of the posterior palatal elements and the braincase (Fig. 2.2). The anatomical data gleaned from personal observations of the exposed surfaces of NCSM 15728 were supplemented by computed tomography (CT) scans of the skull, not including the elements removed from the left side of the skull. The CT scans were conducted at the College of Veterinary Medicine at North Carolina State University using a Siemens Somatom Sensation 16, with a slice thickness of 0.75 mm and a spacing of 0.0 mm (Cleland et al., 2011). Digital models of some of the bones of the cranium that could not be described adequately via visual examination of the specimen were constructed using the program VGSudio Max in the digital morphology lab at The

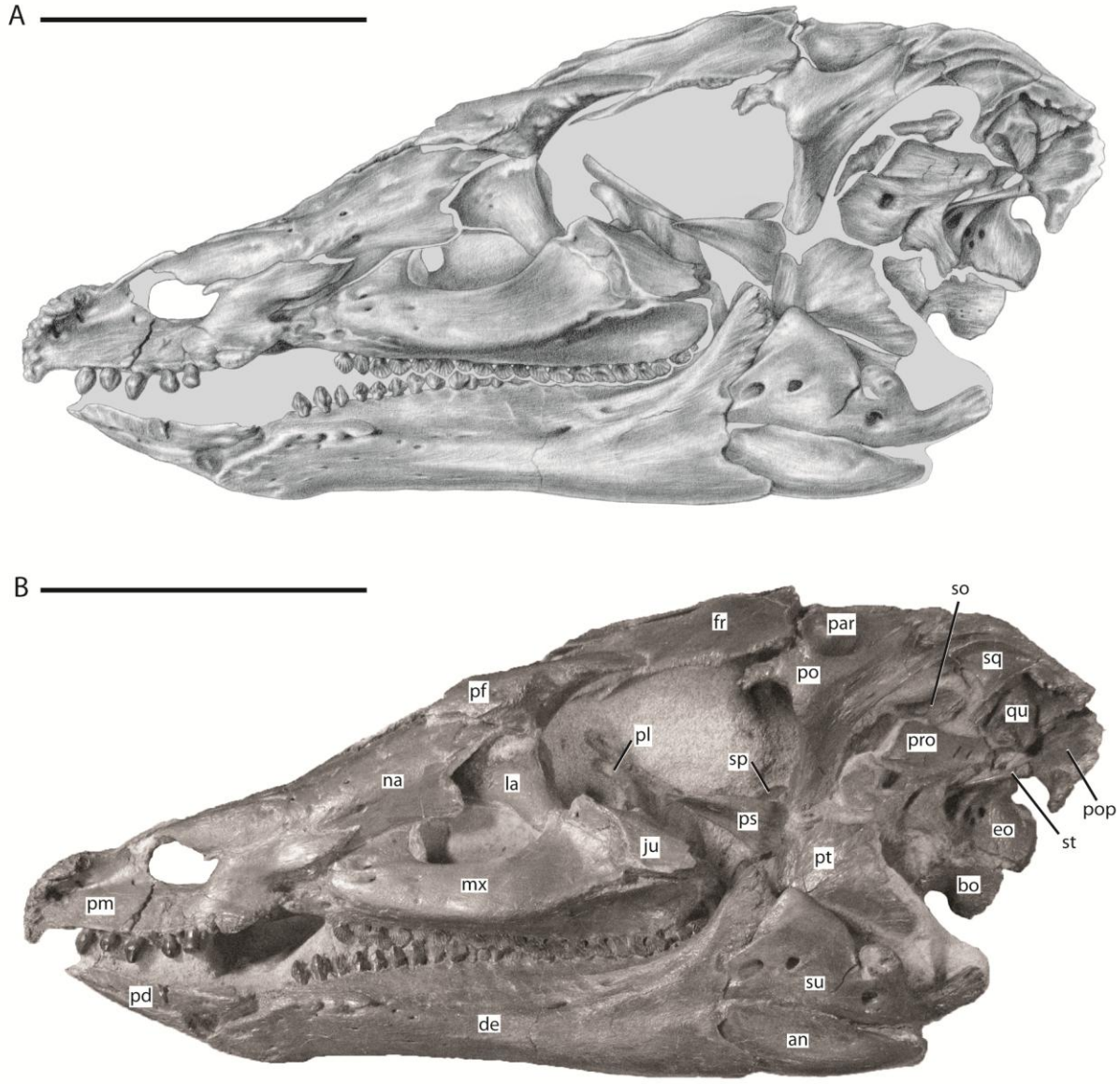

Figure 2.2: Skull of NCSM 15728 in left lateral view. **A**. Illustration of left side of skull. **B**. Photograph of left side of skull. In **A**, grey regions indicate the presence of matrix on the specimen. Scale bars equal 10 cm. See Appendix 2 for anatomical abbreviations.

University of Texas at Austin. These CT data provided insight into areas of the skull that cannot be observed directly owing to the presence of matrix on the specimen, and the manner in which the specimen was mounted for display. The combination of these methods ensures that the elucidation of the anatomy of this specimen is only limited by the preservation of the specimen.

SYSTEMATIC PALEONTOLOGY

DINOSAURIA Owen, 1842

ORNITHISCHIA Seeley, 1887

NEORNITHISCHIA Cooper, 1985 (sensu Butler et al., 2008a)

Thescelosaurus Gilmore, 1913

Bugenasaura Galton, 1995:308

Name Bearing Species:

Thescelosaurus neglectus Gilmore, 1913

Other Included Species:

Thescelosaurus garbanii Morris, 1976

Thescelosaurus assiniboiensis Brown, Boyd, and Russell, 2011

Distribution:

Frenchman Formation, Saskatchewan; Hell Creek Formation, Montana, North Dakota, and South Dakota; Lance Formation, Wyoming; Scollard Formation, Alberta (all Maastrichtian age [70.6–65.5 Ma]; Weishampel et al., 2004; Gradstein et al., 2005).

Diagnosis:

This taxon differs from all other basal ornithischian dinosaurs as follows (Boyd et al., 2009; Brown et al., 2011): 1) Frontals wider at midorbital level than across posterior end; 2) dorsolaterally directed process on surangular; 3) prominent, horizontal ridge on maxilla with at least the posterior portion covered by a series of coarse, rounded, obliquely inclined ridges; 4) depressed posterior half of ventral edge of jugal covered laterally with obliquely inclined ridges; 5) foramen in dorsal surface of prefrontal that opens into the orbit positioned dorsomedial to the articulation surface for palpebral; and 6) shafts of anterior dorsal ribs transversely compressed and laterally concave, with the posterior margin of the distal half characterized by a distinct rugose texture and flattened surface, possibly for articulation with the intercostal plates. Two additional characters are currently uniquely known in *Thescelosaurus*, but are unable to be evaluated in its recovered sister taxon *Parksosaurus* (Boyd et al., 2009): 1) dorsal edge of opisthotic indented by deep, 'Y-shaped' excavation in dorsal view; and, 2) palpebral dorsoventrally flattened and rugose along the medial and distal edges. The latter character also is present in an otherwise distinct basal neornithischian specimen from China housed at IVPP (C. Boyd, pers. obs.) whose relationships remain unknown.

Two additional characters are optimized as local apomorphies of *Thescelosaurus*, but occur convergently within major neornithischian subclades: 1) angle between ventral margin of braincase (occipital condyle, basal tubera, and basipterygoid processes) and a line drawn through center of the trigeminal foramen and posterodorsal hypoglossal foramen less than fifteen degrees; and, 2) femur longer than tibia. The former also is

found in some iguanodontians (e.g., *Tenontosaurus*: Norman, 2004b) and the latter occurs in some iguanodontians and marginocephalians (Maryańska et al., 2004; Norman, 2004b).

***Thescelosaurus neglectus* Gilmore, 1913**

Holotype:

USNM 7757: nearly complete postcranial skeleton.

Paratype:

USNM 7758: fragmentary skeleton including parts of skull.

Type Series Localities:

USNM 7757: Collected by J. B. Hatcher and W. H. Utterback in 1891 from Doegie Creek, Niobrara County, Wyoming. USNM 7758: Collected by O. A. Peterson in 1889 from Lance Creek, Niobrara County, Wyoming.

Distribution:

Lance Formation of Wyoming and Hell Creek Formation of South Dakota (both Maastrichtian age [70.6–65.5 Ma]; Weishampel et al., 2004; Gradstein et al., 2005).

Referred Specimens:

NCSM 15728 (Figs 2.1-2.19): Complete skull (lacking only part of the left quadratojugal), ceratobranchials, articulated vertebral column complete from the atlas to the thirteenth caudal vertebra, cervical, dorsal, and sternal ribs, seven right intercostal plates, nine chevrons, right fused scapulacoracoid, left and right sternal plates, right humerus, right ulna, right radius, right manus consisting of five carpals, all five

metacarpals, and seven phalanges, right ilium, left and right pubes, left and right ischia, right femur, proximal portion of the right tibia, proximal half of the right fibula.

Basis of Referral:

NCSM 15728 displays all of the synapomorphies of *Thescelosaurus* outlined above. The morphology of the frontal, postorbital, and squamosal in this specimen match that reported for the paratype of *Thescelosaurus neglectus* (Boyd et al., 2009), except that NCSM 15728 lacks the extreme rugosities present along the orbital margin of the postorbital in the paratype. The morphology of these elements is significantly different in *Thescelosaurus assiniboiensis* (see Brown et al. [2011] and description below for details). Additionally, NCSM 15728 lacks a supraoccipital foramen, which diagnoses *Thescelosaurus assiniboiensis* (Brown et al., 2011). NCSM 15728 cannot be directly compared to the fragmentary holotype of *Thescelosaurus garbanii* because NCSM 15728 does not preserve any of the tarsal morphologies that are diagnostic of *T. garbanii*; however, NCSM 15728 can be compared to *T. garbanii* via the use of an intermediary specimen. An undescribed, nearly complete specimen of *Thescelosaurus* at the Timber Lake and Area Museum (Timber Lake, South Dakota) closely matches the morphology of the type series of *T. neglectus* (Gilmore, 1915) and NCSM 15728. The Timber Lake specimen does not possess a supraoccipital foramen (distinguishing it from *T. assiniboiensis*) and possesses a calcaneum that is not excluded from the midtarsal joint. These differences distinguish the Timber Lake specimen and, indirectly, NCSM 15728 from *T. garbanii* (C. Boyd, pers. obs.). These morphological observations justify referring NCSM 15728 to *T. neglectus*.

Emended Diagnosis of *Thescelosaurus neglectus*:

Thescelosaurus neglectus differs from all other basal ornithischian taxa as follows: 1) presence of a foramen in the ventral surface of the basioccipital anterior to the midline keel; and, 2) presence of a groove on the medial surface of the prootic extending from the anterodorsal corner of the trigeminal foramen anteriorly to a foramen that passes between the prootic and the laterosphenoid. This species differs from *Thescelosaurus garbanii* as follows: 1) calcaneum not excluded from the midtarsal joint by the astragalus. This species differs from *Thescelosaurus assiniboiensis* as follows: 1) posterior surface of the squamosal concave dorsoventrally and mediolaterally (convex in *T. assiniboiensis*); 2) lack of anteroposteriorly oriented ridges on the articular surface for the postorbital on the squamosal (present in *T. assiniboiensis*); 3) presence of a groove on the pterygoid extending from the lateral ridge on the quadrate process onto the mandibular process (absent in *T. assiniboiensis*); 4) absence of a foramen extending from the roof of the braincase through to the dorsal surface of the supraoccipital (autapomorphy of *T. assiniboiensis*; Brown et al., 2011); 5) less than thirty percent of the dorsal surface of the basioccipital contributes to the ventral margin of the foramen magnum (at least one-third in *T. assiniboiensis*); 6) anterior end of basioccipital 'V-shaped' and inserts into the posterior end of the basisphenoid (anterior surface of basioccipital flattened in *T. assiniboiensis*); and, 7) trigeminal foramen completely enclosed within the prootic (spans between prootic and laterosphenoid in *T. assiniboiensis*).

Several other morphological characters noted on the cranium of NCSM 15728 are apomorphic with respect to all other basal ornithischian taxa. However, owing to the lack

Figure 2.3: Skull of NCSM 15728 in dorsal view. **A**. Illustration of dorsal surface of skull. **B**. Photograph of dorsal surface of skull. In **A**, grey regions indicate the presence of matrix on the specimen. Scale bars equal 10 cm. See Appendix 2 for anatomical abbreviations.

of comparative data for *T. assiniboiensis* and *T. garbanii*, it cannot be determined if these characters represent autapomorphies of *T. neglectus*, synapomorphies of the taxon *Thescelosaurus*, or synapomorphies of a subset of the species referred to *Thescelosaurus*. These characters are: 1) lack of contact between the ventral process of the lacrimal and the anterodorsal process of the palatine; 2) presence of numerous foramina and associated grooves on the dorsal and lateral surface of the nasal; 3) presence of a small, anterodorsal projection off the anterodorsal corner of the posterolateral process of the premaxilla; and,

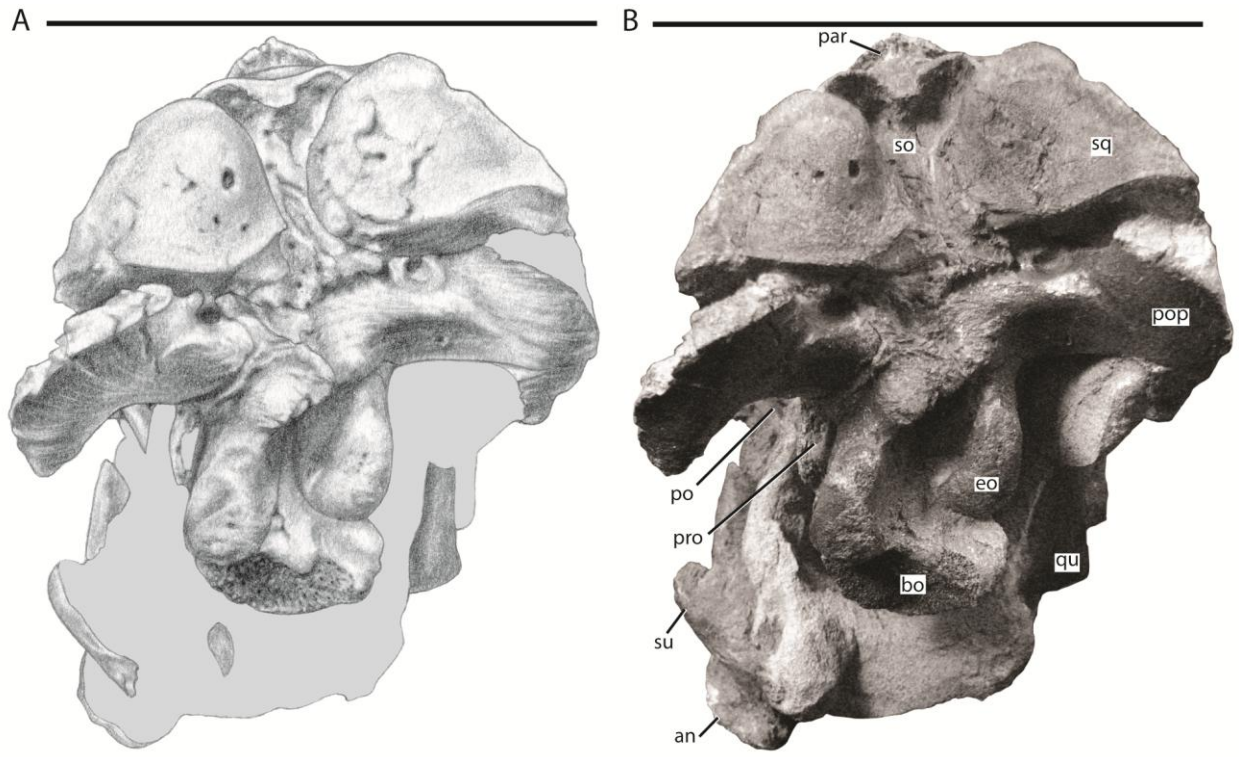

Figure 2.4: Skull of NCSM 15728 in posterior view. **A**. Illustration of posterior side of skull. **B**. Photograph of posterior side of skull. In **A**, grey regions indicate the presence of matrix on the specimen. Scale bars equal 10 cm. See Appendix 2 for anatomical abbreviations

4) presence of a groove in the anterior margin of the quadratojugal into which the posteroventral projection of the jugal inserted, causing the anteroventral corner of the quadratojugal to overlap the lateral surface of the posteroventral corner of the jugal.

DESCRIPTION OF THE SKULL OF NCSM 15728

The skull of NCSM15728 is well preserved, with portions of every cranial bone represented. Only one bone, the left quadratojugal, is highly fragmentary (Figs. 2.1 through 2.4). The bones on the right side of the skull remain in their original positions, and the right lower jaw remains in close contact (Fig. 2.1). Alternatively, many of the

bones on the left side of the skull are slightly displaced, including the left frontal, lacrimal, prefrontal, postorbital, squamosal, and jugal (Figs. 2.2 and 2.3) in addition to the quadrate, which was removed. The posterior bones of the left lower jaw also are slightly displaced from their original positions. The bones of the palate are slightly displaced, but remain in relative close proximity to their presumed original positions. Many of the bones of the braincase are shifted anteriorly and medially from their original positions (Fig. 2.4), preventing the construction of an accurate endocast, though the endocast and inner ear of *Thescelosaurus* was described previously in detail by Galton (1989), and the morphology of this specimen differs only in minor details from that original description.

After my initial observations of the skull, the premaxillae were damaged in an apparent attempt to remove the skull from its display by a visitor. As a result, the figures presented herein and the CT scans obtained before the damage and current morphology of the skull differ slightly. Specifically, slight damage occurred to the anteroventral projection of the premaxillae and possibly to other portions of the anterior-most part of the premaxillae.

Cranium

Premaxilla

The anterior-most portions of the premaxillae are fused. Posterior to the anterior-most edentulous region, the open suture between the premaxillae can be traced on the CT scans throughout their length. The presence of at least partial fusion of the premaxillae is

reported in *Changchunsaurus*, *Oryctodromeus*, and *Zephyrosaurus* (Sues, 1980; Varricchio et al., 2007; Jin et al., 2010). The anterior end of the premaxilla is broadly rounded in lateral view (Fig. 2.5A). A prominent, posteroventrally concave, ventral projection is present along the midline of the anteroventral tip of the premaxilla. The anterodorsal margin of the premaxilla bears a mediolaterally expanded shelf that increases in transverse breadth posteriorly (Figs. 2.5A and B: ads). The anterodorsal shelf ends just anterior to the contact with the nasals, and the posterolateral corners of the shelf formed prominent projections (damaged on left side), giving the anterodorsal shelf a 'V-shaped' outline in dorsal view (Fig. 2.5B). The dorsal surface of the shelf and the anterior tip of the premaxillae are rugose and covered with foramina (Fig. 2.5B), as seen in the basal ornithischian *Lesothosaurus* (Sereno, 1991) and the basal neornithischians *Changchunsaurus*, *Hypsilophodon*, *Jeholosaurus*, *Oryctodromeus*, and *Zephyrosaurus* (Galton, 1974a; Sues, 1980; Varricchio et al., 2007; Barrett and Han, 2009; Jin et al., 2010). This rugose region likely supported a rhamphotheca (Sereno, 1991).

The posterodorsal processes of the premaxillae arise posterior to the anterodorsal shelf, dividing the anterior processes of the nasal and overlapping their dorsal surfaces (Fig. 2.5B: pdp). The posterodorsal processes extend along the dorsal surface of the premaxillae farther than in any other basal neornithischian taxon (Norman et al., 2004c), eventually terminating level with the posterior-most extent of the oral margin of the premaxillae (Fig. 2.5B). The oral margin of the premaxilla is longer than the oral margin of the predentary (Figs. 2.1 and 2.2), as seen in the heterodontosaurid *Heterodontosaurus* (Crompton and Charig, 1962), and the basal neornithischian *Haya* (Makovicky et al.,

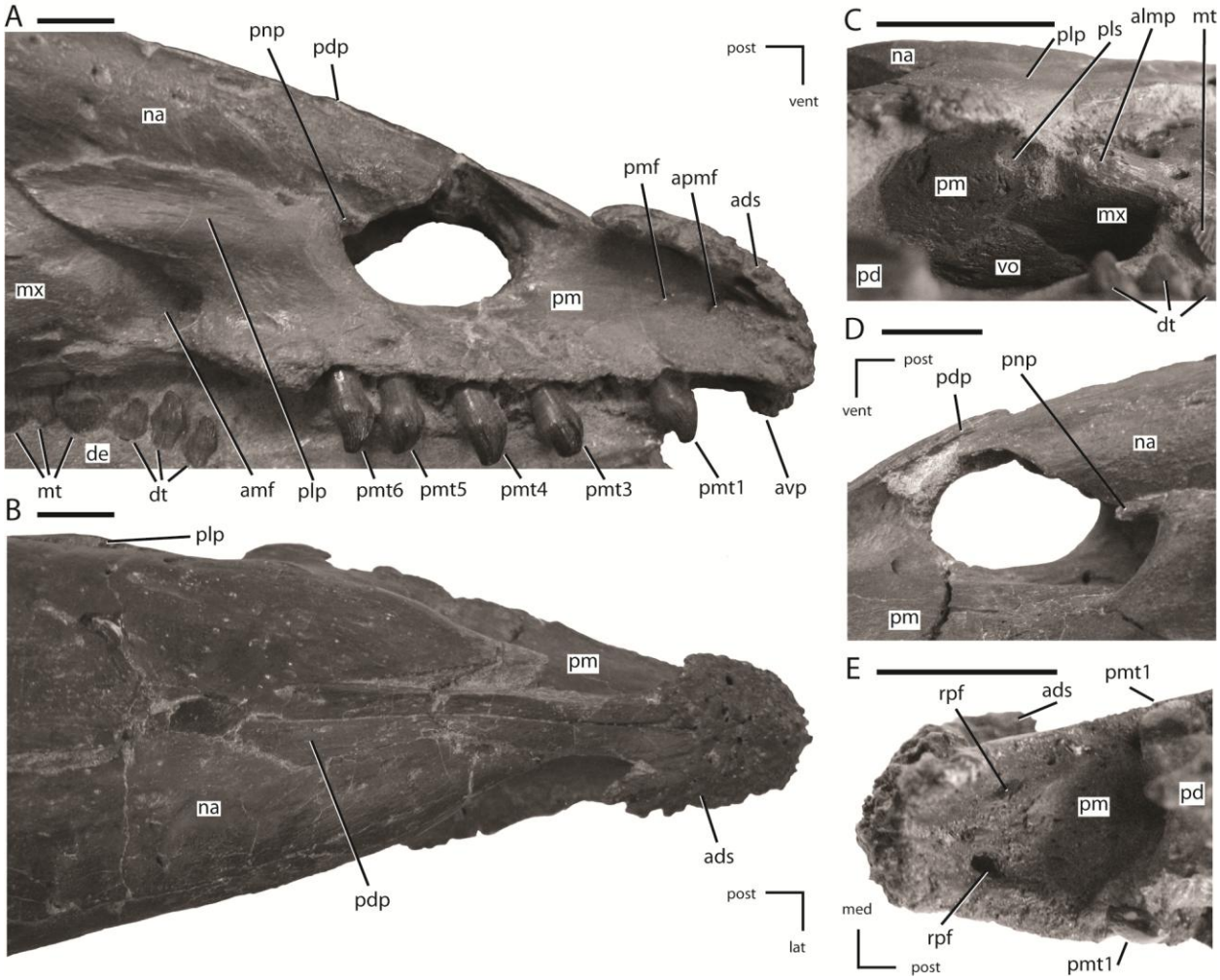

Figure 2.5: Premaxillae of NCSM 15728. **A**. Right premaxilla in lateral view. **B**. Premaxillae in dorsal view. **C**. Posterior portion of the left premaxillary palate in ventrolateral view. **D**. External nares in left lateral view. **E**. Anterior portion of the premaxillary palate. In **A**, **B**, **D**, and **E** the directional arrows indicate the orientation of the specimen. In **C**, anterior is to the left. Scale bars equal 1 cm. See Appendix 2 for anatomical abbreviations.

2011). The lateral surface of the oral margin of the premaxilla is everted (Fig. 2.5B) as in the basal neornithischians *Agilisaurus*, *Changchunsaurus*, *Orodromeus*, *Oryctodromeus*, and *Talenkauen* (Peng, 1992; Scheetz, 1999; Novas et al., 2004; Varricchio et al., 2007; Jin et al., 2010) and the basal iguanodontians *Dryosaurus*, *Dysalotosaurus*, and *Tenontosaurus* (Norman, 2004b), which results in the premaxillary tooth row being

positioned lateral to the maxillary tooth row. The oral margin of the premaxilla is smooth, in contrast to the denticulate oral margin present in basal ankylopollexians (Norman, 2004b), and is situated level with the maxillary tooth row (Fig. 2.5A) and not ventrally deflected as seen in heterodontosaurids (Butler, 2005), the basal neornithischians *Hypsilophodon* and *Orodromeus* (Galton, 1974a; Scheetz, 1999), and the basal iguanodontian *Zalmoxes* (Weishampel et al., 2003). There is a short edentulous region anterior to the premaxillary teeth (Fig. 2.5A), as in all ornithischians (Butler et al., 2008a), and a diastema is present between the premaxillary and maxillary tooth rows (Fig. 2.5A), as in all neornithischian taxa except *Agilisaurus* (Peng, 1992; Barrett et al., 2005). Six premaxillary teeth are present in each premaxilla, a condition also present in the basal ornithischian *Lesothosaurus* (Sereno, 1991), the basal thyreophoran *Scutellosaurus* (Colbert, 1981), and the basal neornithischians *Hypsilophodon* and *Jeholosaurus* (Galton, 1974a; Barrett and Han, 2009; P. Galton, pers. comm. 2008). In the lateral surface of the premaxilla, ventral to the rugose anterodorsal shelf, a premaxillary foramen (sensu Sereno, 1991) and a rostral premaxillary foramen (sensu Sereno, 1991) are present, with the former situated directly posterior to the latter (Fig. 2.5A: pmf and apmf, respectively). Premaxillary foramina also are present in the basal ornithischian *Lesothosaurus* (Sereno, 1991), the basal neornithischians *Changchunsaurus*, *Haya*, *Hypsilophodon*, *Jeholosaurus*, *Oryctodromeus*, and *Zephyrosaurus* (Galton, 1974a; Sues, 1980; Varricchio et al., 2007; Barrett and Han, 2009; Jin et al., 2010; Makovicky et al., 2011), and the basal iguanodontian *Zalmoxes* (Weishampel et al., 2003). The surface of the premaxilla ventral to the anterodorsal shelf

and anterior to the nares is dorsoventrally concave, though a distinct subnarial fossa is not present.

The posterolateral process arises just anterior to the posterior end of the premaxilla, and first angles posterodorsally before curving directly posteriorly, with its ventral margin roughly following the contact between the maxilla and the nasals (Fig. 2.5A). At the anterodorsal corner of the posterolateral process, a small, anterodorsal projection, the premaxillary narial process, is present. It wraps around the posterior edge of the external nares (Figs. 2.5A and D: pnp). That feature is not present in any other basal neornithischian taxon and is an apomorphic trait of either *Thescelosaurus neglectus*, or of the taxon *Thescelosaurus*. The posterolateral process of the premaxilla does not extend far enough posteriorly to contact the lacrimal (Fig. 2.1), unlike in the heterodontosaurid *Heterodontosaurus* (Norman et al., 2004c), the basal neornithischian *Jeholosaurus* (Barrett and Han, 2009), the basal ceratopians *Liaoceratops* and *Yinlong* (You and Dodson, 2003; Xu et al., 2006), and most basal iguanodontians (e.g., *Tenontosaurus*; Norman, 2004b). The posterolateral process is not as dorsoventrally tall as in *Parksosaurus* (Galton, 1973).

The palatal surface of the premaxillae is concave anteriorly (Fig. 2.5E). At the level of the second tooth position a ridge is present along the midline of the premaxillae, extending to the posterior end of the premaxillae. Based on examination of the CT data and the presence of slight transverse crushing in this specimen, the ridge is likely a taphonomic feature. The majority of the palatal surface was flat. A pair of rostral palatal foramina (sensu Sereno, 1991) are present anterior to the first premaxillary tooth (Fig.

2.5E: rpf). Similar foramina are present in the basal ornithischian *Lesothosaurus* (Sereno, 1991), the basal neornithischians *Changchunsaurus* and *Zephyrosaurus* (Sues, 1980; Jin et al., 2010), and some marginocephalians (e.g., *Archaeoceratops*; You and Dodson, 2003). The rostral palatal foramina connect to the rostral premaxillary foramina, as suggested previously by several authors (e.g., Sereno, 1991; Jin et al., 2010). The slit-like opening present along the midline of the palatal surface seen in *Changchunsaurus* is absent in NCSM 15728 (Jin et al., 2010). In the ventrolateral corner of the posterior end of the premaxilla a concavity is present. The concavity receives the short anterolateral process of the maxilla (Fig. 2.5C:pls), as in *Changchunsaurus*, *Haya*, *Orodromeus*, *Oryctodromeus*, and *Zephyrosaurus* (Sues, 1980; Scheetz, 1999; Varricchio et al., 2007; Jin et al., 2010; Makovicky et al., 2011). Posteromedially, the anterior processes of the maxillae meet along the midline and insert into the posterior end of the premaxilla dorsal to the palatal shelf. The anterior end of the vomer is positioned ventral to the anterior-most end of the maxilla and its anterior tip inserts into a shallow concavity in the posteromedial end of the premaxillae ventral to the paired maxillae (Fig. 2.5C).

Nasal

The nasal is an anteroposteriorly long element that is strongly concave ventromedially, equal in length to the frontal, and thin throughout its length. The nasals meet along the midline, but transverse compression of the specimen caused the nasals to crush together slightly, obscuring the original morphology of their contact. There is no evidence of midline depression on the nasals (Fig. 2.3) as seen in the heterodontosaurid

Heterodontosaurus, the basal neornithischians *Agilisaurus*, *Changchunsaurus*, *Haya*, *Hexinlusaurus*, *Jeholosaurus*, and the basal ceratopsian *Yinlong* (Jin et al., 2010; Makovicky et al., 2011). The anterior end of the element was sharply pointed and its anterolateral margin formed the posterodorsal corner of the external nares (Figs. 2.1 and 2.2). The anterior tips of the nasals were separated by the posterodorsal processes of the premaxillae (Figs. 2.3 and 2.5B), which inserted between the nasals anteriorly and then transitioned to overlapping the nasals at their posterior ends. The nasals are also divided anteriorly by the posterodorsal processes of the premaxillae in *Hypsilophodon*, but this condition is absent in other basal neornithischian taxa (e.g., *Haya* and *Jeholosaurus*: Barrett and Han, 2009; Makovicky et al., 2011).

The lateral edge of the nasal is curved ventrally and overlapped the lacrimal and maxilla laterally (Figs. 2.1 and 2.2). The posterolateral corner of the nasal forms part of the dorsal margin of the antorbital fenestra (Figs. 2.1 and 2.2). The posterolateral process of the premaxilla overlapped the anterior half of the ventrolateral margin of the nasal, but this contact did not extend all the way to the lacrimal as in the heterodontosaurid *Heterodontosaurus* (Crompton and Charig, 1962), the basal neornithischian *Jeholosaurus* (Barrett and Han, 2009), and the basal ceratopsians *Liaoceratops* and *Yinlong* (Xu et al., 2002; 2006). The posterior ends of the nasal were separated by the anterior processes of the frontals and overlapped posterolaterally by the prefrontals. These contacts resulted in the exposure of only a small, tapering wedge of the posterior end of the nasal in dorsal view (Fig. 2.3). A series of foramina pierce the dorsal and lateral surfaces of the nasal in the area between the posterior-most extent of the posterodorsal processes of the

premaxillae and the anterior-most extent of the prefrontals (Figs. 2.1, 2.2, and 2.3). Shallow grooves extend from some of these foramina onto the surface of the nasal, and examination of the CT images shows that many of these foramina are interconnected and exit the medial surface of the nasal. Their positions and number vary on each side of the skull. In *Jeholosaurus*, a row of three foramina are present along the ventrolateral margin of the nasals (Barrett and Han, 2009). By contrast, a single foramen is present on the surface of the nasal in *Haya* (Makovicky et al., 2011). No foramina are reported on the nasal in *Hypsilophodon* (Galton, 1974a) and none are observed in the preserved portion of the nasal in the holotype of *Parksosaurus* (Galton, 1973, C. Boyd, pers. obs.).

Prefrontal

The prefrontal is a triradiate bone that forms the anterodorsal corner of the orbit and is exposed on the dorsal and lateral surfaces of the skull (Figs. 2.1 and 2.2). In lateral view the prefrontal is triangular, with the posterior portion dorsoventrally thicker than the anterior portion (Fig. 2.6C). A rugose boss is present on the lateral surface of the prefrontal at its dorsoventrally thickest point, immediately adjacent to the anterodorsal corner of the orbit (Fig. 2.6C: rso). This boss formed part of the articulation surface for the supraorbital along with an adjacent area on the lacrimal (Figs. 2.6A and C) as in other basal neornithischians (e.g., *Hypsilophodon*, *Parksosaurus*: Galton, 1973, 1974a). The orbital margin of the prefrontal transitions from broadly convex immediately posterior to the supraorbital boss to sharply pointed and slightly rugose posteriorly (Fig. 2.6C).

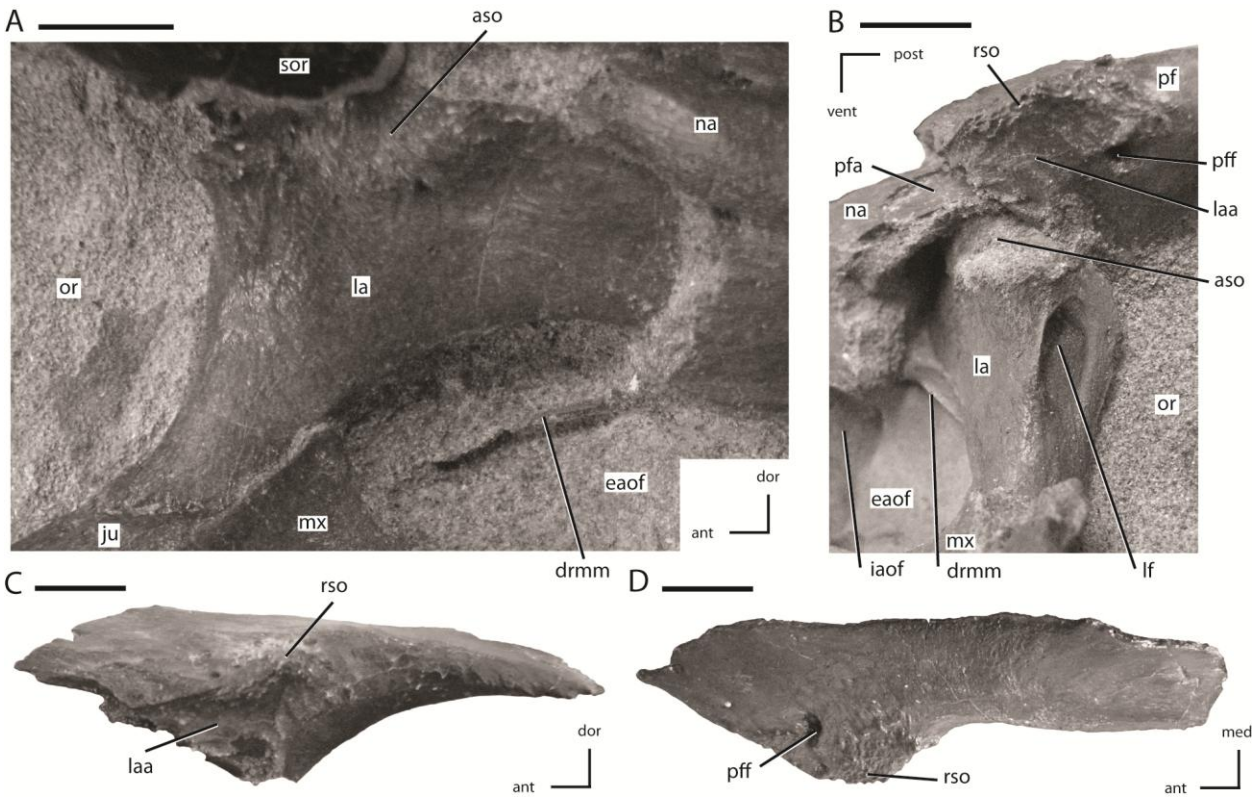

Figure 2.6: Lacrimal and prefrontal of NCSM 15728. **A**. Right lacrimal in lateral view. **B**. Left lacrimal in posterolateral view. **C**. Left prefrontal in lateral view (note: ventral process not shown). **D**. Left lacrimal in dorsal view. The directional arrows indicate the orientation of the specimen in each view. Scale bars equal 1 cm. See Appendix 2 for anatomical abbreviations.

The dorsal surface of the prefrontal is anteroposteriorly convex and is pierced by a foramen along the dorsomedial margin of the supraorbital boss (Fig. 2.6C), a condition that is unique to *Thescelosaurus* (Boyd et al., 2009). This foramen passes ventrolaterally through the prefrontal, exiting into anterodorsal corner of the orbit just ventral to the supraorbital boss. The anterior process of the prefrontal is dorsoventrally thin, ventromedially concave, and rests in a shallow fossa on the dorsal surface of the nasal. The pointed, triangular tip of this process is positioned dorsal to the lacrimal and is bordered anteriorly by the nasal, a condition seen in most basal ornithischians (Norman et

al., 2004a, 2004c), but not in *Parksosaurus* wherein the anterior tip inserts between the lacrimal and the dorsal process of the maxilla, nearly preventing the anterior process of the lacrimal from contacting the dorsal process of the maxilla (Galton, 1973; C. Boyd, pers. obs.). The posterior process of the prefrontal is dorsoventrally thicker than the anterior process (Fig. 2.6C). The posterior process wraps around the dorsolateral corner of the anterior end of the frontal while only overlapping the dorsal surface at its posterior-most extent. The ventral process of the prefrontal is not exposed on the exterior of the skull. It arises ventral and slightly posterior to the supraorbital boss and extends ventromedially. The distal end of the ventral process is flattened to slightly concave to fit against a facet on the dorsomedial edge of the lacrimal.

Lacrimal

The lacrimal forms much of the anterior margin of the orbit and the posterodorsal corner of the external antorbital fenestra (Figs. 2.1, 2.2, and 2.6A). It is composed of posteroventral and anterior processes oriented at an angle of approximately 100 degrees (Fig. 2.6A). The lateral surface of the posteroventral process is dorsoventrally concave and anteroposteriorly convex. The distal end of the posteroventral process is positioned posterior to the maxilla, and dorsal to the anterior tip of the jugal (Fig. 2.6A), a condition also seen in *Orodromeus* (Scheetz, 1999). Alternatively, in *Gasparinisaura* and *Jeholosaurus* the posteroventral tip of the lacrimal is situated anterior to the jugal and posterodorsal to the maxilla (Coria and Salgado, 1996; Barrett and Han, 2009) and in *Hypsilophodon* it is dorsal to both the jugal and the maxilla (Galton, 1974a). The anterior

process also did not contact the dorsal process of the maxilla on the lateral surface of the skull (Fig. 2.6A), unlike the condition seen in the basal neornithischians *Changchunsaurus*, *Haya*, and *Parksosaurus* (Galton, 1973; Jin et al., 2010; Makovicky et al., 2011).

The foramen for the prominent lacrimal duct is present on the dorsal portion of the posterior surface of lacrimal (Fig. 2.6B). This foramen penetrates the middle of the anterior process and eventually opens along the medial surface near the distal end of the anterior process. The posterodorsal corner of the lateral surface of the lacrimal is rugose where it contacted the base of the supraorbital (Fig. 2.6A: aso). Anteroventral to this rugose area, foramina pierce the lateral surface of the lacrimal. On the right side there are two foramina, while on the left there are three. The posterodorsal margin of the lacrimal contacts the prefrontal. The nasal overlaps much of the dorsal and lateral surfaces of the anterior process of the lacrimal, preventing the anterior process from contacting the posterolateral process of the premaxilla. Contact between the lacrimal and the premaxilla is present in *Heterodontosaurus* (Crompton and Charig, 1962), *Jeholosaurus* (Barrett and Han, 2009), some basal ceratopsians (e.g., *Liaoceratops* and *Yinlong*: Xu et al., 2002, 2006), and some basal iguanodontians (e.g., *Tenontosaurus*, *Dryosaurus*; Norman, 2004b). The ventrolateral margin of the anterior process projects ventrally as a mediolaterally thin sheet over the posterodorsal corner of the antorbital fossa. A mediolaterally thin sheet of bone extended from the anteromedial margin of the posteroventral process across to the ventromedial margin of the anterior process, forming the posterodorsal portion of the medial wall of the antorbital fossa. The ventral margin of

this sheet is slightly thickened and contacted a corresponding medial sheet of the maxilla (Figs. 2.6A and B: drmm). The medial surface of the ventral process did not contact the palatine, unlike in *Hypsilophodon*, *Jeholosaurus*, and *Lesothosaurus* (Galton, 1974a; Sereno, 1991; Barrett and Han, 2009).

Maxilla

The maxilla forms the anterior and ventral margins of the antorbital fenestra, but is excluded from bordering the external nares anteriorly by the posterolateral process of the premaxilla (Figs. 2.1 and 2.2). The maxillary tooth row is shorter than the dentary tooth row (Figs. 2.1 and 2.2). There is a shallow fossa present on the anteroventral corner of the lateral surface of the maxilla, just posterior to the contact with the premaxilla (Figs. 2.1, 2.2, and 2.5A). This fossa is also present in *Changchunsaurus*, *Haya*, *Hypsilophodon*, *Jeholosaurus*, *Orodromeus*, and *Zephyrosaurus* (Butler et al., 2008a; Jin et al., 2010; Makovicky et al., 2011). There are twenty tooth positions present in the maxilla. The maxillary tooth row ends even with the posterior edge of this lateral maxillary fossa, creating a flat diastema between the maxillary and premaxillary tooth rows. In heterodontosaurids, the maxillary diastema is anteroposteriorly concave (Butler et al., 2008a). Just anterior to the lateral maxillary fossa a short, anterolateral boss is present that inserted into a posterolateral recess in the premaxilla (Fig. 2.5C: almp), a character shared by *Changchunsaurus*, *Haya*, *Orodromeus*, *Oryctodromeus* (inferred based on the morphology of the premaxillae), and *Zephyrosaurus* (Sues, 1980; Scheetz, 1999; Jin et al., 2010; Makovicky et al., 2011; C. Boyd, pers. obs.). This boss is separate

from the long, ‘spike-like’ process that forms the anterior-most end of the maxilla and inserts deeply into the posterior end of the premaxilla (Scheetz, 1999). The anterior ends of the maxillae contact each other medially, after inserting into the premaxillae. Where the maxillae are in contact medially, the vomer overlaps their ventral surfaces until the maxillae insert into the posterior end of the premaxillae, though posterior to this contact the vomer inserts between the medial surfaces of the maxillae.

The lateral surface of the maxilla is overlapped dorsally by the nasal and anteriorly by the posterolateral process of the premaxilla (Figs. 2.1 and 2.2). A small, dorsally directed, triangular projection is positioned ventral to the nasal and formed the anterior boarder of the antorbital fenestra. A prominent anteroposteriorly oriented ridge is present on the lateral surface of the maxilla, causing the tooth row to be inset medially. In *Lesothosaurus* and *Scutellosaurus* this ridge is reduced in size, resulting in only a slight emargination (Colbert, 1981; Sereno, 1991). A few small foramina pierce the surface of this ridge near its apex, and a row of larger foramina are present ventral to this ridge. The maxillary border of the external antorbital fenestra is anteroposteriorly concave and is sharply defined along its entire length, unlike in the heterodontosaurid *Abrictosaurus* (Thulborn, 1974), the thyreophorans *Emausaurus* and *Scelidosaurus* (Butler et al., 2008a), the basal ornithischian *Lesothosaurus* (Sereno, 1991), the basal neornithischian *Zephyrosaurus* (Sues, 1980), and the basal ceratopsian *Archaeoceratops* (You and Dodson, 2003) where the external antorbital fenestra rounds smoothly on the maxilla along at least a portion of its margin. Unlike in the basal neornithischians *Haya* and *Hypsilophodon* (Galton, 1974a; Makovicky et al., 2011), there is no maxillary fenestra

present anterior to the antorbital fenestra. The posterodorsal margin of the maxilla contacts the lacrimal and jugal along a continuous butt joint (Figs. 2.1 and 2.2).

The medial surface of the maxilla is dorsoventrally concave. Near the ventral margin a row of replacement foramina are present dorsomedial to the tooth row, as in all neornithischians and the heterodontosaurid *Fruitadens* (Norman et al., 2004c; Butler et al., 2010). Just anterior to the external antorbital fenestra a mediolaterally thin medial process extends dorsally. Anteriorly, this medial process extends dorsally and connects to the dorsomedial surface of the triangular projection of the maxilla anterior to the antorbital fenestra, creating a small internal antorbital fenestra in the anteroventral corner of the antorbital fossa (Fig. 2.6B: iaof). This medial process extends posteriorly, forming the medial and much of the dorsal walls of the antorbital fossa. Posteriorly, the medial process contacts a medial sheet of bone extending from the lacrimal and gradually reduces in dorsoventral height until it reaches the contact between the maxilla and the ventral process of the lacrimal. The dorsal margin of the medial process of the maxilla is mediolaterally expanded where it contacts the lacrimal (Fig. 2.6A: drmm). A small fenestra is also present in the posteroventral corner of the antorbital fenestra, between the maxilla and the lacrimal, that opened posteriorly into the orbit.

Jugal

The jugal forms the entire ventral, and part of the anterior, margin of the infratemporal fenestra as well as the entire ventral, and part of the posterior, margin of the orbit (Fig. 2.1). The lateral surface of the jugal lacks the ornamentation seen in

Jeholosaurus (Barrett and Han, 2009) and either a low (*Changchunsaurus*: Jin et al., 2010) or pronounced jugal boss (*Orodromeus*, *Skaladromeus*, and *Zephyrosaurus*: Sues, 1980; Scheetz, 1999, C. Boyd, pers. obs.). The anterior process of the jugal is straight in lateral view (Fig. 2.1), unlike the curved anterior process seen in the basal neornithischians *Agilisaurus* and *Zephyrosaurus* (Peng, 1992; Scheetz, 1999). It is dorsoventrally deeper than mediolaterally broad, unlike in thyreophorans (Norman et al., 2004b). The anterior process of the jugal is excluded from contacting the margin of the antorbital fenestra by the lacrimal and the maxilla, as in all non-cerapodan basal neornithischians (Norman et al., 2004c), *Hypsilophodon* (Galton, 1974a), and many basal iguanodontians (e.g., *Gasparinisaura*, *Zalmoxes*: Coria and Salgado, 1996; Weishampel et al., 2003). The tip of the anterior process is triangular in shape, and ends dorsal to the maxilla (Fig. 2.1), in contrast to the basal neornithischians *Agilisaurus* and *Hypsilophodon* (Galton, 1974a; Peng, 1992) and most iguanodontians (e.g., *Dysalotosaurus*, *Gasparinisaura*, and *Tenontosaurus*: Coria and Salgado, 1996; Norman, 2004b) where the anterior process of the jugal inserts into the maxilla. The dorsal surface of the tip of the anterior process of the jugal forms an extensive butt-joint against the ventral process of the lacrimal (Fig. 6A)

Medially, the dorsal and ventral margins of the anterior process are thickened, the jugal forms an extensive butt-joint against the ventral process of the lacrimal (Fig. 2.6A). making the medial surface dorsoventrally concave. On the medial surface of the anterior process, an elongate, anteroposteriorly oriented groove is present that formed the. articulation surface for the ectopterygoid (Fig. 2.7B: mgj), as in all basal ornithischians.

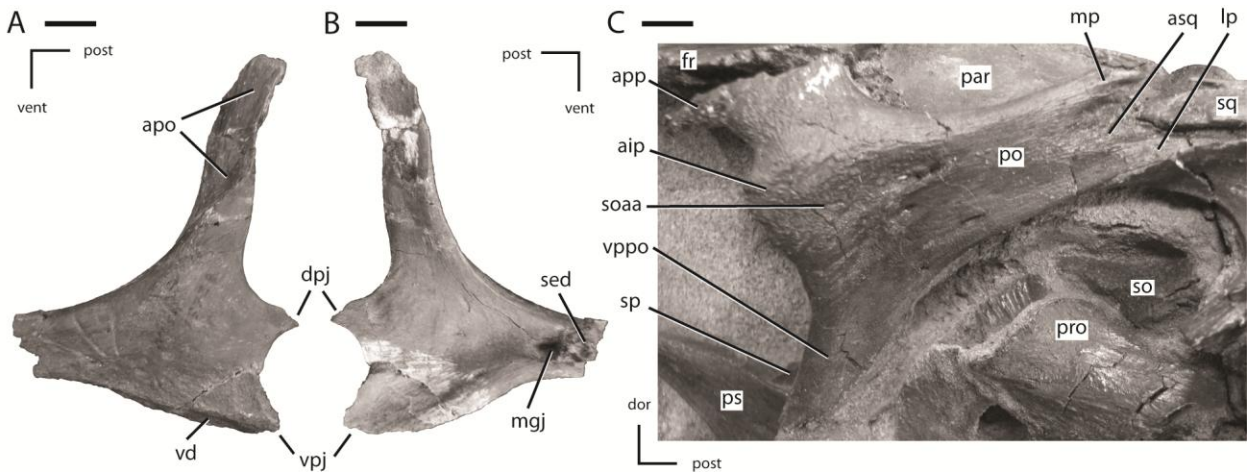

Figure 2.7: Jugal and postorbital of NCSM 15728. **A**. Partial left jugal in lateral view. **B**. Partial left jugal in medial view. **C**. Right postorbital in lateral view. The directional arrows indicate the orientation of the specimen in each view. Scale bars equal 1 cm. See Appendix 2 for anatomical abbreviations

The dorsal process of the jugal is the most gracile of the three processes on the jugal and angles posterodorsally to contact the postorbital. The contact surface for the postorbital on the dorsal process of the jugal faces laterally and slightly anteriorly (Fig. 2.7A: apo).

The medial surface of the dorsal process is concave anteroposteriorly, and its anterior edge is thicker than the posterior edge. The dorsal and posterior processes of the jugal form an oblique angle at the anteroventral corner of the infratemporal fenestra. The dorsoventral height of the posterior process is less than 25% of the total height of the skull, as in the basal neornithischians *Agilisaurus*, *Haya*, *Hexinlusaurus*, *Jeholosaurus*, and *Orodromeus* (He and Cai, 1984; Peng, 1992; Scheetz, 1999; Barrett and Han, 2009; Makovicky et al., 2011) and the basal ceratopsian *Yinlong* (Xu et al., 2006). The posterior process is bifurcated at its distal end, giving rise to an elongate, 'tab-shaped' dorsal projection and a triangular ventral projection. The dorsal projection overlapped the lateral surface of the quadratojugal along the ventral margin of the infratemporal fenestra (Figs.

2.7A and B: dpj), while the ventral projection inserted medial to the quadratojugal (Figs. 2.7A and B: vpj). The lateral surface of the ventral margin of the posterior process is depressed and covered by a series of ridges (Fig. 2.7A: vd), a feature only known in the taxon *Thescelosaurus* (Boyd et al., 2009).

Quadratojugal

The quadratojugal is a mediolaterally thin, 'plate-like' bone that formed a small part of the posterior margin of the infratemporal fenestra (Fig. 2.1). A thin, anteroposteriorly flattened projection of bone expands dorsally along the anterior margin of the quadrate, wrapping anteriorly and medially to the dorsal portion of the jugal wing on the quadrate. This dorsal process did not reach the ventral process of the squamosal, unlike in the heterodontosaurid *Heterodontosaurus* (Crompton and Charig, 1962), the basal neornithischian *Lesothosaurus* (Sereno, 1991), and the basal iguanodontians *Dryosaurus* and *Dysalotosaurus* (Norman et al., 2004c). The dorsal margin of the quadratojugal posterior to the dorsal process is posterodorsally concave to wrap around the anterior margin of the jugal wing of the quadrate. The posterior margin of the quadratojugal is slightly concave with rounded posterodorsal and posteroventral corners. The medial surface of the posteroventral corner of the quadratojugal contacted the quadrate along a laterally flattened facet just dorsal to the distal condyles (Fig. 2.8B: aqj). The ventral margin of the quadratojugal is sloped anterodorsally.

The anterior portion of the quadratojugal participates in a complicated contact with the posterior process of the jugal. The majority of the anterior end of the

quadratojugal inserted medial to the posterior process of the jugal; however, the anteroventral corner of the quadratojugal possesses a dorsoventrally oriented groove that the posterior process of the jugal inserted into, which causes the posteroventral corner of the posterior process of the jugal to insert medial to the quadratojugal (Fig. 2.1). Thus, the jugal overlaps the lateral surface of the quadratojugal dorsally and inserts medial to the quadratojugal ventrally. This morphology is unique to this specimen, but since the quadratojugal is not preserved in *Thescelosaurus assiniboiensis* or *Thescelosaurus garbanii* (Morris, 1976; Brown et al., 2011), it is uncertain if this morphology is an autapomorphy of *Thescelosaurus neglectus* or a synapomorphy of *Thescelosaurus*. A similar condition is seen in the basal iguanodontians *Tenontosaurus* and *Zalmoxes*, except that in those taxa the quadratojugal sits in a dorsoventral groove in the jugal, producing the same pattern of overlap on the lateral surface of the skull (Weishampel et al., 2003; Godefroit et al., 2009). A small quadratojugal foramen is present slightly posterior to the contact between the jugal and the quadratojugal (Fig. 2.1), which is also present in the basal neornithischians *Haya*, *Hypsilophodon*, *Jeholosaurus*, *Parksosaurus*, and some specimens of *Orodromeus* (e.g., MOR 1141) and the basal iguanodontian *Tenontosaurus tilletti* (Galton, 1973, 1974a; Scheetz, 1999; Norman, 2004b; Barrett and Han, 2009; Makovicky et al., 2011).

Postorbital

The postorbital formed the posterodorsal corner of the orbit, the anterodorsal margin of the infratemporal fenestra, and the anterolateral margin of the supratemporal

fenestra (Fig. 2.1). The postorbital consists of two prominent processes directed ventrally and posteriorly, and a third, reduced process directed anteriorly (Fig. 2.7C). The ventral process is triangular in transverse section, with the lateral surface anteroposteriorly concave. The ventral process overlaps the lateral surface of the dorsal process of the jugal, as in the basal neornithischians *Agilisaurus*, *Jeholosaurus*, *Parksosaurus*, and *Zephyrosaurus* (Galton, 1973; Sues, 1980; Peng, 1992; Barrett and Han, 2009). The short anterior process extends anterior from the contact between the frontal and postorbital and envelopes the lateral and ventral margins of the frontal (Fig. 2.7C: app). The orbital margin of the main body of the postorbital and the anterior process is rugose as seen in the basal neornithischians *Haya*, *Orodromeus*, and *Zephyrosaurus* (Sues, 1980; Scheetz, 1999; Makovicky et al., 2011) and the basal ceratopsians *Archaeoceratops* and *Liaoceratops* (Xu et al., 2002; You and Dodson, 2003). A distinct anteriorly directed inflation is present along the orbital margin (Fig. 2.7C: aip), as in the basal neornithischians *Haya*, *Hexinlusaurus*, *Jeholosaurus*, *Orodromeus*, *Thescelosaurus assiniboiensis*, and *Zephyrosaurus* (Sues, 1980; He and Cai, 1984; Scheetz, 1999; Barrett and Han, 2009; Brown et al., 2011; Makovicky et al., 2011, C. Boyd, pers. obs.). A prominent, anteroposteriorly oriented ridge extends from the dorsal margin of this projection posteriorly along the lateral surface of the postorbital onto the posterior process. Ventral to this ridge the surface of the postorbital is flattened (Fig. 2.7C: soaa). It was proposed that this anterior projection into the orbit served as a site of attachment for the supraorbital or, when present, the accessory supraorbital (Norman et al., 2004c). This hypothesis is confirmed by the fact that the accessory supraorbital in this specimen rests

on the flattened lateral surface of this projection ventral to the anteroposteriorly oriented ridge (Fig. 2.1). Posterior to this contact surface for the accessory supraorbital a series of small foramina are present, though the number and position vary on each side of the specimen.

The posterior process angles posterodorsally and its lateral surface is dorsoventrally concave. The posterior process twists about its long axis so that its lateral surface rotates to face dorsolaterally (Figs. 2.3 and 2.7C). The distal end is bifurcated into medial and lateral projections, with the lateral projection extending farther posteriorly (Fig. 2.8E: mp and lp, respectively). These projections insert into the anterior process of the squamosal, which is also bifurcated into mediolaterally broad dorsal and ventral projections, with the ventral projection extending further anteriorly than the dorsal projection. These four projections tightly interlock with each other, forming a secure contact between these two elements (Fig. 2.8E). The main body of the postorbital is relatively mediolaterally thin, unlike the robust postorbital seen in some basal iguanodontians (e.g., *Tenontosaurus* and *Zalmoxes*: Norman, 2004b, Weishampel et al., 2003) and ankylopollexians (e.g., *Camptosaurus*: Norman, 2004b). On the ventromedial surface adjacent to the contact surface for the frontal, a prominent facet is present for the head of the laterosphenoid. This contact surface extends medially onto the frontal.

Frontal

The frontals are dorsally flattened, anteroposteriorly longer than wide, and approximately the same length as the nasals (Fig. 2.3). Each frontal is roughly triangular

in dorsal view, with the anterior end pointed and the posterior end transversely wide. The medial margins of the frontals remain in contact throughout their entire length and the medial contact surface consists of a series of anteroposteriorly oriented ridges and grooves. The anterior tips of the frontals insert in between the posterior ends of the nasals and overlap the dorsal surface of the posteromedial corners of the nasals. The anterolateral portion of the frontal is dorsally depressed, creating a facet into which the posterior process of the prefrontal inserted. The frontals extend over the entire orbit, unlike in *Zalmoxes* and some Ankylopollexians where the frontals are only positioned over the posterior half of the orbit (Weishampel et al., 2003; Norman, 2004b). The frontal forms the middle portion of the orbital margin, and is dorsoventrally thin and rugose along this margin as most basal neornithischian taxa (e.g., *Haya*, *Skaladromeus*, and *Zephyrosaurus*: Sues, 1980, Makovicky et al., 2011; C. Boyd, pers. obs.) The orbital contribution of the frontal is less than 25% of the total length of the frontal, as in *Thescelosaurus assiniboiensis* (Brown et al., 2011) and some basal iguanodontians (e.g., *Muttaburrasaurus*: Bartholomai and Molnar, 1981). The width of the frontals is greatest at mid-orbit level, not across the posterior end (Fig. 2.3), a condition unique to *Thescelosaurus* (Boyd et al., 2009).

The postorbital contacts the posterolateral corner of the frontal, and the articulation facet for the postorbital is oriented laterally and wraps around to the ventral surface, as in *Zephyrosaurus*, but unlike the dorsally facing articulation facet seen in *Skaladromeus* (C. Boyd, pers. obs.). The articulation between the frontal and postorbital consists of a series of pronounced, interlocking projections, as in *Hypsilophodon*,

Orodromeus, and *Zephyrosaurus* (Galton, 1974a; Scheetz, 1999; C. Boyd, pers. obs.). The articulation surface for the dorsal head of the laterosphenoid is positioned on the ventral surface along the contact between the frontal and the postorbital, which is also seen in the basal neornithischians *Agilisaurus*, *Jeholosaurus*, *Lesothosaurus*, *Thescelosaurus assiniboiensis*, *Skaladromeus*, and *Zephyrosaurus* (Sues, 1980; Sereno, 1991; Barrett et al.,. 2005; Barrett and Han, 2009; Brown et al., 2011; C. Boyd, pers. obs.). The frontals form the anteromedial margins of the supratemporal fenestrae. The posterior-most extent of each frontal is along the midline. These projections inserting into corresponding slots in the anterodorsal surface of the parietal, as in *Thescelosaurus assiniboiensis* (Brown et al., 2011). In *Hypsilophodon* posterior projections are also present, but they are positioned slightly lateral to the midline (Galton, 1974a), and in *Haya, Lesothosaurus,* and *Orodromeus* the posterior contact with the parietals is relatively straight (Sereno, 1991; Scheetz, 1999; Makovicky et al., 2011). There is a broad, ventrolaterally oriented concavity on the ventral surface along the orbital margin, the limits of which are denoted by the presence of a sharp, ventrally pointing ridge. Medial to this ridge, the ventromedial surface of the frontal is concave where the olfactory bulb and tract and the anterior portion of the cerebrum were positioned (Galton, 1989). This ventromedial concavity is more pronounced than the ventrolateral concavity. The posterior end of the frontal is dorsoventrally thicker than the anterior end.

Parietal

The parietals are completely fused, and form much of the anterior, medial, and posterior margins of the supratemporal fenestrae (Fig. 2.3). Anteriorly, the parietals make a mediolaterally broad contact with the posterior margin of the frontals (Fig. 2.3). The median process (sensu Galton, 1974a) is situated along the midline of the anteroventral margin of the parietals and inserted into a shallow notch in the posteroventral surface of the frontals. Dorsoventrally thin, mediolaterally wide processes extend anteriorly from the anterolateral corners of the parietals. These processes were appressed to the ventral surface of the frontals, slightly overlapped the posteroventral portion of the contact between the postorbital and the frontal, and ended just posterior to the articulation surface on the frontal and postorbital for the laterosphenoid. The ventral surface of these processes formed an anteroposteriorly long, mediolaterally concave contact with the dorsal surface of the laterosphenoid.

The dorsomedial portion of the anterior margin of the parietals is indented to receive the two posteromedial projections of the frontals. Just posterior to these indentations on the dorsal surface of the parietals, a flattened, triangular-shaped surface is present that narrows posteriorly leading to the sagittal crest. The sagittal crest is a narrow ridge with steeply sloped lateral surfaces that extends to the posterior margin of the parietals. The lateral surfaces of the parietals are anteroposteriorly concave and dorsoventrally convex below the sagittal crest, giving the parietals an hourglass shape in dorsal view (Fig. 2.3). In the middle of the lateral surface, the ventral half is covered by a series of posterodorsally inclined ridges, though matrix obscures exactly how many

ridges were present and how far posteriorly they extend. In each of the posterodorsal corners of the lateral surfaces a pronounced fossa is present. In dorsal view, the posterior margin is posteriorly concave, with the lateral wings meeting along the midline at a sharp angle, and a thickened ridge is present along the entire posterior border. The posterolateral surfaces contacted mediolaterally thin, ventromedially directed processes of the squamosals. Ventrally, the parietals are deeply concave for receipt of the dorsal surface of the supraoccipital. At the posterior margin there is a ventrally directed wedge of bone along the midline of the element (Fig. 2.4). The lateral walls of the parietals are mediolaterally thin posteriorly, with their ventral tips wedged between the squamosal and the supraoccipital. The lateral walls thicken and decrease in dorsoventral height anteriorly, reaching their maximum mediolateral thickness at the posterior margin of their contact with the laterosphenoids.

Squamosal

The squamosal forms the dorsal margin of the infratemporal fenestra and the posterolateral margin of the supratemporal fenestra (Figs. 2.1, 2.3, and 2.8A). It has four distinct processes. The anterior process curves ventrally as it approaches and contacts the postorbital (Fig. 2.8A). The contact surface for the postorbital consists of two anteriorly directed projections, the ventral projection being longer than the dorsal projection (Fig. 2.8A: vsq and dsq, respectively). The ventral projection was positioned ventromedial to the posterior process of the postorbital, while the dorsal projection overlapped the dorsolateral surface of the posterior process (Fig. 2.8E). The posterior process was forked

into medial and lateral projections that inserted into anteroposteriorly elongate grooves on either side of the dorsal projection of the squamosal (Fig. 2.8B). This same contact is present in the paratype of *Thescelosaurus neglectus* (USNM 7758), but the contact in *Thescelosaurus assiniboiensis* is not as intricate (Boyd et al., 2009; Brown et al., 2011). Additionally, the series of anteroposteriorly oriented ridges present on the dorsal surface of the articulation with the postorbital in *Thescelosaurus assiniboiensis* are absent in NCSM 15728 (Boyd et al., 2009).The anteroventrally directed prequadratic process (sensu Makovicky et al., 2011), is triangular in transverse section, arises anterior to the socket for the head of the quadrate, and extends ventrally along the anterior surface of the quadrate with its distal end tapering to a point (Fig. 2.8A: prq).

The prequadratic process does not extend far enough ventrally to contact the dorsal process of the quadratojugal, unlike in the heterodontosaurid *Heterodontosaurus* (Crompton and Charig, 1962), the basal ornithischian *Lesothosaurus* (Sereno, 1991), and the basal iguanodontians *Dryosaurus* and *Dysalotosaurus* (Norman, 2004b). The posteroventral, or postquadratic (sensu Makovicky et al., 2011) process is an anteroposteriorly thin sheet that forms much of the posterior surface of the squamosal, enclosing the posterior end of the socket for the head of the quadrate (Fig. 2.8A: poq). The lateral margin of the postquadratic process flares posterolaterally, creating a broad lateral wing (Fig. 2.8B). The posterodorsal surface of the squamosal is posteromedially concave in dorsal view and in lateral view the posterior margin is offset at a right angle from the posterodorsal margin (Fig. 2.8A), as in the paratype of *Thescelosaurus neglectus* (USNM 7758: Boyd et al., 2009). Alternatively, the posterodorsal corner of the

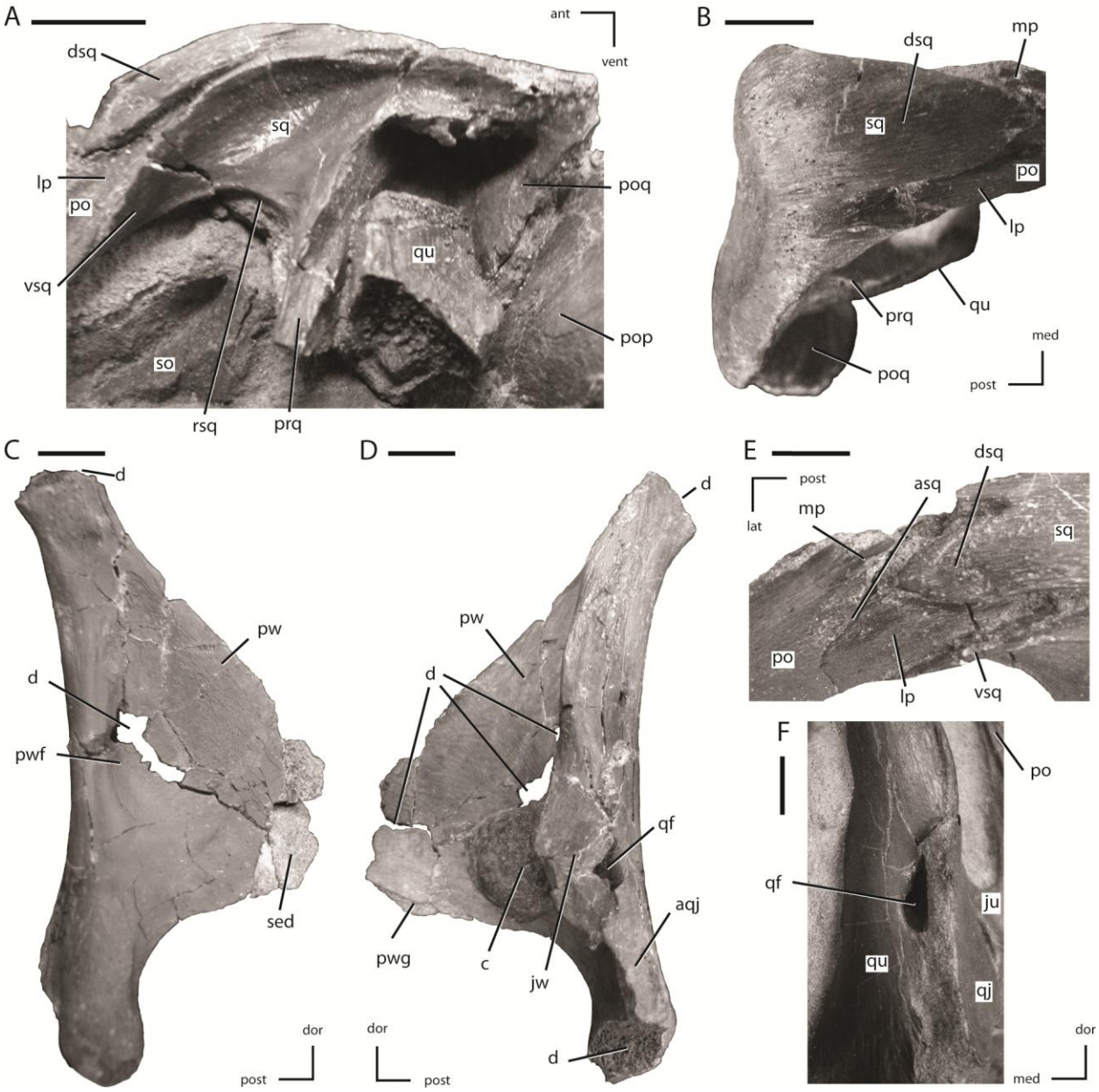

Figure 2.8: Squamosal and quadrate of NCSM 15728. **A**. Left squamosal in lateral view. **B**. Right squamosal in dorsal view. **C**. Partial left quadrate in medial view. **D**. Partial left quadrate in lateral view. **E**. Contact between the left squamosal and postorbital in dorsal view. **F**. Foramen between the right quadrate and quadratojugal in posterolateral view. The directional arrows indicate the orientation of the specimen in each view. Scale bars equal 1 cm. See Appendix 2 for anatomical abbreviations.

squamosal is convex in lateral views and the posterior margin is concave to straight in dorsal view in *Thescelosaurus assiniboiensis* (Brown et al., 2011). The convex anterior surface of the paroccipital process fit into the posterior concavity on the squamosal. The medial process of the squamosal is a stout sheet of bone that extends anteromedially from the posteromedial margin of the postquadratic process (Fig. 2.4).

The medial process narrows in dorsoventral height as it extends medially, and its medial end possesses an anteroposteriorly elongate groove. The posteroventral end of the parietals inserted into this groove, and a small projection of the medial process of the squamosal cupped the ventral surface of the parietal, preventing the latter element from contacting the supraoccipital along is posteroventral surface. The dorsal surface of the squamosal is medially expanded to unite the dorsomedial margin of the anterior process and the anterodorsal margin of the medial process (Fig. 2.8B), creating a dorsally enclosed pocket in the posterolateral corner of the supratemporal fenestra.

A thin, sharply defined, anteroposteriorly oriented ridge arises on the ventral surface of the anterior process of the squamosal (Fig. 2.8A: rsq). This ventral ridge extends posteriorly to the base of the prequadratic process of the squamosal, becoming dorsoventrally taller. A ventral ridge also extends between the posterior margin of the prequadratic process and the anterior margin of the postquadratic process, enclosing the medial surface of the socket for the head of the quadrate. In ventral view, these ventral ridges divide the ventral surface of the squamosal into lateral and medial fossae. The medial fossa is twice the transverse breadth of the lateral fossa on average. Anterior to the prequadratic process the lateral fossa forms a well-developed, ventrolaterally oriented

concavity (Fig. 2.8A) for the adductor musculature (M. adductor mandibulae superficialis; Galton, 1974a; Jin et al., 2010). A smooth, laterally facing surface extends posteriorly from this concavity dorsal to the socket for the head of the quadrate, reaching the anterior margin of the postquadratic process. There is no parietosquamosal shelf, unlike the condition in all known marginocephalian taxa (Butler et al., 2008a).

Palatoquadrate

The palatoquadrate region of NCSM 15728 is relatively well preserved, though many of the elements have been slightly displaced from their natural positions. Elements from the left side of the skull are figured, but their morphology is congruent with that of their antimeres.

Quadrate

The quadrate shaft leans posteriorly in lateral view (Fig. 2.1). The ventral portion of the quadrate shaft angles slightly anteroventrally, unlike in some basal ceratopsians (e.g., *Yinlong*) where the shaft angles posteroventrally (Xu et al., 2006). The distal condyles of the quadrate are dorsolaterally sloped in posterior view, as seen in the basal neornithischians *Jeholosaurus*, *Orodromeus*, *Oryctodromeus*, and *Zephyrosaurus* (Sues, 1980; Scheetz, 1999; Barrett and Han, 2009; C. Boyd, pers. obs.). The quadrate was separated from the jugal by the quadratojugal, unlike in some basal iguanodontians and ankylopollexians (e.g., *Dryosaurus*, *Camptosaurus*: Norman, 2004b). The contact surface for the quadratojugal begins ventrally on the lateral surface of the quadrate, just dorsal to the distal condyles (Fig. 2.8D: aqj), which is the basal ornithischian condition. The

contact extends dorsally along the lateral surface of the ventral third of the quadrate shaft, then wraps around to the anteromedial surface where the dorsal process of the quadratojugal contacts the quadrate shaft. Overall, the contact between the quadrate and the quadratojugal extends along more than half of the dorsoventral height of the quadrate, unlike the reduced contact seen in the basal neornithischian *Changchunsaurus* (Jin et al., 2010), the basal ceratopsians *Archaeoceratops* and *Yinlong* (You and Dodson, 2003, Xu et al., 2006), and the basal iguanodontians *Dryosaurus* and *Dysalotosaurus* (Norman, 2004b). A foramen is present in the lateral surface of the quadrate, just posterior to the contact with the quadratojugal (Figs. 2.8D and F: qf). A similar foramen is present in the basal neornithischians *Haya* and *Parksosaurus* (Makovicky et al., 2011; C. Boyd, pers. obs.) and in some basal iguanodontian and ankylopollexian taxa (Norman, 2004b). This foramen passes though the base of the jugal wing and opens on the anteromedial surface of the quadrate (Fig. 2.8D). The dorsal head of the quadrate is posteriorly recurved (Figs. 2.8C and D), unlike in the basal neornithischian *Agilisaurus* (Peng, 1992).

Two processes are present on the quadrate, the anteriorly directed jugal wing (Fig. 2.8D: jw) and the anteromedially directed pterygoid wing (Fig. 2.8C: pw). The jugal wing is a mediolaterally thin sheet that arises from the anterolateral margin of the quadrate shaft, is moderately developed, and extends ventrally nearly to the distal condyles (Fig. 2.8D), contrasting with the shortened, more dorsally situated jugal wing in some basal iguanodontians (e.g., *Gasparinisaura*, *Zalmoxes*: Coria and Salgado, 1996; Weishampel et al., 2003). A shallow fossa is present on the lateral surface of the quadrate shaft, just posterodorsal to the jugal wing. The pterygoid wing emerges from the

anteromedial margin and is a large, anteromedially oriented sheet that arises dorsally below the head of the quadrate and ends well dorsal to the distal condyles (Fig. 2.8C). A fossa is present on the posterior side at the base of the jugal wing (Fig. 2.8C: pwf), which is also seen in the basal neornithischians *Jeholosaurus*, *Parksosaurus*, *Orodromeus*, and *Zephyrosaurus* (Galton, 1973; Sues, 1980; Scheetz, 1999; Barrett and Han, 2009; C. Boyd, pers. obs.) and the basal iguanodontian *Dysalotosaurus* (Norman, 2004b). The anteroventral margin of the pterygoid wing is grooved where it inserted into a groove on the ventrolateral surface of the quadrate process of the pterygoid (Fig. 2.8D: pwg).

Pterygoid

The pterygoid consists of three processes oriented roughly orthogonal to each other: the quadrate process (Fig. 2.9E: qap), the mandibular process (Fig. 2.9E: mpp), and the palatine process (Fig. 2.9E: ppp). The quadrate process is a broad, dorsoventrally expanded, mediolaterally thin sheet that projects posterolaterally from the body of the pterygoid (Figs. 2.9E, F, and G). The posteromedial surface of the quadrate process is dorsoventrally concave (Fig. 2.9F). In the anterior corner of the quadrate process where it joins with the other processes a posteromedially facing cup is present that received the basipterygoid process of the basisphenoid (Fig. 2.9G: bpa). The anterolaterally facing surface of the quadrate process is dorsoventrally convex and contacted the pterygoid wing of the quadrate (Fig. 2.9E). The ventral margin of the quadrate process is mediolaterally thickened, creating an expanded ridge just ventral to an associated shallow groove that received the ventral edge of the pterygoid wing of the quadrate (Fig. 2.9E:

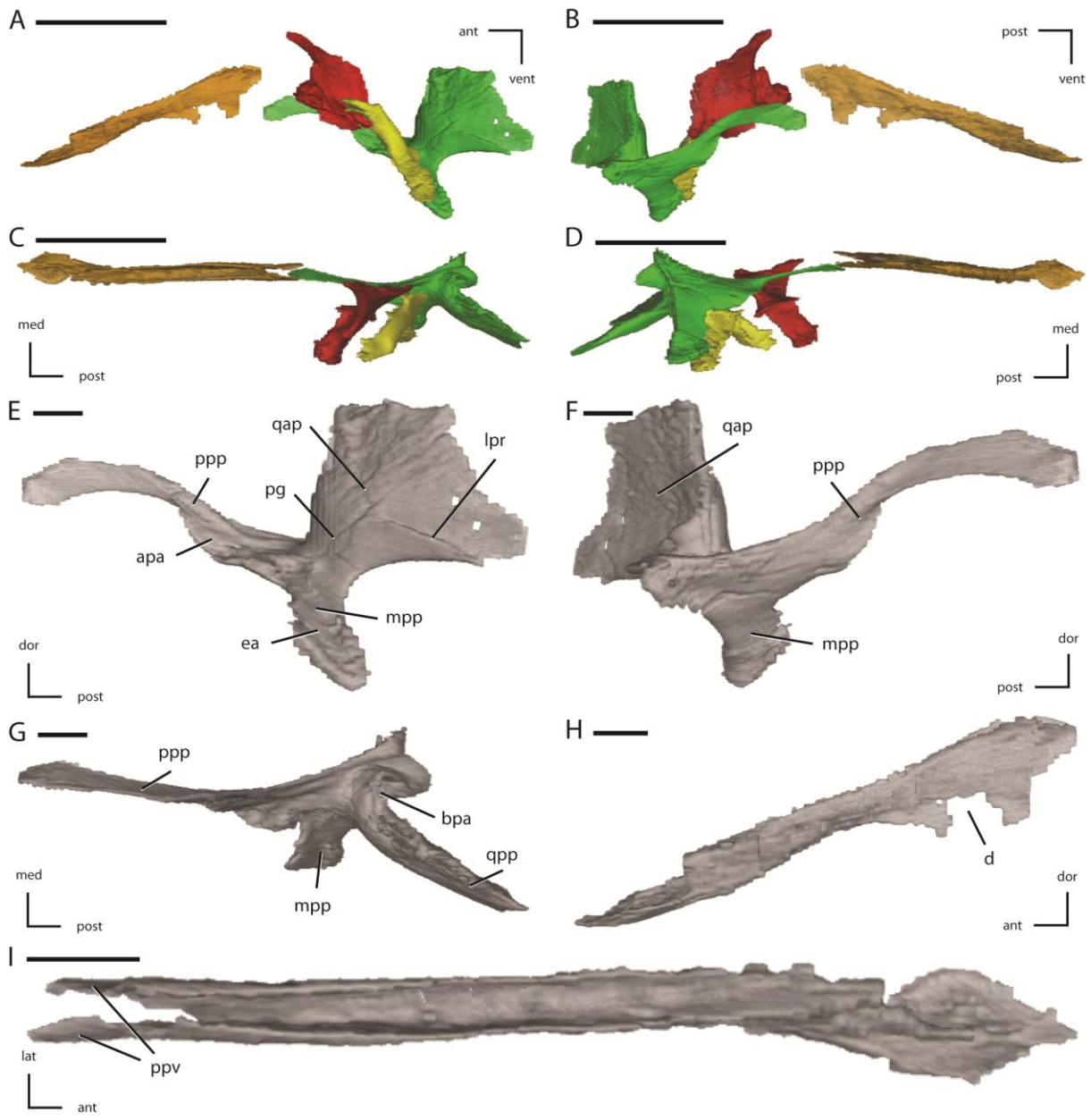

Figure 2.9: Midline and left palatal elements of NCSM 15728. **A**. Left palatal elements in lateral view. **B**. Left palatal elements in medial view. **C**. Left palatal elements in dorsal view. **D**. Left palatal elements in ventral view. **E**. Left pterygoid in lateral view. **F**. Left pterygoid in medial view. **G**. Left pterygoid in dorsal view. **H**. Vomer in left lateral view. **I**. Vomer in dorsal view. Key to colors used in **A** through **D**: Red = Palatine; Green = Pterygoid; Yellow = Ectopterygoid; Orange = Vomer. The directional arrows indicate the orientation of the specimen in each view. In **A** through **D** scale bars equal 5 cm. In **E** through **I** scale bars equal 1 cm. See Appendix 2 for anatomical abbreviations.

lpr). A groove extends from the anterior edge of the lateral pterygoid ridge on the quadrate process ventrally onto the mandibular process (Fig. 2.9E: pg), as seen in *Skaladromeus* (Chapter 3) and *Zephyrosaurus*. This groove is absent in *Thescelosaurus assiniboiensis* (Brown et al., 2011). The mandibular process projects ventrolaterally from the base of the quadrate process. Its surface is anteroposteriorly concave, with nearly the entire dorsal surface forming the articulation surface for the ectopterygoid (Fig. 2.9C). A thickened ridge is present along the anterior, lateral, and posterior margins of the mandibular process (Fig. 2.9E). The palatine process extends anteriorly from the contact between the mandibular and quadrate processes. At its base, a narrow shelf projects off the ventrolaterally from the ventral margin, forming the articulation surface for the palatine (Fig. 2.9E: apa). The remainder of the palatine process consists of a dorsoventrally expanded, mediolaterally thin process that extends anterodorsally from the body of the pterygoid. The distal end of the palatine process curves ventrally, eventually contacting the posterior process of the vomer. The palatal processes of the pterygoids were separated along the midline by a narrow interpterygoid vacuity (sensu Sereno, 1991). The dorsal margin of the palatal process continues posteriorly as a thin ridge that curves medial to the quadrate process, creating a dorsally flattened, medially projecting tab that contacting its antimere (Fig. 2.9G). The pterygoid is excluding from bordering the postpalatine fenestra by the ectopterygoid and palatine (Fig. 2.9C), as occurs in the basal neornithischians *Haya* and basal ceratopsians (Makovicky et al., 2011), but not in the basal neornithischians *Changchunsaurus* and *Hypsilophodon* (Galton, 1974a; Jin et al., 2010).

Palatine

The palatines are preserved slightly displaced from their natural positions, but are undamaged (Figs. 2.9A-D). The palatine is robust laterally where it contacts the medial surface of the maxilla just dorsal to the posterior end of the tooth row. The contact surface for the maxilla is deeply dorsoventrally concave and relatively anteroposteriorly straight (Fig. 2.10A: am). Dorsal to the maxillary contact surface, a robust anterodorsally oriented projection is present that that extends along the medial surface of the maxilla. The posterodorsal margin of this anterodorsal projection (Fig. 2.10A: adp) forms a broad contact surface with the anterior margin of the lateral process of the ectopterygoid (Fig. 2.9C). The dorsal tip of this projection inserts into the anteroposteriorly oriented groove in the medial surface of the anterior process of the jugal, as in *Hypsilophodon* and *Lesothosaurus* (Galton, 1974a; Sereno, 1991), preventing the palatine from contacting the lacrimal. In *Jeholosaurus*, the lacrimal is more ventrally positioned, inserting anterior to the jugal, allowing for a broad contact between the palatine and the lacrimal (Barrett and Han, 2009). Similarly, in *Hypsilophodon* the anterior process of the jugal is both dorsoventrally and anteroposteriorly shorter and does not extend as far anteriorly as in NCSM 15728, facilitating more contact between the lacrimal and the palatine (Galton, 1974a).

A broad sheet extends dorsomedially from the thickened lateral surface, forming the ventromedial wall of the orbit (Figs. 2.2 and 2.10A). The dorsolateral surface of this sheet is mediolaterally convex and anteroposteriorly concave (Fig. 2.10A). A few low, mediolaterally oriented ridges are present on the dorsolateral surface that extend to the

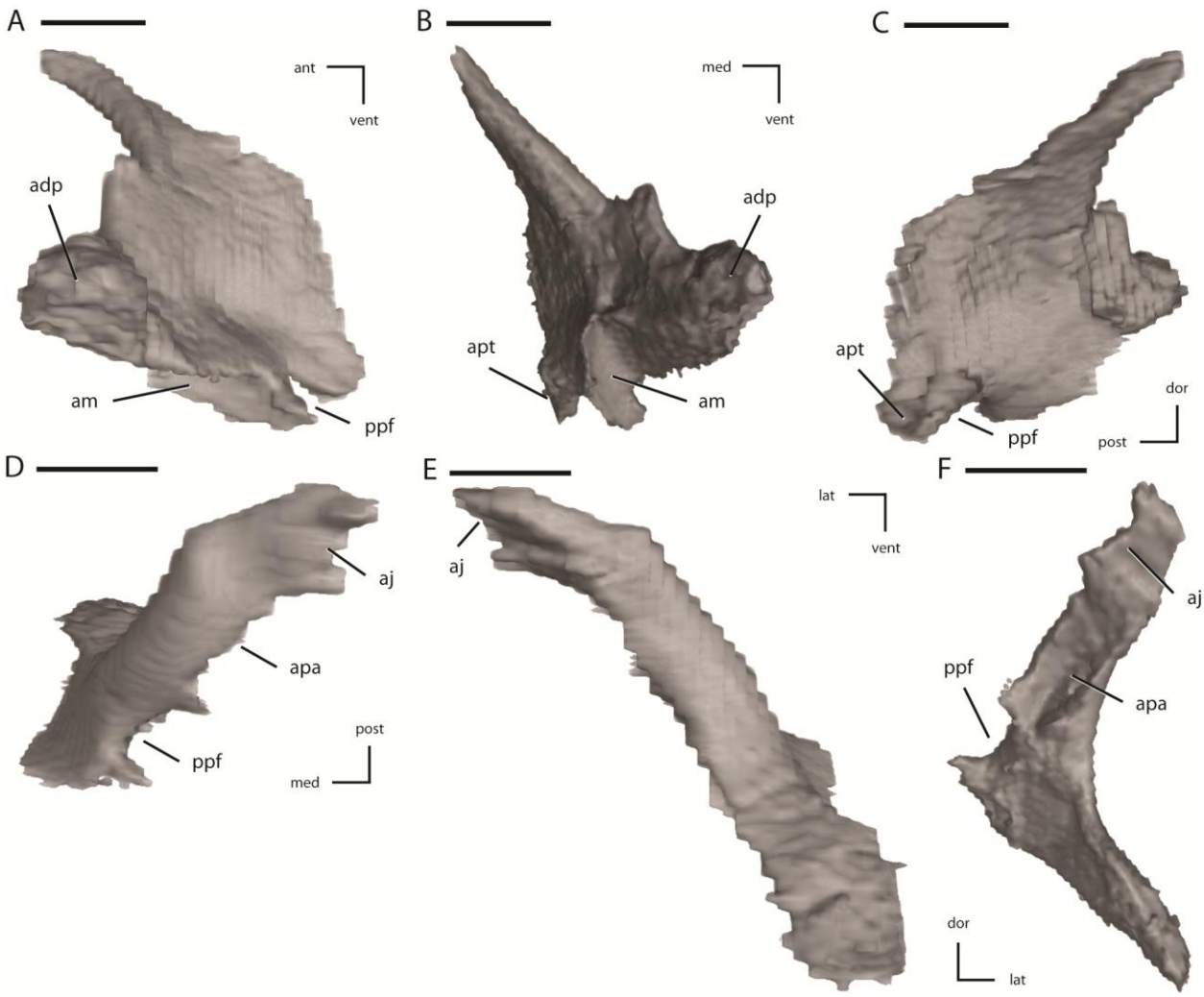

Figure 2.10: Additional illustrations of left palatal elements of NCSM 15728. **A**. Left palatine in lateral view. **B**. Left palatine in anterior view. **C**. Left palatine in medial view. **D**. Left ectopterygoid in dorsal view. **E**. Left ectopterygoid in posterior view. **F**. Left ectopterygoid in anterior view. The directional arrows indicate the orientation of the specimen in each view. Scale bars equal 1 cm. See Appendix 2 for anatomical abbreviations.

dorsal margin. The anterior margin of the palatine is slightly dorsoventrally thickened and has a 'W-shaped' outline in dorsal view, owing to the presence of a triangular anterior projection near the midpoint of the otherwise mediolaterally concave anterior margin (Figs. 2.10A and C). The anteromedial corner of the palatine consists of a

thickened, ‘tab-shaped’ projection. The medial margin of the palatine is dorsoventrally thickened (more pronounced anteriorly) and relatively straight (Fig. 2.10A).

A deep sulcus is present in the posterolateral corner of the palatine (Figs. 2.10A and C: ppf). This sulcus formed the anterior, and part of the medial margin of the postpalatine fenestra (sensu Sereno, 1991: = suborbital fenestra of Makovicky et al., 2011). Medial to this sulcus the posterior margin is slightly mediolaterally concave and angles anteromedially. The posterodorsal corner of the palatine is rounded. The ventromedial surface of the palatine is mediolaterally and anteroposteriorly concave (Fig. 2.10C). The articulation surface for the palatal process of the pterygoid consists of a flattened facet on the ventromedial surface positioned just medial to the sulcus for the postpalatine fenestra (Figs. 2.10B and C: apt). The palatines may have contacted each other along at least part of their medial margins, as in *Orodromeus* (Scheetz, 1999). It does not appear that the palatines extended far enough anteriorly to contact the posterolateral processes of the vomer (Figs. 2.9A through D), as it does in *Hypsilophodon* and *Lesothosaurus* (Galton, 1974a; Sereno, 1991). The palatines of NCSM 15728 match the morphology of the highly fragmentary palatines preserved in the holotype of *Thescelosaurus assiniboiensis* (Brown et al., 2011:fig. 9).

Ectopterygoid

The medial portion of the ectopterygoid consists of an expanded plate with a ventromedially facing articulation surface that contacts nearly the entire dorsolateral surface of the mandibular process of the pterygoid (Fig. 2.10F). The ectopterygoid did

not contact the palatal process of the pterygoid, as it does *Changchunsaurus* (Jin et al., 2010), though its anteromedial corner does just touch the posteromedial corner of the palatine at the base of the palatal process. The anteromedial portion of the ectopterygoid formed the medial margin of the postpalatine fenestra. In ventromedial view the articulation surface for the pterygoid is roughly triangular in shape, with its apex pointed anteromedially.

A 'rod-shaped' lateral process extends from the dorsolateral surface of the medial plate and angles anterodorsally (Figs. 2.10D and F). This process is bowed along its length, being convex dorsally and concave ventrally (Fig. 2.10E). A small fenestra is present between the maxilla and the ventral surface of this lateral process. The lateral process of the ectopterygoid becomes anteroposteriorly wider and dorsoventrally thinner dorsally, as it curves around the posteromedial corner of the maxilla. Near the dorsal end of the lateral process the anteroventral surface overlaps the posterodorsal corner of the maxilla. The distal end of the lateral process bears an anteroposteriorly oriented ridge that inserted into a dorsoventrally narrow groove on the medial surface of the anterior process of the jugal (Figs. 2.10D and E), just dorsal to the posterior end of the maxilla and posterior to the palatine, which also inserts into the groove.

The dorsal half of the anterior margin of the lateral process formed a broad, concave articulation surface for the posterior margin of the anterodorsal projection of the palatine (Fig. 2.10F), though postmortem displacement of the palatines has removed these elements from contact in NSCM 15728 (Fig. 2.9C). Contact between the ectopterygoid and the palatine is also present in *Haya* and *Lesothosaurus* (Sereno, 1991;

Makovicky et al., 2011), but is apparently absent in *Changchunsaurus* and *Hypsilophodon* (Galton, 1974a; Jin et al., 2010). The contact between the lateral process of the ectopterygoid and the palatine terminated medially at the anterolateral corner of the postpalatine fenestra, and together these two bones formed the entire border of this fenestra.

Vomer

The vomer is a midline element that contacted the premaxillae and maxillae anteriorly and the pterygoid posteriorly. The anterior end of the vomer is triangular in dorsal view (Fig. 2.9I), is dorsoventrally thin, and overlapped the maxillae along their ventral surfaces. The anterior tip inserted into a short socket near the ventral margin of the premaxillae. Posterior to the triangular anterior end a mediolaterally narrow neck is present that angles posterodorsally, separating the maxillae along the midline. Shortly after passing between the maxillae the vomer turns posteriorly. A narrow groove indents the dorsal surface of the vomer, and mediolaterally thin, dorsolaterally oriented processes arise from the dorsolateral margins of this groove (Fig. 2.9I). Posteriorly, the dorsal groove deepens and the dorsolateral processes become more dorsoventrally elongate.

A mediolaterally thin process extends from the ventral margin, becoming more elongate posteriorly, which makes the posterior portion of the vomer 'Y-shaped' in transverse section (Fig. 2.9H). A portion of this ventral process is damaged and was lost (Fig. 2.9H: d). Near their posterior end the dorsal groove extends all the way through the ventral process, dividing the posterior end into two lateral wings (Fig. 2.9I: ppv). The

dorsal margins of these lateral wings become mediolaterally thicker as they extend posteriorly, and eventually the wings overlap the lateral surfaces of the palatal processes of the pterygoids (sensu Sereno, 1991) as occurs in all ornithischian taxa (Sereno, 1991). The palatal process of the pterygoid is not reconstructed in contact with the posterior end of the vomer in *Hypsilophodon* (Galton, 1974a), but in all specimens of *Hypsilophodon* the palatal process is largely missing and this may not be accurate. The posterior extent of the vomer is roughly equal with the anterior margin of the orbit; thus, the vomer could not have contacted the palatines (Figs. 2.9A through D).

Braincase

The braincase of NSCM 15728 is slightly transversely crushed (Fig. 2.4), and demonstrates a lack of fusion between most of the individual bones (Fig. 2.11), with a few exceptions. Each opisthotic is fused indistinguishably with its exoccipital (Figs. 2.11A and B, 2.13A through D), as is the general case in basal ornithischians (Norman et al., 2004c), and the parasphenoid and the basisphenoid are indistinguishably fused (Figs. 2.11A, B, and D, 13G through I), which occurs in nearly all dinosaurs (Currie, 1997). The left opisthotic/exoccipital is slightly inset medially from its normal position (Fig. 2.11E), while the right opisthotic/exoccipital is displaced anteriorly and slightly medially (Fig. 2.4). The prootics, laterosphenoids, and the supraoccipital are all slightly displaced anteriorly, so that small gaps are present between each of these bones and most of their adjacent bones (Figs. 2.11A and B). There is no evidence of an ossified orbitosphenoid or presphenoid. The presence of an orbitosphenoid was noted in *Parksosaurus* (Galton,

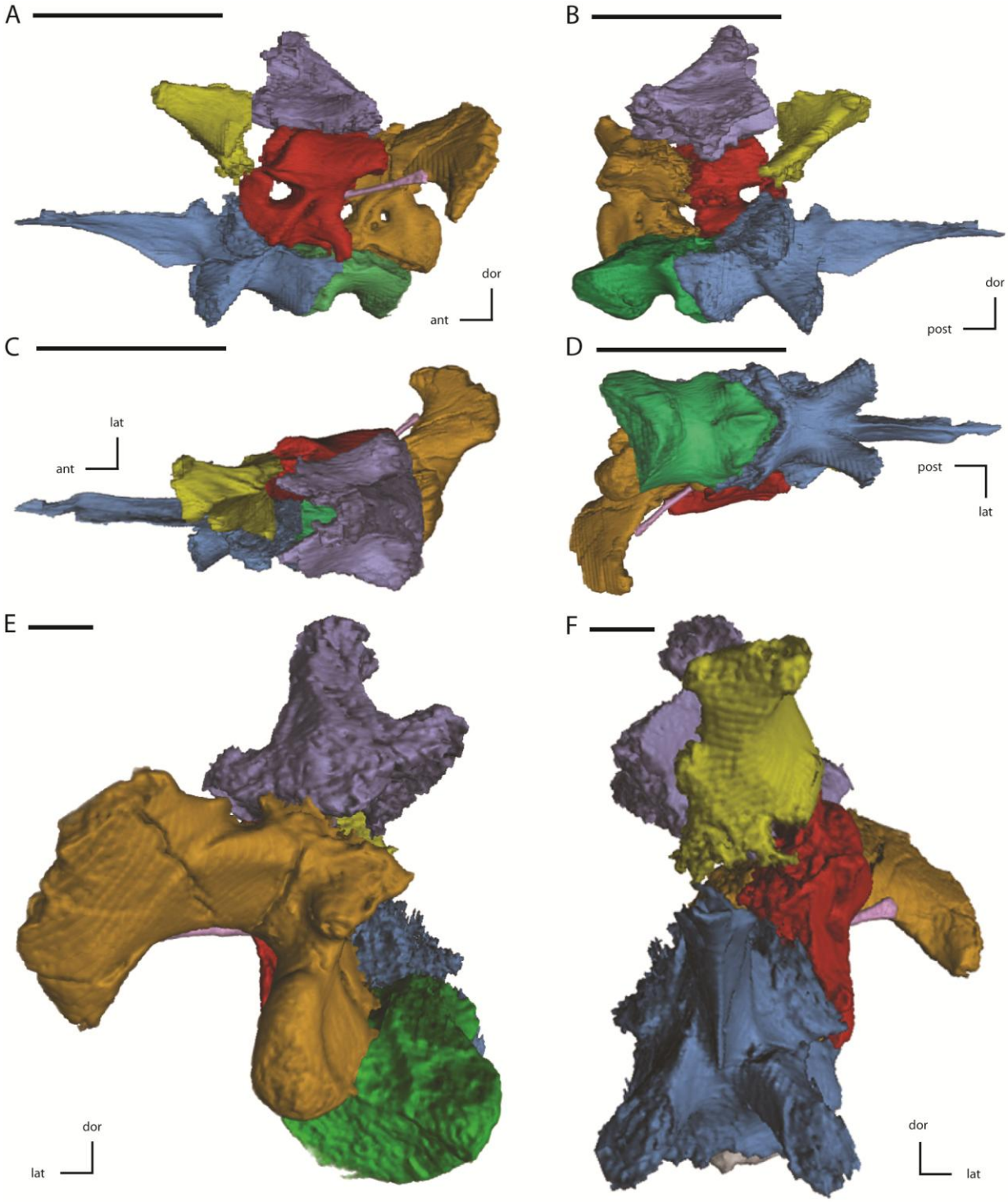
A
dor
ant
B
dor
post
C
lat
ant
D
post
lat
E
dor
lat
F
dor
lat

Figure 2.11: Midline and left side elements of the braincase of NCSM 15728. **A**. Braincase in lateral view. **B**. Braincase in medial view. **C**. Braincase in dorsal view. **D**. Braincase in ventral view. **E**. Braincase in posterior view. **F**. Braincase in anterior view. Key to colors: Red = Prootic; Yellow = Laterosphenoid; Purple = Supraoccipital; Green = Basioccipital; Blue = Fused basisphenoid/parasphenoid; Orange = Fused opisthotic/exoccipital; Pink = Stapes. The directional arrows indicate the orientation of the specimen in each view. Scale bars in **A** through **D** equal 5 cm. Scale bars in **E** and **F** equal 1 cm. See Appendix 2 for anatomical abbreviations.

1973:figs 2 and 3); however, its placement and morphology suggest that this actually a slightly damaged palatine (C. Boyd, pers. obs.). This observation is supported by the fact that this bone was reconstructed in the same position the palatine occupies in NCSM 15728 (Galton, 1973:fig. 5). Thus, the lack of an ossified orbitosphenoid in NCSM 15728 is not unexpected.

Basioccipital

The left posterodorsal corner of the basioccipital is detached from the rest of the basioccipital and preserved on the block containing the anterior cervical vertebrae from NCSM15728 (Figs. 2.12G and I). The anteroposterior length of the basioccipital is greater than the length of the basisphenoid, not including the fused parasphenoid (Fig. 2.11D), as in the basal neornithischians *Jeholosaurus* and *Thescelosaurus assiniboiensis* (Barrett and Han, 2009; Brown et al., 2011) and the iguanodontians *Camptosaurus*, *Dryosaurus*, and *Tenontosaurus tilletti* (Norman, 2004b). The posterior surface of the basioccipital forms the majority of the occipital condyle, along with contributions from the posteromedial portion of the fused opisthotic/exoccipital (Fig. 2.11E). The posterodorsal surface of the basioccipital is indented by the ventral margin of the foramen magnum, which occupies between twenty and thirty percent of the posterodorsal surface

of the basioccipital (Fig. 2.11E), as in the basal neornithischians *Orodromeus*, *Oryctodromeus*, *Othnielosaurus*, and *Zephyrosaurus* (Sues, 1980; Scheetz, 1999; C. Boyd, pers. obs.) and the basal iguanodontian *Zalmoxes* (Weishampel et al., 2003). In *Thescelosaurus assiniboiensis* the ventral margin of the foramen magnum occupies more than one third of the posterodorsal surface of the basioccipital (Brown et al., 2011).

The lateral and ventral sides of the basioccipital are concave, giving the basioccipital an 'hour-glass' shape in ventral and lateral views (Figs. 2.12G and H). A ventrally extending keel is present along the midline of the ventral surface of the basioccipital, extending from the anterior contact with the basisphenoid to about one third of the way toward to posterior end (Fig. 2.12G: bk). A similar keel is present in all non-iguanodontian basal neornithischian taxa except *Othnielosaurus* (Scheetz, 1999). Immediately posterior to this keel a small foramen is present (Fig. 2.12G: bt), which is not known in any other basal neornithischian taxon (Norman et al., 2004c), distinguishing *Thescelosaurus neglectus* from *T. assiniboiensis*. This foramen penetrates dorsally into the basioccipital, but does not appear to penetrate the floor of the braincase based on examination of the CT data. Lateral to the ventral keel along the anterior margin of the basioccipital, two small knobs form the posterior portions of the basal tubera (Figs. 2.12G and H). These basioccipital contributions to the basal tubera extend ventrally to the same level as their counterparts from the basisphenoid (Figs. 2.11A and B).

The posterior margin of the basioccipital forms an anteriorly pointing 'V-shape' in ventral view, inserting into the body of the basisphenoid (Figs. 2.11D and 2.12G). This results in the articulation surface for the basisphenoid extending onto the anterolateral

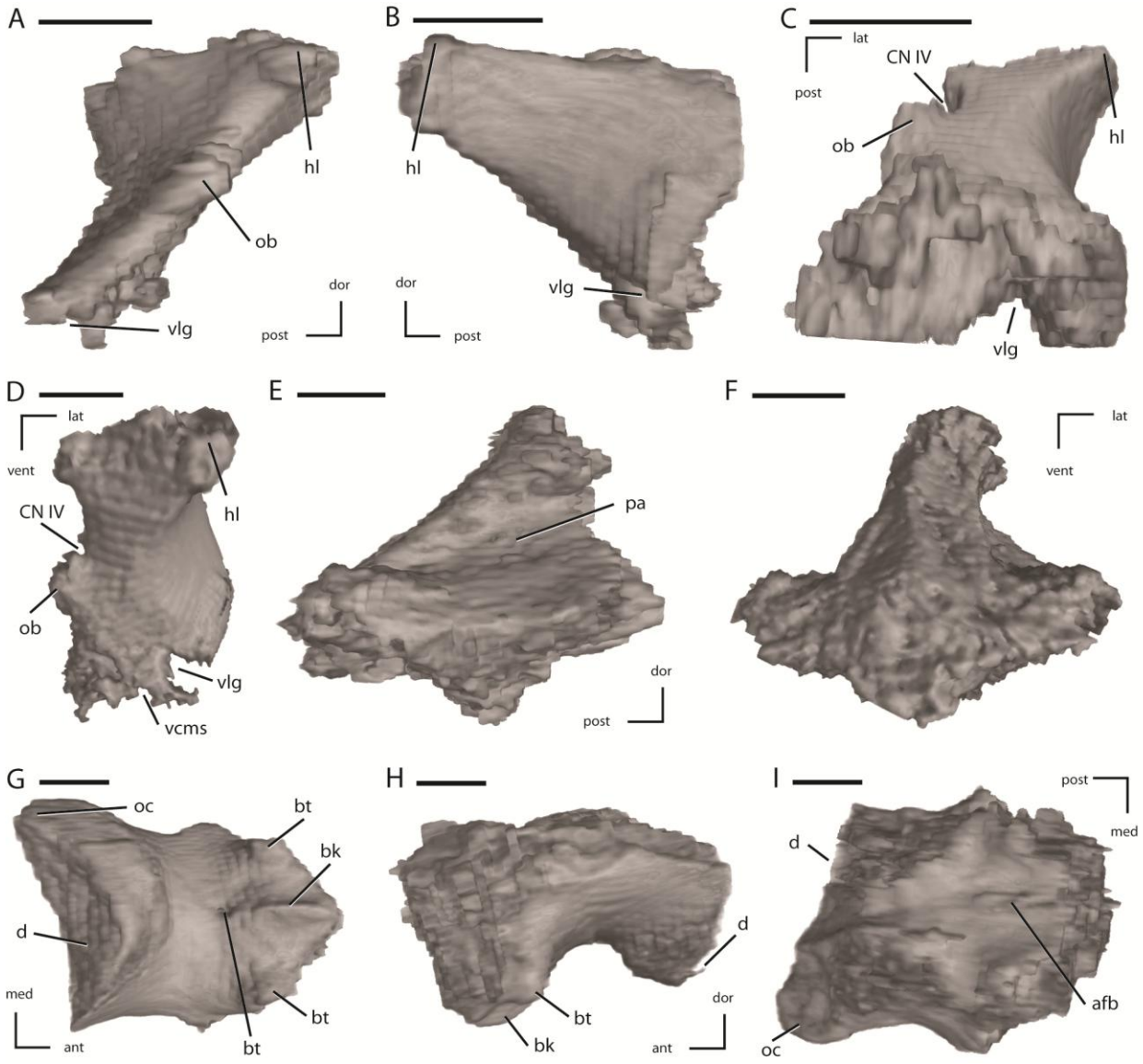

Figure 2.12: Left laterosphenoid, the supraoccipital, and the basioccipital of NCSM 15728. **A**. Left laterosphenoid in medial view. **B**. Left laterosphenoid in lateral view. **C**. Left laterosphenoid in ventral view. **D**. Left laterosphenoid in anterior view. **E**. Left supraoccipital in right lateral view. **F**. Left supraoccipital in posterior view. **G**. Basioccipital in ventral view. **H**. Basioccipital in left lateral view. **I**. Basioccipital in dorsal view. The directional arrows indicate the orientation of the specimen in each view. Scale bars equal 1 cm. See Appendix 2 for anatomical abbreviations.

surfaces of the basioccipital (Figs. 2.11A, 2,11B, 2.11D, and 2.12H), creating a tightly interlocking contact between these two elements. A similar morphology is seen in the basal neornithischians *Changchunsaurus* and *Haya* (Jin et al., 2010; Makovicky et al., 2011) and the basal iguanodontian *Anabisetia* (Coria and Calvo, 2002). Alternatively, the anterior margin of the basioccipital is 'W-shaped' (indented posteriorly along the midline) in *Zephyrosaurs* (Sues, 1980), and is relatively flat in *Thescelosaurus assiniboiensis* (Brown et al., 2011). In *Hypsilophodon* and *Parksosaurus* the basioccipital and basisphenoid are indistinguishably fused, obscuring the shape of their mutual contact (Galton, 1973, 1974a). The lateral portions of the dorsal surface (Fig. 2.12I) form rugose articulation surfaces for the fused opisthotic/exoccipital (posteriorly) and the prootic (anteriorly). Between these articulation surfaces the medial third of the dorsal surface of the basioccipital is slightly depressed and roughly 'hour-glass' shaped, forming the posterior portion of the floor of the braincase. The anterior portion of this depressed surface is dorsally arched along the midline (Fig. 2.12: afb), as in all non-iguanodontian basal neornithischian taxa except *Othnielosaurus* (Scheetz, 1999).

Basisphenoid/Parasphenoid

The anteroposterior length of the basisphenoid, not including the parasphenoid, is shorter than the length of the basioccipital (Fig. 2.11D). The posterodorsal surface of the basisphenoid formed the anteroventral floor of the braincase (Fig. 2.13J). The posteroventral margin of the basisphenoid contribution to the floor of the braincase extended posteriorly and slightly overlapped the dorsal surface of the basioccipital (Fig.

2.13I). The median ridge on the anterodorsal surface of the basioccipital extends onto the basisphenoid. On either side of this median ridge a shallow groove is present that deepens posteriorly, eventually connecting to a set of foramina that penetrate the floor of the braincase and pass into the posterodorsal surface of the sella turcica (Fig. 2.13J). The abducens nerve (CN VI) passed through these foramina. Lateral and slightly ventral to the basisphenoid contribution to the floor of the braincase, the laterally projected preotic pendants are present (Figs 2.13G through K: prp). The dorsal surfaces of the preotic pendants face posterodorsally and formed part of the articulation surface for the prootic (Figs. 2.11A and B). Their lateral margins are slightly dorsoventrally concave. A sharp ridge marks the ventrolateral margin of these processes, and the surface ventral to this ridge is dorsoventrally concave (Fig. 2.13K). This concavity deepens posteriorly, forming a mediolaterally narrow fossa posteroventral to each preotic pendant.

The posterior surface of the basisphenoid forms a ‘V-shaped’ (in ventral view) contact with the anterior surface of the basioccipital (Fig. 2.13H), with the posterolateral margins of the basisphenoid extending onto the posterolateral surfaces of the basioccipital. The basisphenoid contribution to the basal tubera was level with the corresponding contribution from the basioccipital (Figs. 2.11A and B). The lateral surfaces of the basisphenoid were concave anteroposteriorly and convex dorsoventrally posterior to the basipterygoid processes (Fig. 2.13H). The ventral surface is slightly anteroposteriorly concave and mediolaterally convex anterior to the basipterygoid processes. Between the basipterygoid processes the ventral surface is mediolaterally and anteroposteriorly concave. The basipterygoid processes are stout and project

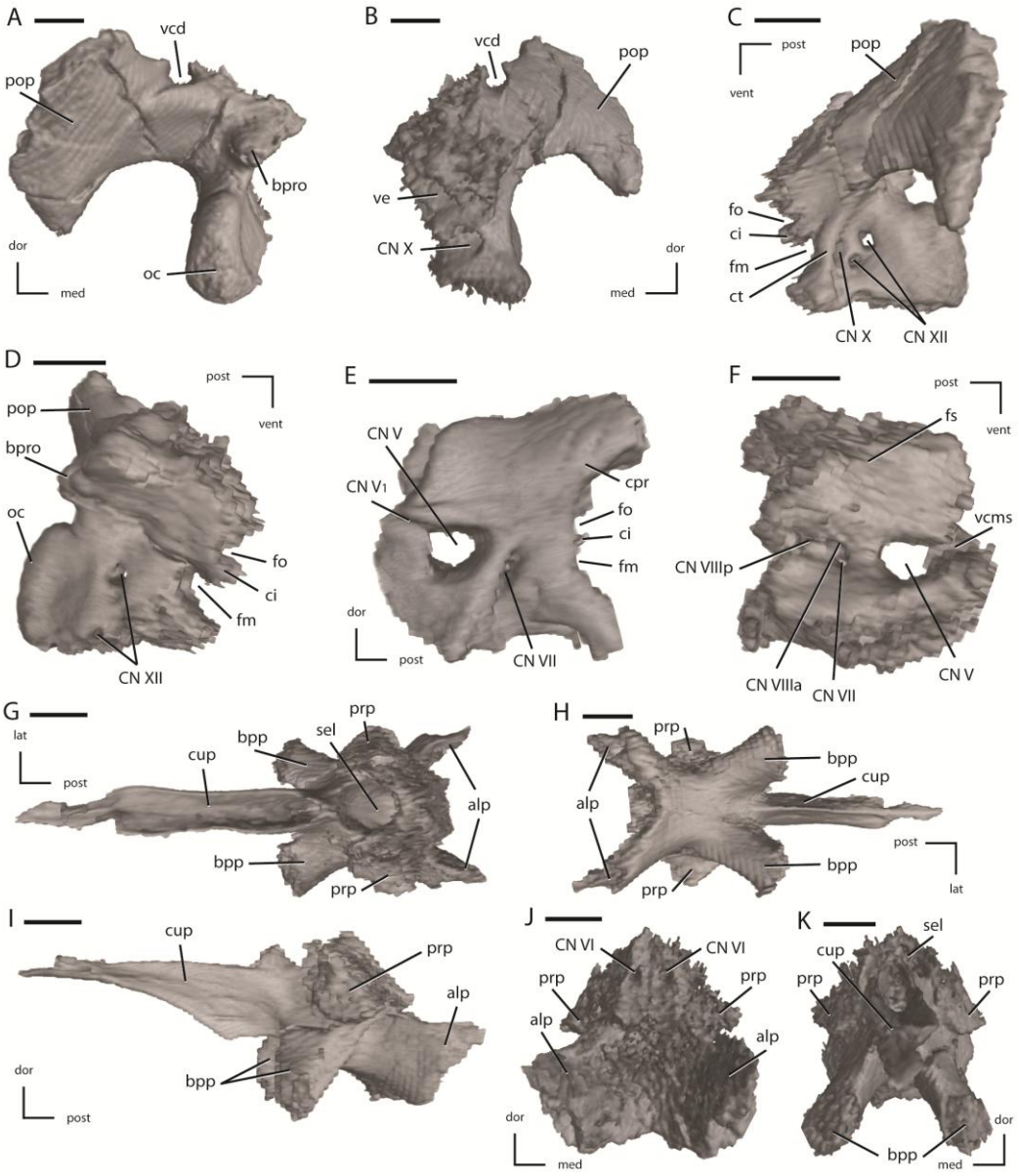

Figure 2.13: Left fused opisthotic/exoccipital, left prootic, and the fused basisphenoid/parasphenoid of NCSM 15728. **A**. Left fused opisthotic/exoccipital in posterior view. **B**. Left fused opisthotic/exoccipital in anterior view. **C**. Left fused opisthotic/exoccipital in lateral view. **D**. Left fused opisthotic/exoccipital in medial view. **E**. Left prootic in lateral view. **F**. Left prootic in medial view. **G**. Fused basisphenoid/parasphenoid in dorsal view. **H**. Fused basisphenoid/parasphenoid in ventral view. **I**. Fused basisphenoid/parasphenoid in left lateral view. **J**. Fused basisphenoid/parasphenoid in posterior view. **K**. Fused basisphenoid/parasphenoid in anterior view. The directional arrows indicate the orientation of the specimen in each view. Scale bars equal 1 cm. See Appendix 2 for anatomical abbreviations.

anterolaterally from the ventrolateral corners of the basisphenoid (Figs. 2.13G, H, I, and K). These processes are oriented approximately sixty degrees from each other (Figs. 2.13H and K). The posterior margins of the basipterygoid processes are mediolaterally convex, while the anterior edges consist of sharply rounded ridges. The anteroventral surfaces of the basipterygoid processes are mediolaterally and dorsoventrally flattened, forming contact surfaces for the pterygoids (Figs. 2.13H, I, and K).

The cutriform process arises just anterior to the bases of the basipterygoid processes and projects anteriorly along the midline (Figs. 2.13G, H, and I), with the anterior tip extending between the palatines. Mediolateral compression of the specimen caused the palatines to compress and damage the anterior end of the cutriform process (Figs. 2.13G and H). The ventral surface of the cutriform process bears a distinct ventral ridge that deepens posteriorly until just anterior to the basipterygoid processes, at which point the ventral ridge decreases in dorsoventral height until it ends approximately level with the anterior margin of the basipterygoid processes. This gives the ventral margin of the cutriform process a triangular shape in lateral view (Fig. 2.13I). The dorsal surface of the cutriform process is mediolaterally concave, with the dorsolateral projections on either side of the dorsal concavity becoming dorsoventrally taller and more vertically oriented posteriorly (Fig. 2.13G). The dorsolateral margins contact each other just anterior to the sella turcica, creating a short foramen (Fig. 2.13G). This foramen passes into the anteroventral surface of the sella turcica.

The sella turcica is enclosed within the anterodorsal portion of the basisphenoid (Fig. 2.13G). The foramina for the internal carotid arteries pass through the

posteroventral corners of the sella turcica, exiting in the fossa ventral to the preotic pendants. Many authors have speculated that the foramina for the internal carotid arteries were present ventral to the preotic pendants (e.g., Galton, 1974a, 1989; Sues, 1980; Sereno, 1991; Butler et al., 2007), but their presence was never previously observed either via visual inspection or examination of CT data (Butler, 2010). The CT data collected from NCSM 15728 confirms the presence of these foramina ventral to the preotic pendants in at least this taxon. The fused basisphenoid/parasphenoid of NCSM 15728 differs substantially from that of the basal neornithischian *Zephyrosaurus*. In the latter taxon the basipterygoid processes projected ventrally, but not anteriorly (Sues, 1980). The ventral surface of the basisphenoid bears an elongate groove extending from the posterior contact with the basioccipital to the base of the cutriform process anteriorly (Sues, 1980). Additionally, the posterolateral surface of the basisphenoid bears a prominent depression (Sues, 1980), which is lacking in NCSM 15728.

Opisthotic/Exoccipital

The ventral margin of the fused opisthotic/exoccipital formed an extensive contact with the dorsolateral surface of the basioccipital (Figs. 2.13C through D). The posteroventral portion of the fused opisthotic/exoccipital forms the dorsolateral corner of the occipital condyle (Fig. 2.13A: oc), unlike in ankylopollexians where the exoccipital is excluded from the occipital condyle (Norman, 2004b). The ventral margin of this posterior process is mediolaterally wider than the dorsal margin, and the dorsal edge is mediolaterally convex (Fig. 2.13A). The medial surface of the fused

opisthotic/exoccipital is broadly dorsoventrally concave, forming the posterolateral wall of the braincase (Fig. 2.13A). A small, shallow fossa is present on the medial surface for the remnant of the vena cerebralis posterior (Galton, 1989). The posteromedial margin of the fused opisthotic/exoccipital forms the majority of the foramen magnum. On the posterior surface of the dorsomedial corner of the fused opisthotic/exoccipital a posteriorly projecting boss is present (Fig. 2.13A and D: pbro) that served as the articulation surface for the proatlas (Sereno, 1991). The anterodorsal surface of the fused opisthotic/exoccipital forms a complex articulation surface with the supraoccipital that is pierced by the foramen for the posterior semicircular canal. The anterior margin formed an extensive contact with the prootic, and the foramen for the lateral semicircular canal is present on the dorsal portion of this contact. Medial to the foramen for the lateral semicircular canal a fossa is present that formed the posterior portion of the vestibule (Fig. 2.13B).

The paroccipital process arises from the dorsolateral body of the fused opisthotic/exoccipital and extends dorsolaterally (Fig. 2.13A). The paroccipital process is anteroposteriorly thinner than anteroventrally tall. The distal end of the paroccipital process expands ventrally, giving it a ‘pendent-shape’ in posterior view (Fig. 2.13A), unlike in the basal ornithischian *Lesothosaurus* (Sereno, 1991), basal thyreophorans (Norman et al., 2004b), and the basal neornithischians *Agilisaurus*, *Gasparinisaura*, and *Hypsilophodon* (Galton, 1974a; Peng, 1992; Coria and Salgado, 1996) where the distal end is at most slightly widened. There is no enclosed posttemporal foramen in the paroccipital process; instead, the dorsal margin of the paroccipital process is notched by a

‘Y-shaped’ groove that is open dorsally through which passed the vena capitis dorsalis (Figs. 2.13A and B), as in *Thescelosaurus assiniboiensis* (Brown et al., 2011). This groove begins on the posteromedial surface of the paroccipital process and extends anteromedially over the dorsal margin of the neck of the paroccipital process. At the apex of the dorsal margin the paroccipital process this groove bifurcates, with one branch passing anteriorly through a deep, nearly enclosed groove and the other branch angling dorsomedially to the contact with the supraoccipital. This latter groove continued onto the dorsal margin of the supraoccipital, while the former penetrates the medial process of the squamosal. The anterior surface of the paroccipital process broadly contacted the posterior surface of squamosal.

The crista tuberalis is a prominent ridge that arises along the ventral margin of the paroccipital process and extends anteroventrally to the contact with the basioccipital (Figs. 2.13C and D). Anterior to the crista tuberalis portions of three foramina/fenestra are present. The anterior-most of these is the posterior margin of the fenestra ovalis (Figs. 2.13C and D), into which the stapes inserts. Posterior to the fenestra ovalis an anteroventrally projecting process, the crista interfenestralis, separates the fenestra ovalis from the foramen metoticum (Figs. 2.13C and D). The foramen metoticum facilitates the passage of the glossopharyngeal nerve (CN IX), the accessory nerve (CN XI), and the vena jugularis interna from the braincase (Galton, 1989). Dorsal to these foramina the anteroventral surface of the paroccipital process is very shallowly concave (Figs. 2.13C) and lacks the dorsoventrally deep and anteroposteriorly narrow lateral opisthotic fossa seen in *Orodromeus*, *Skaladromeus*, and *Zephyrosaurus* (Sues, 1980; Scheetz, 1999; C.

Boyd, pers. obs.). A foramen present on the anterior surface of the crista tuberalis (Fig. 2.13B) passes posteriorly through this ridge, emerging on its posterior surface (Fig. 2.13C). The vagus nerve (CN X) exits the braincase via the foramen metoticum and then passes posteriorly through this foramen. Posterior to the crista tuberalis, the ventrolateral surface of the fused opisthotic/exoccipital is pierced by two closely spaced foramina (Fig. 2.13C). The more dorsally positioned foramen penetrates medially to the lateral wall of the braincase and housed the posterior ramus of the hypoglossal nerve (CN XII). The ventral-most foramen also penetrated directly medially to the lateral wall of the braincase and housed the anterior ramus of the hypoglossal nerve (Fig. 2.13D). In the basal neornithischian *Jeholosaurus* only a single foramen is present on the lateral surface for the passage of the hypoglossal nerve (Barrett and Han, 2009).

Prootic

The prootic formed the lateral wall of the braincase and was bordered posteriorly by the opisthotic, posteroventrally by the basioccipital, anteroventrally by the basisphenoid, anteriorly by the laterosphenoid, and dorsally by the supraoccipital (Figs. 2.11A and B). The dorsal margin is slightly anteroposteriorly concave, with the posterior end rising dorsally to overlap the posterodorsal surface of the fused opisthotic/exoccipital (Fig. 2.11A). The dorsal articulation surface for the supraoccipital is roughly triangular in shape, being mediolaterally broad posteriorly and narrowing anteriorly, and is pierced by the foramen for the anterior semicircular canal. The anterodorsal corner or the prootic bears a dorsoventrally elongate projection that inserted into the posterior end of the

laterosphenoid (Fig. 2.13E). The anteroventral corner of the prootic is broadly rounded to contact the basisphenoid.

The lateral surface of the prootic is pierced by two foramina (Fig. 2.13E). The trigeminal, or prootic, foramen for CN V (the trigeminal nerve) is located near the anterior end of the prootic and is entirely enclosed within the prootic (Fig. 2.13E), unlike in *Thescelosaurus assiniboiensis* (Brown et al., 2011). A narrow groove extends from the anterodorsal corner of this foramen and extends anterodorsally onto the posteroventral margin of the laterosphenoid (Fig. 2.13E). The ramus ophthalamicus (CN V_1) of the trigeminal nerve likely passed anteriorly through this groove before passing through a similar groove in the laterosphenoid. A narrow ledge projects over the dorsal margin of the trigeminal foramen, beginning at the anterior margin of the prootic and extending posteriorly about half the length of the prootic. The facialis foramen (sensu Galton, 1989) for CN VII is a relatively small foramen positioned posteroventral to the trigeminal foramen (Fig. 2.13E). A flat sheet of bone extends posterolaterally between these foramina, laterally overhanging the facialis foramen. This sheet of bone runs anteroventrally and is confluent with the posterolateral margin of the basipterygoid process of the basisphenoid. A depression extends ventral to the facialis foramen medial to this sheet, through which passed the ramus palatines (CN $VII_{p:}$ Galton, 1989). The posteroventral corner of the prootic extends ventral to the fenestra ovalis to contact the dorsal margin of the basioccipital and the anteroventral corner of the fused opisthotic/exoccipital. The crista prootica (Fig. 2.13E: cpr) forms a sharp edge overhanging the anterodorsal margin of the foramen ovale (Fig. 2.13E: fo) and, more

ventrally, the lateral surface of the lagenar recess. The fenestra ovalis, into which the stapes inserts, notches the posterior margin of the prootic at approximately mid-height, with the fused opisthotic/exoccipital forming the posterior margin of this fenestra (Fig. 2.11A). Just ventral to the fenestra ovalis the posterior margin is indented to form the ventral margin of the foramen metoticum (Fig. 2.13E). Dorsal to the fenestra ovalis, the posterodorsal contact surface for the fused opisthotic/exoccipital is penetrated by the foramen for the lateral semicircular canal.

On the dorsomedial surface of the prootic, near the suture for the supraoccipital, the shallow, anteriorly facing fossa subarcuata is present (Fig. 2.13F: fs). Near the anterior margin of the medial surface the foramen for the trigeminal nerve is present. Extending from the anteromedial margin of the trigeminal foramen is a deeply recessed groove that runs anteriorly to the contact with the ventral edge of the laterosphenoid (Fig. 2.13F: vcms). It is likely that at least the vena cerebralis media secunda, if not the entire vena cerebralis media, occupied this medial groove and exited the foramen at the posteroventral margin of the laterosphenoid. The ramus ophthalamicus (CN V_1) of the trigeminal nerve likely did not pass through this groove; rather, it occupied the groove on the lateral surface of the prootic (Fig. 2.13E). Posterior to the trigeminal foramen, a fossa is present on the medial surface that contains three foramina (Fig. 2.13F), as in *Dysalotosaurus* (Galton, 1989).The facialis foramen for CN VII passes laterally out of the anteroventral corner of this fossa. The foramen for the anterior ramus of the acoustic nerve (Fig. 2.13F: CN $VIII_a$) is positioned in the anterodorsal portion of this fossa and travels dorsolaterally into the anterior utricular recess within the prootic. The foramen for

the posterior ramus of the acoustic nerve (CN $VIII_p$) is positioned posterodorsally in the fossa and extends posterodorsally into the lagenar recess. This differs from the morphology seen in the basal neornithischian *Hypsilophodon* and the basal iguanodontian *Dryosaurus* where a fossa does not connect the former two foramina with the foramen for the posterior ramus of the acoustic nerve (Galton, 1989).

Stapes

The stapes is a 'rod-shaped' bone that extends from the fenestra ovalis (formed by the fused opisthotic/exoccipital and the prootic) to the anterolateral surface of the paroccipital process, medial to the dorsal end of the quadrate (Fig. 2.11A), the presumed location of the otic notch (You and Dodson, 2004). The proximal end is broadened dorsoventrally where it enters the fenestra ovalis, with a thin ridge present on the dorsal surface. The full morphology of the proximal end cannot be determined because it is closely appressed to the braincase and difficult to fully distinguish in the CT scans and is covered by matrix, making it impossible to fully describe via visual examination. After exiting the fenestra ovalis, the stapes angles posteroventrally, and slightly dorsally as well. The mid-shaft portion is rounded in transverse section. Near the distal end the stapes narrows mediolaterally while expanding dorsoventrally, giving the distal end a triangular shape in lateral view.

The morphology of the stapes in NCSM 15728 closely matches that figured (though not described) for the basal ornithischian *Lesothosaurus* by Sereno (1991). Among basal neornithischians, a stapes is only identified for a single specimen of

Jeholosaurus (IVPP V15716: Barrett and Han, 2009). However, the position (near the distal condyles of the quadrate pointing posteriorly) and morphology of the presumed stapes in the referred specimen of *Jeholosaurus* (Barrett and Han, 2009:fig. 6) matches that of the element identified as a ceratobranchial in the holotype of *Changchunsaurus* (Jin et al., 2010:fig. 1b). In the same specimen of *Jeholosaurus*, a slender, 'rod-shaped' element exposed displaced in the infratemporal fenestra was identified as a possible epipterygoid (Barrett and Han, 2009:fig. 6). Among ornithischian dinosaurs, ossified epipterygoids are only known in a few ankylosaurian and pachycephalosaurian dinosaurs (Maryańska et al., 2004; Vickaryous et al., 2004). Thus, it seems most likely that the element identified as an epipterygoid in the referred specimen of *Jeholosaurus* (IVPP V15716) is actually a slightly displaced stapes, especially given that the specimen is extensively transversely crushed. A slender element in the holotype of *Jeholosaurus* positioned dorsolateral to the basisphenoid and exposed in ventral view was also identified as a possible epipterygoid (Barrett and Han, 2009). However, this bone is triangular to 'T-shaped' in cross section, owing to the presence of a ventrally projecting ridge and concave lateral and medial surfaces, and appears to be the tip of a larger element that is obscured by the basisphenoid (C. Boyd, pers. obs.). This morphology does not match the morphology of any epipterygoid previously reported for an ornithischian dinosaur (Maryańska et al., 2004; Vickaryous et al., 2004) or that of the stapes, and it seems likely this exposed end of bone is part of one of the bones of the palate. A stapes is preserved in original position in another referred (but undescribed) specimen of

Jeholosaurus (PKUP V 1601), and its morphology generally conforms with that here reported in NCSM 15728 (C. Boyd, pers. obs.).

Laterosphenoid

The laterosphenoid contacted the prootic along an obliquely inclined surface along it posteroventral margin (Fig. 2.11A). A dorsoventrally elongate, mediolaterally thin dorsomedial process of the prootic inserted into the posterior end of the laterosphenoid. There is no evidence of the posteroventrally projected prootic boss along the contact surface that inserted into the prootic that is seen in *Skaladromeus* (Chapter 3). The trigeminal, or prootic, foramen for CN V does not notch the posterior end of the laterosphenoid, unlike in the heterodontosaurid *Heterodontosaurus* (Norman et al., 2004c), the basal ornithischian *Lesothosaurus* (Sereno, 1991), the basal ornithischians *Gasparinisaura*, *Hypsilophodon*, *Jeholosaurus*, *Parksosaurus*, *Thescelosaurus assiniboiensis*, and *Zephyrosaurus* (Galton, 1973, 1974a; Sues, 1980; Coria and Salgado, 1996; Brown et al., 2011; C. Boyd, pers. obs.), the basal iguanodontians *Tenontosaurus* and *Zalmoxes* (Norman, 2004b; Weishampel et al., 2003), and the ankylopollexians *Camptosaurus* and *Iguanodon* (Norman, 2004b).

On the posteroventral corner of the anterior surface of the laterosphenoid, along the contact with the prootic, a deep groove is present through which a portion of the trigeminal nerve (CN V), the ramus ophthalamicus, (CN V_1: Galton, 1989) passed through after exiting the prootic foramen and traveling through an anterodorsally oriented groove on the lateral surface of the prootic (Figs. 2.12A through D: vlg). A similar

groove is seen in the basal ornithischian *Lesothosaurus* (Sereno, 1991) and the basal neornithischians *Orodromeus* and *Zephyrosaurus* (Sues, 1980; Scheetz, 1999). Just ventromedial to this groove the dorsal edge of a foramen notches the ventral margin of the laterosphenoid, along the contact with the prootic (Fig. 2.12D: vcms). The vena cerebralis media passes through a channel between the prootic and the laterosphenoid anterodorsal to the trigeminal foramen in the basal neornithischian *Zephyrosaurus* and the basal iguanodontian *Dryosaurus* (Galton, 1989), with the vena cerebralis media secunda then passing anteriorly through a groove in the posteroventral margin of the laterosphenoid. Thus, it is likely that at least the vena cerebralis media secunda passed through this foramen in NCSM 15728, if not the entire vena cerebralis media.

The lateral surface of the laterosphenoid is dorsoventrally convex and anteroposteriorly concave and lacks the foramen in the posteroventral corner seen in *Lesothosaurus* that is hypothesized as the foramen for the oculomotor nerve (CN III: Sereno, 1991). The dorsal margin articulates with the ventral margin of the parietal, and this contact consists of a sharp ridge anteriorly that becomes mediolaterally broader posteriorly and bears a series of low ridges and grooves that interlocks with corresponding ridges and grooves on the parietal. This ridge extends anterior to the medial margin of the head of the laterosphenoid. The anterodorsal head of the laterosphenoid turns laterally (Fig. 2.12D), forming a broad contact surface with the frontal and the postorbital, as in all basal neornithischians except *Orodromeus* (Scheetz, 1999) and in the basal iguanodontians *Tenontosaurus dossi* and *Zalmoxes* (Weishampel

et al., 2003; Norman, 2004b). The anterior margin of the head is concave (Fig. 2.12C), while the posteromedial and lateral margins are slightly convex (Figs. 2.12A and B).

The dorsomedial surface is broadly concave both dorsoventrally and anteroposteriorly (Fig. 2.12A). The medial margin consists of a rounded ridge that extends from the posteromedial corner of the laterosphenoid to the anterodorsal head. Midway along this ridge an expanded, anteromedially projected boss is present (Fig. 2.12A, C, and D: ob). In *Hypsilophodon*, a similar boss, or step, on the anteromedial edge is hypothesized to demarcate the ventral extent of the unossified orbitosphenoid (Galton, 1974a), and in *Dryosaurus* a similar boss is present at the ventral margin of the contact between the laterosphenoid and the ossified orbitosphenoid (Galton, 1989). Just dorsal to this boss a semicircular depression is present, indicating the presence of a foramen that passed between the laterosphenoid and the orbitosphenoid (Figs. 2.12C and D). In *Dryosaurus*, the foramen for the trochlear nerve (CN IV) passes between the laterosphenoid and the orbitosphenoid dorsal to the medially projecting boss (Galton, 1989), making it likely that this foramen served the same function.

Supraoccipital

The posteroventral tip of the supraoccipital just barely contacts the dorsal margin of the foramen magnum, as seen in *Thescelosaurus assiniboiensis* (Brown et al., 2011) and unlike all other basal ornithischians where the supraoccipital forms a substantial portion of the dorsal margin of the foramen magnum (Norman et al., 2004c). A few small foramina pierce the dorsal surface of the posteromedial portion of the supraoccipital (Fig.

2.4); however, none of these foramina penetrate through to the ventral surface of the supraoccipital and do not represent the relatively large, medially situated supraoccipital foramen present in *Thescelosaurus assiniboiensis* (Brown et al., 2011). Two narrow grooves extend along the dorsal surface of the supraoccipital, beginning at the posterolateral margins and extending anteromedially until they reach distinct foramina that pierce the dorsal surface of the supraoccipital. These grooves are continuations of the dorsally open grooves present on the fused opisthotic/exoccipital that contained vena capitis dorsalis, as seen in *Thescelosaurus assiniboiensis* (Brown et al., 2011).

The dorsal process of the supraoccipital is triangular-shaped in lateral view (Fig. 2.12E), being dorsoventrally tall anteriorly and tapering posteriorly. This dorsal process inserted into the concave ventral surface of the parietal. The posterodorsal surface of the dorsal process is slightly mediolaterally convex, but lacks the distinct nuchal crest seen in the basal ornithischians *Eocursor* and *Lesothosaurus* (Sereno, 1991; Butler, 2010), the basal neornithischians *Gasparinisaura* and *Orodromeus* (Scheetz, 1999), the basal iguanodontian *Tenontosaurus* (Norman, 2004b), and in some ankylopollexians (Norman, 2004b). The lateral surfaces of this dorsal process are gently dorsoventrally concave (Fig. 2.12E).

The ventrolateral processes of the supraoccipital are relatively thin posteriorly, but thicken anteriorly. The posteroventral margin of the ventrolateral processes sutured to the dorsomedial surface of the fused opisthotic/exoccipital. Posterior to this contact, the ventral surface formed an elongate contact with the prootic. The anterior margins of the ventrolateral processes thin to form narrow, posterodorsally inclined ridges. The medial

surface of the supraoccipital is deeply concave, forming the posterodorsal roof of the braincase. A separate or co-ossified epiotic forming an anterolaterally extending flange that was directed under the parietal wings, forming the posterodorsal part of the lateral wall of the braincase, which is seen in the basal ornithischians *Eocursor* and *Lesothosaurus* (Sereno, 1991; Butler, 2010), is absent in NCSM 15728.

Dorsally directed fossae that formed the dorsal portions of the vestibules are present along the ventral margins of the ventrolateral processes of the supraoccipital, along the shared contacts between the supraoccipital, prootic, and fused opisthotic/exoccipital. On each side, the dorsomedial surface of the fossa for the vestibule is penetrated by the foramen for the crus communis that extends dorsally into the supraoccipital close to the medial surface. The foramen for the crus communis bifurcates dorsally into the foramina for the anterior and posterior semicircular canals. The foramen for the posterior semicircular canal does not extend as far dorsally into the supraoccipital as the foramen for the anterior semicircular canal. The foramen for the posterior semicircular canal exits the posteroventral surface of the ventrolateral process of the supraoccipital along the articulation surface with the fused opisthotic/exoccipital. The foramen for the anterior semicircular canal extends high into the supraoccipital, then arcs ventrolaterally, eventually exiting the ventral margin of the supraoccipital along the articulation surface for the prootic. The fossa subarcuata (sensu Galton, 1989), a depression in the ventromedial surface of the supraoccipital adjacent to the prootic articulation surface that housed the floccular lobe of the cerebellum, lies within the loop formed by the anterior semicircular canal as in the basal neornithischians *Hypsilophodon*

and *Zephyrosaurus* and in basal iguanodontians (e.g., *Dryosaurus, Tenontosaurus*: Galton, 1989). The fossa subarcuata is greatly reduced relative to its development in the basal neornithischians *Hypsilophodon* and *Orodromeus* (Galton, 1974a; Scheetz, 1999), as also occurs in *Thescelosaurus assiniboiensis* (Brown et al., 2011).

Mandible

The mandibles of NSCM15728 are well preserved and remain in close contact with the rest of the skull (Figs. 2.1 and 2.2). Unfortunately, this resulted in much of the dentary dentition being obscured by the overhanging maxillary dentition. The post-dentary elements on the left side of the skull are slightly displaced from their original positions, making it easier to define the boundaries of the individual elements. Therefore, the post-dentary elements from the left side were used for the figures.

Predentary

The anterior tip of the predentary is sharply pointed in ventral view (Fig. 2.14B) as in heterodontosaurids (e.g., *Heterodontosaurus*: Butler et al., 2008b), basal neornithischians (e.g., *Jeholosaurus, Changchunsaurus*; Barrett and Han, 2009; Jin et al., 2010), and marginocephalians (e.g., *Archaeoceratops*, *Liaoceratops*, *Yinlong*: Xu et al., 2002; You and Dodson, 2003; Xu et al., 2006), and *Hypsilophodon* (Galton, 1974b), but unlike the rounded anterior margin seen in most basal iguanodontians (e.g., *Tenontosaurus*, *Zalmoxes*: Ostrom, 1970; Weishampel et al., 2003). The anteroventral surface is broadly rounded. A single, prominent foramen pierces the lateral surface of the main body of the predentary, though its placement varies slightly on each side (Figs.

2.14A and B: lfpd). Several smaller foramina are also present on the lateral surfaces, but their number and placement varies on each side. A broad, shallow groove extends posteroventrally along the lateral surface from near the anterior tip, passing through the lateral foramen, and ending near the middle of the embayment formed between the posterolateral and posteroventral processes that received the anterior tip of the dentary (Figs. 2.14A and B: lg). This groove is similar to the shallow groove seen in *Hypsilophodon* (Galton, 1974a), but not as prominent as the lateral groove seen in *Changchunsaurus* and *Jeholosaurus* (Barrett and Han, 2009; Jin et al., 2010). Prominent posterolateral processes extend posteriorly onto the dorsal surface of the anterior portion of the dentary (Figs. 2.14A and B: plpd) and are pierced at approximately mid-length by a foramen. The posterolateral processes are anteroposteriorly longer than dorsoventrally tall, and the posterior ends are bluntly pointed. The posterior end of the posterolateral processes are separated from the first dentary tooth by a gap that is between one and two tooth positions long.

The posteroventral process extends further posteriorly than the posterolateral processes (Fig. 2.14B: vppd), and the posterior third is distinctly bifurcated as in the basal neornithischians *Changchunsaurus, Haya*, and *Talenkauen* (Novas et al., 2004; Jin et al., 2010; Makovicky et al., 2011), basal ceratopsians (e.g., *Archaeoceratops, Liaoceratops*, *Yinlong*: Xu et al., 2002; You and Dodson, 2003; Xu et al., 2006), and some iguanodontians (e.g., *Zalmoxes, Dryosaurus*: Weishampel et al., 2003; Norman, 2004). The oral margin of the predentary is smooth and relatively straight, though the anterior tip is slightly dorsally projected (Fig. 2.14A), though not to the extent seen in some basal

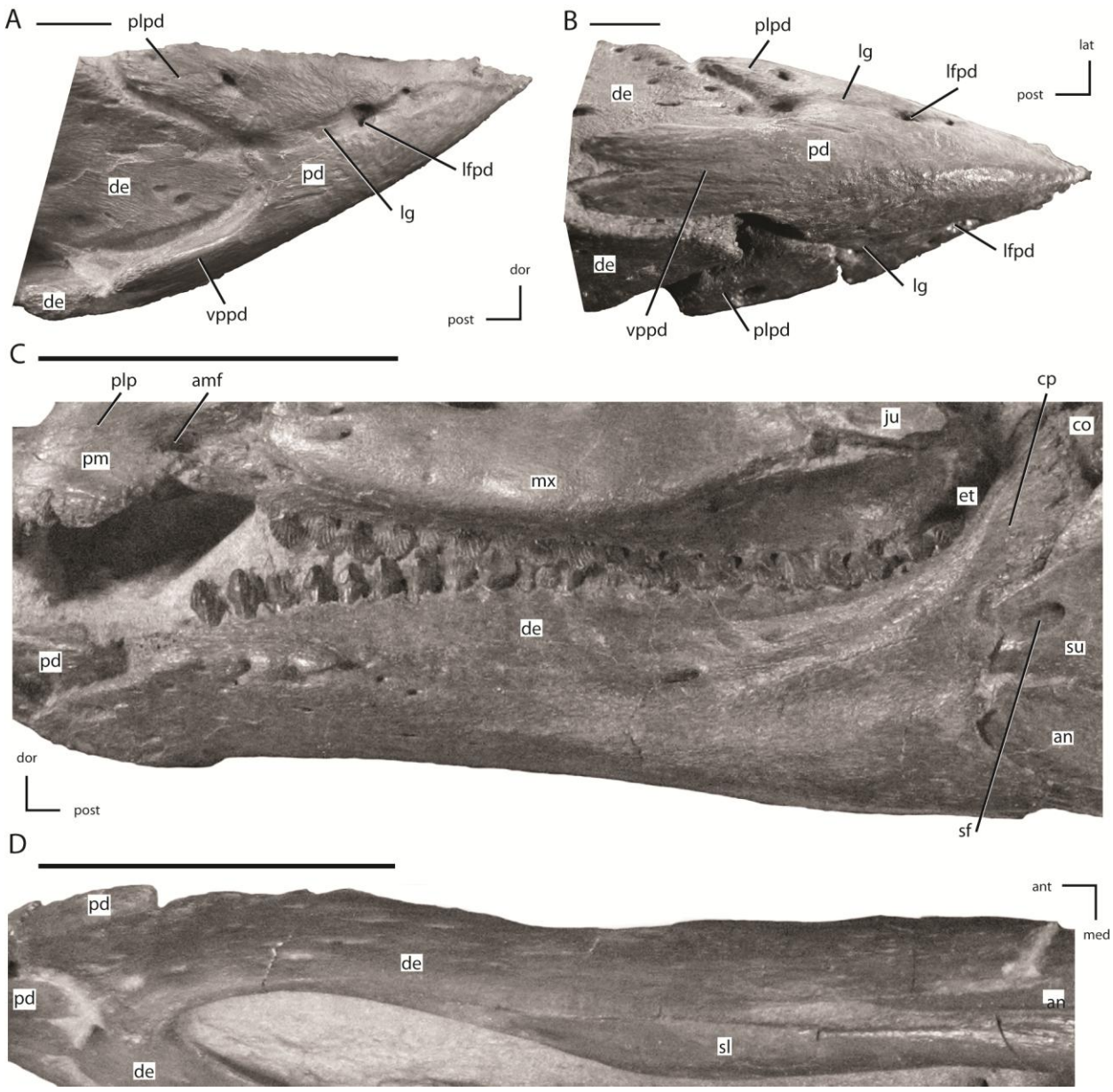

Figure 2.14: The predentary and dentary of NCSM 15728. **A**. Predentary in right lateral view. **B**. Predentary in ventral view. **C**. Left dentary in lateral view. **D**. Left dentary in ventral view. The directional arrows indicate the orientation of the specimen in each view. Scale bars in **A** and **B** equal 1 cm. Scale bars in **C** and **D** equal 5 cm. See Appendix 2 for anatomical abbreviations.

ceratopsians (e.g., *Ajkaceratops*, *Liaoceratops*: Xu et al., 2002; Osi et al., 2010). The anterior-most portion of the oral margin consists of a sharp ridge. This ridge flattens out and becomes mediolaterally wider posteriorly to form a triangular shaped, dorsally flattened surface that is broadly concave. The posterior-most premaxillary tooth ends just anterior to the posterior end of the oral margin of the predentary, and elongation of the premaxilla prevents the anterior maxillary teeth from occluding with the predentary. The articulation surface for the dentary consists of a broad, 'u-shaped' sulcus that extends from the posterior-most tip of the posterolateral processes down to the posterior-most tip of the posteroventral process (Fig. 2.14A).

Dentary

The dentary forms the majority of the mandibular ramus and is the only tooth bearing element of the lower jaw. There are twenty tooth positions within the dentary. The thyreophoran dinosaur *Scutellosaurus* and the basal neornithischians *Agilisaurus* and *Hexinlusaurus* all possess at least 18 dentary tooth positions (Colbert, 1981; He and Cai, 1984; Peng, 1992). The tooth row is not sinuous like it is derived thyreophorans (Norman et al., 2004b; Butler et al., 2008a), but the anterior portion of the dorsal surface slopes anteroventrally, causing the anterior three tooth positions to be offset ventrally below the rest of the dentary tooth row and the crowns are angled anterodorsally (Fig. 2.14C), a condition not seen in any other basal neornithischian taxon (Norman et al., 2004c). The anterior-most tip of the dentary is spout-shaped (Fig. 2.14D), as in all ornithischians

except *Eocursor* and heterodontosaurids (Butler et al., 2007, Butler et al., 2008a), and is positioned nearly level with the ventral margin of the dentary.

The dorsal and ventral margins of the dentary converge anteriorly (Figs. 2.14C), which is the primitive condition within Ornithischia. As in all ornithischians, the posterodorsal portion of the dentary forms the anterior portion of the coronoid process, contacting the coronoid medially and the surangular posteriorly. The posterior-most portion of the tooth row is situated medial to the rising coronoid process, as in the basal neornithischian taxa *Changchunsaurus* and *Jeholosaurus,* and in most iguanodontians (Jin et al., 2010; Norman, 2004; Barrett and Han, 2009). The lateral surface of the dentary is convex dorsoventrally with a pronounced ridge present that begins posteriorly at the base of the dentary contribution to the coronoid process, extends slightly anteroventrally to mid-length, then arcs anterodorsally, gradually becoming less pronounced and terminating near the first dentary tooth position (Fig. 2.14C). The lateral surface of the anterior third of the dentary is covered by numerous, irregularly distributed foramina, while posteriorly a few foramina are present in a row just dorsal to the lateral ridge.

The medial surface of the posterior end of the dentary is dorsoventrally concave and overlapped the lateral surfaces of the angular, coronoid, and surangular. The ventral surface is anteroposteriorly concave and mediolaterally convex. The medial surface of the dentary is convex both anteroposteriorly and dorsoventrally (Fig. 2.14D), as in all neornithischians except *Othnielosaurus* and *Zalmoxes* (C. Boyd, pers. obs., Weishampel et al., 2003; Norman et al., 2004c; Godefroit et al., 2009). There is a row of replacement foramina positioned ventromedial to the tooth row, as in all genasaurians and the

heterodontosaurid *Fruitadens* (Norman et al., 2004a; Butler et al., in press). The Meckelian groove is situated near the ventral margin. It begins near the anterior end as a shallow groove that is dorsoventrally broader than mediolaterally deep. As the groove extends posteriorly, it becomes slightly taller and substantially deeper, angling dorsolaterally into the dentary lateral to the roots of the dentary teeth. Near the posterior end, the anterior portions of the angular, prearticular, and surangular insert into this groove. The splenial overlaps the medial surface of the dentary, with its thickened, slightly ventrolaterally curved ventral margin sitting over the Meckelian groove.

Coronoid

The coronoid is composed of three processes (Figs. 2.16H and I), which differs from the strap-like coronoid present in *Lesothosaurus*, the thyreophoran *Scelidosaurus*, and the heterodontosaurid *Lycorhinus* (Sereno, 1991). The lobate dorsal process of the coronoid is positioned medial to the coronoid rise of the dentary and contacted the anterodorsal margin of the surangular (Figs. 2.16A and B). The morphology and position of the dorsal process is similar to that of the basal neornithischians *Changchunsaurus* (Jin et al., 2010) and *Hypsilophodon* (Galton, 1974a) and the basal ceratopsian *Psittacosaurus* (Sereno, 1987). A short ventral process was overlapped medially by the splenial, and was separated from the anterior process by a shallow sulcus (Figs. 2.16 H and I). This morphology differs from that seen in *Hypsilophodon*, in which the coronoid is triangular in medial view, lacking an anteroventral sulcus between the ventral and anterior projections (Galton, 1974a). The posteroventral portion of the coronoid is obscured by

the splenial in *Changchunsaurus* (Jin et al., 2010). The anterior process of the coronoid tapered anteriorly (Figs. 2.16H and I) and was relatively short compared to the elongate coronoids of *Changchunsaurus* (Jin et al., 2010) and *Lesothosaurus* (Sereno, 1991), but similar in length and shape to the coronoid of *Hypsilophodon* (Galton, 1974), extending medial to the posterior five dentary tooth positions.

Surangular

The anterior portion of the surangular is slightly medially deflected in dorsal view (Fig. 2.15G), mediolaterally thin, and was situated medial to the dentary (Fig. 2.15A). The anterior two-thirds of the ventral margin angles medioventrally and was overlapped laterally by the lateral wall of the angular (Fig. 2.15H). The dorsal margin of the surangular is convex in lateral view (Fig. 2.15E), which is the basal ornithischian condition. The dorsal-most portion of the surangular is triangular in lateral view, is convex medially, and forms the posterodorsal portion of the coronoid eminence (Fig. 2.16A). The anterodorsal margin contacted the dentary along its lateral half and the coronoid along its medial half.

The lateral surface of the surangular is flattened and oriented slightly posteriorly. Two distinct foramina are present on the lateral surface of the left surangular just posterior to the contact with the dentary (Fig. 2.15E: sf1 and sf2), but only a single foramen is present in the same area on the right surangular (Fig. 2.15A). The lateral foramina on the left surangular converge and exit the medial surface of the surangular through a single foramen (Fig. 2.15F: sf). Thus, the two foramina on the left surangular

and the single foramen on the right surangular represent the surangular foramen that is also present in the basal neornithischians *Changchunsaurus*, *Gasparinisaura*, *Hypsilophodon*, *Jeholosaurus*, *Orodromeus*, and *Oryctodromeus*, the basal ceratopsian *Yinlong*, and most basal iguanodontians (Galton, 1974a; Coria and Salgado, 1996; Scheetz, 1999; Norman, 2004; Xu et al., 2006; Barrett and Han, 2009; Jin et al., 2010; C. Boyd, pers. obs.). On the left dentary of the holotype of *Thescelosaurus edmontonensis* (CMN 8537; now referred to *Thescelosaurus* sp. [Boyd et al., 2009]) the surangular foramen consists of a single opening laterally, but bifurcates into two foramina by the time it exits the medial surface of the surangular (Galton, 1974b:figs. 1E and G). These observations indicate there is considerable variation in the morphology of the surangular foramen in *Thescelosaurus*, even within a single specimen.

There is a distinct, dorsolaterally directed, 'finger-like' process on the lateral surface of the surangular next to the glenoid (Figs. 2.15E through H), similar to the structure seen in the basal iguanodontians *Tenontosaurus tilletti* and *Zalmoxes robustus* (Weishampel et al., 2003; Norman, 2004). However, the dorsolateral process present in NCSM 15728 is dorsoventrally taller than anteroposteriorly wide (Fig. 2.15E), while the reverse condition is present in *Tenontosaurus tilletti* and *Zalmoxes robustus* (Weishampel et al., 2003; Norman, 2004). In several basal neornithischian taxa a low boss is present in this same region (e.g., *Changchunsaurus*, *Haya*, *Hypsilophodon*, *Orodromeus*, *Zephyrosaurus*: Galton, 1974a, 1997; Scheetz, 1999; Jin et al., 2010; Makovicky et al., 2011), though there is no boss or process present in the basal ornithischian *Lesothosaurus* (Sereno, 1991). Just anterior to the base of the dorsolateral process a single foramen is

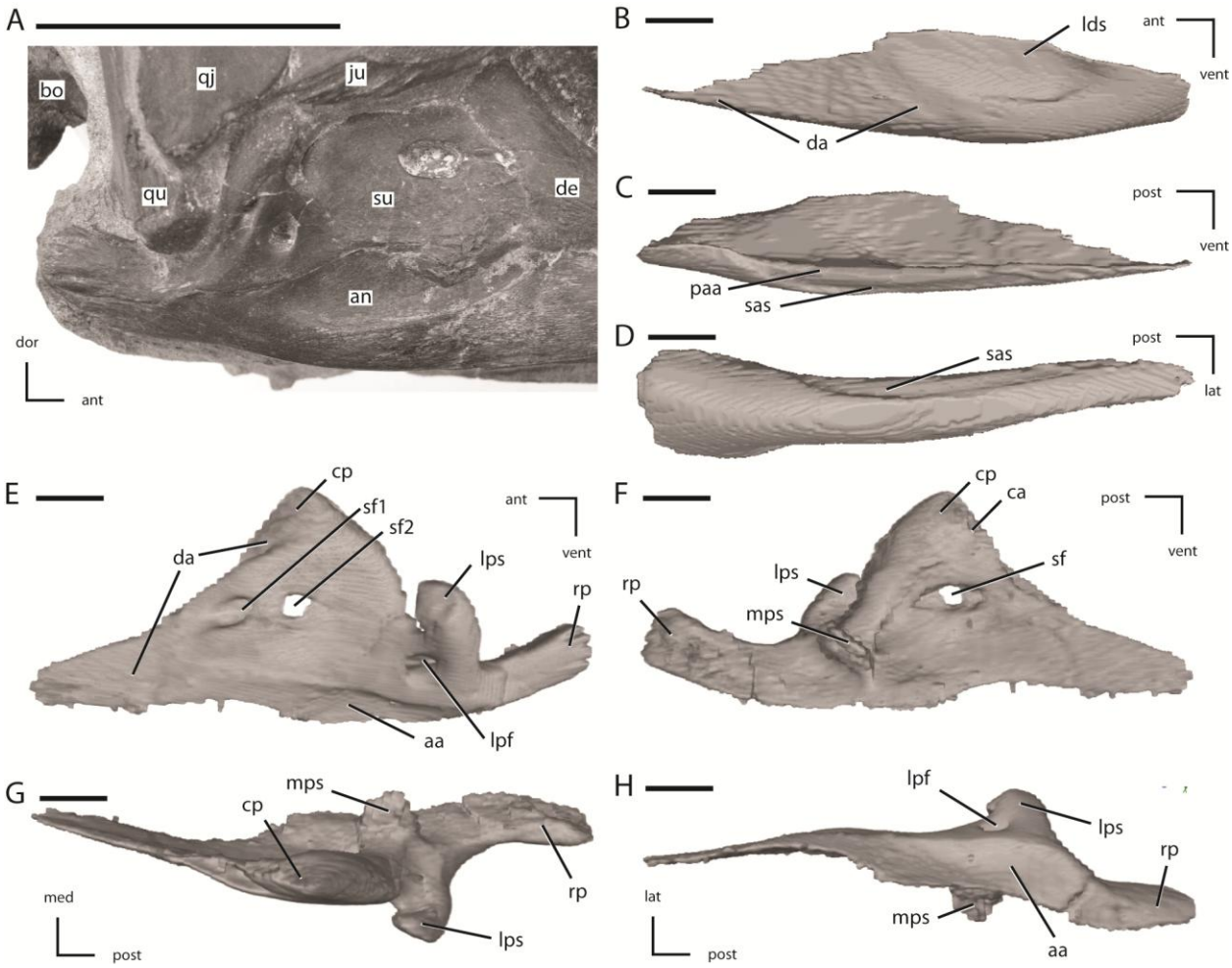

Figure 2.15: Posterior jaw elements of NCSM 15728. **A**. Photograph of the right post-dentary jaw elements in natural position. **B**. Left angular in lateral view. **C**. Left angular in medial view. **D**. Left angular in ventral view. **E**. Left surangular in lateral view. **F**. Left surangular in medial view. **G**. Left surangular in dorsal view. **H**. Left surangular in ventral view. The directional arrows indicate the orientation of the specimen in each view. Scale bar in **A** equals 5 cm. Scale bars in **B** through **H** equal 1 cm. See Appendix 2 for anatomical abbreviations.

present on the left surangular (Fig. 2.15E: lpf), while two foramina are present on the right surangular, with the second foramen positioned on the dorsolateral process (Fig.2.15A). Both foramina on the right surangular connect in the inside of the surangular and exit through a single, anteriorly facing foramen on the medial surface of the surangular just anterior to the medial process of the surangular, which is the same

location of the exit of the single foramen on the left surangular. A foramen is also present in this area in other basal neornithischian taxa (e.g., *Changchunsaurus*, *Haya*, *Hypsilophodon*: Galton, 1974a; Jin et al., 2010; Makovicky et al., 2011).

The posterior portion of the surangular is anteroposteriorly elongate and dorsoventrally narrow, forming the lateral and part of the ventral cup for the articular (Fig. 2.15E: rp). The lateral surface of the posterior margin of the retroarticular process is covered by a series of anteroposteriorly oriented grooves. The medial surface of the surangular is dorsoventrally and mediolaterally concave. Directly medial to the base of the dorsolateral process, a dorsoventrally flattened process projects medially (Figs. 2.15F and G), contacting a small process on the prearticular and forming a distinct foramen posterior to the articular (Fig. 2.16B). This process is also present in the holotype of *Thescelosaurus edmontonensis* (Galton, 1997). A similar process is not present in *Hypsilophodon* (Galton, 1974a), but the morphology of the medial surface of the surangular is poorly known in other basal neornithischian taxa.

Angular

The angular forms the posteroventral portion of the mandible (Figs. 2.15A, 2.16A, and 2.16C). The lateral wing of the angular extends dorsally much higher than the medial wing (Figs. 2.15B versus 2.15C). The anterior portion of the lateral wing is triangular-shaped and positioned medial to the dentary (Fig. 2.15B). Much of the medial surface of the lateral wing overlapped the ventrolateral surface of the surangular. The majority of the exposed lateral surface forms a shallow fossa that extends dorsally onto the

surangular (Figs. 2.15A, B, and E). The ventral margin of the angular is broadly convex anteroposteriorly and rounded mediolaterally (Figs. 2.15B and D). The ventral surface is mediolaterally widest posteriorly where it formed the ventral portion of the retroarticular process (Fig. 2.15D). The short medial wing has a complex contact with the prearticular (Figs. 2.15C and D). The posterior-most portion of the medial wall overlapped the ventral surface of the prearticular medially, but the majority of the medial wing of the angular was positioned lateral to a short ventral flange of the prearticular, resulting in the presence of a narrow, dorsomedially facing contact surface on the medial wing of the angular (Fig. 2.15C: paa). Ventral to this contact surface for the prearticular, a second, dorsoventrally narrow contact surface is present for the posterior process of the splenial (Figs. 2.15C and D: sas).

Splenial

The splenial is a thin, 'plate-like' bone positioned along the posteromedial portion of the mandible (Fig. 2.16A). The majority of the splenial is mediolaterally thin, except for the ventral margin which is thickened where it overlapped the Meckelian groove of the dentary (Fig. 2.16E). The medial surface is dorsoventrally concave. The anterior two-thirds is triangular (Fig. 2.16D) with the narrow anterior tip positioned near the Meckelian groove along the ventral margin of the dentary and the maximum dorsoventral height positioned close to the level of the posterior-most tooth position of the dentary. No foramen is present near the anterior tip of the splenial, unlike in the basal

neornithischians *Changchunsaurus* and *Haya* (Jin et al., 2010; Makovicky et al., 2011) and in saurischian dinosaurs (Rauhut, 2003).

The posterior third of the splenial consist of a dorsoventrally narrow posterior process that contacted the prearticular and angular medially (Fig. 2.16A). This posterior process is not bifurcate, unlike the basal neornithischian *Changchunsaurus* and the marginocephalians *Archaeoceratops* (Jin et al., 2010). The splenial is not visible in lateral view along the ventral margin of the dentary in this specimen (Figs. 2.1 and 2.2), but because both splenials are slightly displaced from life position this may not have been the natural condition.

Prearticular

The prearticular is a mediolaterally flatted bone that forms the posteromedial-most portion of the mandible (Figs. 2.16A and C). The posterior end is laterally concave where it rested against the articular, forming the medial surface of the retroarticular process. The anterior portion of the prearticular consists of two processes (Figs. 2.16D and E). The anterodorsal process is dorsoventrally tall and mediolaterally thin, angled anterodorsally, and was situated lateral to the splenial. Unlike the prearticular of *Changchunsaurus*, the anterior end is not twisted to face ventromedially (Jin et al., 2010). The anteroventral process was dorsoventrally narrow and was situated between the angular and the splenial. A prominent ridge is present on the lateral surface of the anteroventral process that extends posterior about two-thirds of the length of the prearticular (Fig. 2.16G: ra). The surface ventral to this ridge demarcates the contact for

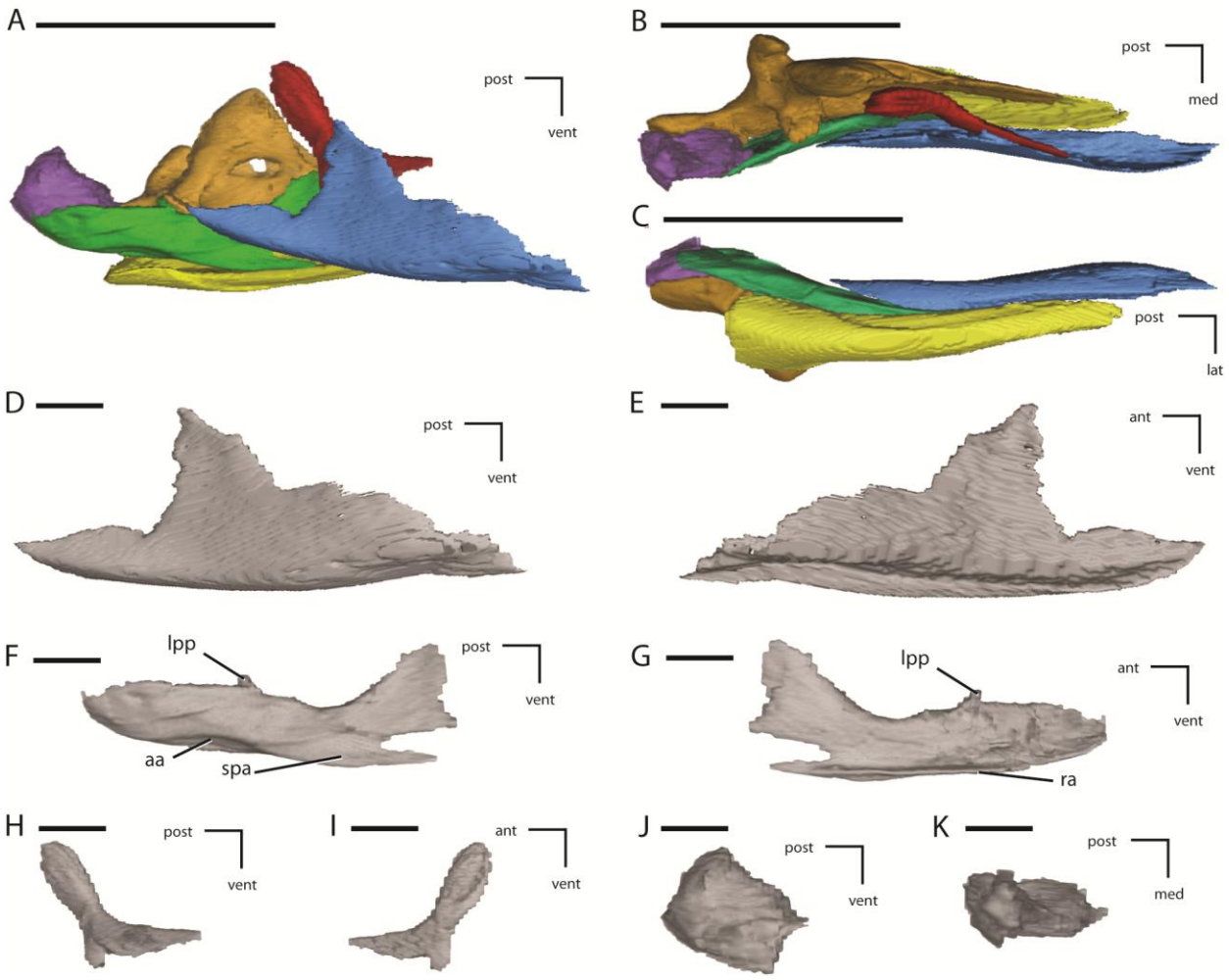

Figure 2.16: Additional figures of teft posterior jaw elements of NCSM 15728. **A**. Left post-dentary elements in medial view. **B**. Left post-dentary elements in dorsal view. **C**. Left post-dentary elements in ventral view. **D**. Left splenial in medial view. **E**. Left splenial in lateral view. **F**. Left prearticular in medial view. **G**. Left prearticular in lateral view. **H**. Left coronoid in medial view. **I**. Left coronoid in lateral view. **J**. Left articular in medial view. **K**. Left articular in dorsal view. Key to colors: Red = Coronoid; Orange = Surangular; Yellow = angular; Blue = Splenial; Green = Prearticular; Purple = articular. The directional arrows indicate the orientation of the specimen in each view. Scale bars in **A** through **C** equal 5 cm. Scale bars in **D** through **K** equal 1 cm. See Appendix 2 for anatomical abbreviations.

the angular. Posteriorly, this contact surface rotates from ventrally facing to medially facing, where the posterior-most portion of the angular overlapped the lateral surface of the prearticular (Fig. 2.16F: aa).

This complex contact with the angular is atypical for basal neornithischians, where the angular generally overlaps the ventral edge of the prearticular medially (e.g., *Hypsilophodon*: Galton, 1974a). There is no evidence of the narrow slit in the posterior portion of the prearticular noted in *Hypsilophodon* (Galton, 1974a). At approximately midlength along the dorsal margin a short, laterally projecting process is present that contacted a corresponding medially directed process on the surangular (Figs. 2.16F and G: lpp), creating a foramen anterior to the articular (Fig. 2.16B).

Articular

The articular is roughly rectangular in both lateral (Fig. 2.16J) and dorsal views (Fig. 2.16K), being slightly anteroposteriorly longer than dorsoventrally tall, unlike the triangular articular of *Hypsilophodon* or the elliptical articular of *Agilisaurus* (Galton, 1974a; Peng, 1992). The articular is positioned within a distinct cup formed by the prearticular medially, the angular ventrally, and the surangular laterally, which is generally the case in basal neornithischians (e.g., *Hypsilophodon*, *Orodromeus*: Galton, 1974a; Scheetz, 1999). The anterodorsal surface is mediolaterally convex, for articulation with the distal condyles of the quadrate (Fig. 2.16K).

Accessory Ossifications

Supraorbital

The supraorbital bar is composed of two elements (Figs. 2.17A and B): the supraorbital, often referred to as a palpebral (e.g., Barrett et al., 2005; Barrett and Han, 2009; Jin et al., 2010; Makovicky et al., 2011); and, an accessory supraorbital (= postpalpebral of Makovicky et al. [2011] and the supraorbital of Barrett et al. [2005]). An accessory supraorbital is also present in the basal neornithischian taxa *Agilisaurus* and *Haya* (Barrett et al., 2005; Makovicky et al., 2011) and multiple supraorbitals (up to 3) are present in some derived thyreophorans and pachycephalosaurians (Maryańska et al., 2004; Norman et al., 2004b). The supraorbitals are free of the orbital margin and project across the orbit (Figs. 2.1 and 2.3), unlike in derived thyreophorans and pachycephalosaurids where it is incorporated into the orbital margin (Maryańska et al., 2004; Norman et al., 2004b). The supraorbital bar transverses the entire width of the orbit (Figs. 2.1 and 2.3), as in the basal neornithischians *Agilisaurus* and possibly *Haya* (the two supraorbitals may not contact each other in this taxon; Makovicky et al., 2011) and the basal iguanodontian *Dryosaurus altus* (Galton, 1983). A supraorbital bar that transverses the entire orbit was proposed to be a local autapomorphy of *Agilisaurus* (Barrett et al., 2005), but this feature is more widespread among basal neornithischians than previously suspected.

The anterior facet is medially concave and rugose where it formed a loose articulation against the roughened surfaces on the prefrontal and the lacrimal at the

anterodorsal corner of the orbit (Fig. 2.17C). The supraorbital articulation also spans the prefrontal and lacrimal in the heterodontosaurid *Heterodontosaurus* (Crompton and Charig, 1962), the basal neornithischians *Agilisaurus* and *Orodromeus* (Peng, 1992; Scheetz, 1999), and in some ceratopsians (e.g., *Archaeoceratops*: You and Dodson, 2003). The supraorbital formed the anterior two-thirds of the supraorbital bar. The anterior facet is medially concave with a prominent dorsomedially directed process extending from the posterodorsal margin that overlapped the posterior surface of the prefrontal, giving the proximal end a triangular outline in proximal view (Fig. 2.16C). The dorsal margin of the anterior facet is lined with a series of small rugose projections. The rod-shaped posterior process of the supraorbital is posterodorsally oriented in lateral view (Figs. 2.1 and 2.17B), the dorsal and ventral margins converge posteriorly, and the distal tip curves to face nearly directly posterior. In dorsal view the posterior process angles posterolaterally along most of its length, is mediolaterally broad with a slightly convex surface, and remains a nearly constant thickness until the distal end, which curves posteriorly and tapers to a blunt point (Fig. 2.17A). The distal tip is covered with a series of anteroposteriorly oriented ridges they may have facilitated a soft tissue connection to the accessory supraorbital. The entire surface of the supraorbital is covered with a series of anteroposteriorly oriented striations (Fig. 2.17B). The dorsomedial margin is covered with a series of rugose projections (Fig. 2.17B), possibly for connection to associated soft tissues (Scheetz, 1999).

The accessory supraorbital forms the posterior third of the supraorbital bar and is approximately half the length of the supraorbital (Figs 2.17A and B). The accessory

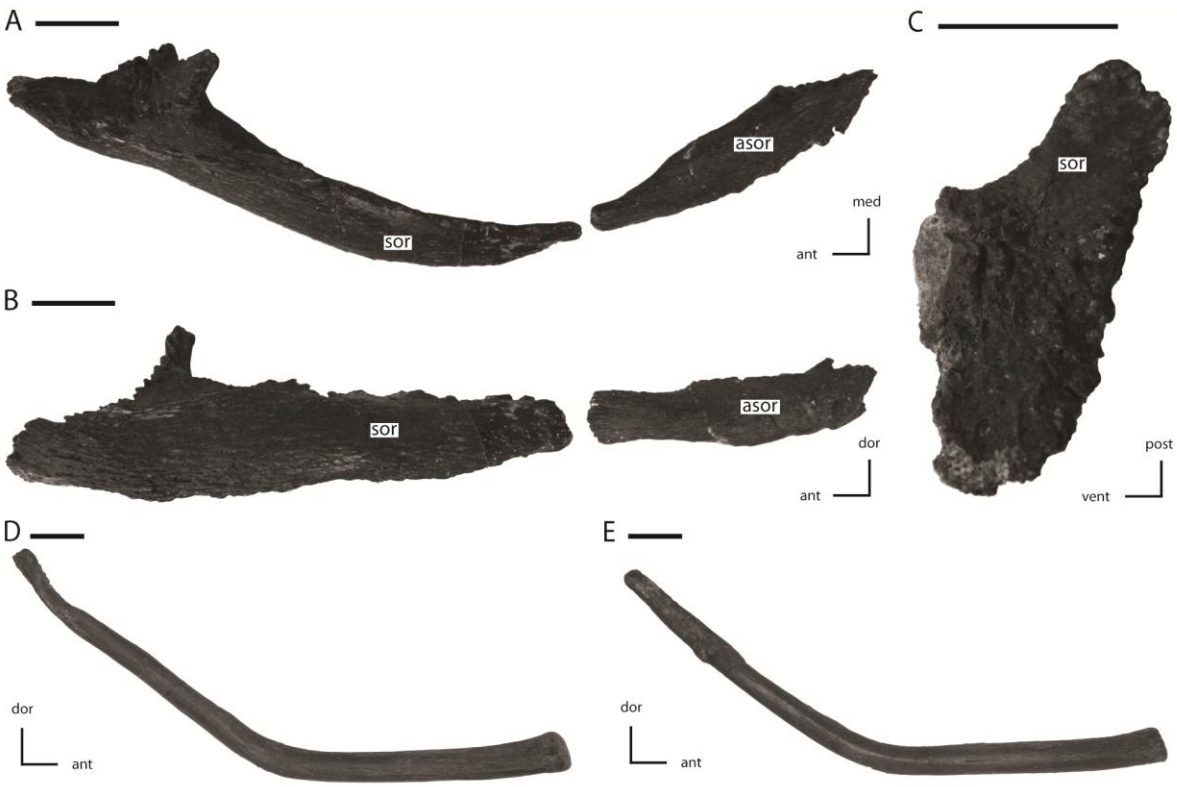

Figure 2.17: Supraorbital, accessory supraorbital, and ceratobranchial of NCSM 15728. **A**. Left supraorbital and accessory supraorbital in dorsal and slightly medial view. **B**. Left supraorbital and accessory supraorbital in lateral and slightly dorsal view. **C**. Anterior articulation facet of left supraorbital in proximal view. **D**. Left ceratobranchial in medial view. **E**. Right ceratobranchial in lateral view. The directional arrows indicate the orientation of the specimen in each view. Scale bars equal 1 cm. See Appendix 2 for anatomical abbreviations.

supraorbital is proportionally larger than those in the basal neornithischians *Agilisaurus* and *Haya* (Peng, 1992; Makovicky et al., 2011). The medial surface is flattened both anteroposteriorly and dorsoventrally, while the lateral surface is convex in both directions (Fig. 2.17A). In lateral view the dorsal margin is concave and the ventral margin is convex. The anterior third of the accessory supraorbital is oriented anterodorsally, is dorsoventrally narrower than the posterior two-thirds, and is covered laterally with a series of fine, anteroposteriorly oriented ridges (Fig. 2.17B). The posterior two-thirds is

oriented posteriorly and the margins are rugose where it overlapped a flattened facet on the lateral surface of the postorbital (Figs. 2.3 and 2.17A).

Hyoid

The ceratobranchials were preserved near the posteroventral corner of the mandible. They were subsequently separated from the specimen and are now isolated elements. Each ceratobranchial consists of an elongate, 'rod-shaped' bone that is strongly curved so that it is dorsally concave and ventrally convex in lateral view (Figs. 2.17D and E). The anterior half was apparently oriented near the ventral margin of the posterior portion of the mandible, while the posterior half curved dorsally around the posterior end of the mandible, closely matching the general morphology and position of the ceratobranchial in iguanodontian ornithischians and basal sauropods (Norman, 2004b; Upchurch et al., 2004). The anterior portion of the ceratobranchial is oriented roughly horizontal and the anterior end is slightly dorsoventrally expanded and ovate in cross-section. The posterior portion is oriented posterodorsally at an angle of approximately forty-five degrees from the anterior portion. The posterior portion tapers dorsoventrally and becomes progressively mediolaterally flattened towards the posterodorsal tip (Figs. 2.17D and E). The morphology of the ceratobranchial differs from those preserved in the basal neornithischians *Changchunsaurus*, *Jeholosaurus*, *Hypsilophodon*, and *Parksosaurus* (Galton, 1973, 1974a; Barrett and Han, 2009; Jin et al., 2010), which are relatively straight and do not show the strong curvature present in NCSM 15728. The ceratobranchials may be curved in the taxon *Agilisaurus* (Peng, 1992:fig. 1) and are

preserved in a more anterior position than in NCSM 15728, though it is uncertain if they are distorted or if they were displaced from their original position.

Sclerotic Plates

Isolated sclerotic plates are present, randomly distributed throughout the orbit. These plates are extremely mediolaterally thin and fragile. The best exposed of these is preserved lying on the dorsal surface of the parasphenoid (Fig. 2.2: sp), though it is distorted from being pressed against the underlying bone. As a result, not much can be said regarding the morphology of these plates or of the morphology of the sclerotic ring.

Dentition

Premaxillary Dentition

Six teeth are present in each premaxilla, as in the basal ornithischian *Lesothosaurus* (Sereno, 1991), the basal thyreophoran *Scutellosaurus* (Colbert, 1981), and the basal neornithischians *Hypsilophodon* and *Jeholosaurus* (Galton, 1974a; Barrett and Han, 2009). However, it appears that the number of premaxillary teeth increases during ontogeny in on examination of multiple specimens of the basal ornithischian taxa *Hypsilophodon* (P. Galton, pers. com.), *Jeholosaurus* (C. Boyd, pers. obs.), and *Thescelosaurus* (C. Boyd, pers. obs.). Thus, the lower tooth counts observed in some other basal neornithischian taxa may not reflect the number present in mature individuals of all of those taxa.

The premaxillary crowns are slightly mediolaterally compressed and slightly constricted at their bases (Fig 2.18A). The bluntly pointed distal tips of the crowns are recurved posteriorly. Serrations are absent on both the anterior and posterior margins just as in the basal neornithischians *Changchunsaurus*, *Haya*, and *Jeholosaurus* (Barrett and Han, 2009; Jin et al., 2010; Makovicky et al., 2011), but weakly developed carinae are present that are more pronounced on the anterior margins. On some premaxillary crowns (e.g., Fig. 2.18A: pmt6) a dorsoventrally oriented groove is present adjacent to the carina, which is also seen in the basal ornithischian *Lesothosaurus* (Sereno, 1991) and the basal neornithischian *Jeholosaurus* (Barrett and Han, 2009). The surfaces of the premaxillary crowns are ornamented by numerous fine ridges that extend from the distal tip to the base of the crown. Similar ornamentation is present in *Hypsilophodon* (Galton, 1974a), but is absent in *Changchunsaurus*, *Jeholosaurus*, and *Zephyrosaurus* (Sues, 1980; Barrett and Han, 2009; Jin et al., 2010). In NCSM 15728, these ridges are less prominent in teeth that display a higher degree of wear (Fig. 2.18A: pmt3). Enamel is evenly distributed on all sides of the crowns. The premaxillary tooth crowns of NCSM 15728 differ from those of most heterodontosaurids (except *Friutadens*: Butler et al., 2010; Butler et al., in press), in which the crowns are straight, subcylindrical, and unconstricted at their base (Butler et al., 2008a).

The roots of the premaxillary teeth are elliptical in *Jeholosaurus* (Barrett and Han, 2009), but round in *Hypsilophodon* and *Zephyrosaurus* (Galton, 1974a; Sues, 1980). In NCSM 15728, the shape of the premaxillary tooth roots vary based on tooth position, with the more anteriorly positioned teeth possessing roots that are elliptical in cross section

(mediolaterally compressed), while the posterior-most teeth possess roots that are roughly circular in cross section. The roots of premaxillary teeth four through six are oriented dorsomedially away from the crowns; however, the roots of the anterior three premaxillary teeth progressively angle more posteriorly as well, with the root for the first premaxillary tooth oriented posteriorly at roughly a forty-five degree angle from the long axis of the body of the premaxilla. This same pattern is observed in the partial premaxillae of the holotype of *Bugenasaura* (SDSM 7210), which is now referred to *Thescelosaurus* (Boyd et al., 2009). Medially oriented wear facets were reported on isolated premaxillary teeth referred to *Thescelosaurus* (Galton, 1974b). Medially facing wear facets are also reported for the basal neornithischian *Zephyrosaurus* (Sues, 1980). Alternatively, the wear facets on the premaxillary teeth of NCSM 15728 are on the distal tips of the crowns and progressive wear decreases the height of the crown. In *Jeholosaurus*, both patterns of wear are observed (Barrett and Han, 2009). Replacement teeth are present in some of the premaxillary alveoli, with a single replacement tooth positioned medial to the root of the erupted tooth. No set pattern of tooth replacement is readily apparent from examination of the CT data.

Maxillary Dentition

The maxillary tooth row is inset from the lateral margin of the maxilla and overhung by a prominent, anteroposteriorly oriented ridge on the maxilla (Figs. 2.1 and 2.2). In *Lesothosaurus* and *Scutellosaurus* the maxillary teeth are only modestly inset from the lateral margin (Colbert, 1981; Sereno, 1991). Twenty teeth are present in each

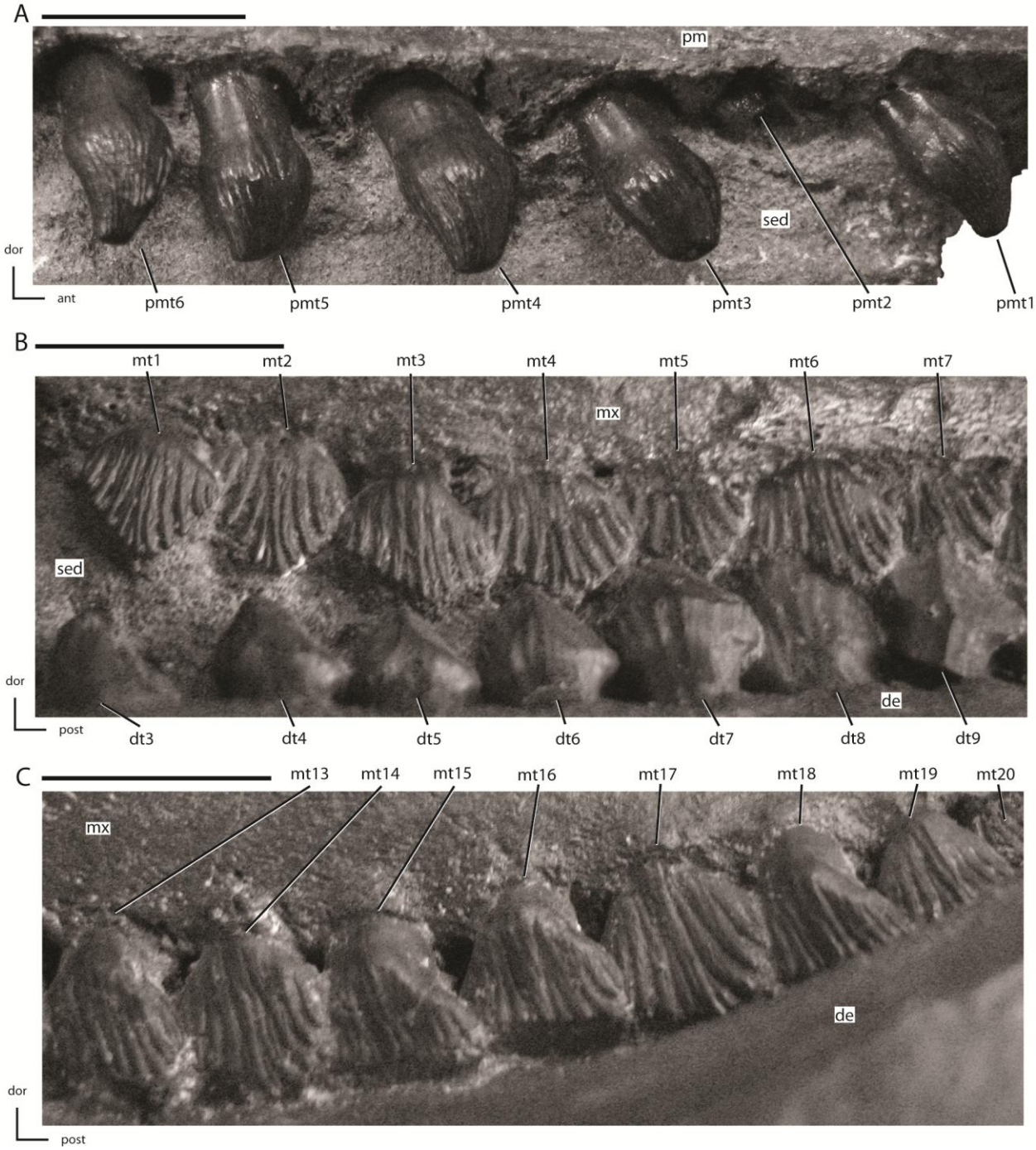

Figure 2.18: Premaxillary and maxillary dentition of NCSM 15728. **A**. Right premaxillary dentition in lateral view. **B**. Anterior portion of left maxillary dentition in ventrolateral view. **C**. Posterior portion of left maxillary dentition in ventrolateral view. The directional arrows indicate the orientation of the specimen in each view. Scale bars equal 1 cm. See Appendix 2 for anatomical abbreviations.

maxilla, more than in any other basal neornithischian (Norman et al., 2004c). The anterior end of the maxillary tooth row is more posteriorly positioned than the anterior end of the dentary tooth row (Figs. 2.1 and 2.2). As a result, the first maxillary crown occludes with anterior margin of the fourth dentary crown and possibly with the posterior margin of the third dentary crown (Fig. 2.18B). Posteriorly the tooth row wraps around the posterior end of the maxilla, causing the posterior-most maxillary crowns to be oriented posteroventrally instead of directly ventrally (Fig. 2.18C). This does not appear to be a result of distortion of the specimen because it occurs on both sides of the specimen, and in the CT data the posterior ends of the maxillae appear undamaged. Instead, this may result from the high number of teeth present in the maxillary and dentary tooth rows compared to other basal neornithischians and the fact that the posterior end of the dentary tooth row extends medial to the rising coronoid process and, as a result, the posterior-most dentary teeth are slightly more dorsally positioned than the anterior portion of the dentary tooth row.

Unworn maxillary crowns are roughly triangular in shape in lateral view and their dorsoventral height is approximately equal to their anteroposterior width (Figs. 2.18B and C), as in the heterodontosaurid *Echinodon* (Galton, 2007), the basal thyreophoran *Scutellosaurus* (Colbert, 1981), the basal neornithischians *Changchunsaurus*, *Jeholosaurus*, *Orodromeus*, *Othnielosaurus*, and *Zephyrosaurus* (Sues, 1980; Scheetz, 1999; Barrett and Han, 2009; Jin et al., 2010; C. Boyd, pers. obs.), and the basal ceratopsian *Yinlong* (Xu et al., 2006). The maxillary teeth are arranged en echelon, with the posterior portion of each crown positioned lateral to the anterior portion of the

proceeding crown (Figs. 2.18B and C). The roots of the maxillary teeth are spaced apart from each other (Fig. 2.18C), unlike in more derived ornithopod and ceratopsian dinosaurs where the roots of adjacent teeth tightly contact each other (Norman, 2004b; You and Dodson, 2004). There is a distinct constriction, or neck, present at the base of the crown, as in all basal neornithischians except *Hypsilophodon* and *Jeholosaurus* (Galton, 1974a; Barrett and Han, 2009). Distal to this constriction, a distinct cingulum is present at the base of the crown, as in all basal neornithischians (Norman et al., 2004c). The medial surfaces of the maxillary crowns are convex, as in the basal neornithischians *Hypsilophodon*, *Leaellynasaura*, and *Zephyrosaurus* (Galton, 1974a; Sues, 1980; Rich and Vickers-Rich, 1999) and in iguanodontians (Norman, 2004b). The distribution of enamel on the maxillary crowns is rather symmetrical, as in all basal neornithischians except *Hypsilophodon* (Galton, 1974a) and in most heterodontosaurids except *Abrictosaurus* and *Heterodontosaurus* (Butler et al., 2008a).

Marginal denticles are present on the maxillary crowns and extend to near the base of the crown, unlike in all heterodontosaurids except *Echinodon* (Galton, 2007) and the basal ceratopsian *Chaoyangsaurus* (Zhao et al., 1999). The marginal denticles are confluent with ridges that extend to the base of the crown, unlike in *Skaladromeus* (Chapter 3), though in this latter taxon the absence of these ridges may reflect the early ontogenetic stage of the specimen that preserves the partial maxilla. A prominent, primary ridge on the lateral surface near the apex of the crown is absent in NCSM 15728, unlike in the heterodontosaurid *Heterodontosaurus* (Crompton and Charig, 1962), the basal neornithischian *Talenkauen* (Novas et al., 2004), some basal ceratopsians (e.g.,

Archaeoceratops: You and Dodson, 2003), and most basal iguanodontians except *Rhabdodon*, *Tenontosaurus*, and *Zalmoxes* (Norman, 2004b; Weishampel et al., 2003). The presence of ridges on the lateral surface of the maxillary crowns that form two converging crescentic patterns was proposed to be an autapomorphy of *Thescelosaurus* by Galton (1997). However, the presence of this feature is variable in NCSM 15728, with some teeth displaying this feature (e.g., Fig. 2.18B: mt2) while adjacent teeth display nearly vertical ridge (e.g., Fig. 2.18B: mt3). Thus, this character was dismissed as a autapomorphy of *Thescelosaurus* in the recent review of the taxon by Boyd et al. (2009).

The maxillary tooth roots are dorsoventrally straight, as in all basal ornithischians. In general, the maxillary teeth do not form a continuous occlusion surface, with each maxillary crown offset in between two dentary crowns, creating distinct anterolingual and posterolingual wear surfaces on the maxillary crowns. However, on the posterior maxillary teeth a single, roughly horizontal wear facet is present on each crown that closely matches the height of the wear facets on the adjacent teeth, creating a nearly continuous occlusion surface (Figs. 2.18C).

Dentary Dentition

The dentary teeth are poorly exposed in NCSM 15728. On the right side of the skull, only the anterior three dentary teeth are visible, and the maxillary dentition obscures the more posterior dentary crowns (Fig. 2.1). On the left side of the skull the dentary and maxilla are slightly separated, allowing the lateral surfaces of the anterior nine dentary crowns to be seen, and parts of the next three crowns, but the posterior eight crowns are entirely

obscured by the overlapping maxillary dentition (Figs. 2.2 and 2.19). CT data was used to gather additional information regarding the morphology of the dentary teeth, but the resolution of the scans is insufficient to fully elucidate their morphology. The dentary tooth row is inset from the lateral margin of the dentary, and a prominent anteroposteriorly oriented ridge present on the dentary ventral to the tooth row (Figs. 2.1 and 2.2). Twenty teeth are present in the dentary. The basal neornithischian taxa *Agilisaurus* and *Hexinlusaurus* also possess twenty dentary teeth (He and Cai, 1984; Peng, 1992), but in these taxa the number of dentary teeth is greater than the number of maxillary teeth, while NCSM 15728 possesses an equal number of dentary and maxillary teeth. The roots of the dentary teeth are dorsoventrally straight, unlike the dorsoventrally curved dentary tooth roots seen in the basal neornithischians *Hypsilophodon* and *Parksosaurus* (Galton, 1974a; C. Boyd, pers. obs.) and in iguanodontians (Norman, 2004b).

The anterior-most dentary tooth is more anteriorly positioned than the anterior-most maxillary tooth (Fig. 2.19). As a result, the anterior two, and possibly also the third, dentary teeth do not occlude with the maxillary dentition; rather, they are situated ventral to the premaxillary-maxillary diastema. In *Agilisaurus*, the anterior three dentary teeth extend anterior beyond the maxillary tooth row, but they occlude with the premaxillary teeth owing to the lack of a premaxillary-maxillary diastema in that taxon (Barrett et al., 2005). None of these anterior dentary teeth match the morphology of the enlarged, anteriorly positioned caniniform tooth present in the heterodontosaurids *Fruitadens*, *Heterodontosaurus*, *Lycorhinus*, and *Tianyulong* (Crompton and Charig, 1962; Hopson,

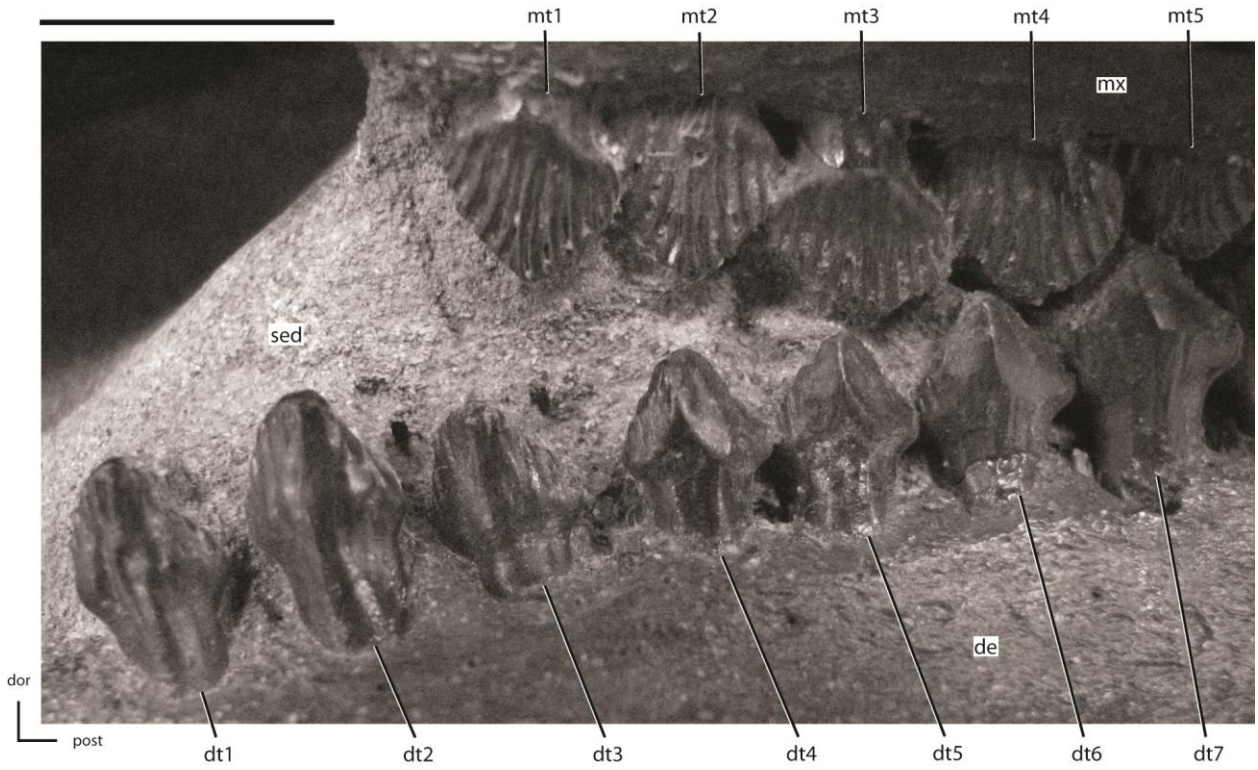

Figure 2.19: Anterior portion of the left dentary dentition from NCSM 15728. The directional arrows indicate the orientation of the specimen. Scale bar equals 1 cm. See Appendix 2 for anatomical abbreviations.

1975; Zheng et al., 2009; Butler et al., 2010). The anterior-most dentary tooth is not reduced relative to the other dentary teeth, as is the first dentary tooth in *Agilisaurus* (Barrett et al., 2005). The anterior two dentary teeth are slightly more enlarged than dentary teeth 3-5 and they are anteroposteriorly narrower than the other dentary crowns (Fig. 2.19). The posterior margins of the first three dentary crowns are slightly concave, but the crowns are not recurved like the anterior three dentary teeth in *Agilisaurus* (Barrett et al., 2005). The anterior three dentary teeth bear marginal denticles and confluent ridges, but they are reduced in number and prominence compared to the more posterior dentary crowns.

The remainder of the dentary crowns are roughly 'triangular-shaped' in lateral view and their dorsoventral height is less than 150% of the anteroposterior width of the crown. In all of the dentary teeth, a distinct constriction, or neck, is present between the base of the dentary crown and its corresponding root. A cingulum is present along the base of the crown, as in all basal neornithischian dinosaurs (Norman et al., 2004c). Marginal denticles are present on both the anterior and posterior edges of the dentary crowns, and these denticles are confluent with ridges that extend to the base of the crown, as in the heterodontosaurids *Heterodontosaurus* and *Tianyulong* (Crompton and Charig, 1962; Zheng et al., 2009), the basal neornithischians *Haya*, *Hypsilophodon*, *Jeholosaurus*, *Othnielosaurus*, *Parksosaurus*, and *Talenkauen* (Galton, 1973, 1974a, 2007; Novas et al., 2004; Barrett and Han, 2009; Makovicky et al., 2011), some basal ceratopsians (e.g., *Archaeoceratops* and *Liaoceratops*: Xu et al., 2002; You and Dodson, 2003), and basal iguanodontians (Norman, 2004b). These ridges are present on both the medial and lateral surfaces of the dentary crowns, unlike in heterodontosaurid *Heterodontosaurus* (Norman et al., 2004c), the basal neornithischian *Hypsilophodon* (Galton, 1974a), some basal ceratopsians (e.g., *Liaoceratops:* Xu et al., 2002), and most basal iguanodontians (Norman, 2004b) where ridges are limited to the medial side of the crown. The apex of the dentary crowns is centrally to slightly anteriorly positioned on the crown, unlike in the basal ornithischian *Lesothosaurus* (Sereno, 1991), the basal marginocephalian *Wannanosaurus* (Butler and Zhao, 2009), and dryomorph iguanodontians (Norman, 2004b) where the apex is positioned posteriorly on the crown. Well-developed wear facets are present on the anterolateral and posterolateral surfaces of

the anterior dentary crowns, indicating that each dentary crown occluded with two maxillary teeth and that a continuous occlusion surface was not present on the anterior dentary teeth (Fig. 2.19). It cannot be determined if the wear pattern on the posterior dentary teeth resembled that seen on the anterior dentary crowns or if a nearly continuous occlusion surface was developed as seen in the posterior maxillary teeth.

DISCUSSION

The conflicting cranial character data of *Thescelosaurus neglectus*

Thescelosaurus neglectus is an unusual basal neornithischian. Its large body size (> four meters: Fisher, et al., 2000; C. Boyd, pers. obs.) is in sharp contrast to the general body size range displayed by most other basal neornithischians (~ 1-2 meters: Norman et al., 2004c). Additionally, *T. neglectus* displays an eclectic set of plesiomorphic and apomorphic characters that complicates attempts to resolve its systematic placement within Neornithischia and to identify its sister taxon. The detailed cranial description of *T. neglectus* presented above highlights an even more discordant mixture of plesiomorphic and apomorphic characters in this taxon than was previously recognized. The systematic relationships of *T. neglectus* are thoroughly analyzed elsewhere using these new character data (see Chapter 5), but a detailed discussion of plesiomorphic and apomorphic traits displayed in the skull of this taxon in light of the new character evidence presented herein and new character data from other basal neornithischian taxa is pertinent to the current discussion.

The dentition of *T. neglectus* displays a suite of characters unique to this taxon. The presence of six premaxillary teeth in *Thescelosaurus neglectus* and *Jeholosaurus* would seem to indicate independent reversals in those taxa to the plesiomorphic condition based on the presence of six premaxillary teeth in the basal ornithischian *Lesothosaurus* and the basal thyreophoran *Scutellosaurus* (Colbert, 1981; Sereno, 1991). However, the presence of six premaxillary teeth was recently recognized in some specimens of *Hypsilophodon* (P. Galton, pers. comm.) and the number of premaxillary teeth was found to vary during ontogeny in *Jeholosaurus* and *Thescelosaurus* (C. Boyd, pers. obs.). Based on these new data, the presence of six premaxillary teeth may be more widespread among basal neornithischian taxa, with the full distribution of this character clouded by the fact that some taxa are known only from ontogenetically immature specimens (e.g., *Orodromeus*: Scheetz, 1999). *Thescelosaurus neglectus* also shares with *Lesothosaurus* (and *Jeholosaurus*) the presence of a dorsoventrally oriented groove adjacent to the carina on the premaxillary crowns (Sereno, 1991; Barrett and Han, 2009). Alternatively, *T. neglectus* and *Hypsilophodon* are unique in possessing fine, dorsoventrally oriented ridges on the premaxillary crowns (Galton, 1974a), and the premaxillary crowns of *T. neglectus*, *Changchunsaurus*, *Haya*, and *Jeholosaurus* differ from other basal ornithischians in lacking serrations (Barrett and Han, 2009; Jin et al., 2010; Makovicky et al., 2011).

The maxillae and dentaries both contain twenty tooth positions, a condition that more closely resembles the basal genosaurian condition, and deviates from a general trend in basal neornithischians and basal iguanodontians of reducing the number of tooth

positions in both the maxillae and dentaries (Norman, 2004b; Norman et al., 2004c). The roots of the dentary and maxillary teeth are dorsoventrally straight and the enamel is symmetrically distributed on the dentary and maxillary crowns in *T. neglectus*, which are ornithischian symplesiomorphies (Scheetz, 1999; Butler, 2005; Butler et al., 2008a). A distinct constriction, or neck, is present at the base of each crown, and just dorsal to that constriction a distinct cingulum is present, both of which are plesiomorphic for Neornithischia (Weishampel and Heinrich, 1992; Scheetz, 1999). The presence of both a convex medial surface on the maxillary crowns and the presence of ridges on the surfaces of the maxillary and dentary crowns that extend from the marginal denticles to the base of the crown are shared with basal iguanodontian taxa, along with some other basal neornithischians (Scheetz, 1999; Weishampel et al., 2003). Additionally, the posterior end of the dentary tooth row extends medial to the rising coronoid process, a feature seen in *Changchunsaurus*, *Jeholosaurus*, and most iguanodontians (Weishampel et al., 2003; Barrett and Han, 2009; Jin et al., 2010).

The lower jaw of *T. neglectus* displays two apomorphic features generally seen in basal iguanodontians. The posteroventral process of the predentary is bifurcated in *T. neglectus*, which is a character commonly associated with basal iguanodontians; however, the basal neornithischians *Changchunsaurus* and *Haya* (Jin et al., 2010; Makovicky et al., 2011) and some basal ceratopsians (You and Dodson, 2003, 2004) also display this feature, suggesting the character state has a much wider distribution than previously assumed. The surangular of *T. neglectus* bears a dorsolateral process near the lateral margin of the glenoid, similar in appearance to the dorsally projecting lip

positioned lateral to the glenoid in the basal iguanodontians *Tenontosaurus tilletti* and *Zalmoxes robustus* (Weishampel et al., 2003; Norman, 2004). Some other basal neornithischian taxa possess small bosses near the lateral margin of the glenoid (e.g., *Changchunsaurus*; Jin et al., 2010), but none of these are as well developed as seen in *T. neglectus*.

The morphology of the braincase in *T. neglectus* is relatively derived with respect to basal ornithischians, and most closely resembles that of *Dysalotosaurus* (Galton, 1989), though it lacks an ossified orbitosphenoid. The basioccipital bears a ventral midline keel and an arched floor of the braincase, both of which are plesiomorphic for Neornithischia (Scheetz, 1999) and present in some basal iguanodontians (e.g., *Dysalotosaurus*: Scheetz, 1999; Norman, 2004b). The anteroposterior length of the basioccipital is less than that of the basisphenoid (not including parasphenoid) in *T. neglectus*, *T. assiniboiensis*, *Jeholosaurus*, and some basal iguanodontians (Norman, 2004b; Barrett and Han, 2009; Brown et al., 2011; C. Boyd, pers. obs.). The trigeminal foramen is entirely enclosed within the prootic, which is also seen in the basal iguanodontians *Dryosaurus* and *Dysalotosaurus* (Scheetz, 1999), and in some basal ceratopsians (e.g., *Yinlong*; C. Boyd, pers. obs.). The presence of a fossa on the medial surface of the prootic containing the foramina for CN VII and both branches of CN VIII is shared only with the basal iguanodontian *Dysalotosaurus* (Galton, 1989). In addition to these features, both autapomorphies of *T. neglectus* also are present on the braincase, as are four of the seven characters used to differentiate *T. neglectus* from *T. assiniboiensis*

(see Emended Diagnosis above), making this a critical region of the skull for evaluating the relationships of this species.

Relationship to *Parksosaurus warreni*

Some prior phylogenetic analyses of the relationships of *Thescelosaurus* positioned it in a monophyletic group with *Parksosaurus* (Weishampel et al., 2003; Boyd et al., 2009; Brown et al., 2011). Alternatively, other analyses place *Parksosaurus* as the sister taxon to *Gasparinisaura* (Buchholz, 2002; Butler et al., 2008a; Makovicky et al., 2011). This latter position was based upon character evidence that requires revision in light of new discoveries, recent preparation work on the holotype of *Parksosaurus*, and the new cranial data for *T. neglectus* described above. The analysis by Butler et al. (2008a) recovered three characters that unambiguously supported the monophyly of a *Parksosaurus* + *Gasparinisaura* clade. The first character (jaw joint strongly depressed ventrally, with more than 40% of the height of the quadrate below the level of the maxilla: Butler et al., 2008a), is inaccurately scored for *Parksosaurus* based on misinterpretation of the holotype. The quadrate of *Parksosaurus* often is reconstructed as extremely dorsoventrally elongate, with the quadratojugal contacting the quadrate within the dorsal two-thirds of the quadrate shaft and a ventrally displaced jaw joint (e.g., Parks, 1926; Galton, 1973), a condition similar to that seen in *Gasparinisaura* (Coria and Salgado, 1996). However, on the holotype and only specimen of *Parksosaurus*, the left quadrate is displaced posteroventrally, rotated laterally about its long axis, and most of its jugal wing and ventrolateral margin are damaged and lost (C. Boyd, pers. obs.). The

preserved, and newly prepared, morphology of the left quadrate of *Parksosaurus* exactly matches that of *T. neglectus* (Figs. 2.8C and D), including the presence of a foramen in the posterolateral side of the quadrate along the contact with the quadratojugal (Fig. 2.8F: C. Boyd, pers. obs.). Additionally, the distal end of the better preserved right quadrate is complete and exposed in posteromedial view, confirming the above observations regarding the length and morphology of the quadrate. The posterior portion of the lower jaw also is damaged in the holotype and displaced posteroventrally, enhancing the false impression that the jaw joint was positioned farther ventrally than it actually was. Thus, the position of the jaw joint and the morphology of the quadrate actually were similar to that of *T. neglectus* (Fig. 2.1).

The second character supporting a sister taxon relationship between *Parksosaurus* and *Gasparinisaura* in Butler et al. (2008a) is the presence of chevrons with anteroposteriorly expanded distal ends. That feature is present in both taxa, but it is also present in middle to distal caudals of *Macrogryphosaurus*, while the more anteriorly positioned chevrons of *Macrogryphosaurus* are relatively unexpanded (Calvo et al., 2007). This same variation was noted in *Parksosaurus* as well (Parks, 1926; C. Boyd, pers. obs.). In many specimens referred to *Thescelosaurus*, including the holotype and NCSM 15728, the middle to distally placed chevrons are damaged at their distal ends, making it impossible to determine if the same morphological variation is present. However, a well-preserved specimen of *Thescelosaurus* in the privately held collection at Triebold Paleontology (Woodland Park, CO) includes an articulated tail with chevrons that are anteroposteriorly expanded at their distal ends (C. Boyd, pers. obs.). This

indicates that *Thescelosaurus* was at least polymorphic for this character, and may indicate a wider distribution of the character amongst basal neornithischians because few specimens include well-preserved chevrons from the middle or distal caudals.

The final character is the absence of a well-developed acromion process on the scapula. Although the acromion process is relatively pronounced in smaller specimens referred to *Thescelosaurus* (e.g., AMNH 5031: Galton, 1974b), in larger specimens of *Thescelosaurus* the acromion is less pronounced or nearly absent (e.g., MOR 989; NCSM 15728: C. Boyd, pers. obs.), suggesting that this character should be scored as polymorphic for *Thescelosaurus*. Given these observations, the characters outlined above do not provide strong support for the monophyly of a *Parksosaurus* + *Gasparinisaura* clade.

The monophyly of a *Parksosaurus* + *Gasparinisaura* clade in the study by Buchholz (2002) was supported by four characters, one of which is the shape of the chevrons (discussed above). The other three are a reduced or absent posterior process of the jugal, a long and thin anterior process of quadratojugal, and the presence of a large descending process of the quadratojugal (Buchholz, 2002). The first character is inaccurate for *Parksosaurus* because the posterior process of the jugal in *Parksosaurus* is elongate, forming nearly the entire ventral margin of the infratemporal fenestra, as in *Thescelosaurus,* and is incomplete ventrally so that its dorsoventral height cannot be determined. The scoring of the second character for *Parksosaurus* is suspect for two reasons. First, the quadratojugal is damaged and its exact dimensions cannot be determined. Second, in *Thescelosaurus* a long anterior process of the quadratojugal

inserts medial to the jugal. Given the damage to the jugal in *Parksosaurus*, it cannot be determined if the increased anteroposterior length of the quadratojugal is merely the result of the quadratojugal being displaced, exposing the long anterior process. Finally, the third character is impossible to score with certainty in *Parksosaurus* owing to the incomplete preservation of the quadratojugal. Thus, reevaluation of the characters proposed to support a *Parksosaurus* + *Gasparinisaura* clade by Buchholz (2002) finds little support for this relationship.

Alternatively, *Parksosaurus* shares several characters in common with *Thescelosaurus* that are lacking in *Gasparinisaura*. Both *Thescelosaurus* and *Parksosaurus* possess in the posterolateral surface of the quadrate a foramen that passed medial to the quadratojugal (also seen in *Haya* and some iguanodontians: Norman, 2004b; Makovicky et al., 2011). *Thescelosaurus* and *Parksosaurus* also possess ossified sternal ribs and intercostal plates (sensu Butler and Galton, 2008), both of which are also present in *Hypsilophodon*, *Macrogryphosaurus*, and *Othnielosaurus* (Butler and Galton, 2008; Boyd et al., 2011b) and the latter is present in *Talenkauen* (Boyd et al., 2011b). Finally, among basal neornithischians the fourth trochanter extends onto the distal half of the femur in *Parksosaurus*, *Thescelosaurus*, and *Talenkauen* (Gilmore, 1915; Galton, 1973; Novas et al., 2004). Additional characters supporting a close relationship between *Thescelosaurus* and *Parksosaurus* cannot be evaluated in *Gasparinisaura*, including the presence of a broad fossa at the base of the pterygoid wing of the quadrate (Fig. 2.8C). These observations suggest that *Parksosaurus* shared a closer relationship with

Thescelosaurus than with *Gasparinisaura*, though the exact relationships of these taxa need to be reevaluated via a phylogenetic analysis incorporating these new character data.

Future directions in the study of *Thescelosaurus*

All three species of *Thescelosaurus* that are currently considered valid (*T. assiniboiensis*, *T. garbanii*, and *T. neglectus*) are from contemporaneous deposits, with the latter two present in the same formation (i.e., Hell Creek Formation; Boyd et al., 2009). The presence of multiple contemporaneous basal neornithischian taxa is not unique to the Western Interior Basin of North America during the late Maastrichtian. The taxa *Agilisaurus louderbacki*, *Hexinlusaurus multidens*, *Yandusaurus hongheensis*, and *Xiaosaurus dashanpensis* are all from the Lower Shaximiao Formation of Sichuan Province, China (Barrett et al., 2005). Additionally, within the Western Interior Basin of North America two contemporaneous taxa are present, *Orodromeus makelai* and *Skaladromeus goldenii* (Scheetz, 1999; Chapter 3). Similarly, two species of the basal iguanodontian taxon *Zalmoxes* are present during the late Maastrichtian in Romania (Weishampel et al., 2003). However, it is still imperative that the validity of all three species of *Thescelosaurus* be thoroughly evaluated. Although there is strong character evidence supporting the separation of *T. neglectus* and *T. assiniboiensis* (Brown et al., 2011: this study), the same cannot be said for the fragmentary holotype of *T. garbanii*. The tentative retention of *T. garbanii* as a distinct taxon by Boyd et al. (2009) was based on review of the published data concerning the anatomy of that taxon because personal observation of the holotype material was not possible owing to the fact that the specimen

was offsite being mounted for future display. Clearly, it is crucial that the holotype material of *T. garbanii* be thoroughly reexamined and its validity confirmed once the material is available again for study.

Despite the excellent anatomical descriptions for *T. neglectus* (Gilmore, 1915; this study) and *T. assiniboiensis* (Brown et al., 2011) now available, referral of additional specimens to individual species within *Thescelosaurus* remain problematic. This is largely a result of two factors. First, the fragmentary nature of the holotype of *Thescelosaurus garbanii*; and second, the lack of recognized postcranial autapomorphies for *T. assiniboiensis* and *T. neglectus*. With regards to the former factor, only the discovery of additional specimens clearly referable to *T. garbanii* can resolve the issue, assuming the validity of that species is upheld. The latter factor requires detailed examination not just of the holotypes of all three taxa, but of all well-preserved specimens referred to *Thescelosaurus* to elucidate any patterns of morphological variation within the taxon and disparity between species. Given the wide range of body sizes represented by specimens referred to *Thescelosaurus*, the possible effects of ontogeny on postcranial (and cranial) skeletal morphology will need to be evaluated and taken into consideration. To begin to address this issue, a histological survey of material referred to *Thescelosaurus* from the Frenchman, Hell Creek, and Lance formations is currently underway. The results of that study will be crucial to deciphering the life history strategy of *Thescelosaurus*, evaluating the ontogenetic status and comparability of specimens referred to *Thescelosaurus*, and identifying taxonomically informative

differences between the postcranial skeletons of the three currently recognized species of *Thescelosaurus*.

CHAPTER 3.

A New Basal Neornithischian (Dinosauria: Ornithischia) from the Kaiparowits Formation of Utah and an Evaluation of Potential Osteological Correlates for Fossorial Behavior in Ornithischians

INTRODUCTION

The fossil record of basal neornithischians (here defined as neornithischian taxa placed outside of the clades Marginocephalia and Iguanodontia) from the Cretaceous in North America is sparse. Only seven species are described from the latter 50 million years of the period (Norman et al., 2004c; Boyd et al., 2009) all restricted to the northern region of the North American Western Interior Basin (i.e., Montana, North Dakota, South Dakota, and Wyoming, USA, Alberta and Saskatchewan, Canada; Norman et al., 2004c; Varricchio et al., 2007; Boyd et al., 2009). A recent phylogenetic analysis of basal neornithischian relationships recovered these seven taxa as a monophyletic group divided into two clades (Boyd et al., 2009:fig. 3b). One clade contains the larger bodied Maastrichtian (70.6-65.5 Myr; Norman et al., 2004c; Gradstein et al., 2005) taxa *Parksosaurus warreni* (Parks 1926), *Thescelosaurus neglectus* Gilmore 1913, *T. garbanii* Morris 1976, and a new species of *Thescelosaurus* from the Frenchman Formation of Saskatchewan (Brown et al., 2009; Brown et al., 2011). The other clade contains the smaller bodied taxa *Orodromeus makelai* Horner and Weishampel 1988, *Oryctodromeus cubicularis* Varricchio et al. 2007, and *Zephyrosaurus schaffi* Sues 1980, ranging in age from the late Aptian (117-112 Myr; Norman et al., 2004c; Gradstein et al., 2005) to the late Campanian (75-70.6 Myr; Norman et al., 2004c; Gradstein et al., 2005).

Recent geologic and paleontologic work within the Kaiparowits Formation within Grand Staircase-Escalante National Monument of southern Utah, USA (Fig. 3.1) yielded

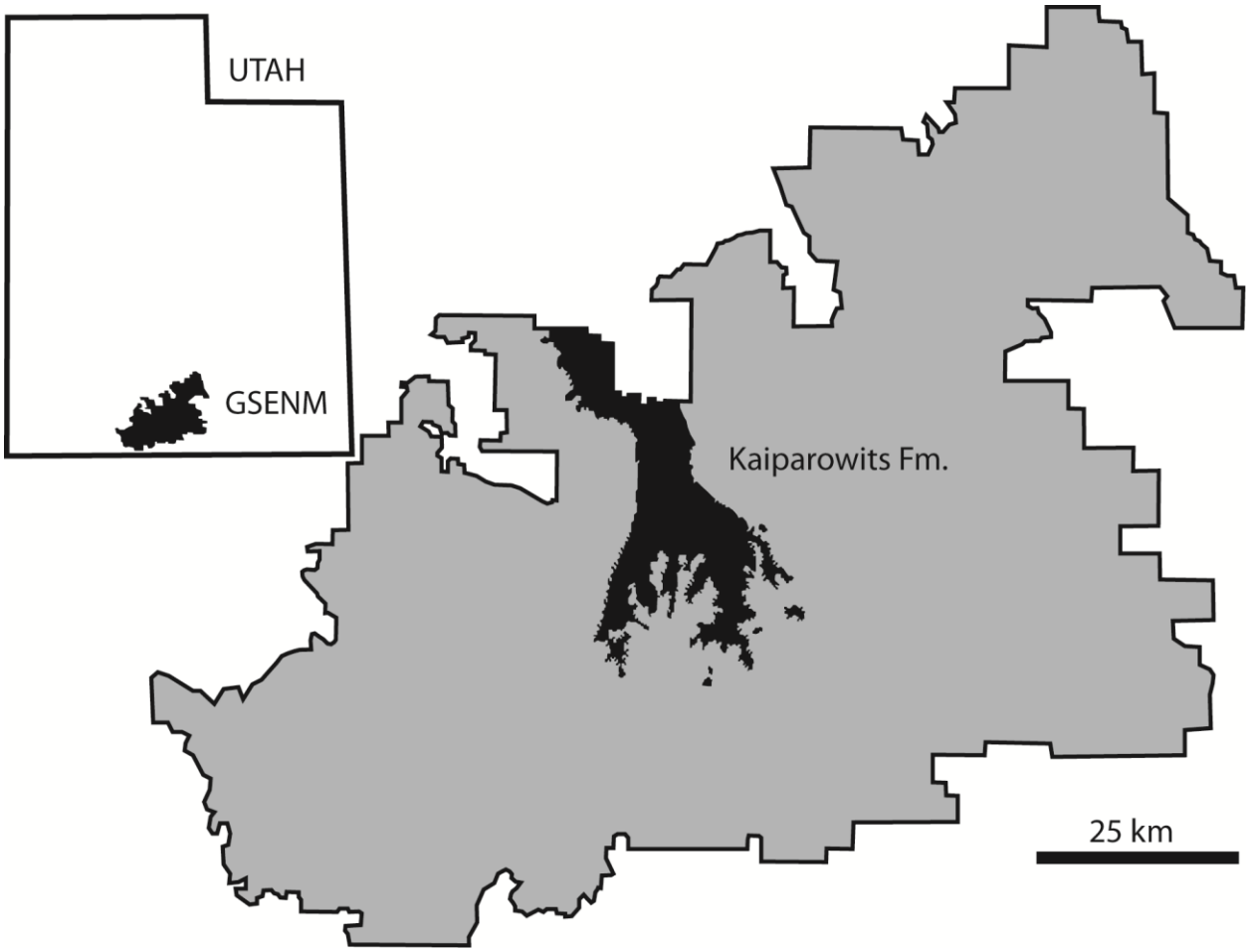

Figure 3.1: Geographic position of surficial exposures of the Kaiparowits Formation within Grand Staircase-Escalante National Monument (GSENM). The top-left diagram shows the geographic position of GSENM within the state of Utah. The larger map indicates the distribution of Kaiparowits Formation outcrops (shaded black) within the boundaries of the GSENM (shaded grey).

several important discoveries that provide insight into the paleobiology and biogeography of basal neornithischians. The Kaiparowits Formation is divided into three informal units (lower, middle, and upper; Roberts, 2007) based on variations in the mudstone to sandstone ratio. The base of the Kaiparowits Formation is dated at approximately 76.1 Myr at its conformable base with the Wahweap Formation and the upper, unconformable contact with the overlying Canaan Peak Formation is dated at 74.0 Myr (^{40}Ar / ^{39}Ar

dating: Roberts et al., 2005). Thus, the Kaiparowits Formation preserves a remarkably well-dated two million year interval that is contemporaneous with several other Judithian formations throughout the Western Interior Basin (e.g., Two Medicine Formation of western Montana).

Within the past decade, research on the dinosaurian fauna of the Kaiparowits Formation revealed at least seven new taxa (Sampson et al., 2010a), including the oviraptorosaurid *Hagryphus giganteus* Zanno and Sampson 2005, the hadrosaurid *Gryposaurus monumentensis* Gates and Sampson 2007, and the chasmosaurine ceratopsians *Utahceratops gettyi* Sampson et al. 2010b and *Kosmoceratops richardsoni* Sampson et al. 2010b. Basal neornithischian (i.e., 'hypsilophodontid') skeletal material was first reported from the Kaiparowits Formation by Zanno (2005), but the fragmentary nature of the material impeded attempts to elucidate its taxonomic identity and systematic relationships. Subsequent discovery of additional basal neornithischian material increased our understanding of the anatomy of the Kaiparowits basal neornithischian taxon. These new data allow a new taxon to be recognized that is diagnosably distinct from all previously described basal neornithischian taxa. Here we describe this new Kaiparowits taxon, discuss its implications for the paleobiology and biogeography of North American basal neornithischian taxa, and reevaluate characters previously proposed to be osteological correlates for fossorial behavior in ornithischians.

See Appendix 1 for institutional abbreviations.

SYSTEMATIC PALEONTOLOGY

DINOSAURIA Owen, 1842

ORNITHISCHIA Seeley, 1887

NEORNITHISCHIA Cooper, 1985 (sensu Butler et al., 2008a)

Orodrominae *clade nov.*

Definition (Stem-Based)

All taxa more closely related to *Orodromeus makelai* than to *Thescelosaurus neglectus* or *Parasaurolophus walkeri* Parks 1922. As defined, this clade includes the North American taxa *Orodromeus makelai*, *Oryctodromeus cubicularis*, *Skaladromeus goldenii* gen. et sp. nov., and *Zephyrosaurus schaffi*, in addition to the Asian taxon *Koreanosaurus boseongensis* Huh et al. 2010.

Diagnosis

Characters discussed in this section that were included in the cladistic analysis are indicated by their corresponding character number and state in Appendix 5. Orodrominae is diagnosed based on the presence of two unambiguously optimized synapomorphies that are confirmed present in all five taxa currently placed within the clade. The fibula is 'D-shaped' in transverse section at midshaft (119:1), and a sharp, pronounced, laterally projecting scapular spine is present on the scapula (88:1). A third character is confirmed present in all orodromine taxa except *Koreanosaurus*, for which the condition is

unknown, and also appears convergently in *Rhabdodon* Matheron, 1869: presence of a distinct facet along the ventrolateral margin of the first sacrodorsal and the first true sacral centrum, just below the articulation surface for the first sacral rib, which supports the medial tubercle of the pubis (83:2).

***Skaladromeus goldenii* gen. et sp. nov.**

Etymology

The clade name is a combination of the Greek words *skala* (σκάλα) and *dromeas* (δρομέας), meaning 'staircase runner,' and refers to the Grand Staircase-Escalante National Monument where this material was recovered. The species name is in honor of the long time Utah Museum of Natural History volunteer Jerry Golden, whose personal, field, and preparation contributions are beyond measure.

Holotype

UMNH VP 19470 (see Table 1 for material preserved).

Locality

Grand Staircase-Escalante National Monument, Kane County, UT.

Distribution

Kaiparowits Formation, Utah (late Campanian [~76.1-74 Myr]; Roberts et al., 2005).

Referred Specimens

See Table 1 for a complete list of referred specimens and the material preserved in each.

Diagnosis

Characters discussed in this section that were included in the cladistic analysis are indicated by their corresponding character number and state in Appendix 5. The holotype differs from all other basal neornithischians in that the ventral ramus of the postorbital inserts into a socket in the anterolateral margin of the dorsal ramus of the jugal. Two additional apomorphic traits are recognized from referred specimens UMNH VP 12665 and UMNH VP 12677, respectively: presence of an ovoid foramen on the ventral margin of the sternal process of the coracoid; reduction of manual digit IV from three to two phalanges, including the ungual (96:1).

Comments

The ontogenetic maturity of type specimens can influence morphological comparisons with other taxa, making it important to assess the maturity of newly designated type specimens before conducting comparisons with other taxa. Histological examinations of fossil bone can be used to assess the age of individual specimens (e.g., Erickson et al., 2004; Horner and Padian, 2004; Erickson et al., 2009) and to determine the relative maturity or growth stage of individual specimens (e.g., Erickson and Tumanova, 2000; Horner et al., 2000; Klein and Sander, 2008). However, these types of

Table 3.1: List of material preserved in each specimen here referred to *Skaladromeus goldenii*. The referral of additional specimens to this taxon is based on general morphological similarity and lack of character disagreement between specimens. Specimens UMNH VP 21091-21099 and 21101-21107 are from the same locality as UMNH VP 12665, and were given separate specimen numbers to make it easier to identify the elements that were used in the supplementary description because there are multiple disarticulated individuals present at this locality.

Specimen Number	Material Preserved
UMNH VP 12665	Skull and Postcranial Fragments from Multiple Individuals of Various Sizes
UMNH VP 12677	Articulated Manus Lacking the Ungual from Digit Three and all of Digit Five, Two Caudal Vertebrae, Two Dorsal Vertebrae, a Fragment of the Postacetabular Portion of the Ilium, Head of the Left Femur, Five Pes Phalanges [II,1; III,3; IV,2; IV,3; IV,4], Distal Portion of Metatarsal I, Distal Portion of Metatarsal II
UMNH VP 16281	Articulated Right and Left Pes, Distal Tarsals, Distal Portions of the Right Tibia And Fibula
UMNH VP 16772	Partial Tibiae, One Complete and One Partial Fibula, Distal Tarsals, And Metatarsals II Through IV
UMNH VP 16773	Dorsal and Caudal Vertebrae, Partial Sacrum, Proximal Portions of Both Femora, Distal Left Tibia, Distal Right Fibula, Several Pes Phalanges
UMNH VP 19470 (Holotype)	Left Frontal, Right Jugal, Partial Left Pterygoid, Left Laterosphenoid, Nearly Complete Left and Partial Right Opisthotic, Left Dentary with Erupted and Unerupted Teeth, Odontoid Process of the Axis, One Nearly Complete and One Partial Cervical Centrum, Three Dorsal Centra, One Sacral Centrum, Six Caudal Centra, Fragmentary Scapula, Proximal Portions of Both Femora, Proximal Portion of a Tibia, Numerous Fragments of Neural Arches, Rib Shafts, Chevrons, Partial Pes Ungual.
UMNH VP 21091	Partial Left Maxilla
UMNH VP 21092	Left Dentary
UMNH VP 21093	Right Dentary
UMNH VP 21094	Cervical Vertebra
UMNH VP 21095	First True Sacral Vertebra
UMNH VP 21096	Proximal Portion of Tibia
UMNH VP 21097	Distal Portion of Tibia
UMNH VP 21098	Chevron
UMNH VP 21099	Left Coracoid
UMNH VP 21101	Distal Portion of Right Humerus
UMNH VP 21102	Proximal Portion of Ulna
UMNH VP 21103	Distal Portion of Ulna
UMNH VP 21104	Left Scapula
UMNH VP 21105	Proximal Portion of Right Humerus
UMNH VP 21106	Proximal Portion of Right Femur
UMNH VP 21107	Distal Portion of Right Femur

investigations are best conducted on the diaphyseal region of long bones (Francillon-Vieillot et al., 1990; Horner et al., 2000), which are not preserved in the holotype. Alternatively, closure of the neurocentral sutures has been used to as a skeletochronological indicator of maturity in archosaurs (e.g., Kirkland et al., 2005;

Kobayashi and Barsbold, 2005; Brusatte et al., 2009; Gangloff and Fiorillo, 2010). Though different patterns of neurocentral suture closure are observed in different archosaurian clades (Irmis, 2007), it has been noted by Brochu (1996:p. 55) that, "the absence of suture closure in the dorsal vertebrae clearly indicates that a particular animal was neither fully mature nor fully grown at death." The largest dorsal centrum preserved in the holotype is 18 mm in length and 15 mm in width, and the neurocentral sutures are fully open in all preserved cervical, dorsal, sacral, and anterior caudal vertebrae, with closure only observed in the distal caudals. Thus, the holotype of *S. goldenii* is here considered to be an immature individual. This conclusion is also supported by the absence of fusion between adjacent sacral centra and between the braincase elements in the holotype (see description below). Additionally, in the largest referred specimen, UMNH VP 12677, the largest dorsal centrum is 24 mm in length and 34.5 mm in width and also exhibits fully open neurocentral sutures. The recognition that most, if not all, of the material here referred to *S. goldenii* is immature requires that caution is taken to ensure differences noted between this taxon and known taxa are not influenced by ontogeny. However, the immaturity of these specimens does not affect the validity of *S. goldenii*, because the distinct autapomorphies of this taxon noted above are unlikely to be affected by ontogeny.

HOLOTYPE DESCRIPTION

The primary description of *S. goldenii* is based solely on the holotype, UMNH VP 19470.

Skull

A partial left frontal is preserved, missing the anterior and much of the medial portions (Figs. 3.2A-C). In dorsal view the frontal is triangular in shape, being transversely broad posteriorly (Fig. 3.2C). The orbital margin of the frontal is rugose (Figs. 3.2A-C; om). The posterior portion of the articulation facet for the prefrontal is preserved and consists of a shallow scarf joint along the anterolateral margin (Fig. 3.2C; pfa). A small portion of the medial frontal suture is preserved and consists of a set of interlocking sagittal ridges and grooves. The articulation surface for the postorbital is dorsolaterally oriented (Fig. 3.2C; poa), resembling the morphology seen in *Orodromeus* (MOR 1136; Scheetz, 1999), but differing from *Zephyrosaurus* (YPM 56695; Figs.3.2D and F; poa) where the articulation consists of a socket that faces laterally. In *S. goldenii* a small portion of the postorbital articulation surface extends around the posterolateral corner of the frontal and the entire articulation surface bears a series of anteroposteriorly oriented ridges. The posteromedial portion of this contact extends dorsal to the articulation surface for the parietals (Fig. 3.2A; pa), indicating the presence of a small amount of contact between the parietals and the postorbital. The anterolateral corners of the parietals inserted into a deep sulcus in the posterior end of the frontal. Medially, the contact between the parietals and the frontal thins, reduced to a narrow butt joint bearing a series of transverse ridges. The ventral surface of the frontal bears an arcuate, sharply defined ridge that demarcates the boundary of the orbital contribution of the frontal (Fig. 3.2B; mor). This ridge extends posterolaterally, terminating at the socket for the

laterosphenoid (Fig. 3.2B; lsa). Lateral to this ridge a series of tiny foramina pierce the frontal.

A partial right jugal is preserved, missing the anterior ramus, much of the posterior ramus, and the tip of the dorsal ramus (Fig. 3.3). A prominent jugal horn core projects posterolaterally from the main body of the jugal, covering the entirety of the preserved lateral surface (Fig. 3.3B; jh). The horn core is subconical, being slightly flattened anteroposteriorly, rugosely textured, and bears a strong ventral ridge. The ventral margin of the jugal thins to a sharp ridge. Two foramina pierce the medial surface of the jugal directly below the dorsal ramus. A rounded depression is present on the medial surface of the posterior ramus of the jugal (Fig. 3.3D; qja). This may indicate the anterior extent of the articulation surface for the quadratojugal, but this facet is not present in *Thescelosaurus* (NCSM 15728). The dorsal and posterior rami are sufficiently preserved to determine that the anteroventral corner of the infratemporal fenestra forms an acute angle (Fig. 3.3B). The dorsal ramus of the jugal is D-shaped in cross-section, being flattened posteromedially (Fig. 3.3C). The ventral ramus of the postorbital overlapped the anterolateral surface of the dorsal ramus of the jugal and the distal end inserted into a shallow socket in the jugal (Fig. 3.3C; pos), a condition unique to this taxon. Previous studies of basal neornithischian systematic relationships noted that the orodromine taxa *Orodromeus* and *Zephyrosaurus* are united in possessing a prominent posterolaterally projecting horn on the body of the jugal (Scheetz, 1999; Varricchio et al., 2007). This feature is also present in *Skaladromeus* (Fig. 3.3; jh), but is absent on the jugal of the juvenile paratype of *Oryctodromeus* (Varricchio et al., 2007). While the size

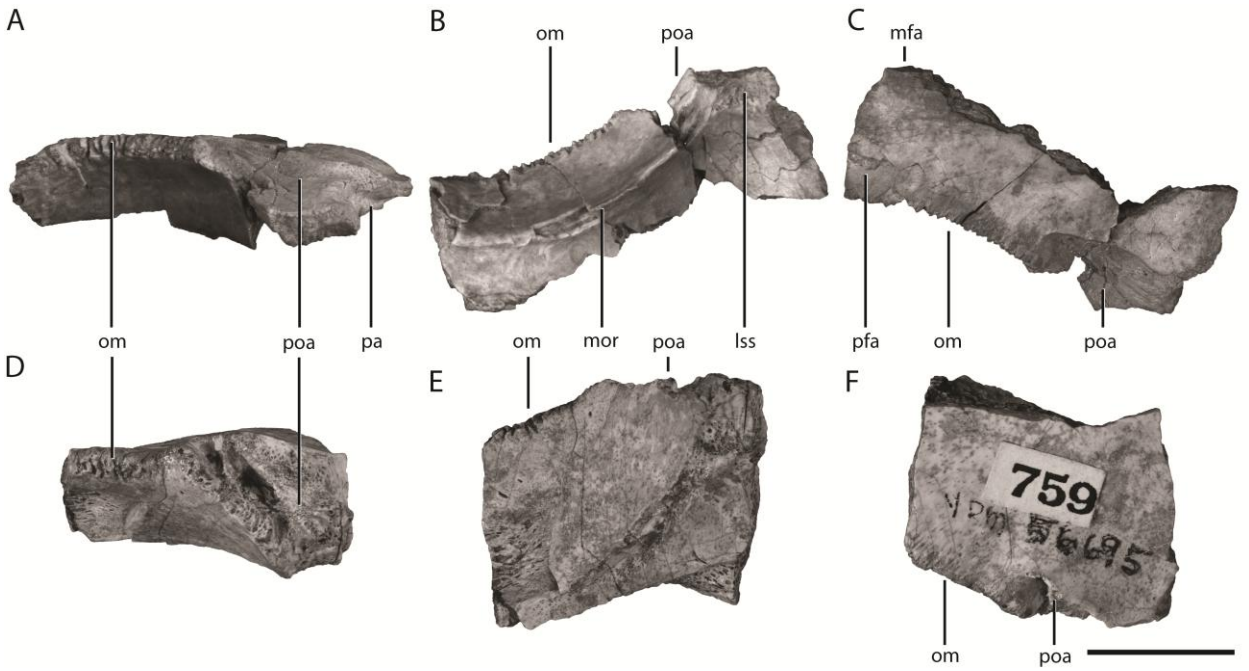

Figure 3.2: Partial left frontals from *Skaladromeus* and *Zephyrosaurus*. The left frontal from the holotype of *Skaladromeus* (UMNH VP 19470) is shown in lateral (**A**), ventral (**B**), and dorsal (**C**) views. The left frontal from a referred specimen of *Zephyrosaurus* (YPM 56696, formally MOR 759) is shown in lateral (**D**), ventral (**E**), and dorsal (**F**) views for comparison. Scale bar equals 1 cm. See Appendix 2 for anatomical abbreviations.

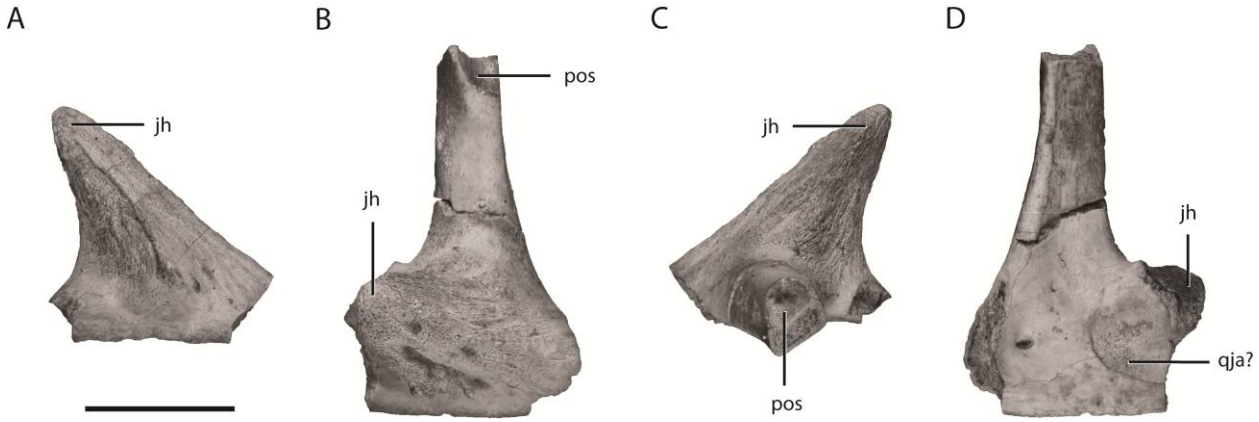

Figure 3.3: Partial left jugal from the holotype of *Skaladromeus*. Specimen shown in ventral (**A**), lateral (**B**), dorsal (**C**), and medial (**D**) views. Scale bar equals 1 cm. See Appendix 2 for anatomical abbreviations.

of the jugal horn in *Orodromeus* does increase during ontogeny and varies in size between individuals (Scheetz, 1999), it is present in all specimens. Additionally, the holotype of *Skaladromeus* is an immature individual, yet the jugal horn is extremely pronounced (Fig. 3.3). Based on this evidence it is reasonable to assume that the absence of a jugal horn in the immature paratype of *Oryctodromeus* reflects the natural state of this taxon and is not an artifact of ontogeny.

A fragmentary left dentary is preserved missing both the anterior and posterior ends (Figs. 3.4A, B, and C). One partial erupted crown and three partially exposed unerupted crowns are visible (Fig. 3.4A). A portion of the Meckelian groove is preserved along the medial surface near the ventral margin, consisting of a 'U-shaped' trough, and it is dorsoventrally wider and mediolaterally deeper posteriorly than anteriorly (Fig. 3.4A; mg). The teeth are inset medially from the lateral margin. Along the lateral surface an anteroposteriorly oriented row of foramina is present (Fig. 3.4B). Anteriorly, the dorsal margin is flared laterally, forming the beginning of the articulation surface for the predentary (Fig. 3.4C).

The pattern of replacement within each alveolus in the dentary consists of a single replacement tooth positioned medial to the root of the erupted tooth (Fig. 3.4A). The crowns are triangular in lateral view, are convex lingually, and possess a centrally to slightly anteriorly placed apical ridge. Numerous denticles are present along the anterior and posterior margins, though the crowns lack ridges on both the labial and lingual surfaces. A distinct neck is present between the crown and the root. The roots are straight in lateral view. The posterior margin of the crown curves lingually, forming a small shelf

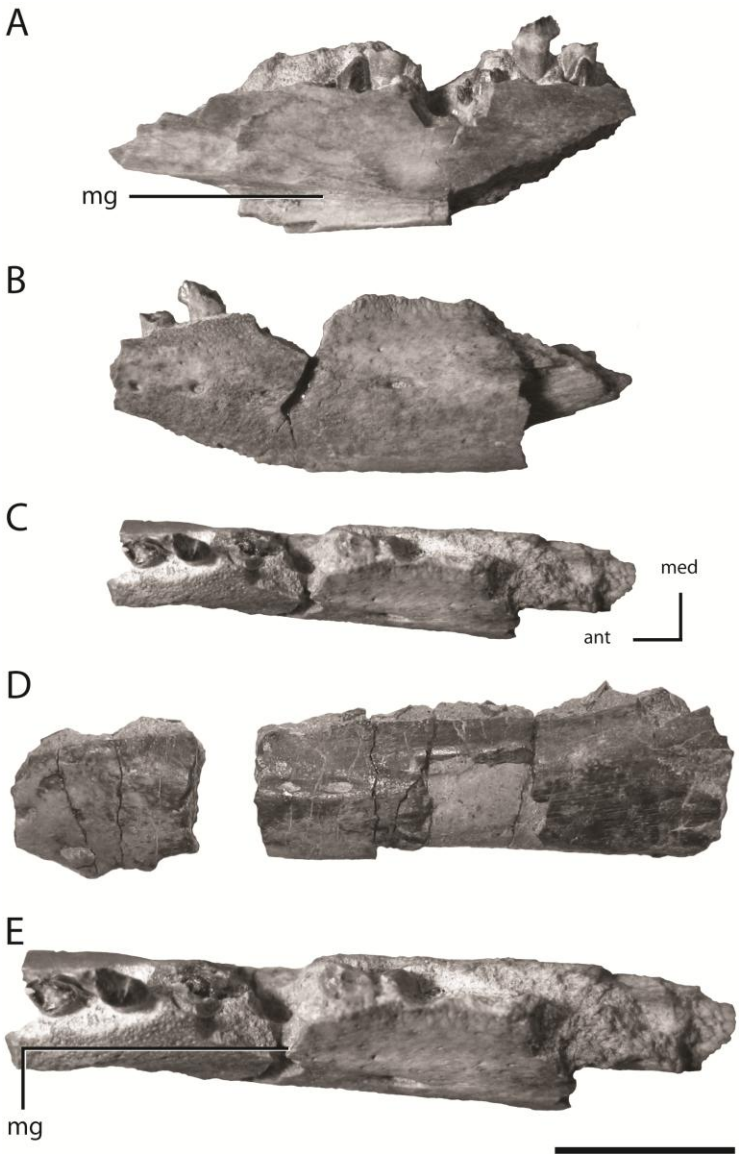

Figure 3.4: Partial dentaries from the holotype of *Skaladromeus*. The partial left dentary from the holotype (UMNH VP 19470) is shown in medial (**A**), lateral (**B**), and dorsal (**C**) views. A more complete left dentary from a smaller individual referred to *Skaladromeus* (UMNH VP 21092) shown in lateral (**D**) and medial (**E**) views. Scale bar equals 1 cm. See Appendix 2 for anatomical abbreviations.

on the posterolingual portion of the crown. A small concavity is also present on the anterolabial portion of the crown. When the tooth row is viewed dorsally, the

posterolingual shelf and anterolabial concavity of overlapping crowns lineup to form a nearly enclosed pocket.

The left pterygoid preserves part of the quadrate alar process, most of the body of the pterygoid, and the base of the ectopterygoid alar process (Figs. 3.5A, B, and C). The quadrate alar process is slightly convex dorsoventrally and flattened anteroposteriorly in lateral view (Fig. 3.5A; qap). On the lateral surface near the posteroventral margin and running parallel to it is a small ridge that becomes more pronounced posteriorly (Fig. 3.5A; lpr). Anterior and slightly dorsal to this ridge there is a shallow, anteroposteriorly elongate depression that extends anteriorly to near the base of the ectopterygoid alar process (Fig. 3.5C; pg). In medial view, the quadrate alar process is divided into two portions by a vertically oriented ridge (Fig. 3.5B; vr). The anterodorsal portion of the pterygoid is concave anteroposteriorly, forming a pocket against which the basipterygoid process of the basisphenoid rested (Figs. 3.5B and C; bpa). The ventral margin of the body is thin and concave anteroposteriorly between the quadrate and ectopterygoid alar processes. The anteromedial margin of the pterygoid just anterior to the quadrate alar process is thickened and concave. Little can be said of the morphology of the ectopterygoid alar process other than the ventromedial surface is concave and the dorsolateral surface is slightly convex.

The left laterosphenoid is missing only a portion of the anterior margin (Figs. 3.5D, E, and F). The laterosphenoid articulates with the parietals along an inclined, dorsally facing surface, with the prootic along the posteroventral margin, and the supraoccipital along the posterodorsal margin. The articulation surface for the parietals is

relatively smooth, while that for both the supraoccipital and prootic consist of a series of irregularly oriented ridges and grooves. The sutural surface for the prootic also bears a prominent, triangular boss that likely inserted into the prootic (Fig. 3.5D; pb). The anterolateral surface is concave dorsoventrally and slightly convex anteroposteriorly. Anterodorsally, a transverse expansion extends dorsolaterally, and a rounded surface on the end of this projection would have contacted at least the frontal (Figs. 3.5D, E, and F; hl). The anteromedial surface displays a marked concavity (Fig. 3.5E; ac). There is no indication that the laterosphenoid contributed to the anterior margin of the foramen ovale, and the groove noted by Sues (1980) along the anterolateral surface in *Zephyrosaurus* is also absent.

There is no distinction between the opisthotic and the exoccipital, as is the case in most basal neornithischians (Galton, 1989); therefore, this description treats them as a single element referred to as the opisthotic because the majority of the region formed by the exoccipitals is missing (i.e., the ventromedial portion). The left opisthotic is missing the extreme lateral margin and ventral tip of the paroccipital process and the ventromedial portion that contacted the basioccipital (Fig. 3.6). Only the dorsomedial portion of the right opisthotic is preserved (Fig. 3.6). The ventromedial surface of the opisthotic contributed to the lateral wall of the braincase, and on this surface the foramen for the vena cerebralis posterior is present (Fig. 3.6A; vcp). The anteroposteriorly compressed paroccipital process extends laterally from the thickened medial portion of the opisthotic and curves ventrally. In the dorsolateral corner of the posterior surface of the paroccipital process the posterior temporal opening for the vena capitis dorsalis is

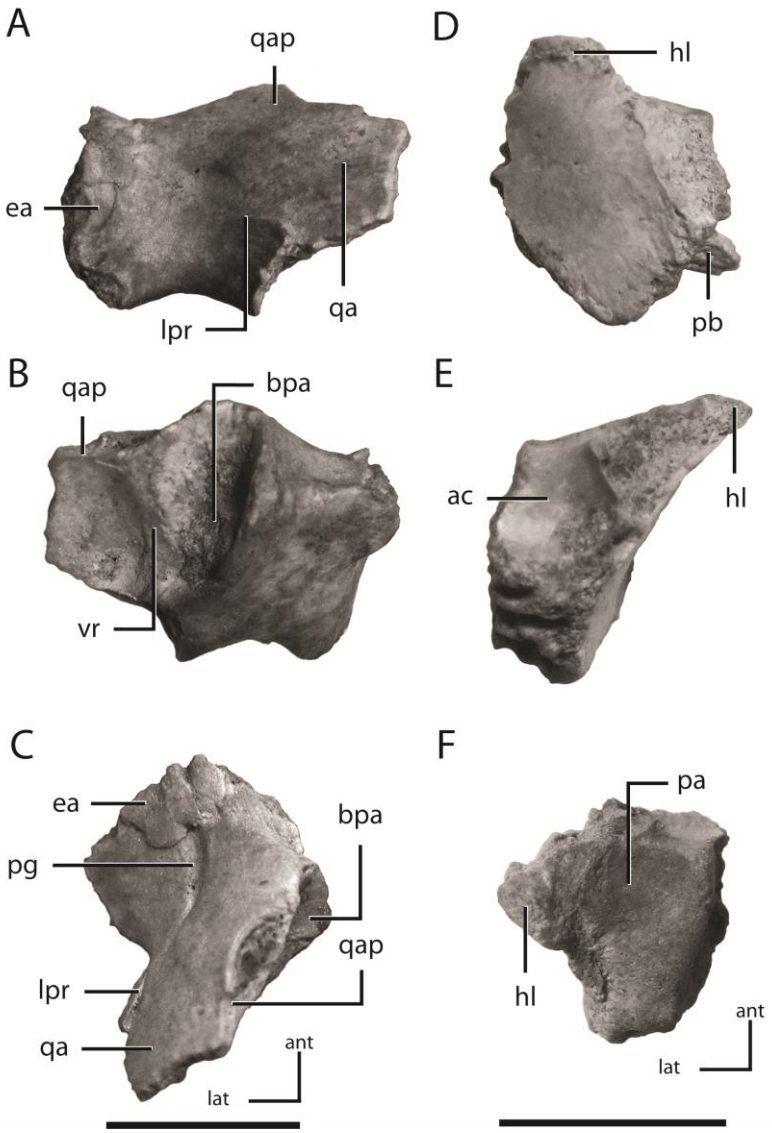

Figure 3.5: Partial left pterygoid and laterosphenoid from the holotype of *Skaladromeus*. The left pterygoid is shown in lateral (**A**), medial (**B**), and dorsal (**C**) views. The partial left laterosphenoid is shown in lateral (**D**), anterior (**E**), and dorsal (**F**) views. Scale bars equals 1 cm, and each scale bar applies to the overlying column of figures. See Appendix 2 for anatomical abbreviations.

temporal foramen is open dorsally in *Dryosaurus* Marsh 1894, *Tenontosaurus* Ostrom, 1970, and *Thescelosaurus* (Galton, 1989). The dorsomedial surface is roughly triangular in shape and forms the articulation surface for the supraoccipital, which consists of a

present as an enclosed foramen, as in *Hypsilophodon* Huxley 1869, *Orodromeus*, and *Zephyrosaurus* (Galton, 1974a; Sues, 1980; Scheetz, 1999). In contrast, the posterior complex set of ridges and grooves. Near the center of this surface is the foramen the posterior semicircular canal. The posterior surface bears the articulation surface for the prootic, which is divided into two parts. The lateral portion faces anteriorly and is roughly triangular in shape, whereas the medial portion is rectangular and faces more medially. The lateral portion consists of a series of mediolaterally oriented ridges and grooves. Along the dorsal margin of this suture the foramen for the vena capitis dorsalis penetrates the posterior surface of the paroccipital process. Along the contact between the lateral and medial portions of the articulation surface for the prootic the foramen for the lateral semicircular canal is present. Medial to the articulation surface for the prootic is the posterior portion of the vestibule (Galton, 1974a; 1997), also referred to as the recessus utricular posterior (sensu Galton, 1989; 1997). In the right opisthotic, the posterolateral wall of the vestibule is missing, exposing the foramen for the semicircular canals positioned within the dorsolateral corner of the vestibule. Ventral to the articulation surface for the prootic there is a mediolaterally elongate fossa that is deeply excavated both dorsally and medially as in *Orodromeus* and *Zephyrosaurus* (Figs. 3.6C-E; lof). Ventromedial to this fossa the dorsal portions of the fenestra ovalis and foramen metoticum are preserved and are separated by the crista interfenestralis (sensu Galton, 1989). The crista tuberalis separates these structures from the more posteriorly positioned foramen for cranial nerve X.

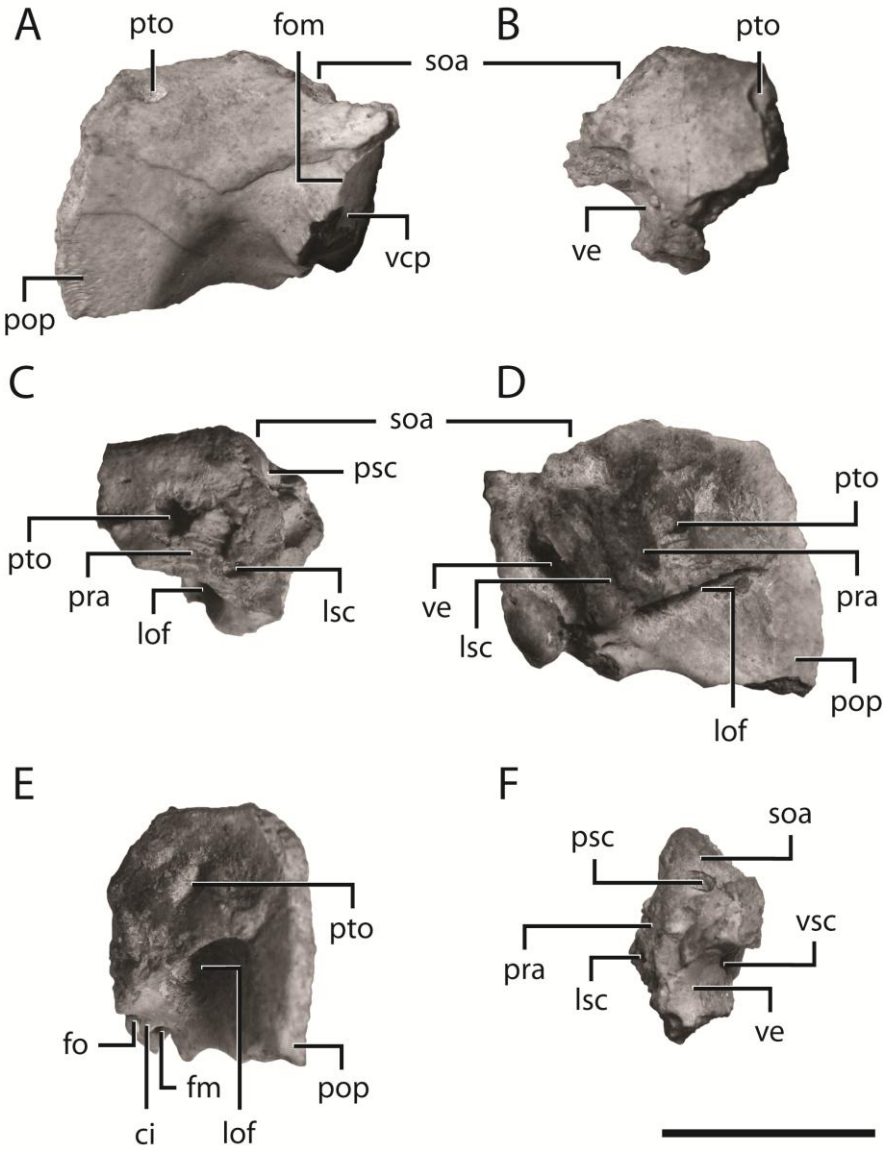

Figure 3.6: Partial left and right opisthotics from the holotype of *Skaladromeus*. The left opisthotic is shown in posterior (**A**), anterior (**D**), and lateral (**E**) views. The right opisthotic is shown in posterior (**B**), anterior (**C**), and medial (**F**) views. Scale bar equals 1 cm. See Appendix 2 for anatomical abbreviations.

Axial Skeleton

The odontoid process is broadly U-shaped in anterior view, with the dorsal surface broadly indented. In ventral view it is saddle-shaped, with the anterior edge broadly rounded and expanded for articulation with the centrum of the atlas, while the

posterior edge is swollen to contact the centrum of the axis. Prominent articulation facets are present on the posterodorsal corners.

The complete cervical centrum preserved in the holotype is laterally concave, causing the centrum to narrow ventrally to form a prominent keel as in *Koreanosaurus*, *Orodromeus*, and *Oryctodromeus* (Huh et al., 2010). The centrum is roughly 1.5 times as long as tall (exact measurements are complicated by slight crushing), as is seen in *Koreanosaurus*. The anterior surface of the centrum is smaller both dorsoventrally and transversely than the posterior surface. Dorsally, a series of prominent ridges and grooves are preserved along the lateral margins indicating the articulation surface for the neural spine, which was unfused to the centrum in this specimen. In approximately the center of the ventral surface of the neural canal a prominent foramen is present. The parapophyses are present as stout pedicles located on the anterodorsal corner of the centrum below the neurocentral suture. No cervical ribs are preserved.

The dorsal centra are 'D-shaped' in transverse section and slightly longer than wide. The centra are amphicoelous, rugose along the lateral margins of the anterior and posterior ends, and concave laterally and ventrally, lacking the ventral keel present in the cervical series. The neurocentral sutures are open and the neural arches are disarticulated. The same elongate foramen noted along the ventral surface of the neural canal in the cervical vertebrae is present in the dorsal centra. Fragmentary neural arches are also preserved in the holotype that resemble those of other basal neornithischian taxa, except in the morphology of the distal ends of the neural spines. The anterior and posterior corners of the distal end of the neural spines are expanded laterally, creating prominent,

dorsally rounded shelves. The location and extent of this feature within the vertebral column is poorly understood owing to preservational issues. Therefore, while this morphology may be an apomorphic trait of *S. goldenii*, we refrain from designating it as such until its distribution in this taxon is better understood.

No complete dorsal ribs are preserved, but the general morphology can be reconstructed my examining all of the preserved fragments. The tuberculum and the capitulum of the preserved dorsal ribs are distinct. The tuberculum is short and closely appressed to the rib shaft. The capitulum is moderately spaced from the tuberculum by a thick neck. The rib shafts are elliptical in transverse section proximally. As the rib shaft curves ventrolaterally, the posterolateral margin extends into a broad wing, creating a moderate sulcus along the posteromedial surface of the rib margin. At the same point a ridge arises along the center of the medial surface, giving the rib shaft a roughly triangular cross-section. Further distally the sharp medial ridge becomes rounded and eventually transitions to a broadly convex surface. The wing along the posterior margin reduces ventrally until it is completely lost at about the same point that the sharp medial ridge becomes more gently rounded. The ventral-most portion of the rib shaft is mediolaterally narrow and anteroposteriorly broad, with a slightly convex medial surface and flattened lateral surface. Some neornithischian taxa possess mediolaterally flattened, 'D-shaped' plates situated along the posterior margin of the anterior dorsal ribs termed intercostal plates (Butler and Galton, 2008). In *Thescelosaurus*, the posterior margin of the anterior dorsal ribs is flattened and rugose where these intercostal plates are positioned (Brown et al., 2011). The preserved dorsal ribs from UNMHVP 19470 do not

show this morphology. However, it has been noted that the differential preservation of intercostal plates in individuals of the same species appears to be influenced by the fact that these plates ossify later in ontogeny (Boyd et al., 2011b), and that this ontogenetic effect may make it difficult to determine the distribution of these structures among neornithischian taxa. Given the evidence outlined above that indicates UMNH VP 19470 is an immature individual, the absence of both intercostal plates and their osteological correlate on the dorsal ribs in this specimen does not necessarily mean these structures were absent in mature individuals of this species.

A partial sacral vertebral centrum is known from the holotype, but its exact position within the series cannot be determined. Distinct articulation facets are present both on the preserved face of the centrum and along the dorsal margin, indicating the centrum was not fused to the adjacent centrum or to its own neural arch. The preserved ventral portion of the neural canal is composed of a deep, 'U-shaped' trough. The portion of the centrum below the neural canal is dorsoventrally thin and transversely wide, though not as transversely expanded as is the contact between the first true sacral and the first sacrodorsal in basal neornithischian taxa (see discussion). The ventral surface in indented by a shallow groove.

Six caudal vertebrae are preserved, representing various portions of the series, and are similar in morphology to that of *Orodromeus* (Scheetz, 1999), which is the only orodromine taxon for which the caudal series is well known. The anterior-most preserved vertebrae are similar to the dorsal centra in length and height, but are transversely narrow. The anterior and posterior surfaces are concave. Dorsally, the lateral margins bear the

prominent ridges and grooves that mark the suture with the neural arch, which is absent and unfused in the anterior-most preserved caudals. The lateral surfaces are concave, and the ventral surfaces display a narrow groove. Articulation facets for the chevrons are present on both the anteroventral and posteroventral corners. The anteroventral facet is broadly rounded, whereas the posteroventral facet consists of a flattened, posteriorly inclined surface that extends further ventrally than the anteroventral facet. The more posteriorly positioned caudals remain consistent in length, but are dorsoventrally shortened, giving them the appearance of being elongate. The ventral groove present on the anterior caudal centra transitions into a slightly concave to flattened ventral surface posteriorly. The neurocentral sutures are fully closed and indistinguishable in the posterior caudals, the only place in the vertebral column where closure is observed in this specimen. The distal caudal vertebrae are transversely narrower than the dorsals.

Two partial chevrons are preserved in the holotype, but both are missing the proximal and distal ends. In lateral view the chevrons are concave posteriorly and convex anteriorly. Distally, the shaft of the chevron is transversely flattened and oval in cross section. The shaft becomes rectangular in cross section proximally, just below where it splits to give rise to the struts that support the proximal articular surfaces. These struts are separated by a 'V-shaped' gap. The struts are broad anteroposteriorly but extremely narrow transversely below the articulation facets. A prominent groove indents the posterior surface of the shaft extending from the ventral margin of the gap between the two lateral struts that support the anterior articulation facets to near the distal end. The anterior margin of the shaft is rounded.

Appendicular Skeleton

Fragmentary portions of both scapulae are preserved, but little can be said of their morphology. The only feature of interest is a small tubercle present on the right scapula along the ventral margin of the scapular blade. This feature is not present in the smaller scapula preserved in UMNH VP 21104, which is from a smaller, and presumably ontogenetically younger individual, though there is some damage in that region on the latter specimen they may account for the difference.

Weathered proximal portions of both femora are preserved. The head of the femur is globular and separated from the greater trochanter by a distinct neck. There is a prominent ventrolaterally oriented groove in the posterior edge of the femoral head, the sulcus for the ligamentum capitis femoris (Novas, 1996; Butler et al., 2011). The lesser trochanter is located anterior and lateral to the greater trochanter and is not separated from the greater trochanter by an intertrochanteric notch.

A badly worn piece of the proximal portion of a tibia is preserved, but it reveals little of the morphology of this element. A fragmentary piece of the shaft of a fibula is also preserved. It is from near the proximal end as noted by the expanding margins at the proximal edge. The fragment is 'D-shaped' in cross section throughout its length.

Four phalanges and a partial ungual from the pes are preserved. Two of the phalanges are complete, and are identified as I-1 and III-1, based on comparisons with UMNH VP 16281 (see supplementary description below). Phalanx I-1 is triangular proximally, being flattened medially and tapered and rounded laterally. The shaft is comparatively long and narrow, and constricted in the middle. The extensor pits are prominent and oriented

slightly dorsolaterally, so that they are visible in dorsal view. The distal end displays a well-developed, but transversely narrow articular surface. Phalanx III-1 is slightly longer than I-1 and much more robust. The proximal surface is concave with a minor swelling present on both the dorsal and ventral margins that define the boundaries of the two articular surfaces for the distal condyles of metatarsal III. The shaft of phalanx III-1 is constricted at mid length, and at the same point just dorsal to the ventral margin on each side a prominent foramen is present. The distal end consists of two well developed articular condyles, and the articular surface is well defined. The extensor pits are unequally developed, being deeper laterally than medially. The two other phalanges are incomplete and their identities cannot be definitively determined. The partial ungual also cannot be referred to a specific digit. The ungual is elongate and narrow, with prominent grooves present on the lateral and medial margins. The proximal articular surface is concave, and a subtle vertical ridge divides the surface roughly in half. The margins of the proximal end are rugose. The ungual is concave ventrally, but is more flattened distally.

SUPPLEMENTARY ANATOMICAL DESCRIPTION

The following description elucidates additional anatomical information gathered from specimens here referred to *Skaladromeus goldenii* (see Table 1). This information is provided separately from the primary description so that if future studies find that one or more of these tentative referrals are inaccurate, the primary description of *S. goldenii* will

remain unaffected. Only anatomical information not provided in the primary description is discussed.

Skull

A small piece of the posteroventral portion of a left maxilla is preserved in UMNH VP 21091. Portions of three alveoli are preserved, containing one nearly complete and another partial crown. On the medial surface dorsal to the alveolar margin the articulation facet for the palatine is indicated by a series of parasagittal ridges.

The partial maxillary crowns are lingually convex and labially concave, triangular in lateral view, and arranged in a slightly imbricated pattern within the maxilla, with the anterior edge of each crown positioned labial to the posterior edge of the preceding crown. A well-developed, steeply inclined wear facet is present on the anterolingual surface of the crown. The unworn posterior edge of the crown displays a few weakly defined marginal denticles, but ridges are absent from both the labial and lingual faces of the crown. A cingulum is present at the base of the crown and there is a distinct neck between the crown and the root of the tooth. The maxillary tooth roots are straight in posterior view.

A nearly complete left dentary is preserved in UMNH VP 21092. A row of foramina runs along the lateral surface of the dentary half way between the tooth row and the ventral margin (Figs. 3.4D and E). Anteriorly, this row of foramina curves ventrally to follow the dentary-predentary symphysis. The anterior tip of the dentary is spout-shaped with the anterior-most point positioned nearly level with the ventral edge of the

body of the dentary. The contact with the predentary consists of a narrow groove between two steep ridges in anterior view. The dentary forms the anterior edge of the coronoid process, the plesiomorphic basal neornithischian condition. The tooth row is inset medially and straight in dorsal view. It originates slightly medial to the dentary-predentary symphysis and ends posteriorly on the anterior edge of the rising coronoid process. The teeth are arranged in an imbricated pattern as in the maxilla.

Axial Skeleton

A disarticulated first true sacral vertebra (see discussion) is preserved in UMNH VP 21095 (Figs. 3.7A-D). The posterior end is 'heart-shaped,' being indented dorsally, whereas the anterior end is transversely expanded to receive the posterior end of the first sacrodorsal (Fig. 3.7A). Below the articulation surface for the posterior portion of the first sacral rib a prominent ventrolaterally directed facet is present that supported the medial protuberance of the main body of the pubis (Figs. 3.11A, B, and D; mta).

A partial, transversely compressed sacrum preserving portions of five fused sacral centra is present in UMNH VP 16773 (Fig. 3.7I). The centra on each end of the sacrum are incompletely preserved, and the majority of the neural arches are missing. The sacral rib articulations transition from spanning adjacent centra anteriorly, to arising from the dorsolateral surface of a single sacral centrum posteriorly. The shape of the ventral surface of the centra cannot be determined due to crushing. In all basal neornithischian taxa the contact between the first true sacral centrum and the first sacrodorsal is transversely expanded, as demonstrated by the disarticulated first true sacral centrum

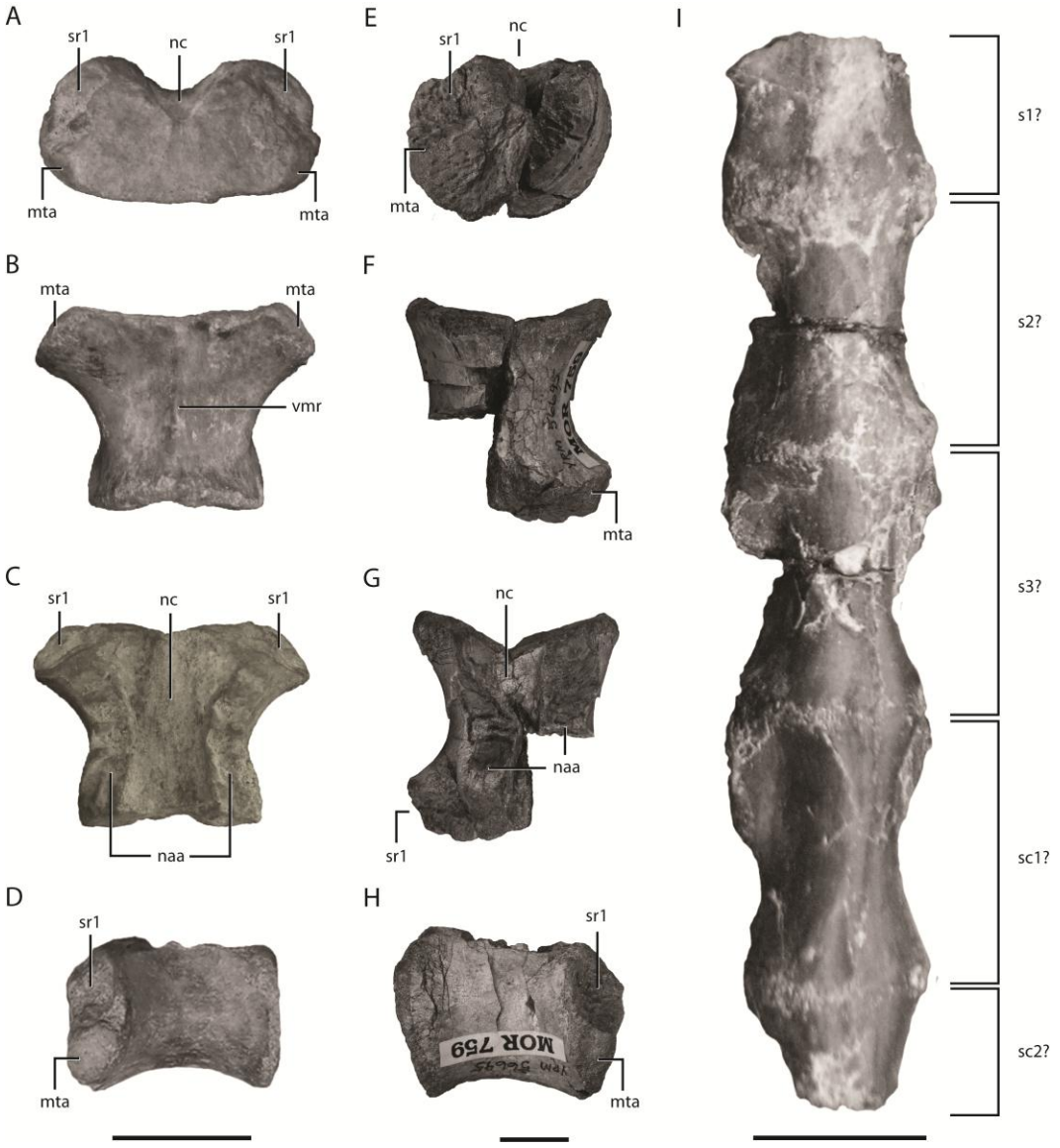

Figure 3.7: Sacral vertebrae from *Skaladromeus* and *Zephyrosaurus*. First true sacral centrum (S1) referred to *Skaladromeus* (UMNH VP 21095) in anterior (**A**), ventral (**C**), dorsal (**E**), and left lateral (**G**) views. The first sacrodorsal (SD1) centrum from *Zephyrosaurus* (YPM 56695, formally MOR 759) is figured for comparison in posterior (**E**), ventral (**F**), dorsal (**G**), and right lateral (**H**) views. A partial sacrum referred to *Skaladromeus* (UMNH VP 16773) shown in ventral view (**I**) with tentative identifications of the preserved sacral centra. In (**B**), (**C**), (**F**), (**G**), and (**I**) anterior is towards the top. In (**D**) and (**H**) anterior is to the left. Scale bars equal 1 cm and each scale bar applies to the overlying column. See Appendix 2 for anatomical abbreviations.

preserved in UMNH VP 21095 (Fig. 3.11A). This feature is not observed in this specimen indicating that at least one sacral vertebra (the first sacrodorsal) is not preserved in UMNH 16773. Based on this observation, it is proposed that the sacrum of *Skaladromeus* contained at least six sacral vertebrae.

Anteriorly in the series the proximal articulation facets of the chevron are joined to form a continuous articular surface (UMNH VP 12665). In lateral view the proximal end resembles an inverted V that points dorsally, creating separate articulation surfaces that face anterodorsally and posterodorsally, respectively (UMNH VP 21098). The chevrons articulate intervertebrally, with each articulation facet contacting a separate caudal centrum. Posteriorly in the series, this united proximal articulation facet separates into two distinct heads that are oval in dorsal view and flared laterally (UMNH VP 12665).

Appendicular Skeleton

A partial left scapula is preserved in UMNH VP 21104 (Fig. 3.8A). The majority of the anterior end of the scapula forms the thickened articulation surface with the coracoid. The scapula contributes to slightly less than half of the anteroventrally facing glenoid fossa (Fig. 3.8A; gf). The preserved portion of the scapular blade is medially concave and the ventral and dorsal margins diverge posteriorly (Fig. 3.8A). The base of the scapular spine is present, angling anteriorly towards the base of the acromion process (Fig. 3.8A; ss). The morphology of the distal end of the scapular blade and the acromion process is unknown.

A partial left coracoid is preserved in UMNH VP 21099 (Figs. 8B and C). The coracoid is concave medially and possesses a small, fully enclosed coracoid foramen (Fig. 8B; cf). The

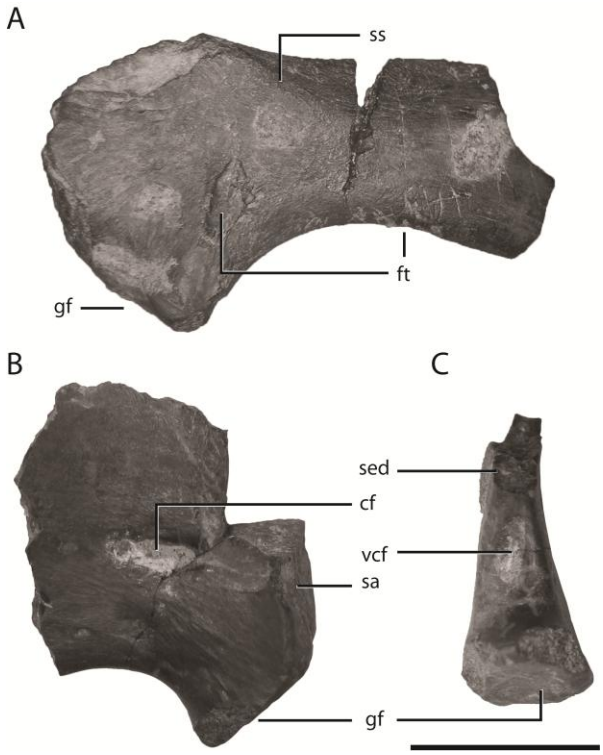

Figure 3.8: Partial left scapula and coracoid referred to *Skaladromeus*. Scapula (UMNH VP 21104) figured in lateral view (**A**) and coracoid (UMNH VP 21099) figured in lateral (**B**) and ventral (**C**) views. Scale bar equals 1 cm. See Appendix 2 for anatomical abbreviations.

coracoid is equal in thickness to the proximal portion of the scapula where they articulate, but thins noticeably away from this contact. On the lateral surface of the coracoid, a shallow groove is present that separates the raised margins along the glenoid fossa from the raised margin along the articular surface for the scapula. The coracoid contribution to the glenoid fossa lies at a forty-five degree angle to the articular surface for the scapula, forming a glenoid fossa that spans approximately ninety degrees when in articulation with the scapula (Fig. 8B; gf). A groove runs along the ventral edge of the coracoid, extending from the sternal process to near the glenoid fossa. Within this groove a prominent elliptical foramen is present slightly anterior to the glenoid fossa (Fig. 8C;

vcf). This feature is not observed in other basal neornithischian taxa. The full extent of the sternal process and the complete dimensions of the coracoid are not preserved.

The description of the humerus is based on a proximal portion of a humerus (UMNH VP 21105; Figs. 3.9A, B, C, and D) and a distal portion of a humerus (UMNH VP 21101; Figs. 3.9E, F, G, H, and I). A well-defined humeral head is centrally placed on the proximal end (Fig. 3.9E). The anterior surface of the proximal half of the humerus is gently concave (Fig. 3.9C), whereas the posterior face is slightly convex (Fig. 3.9A). The deltopectoral crest is a prominent, angular, anteriorly projecting tubercle on the lateral margin of the humerus (Fig. 3.9B, C, and D; dp). The proximal portion of the humerus reclined posteriorly, as in other orodromines. The distal condyles are well defined and separated by a moderate intercondylar groove that deepens anteriorly (Fig. 3.9H; aig). The medial distal condyle (radial) is slightly larger than the lateral (ulnar) condyle (Fig. 3.9I), and a shallow olecranon fossa is present on the posteroventral surface just dorsal to the distal condyles (Fig. 3.9F; of).

The description of the ulna is based on a proximal portion of an ulna (UMNH VP 21102; Figs. 3.10A and B) and a distal portion of an ulna (UMNH VP 21103; Figs. 3.10C and D). The olecranon process is moderately developed (Figs. 3.10A and B; op). The shaft has been crushed laterally so the cross-sectional shape cannot be determined. The distal end of the ulna is slightly reniform in ventral view, being concave medially (Fig. 3.10D).

Five carpals are present in UMNH VP 12677 (Fig. 3.11). The ulnare (Fig. 3.11; pc1) is positioned over a transversely wide and proximodistally narrow distal carpal (Fig.

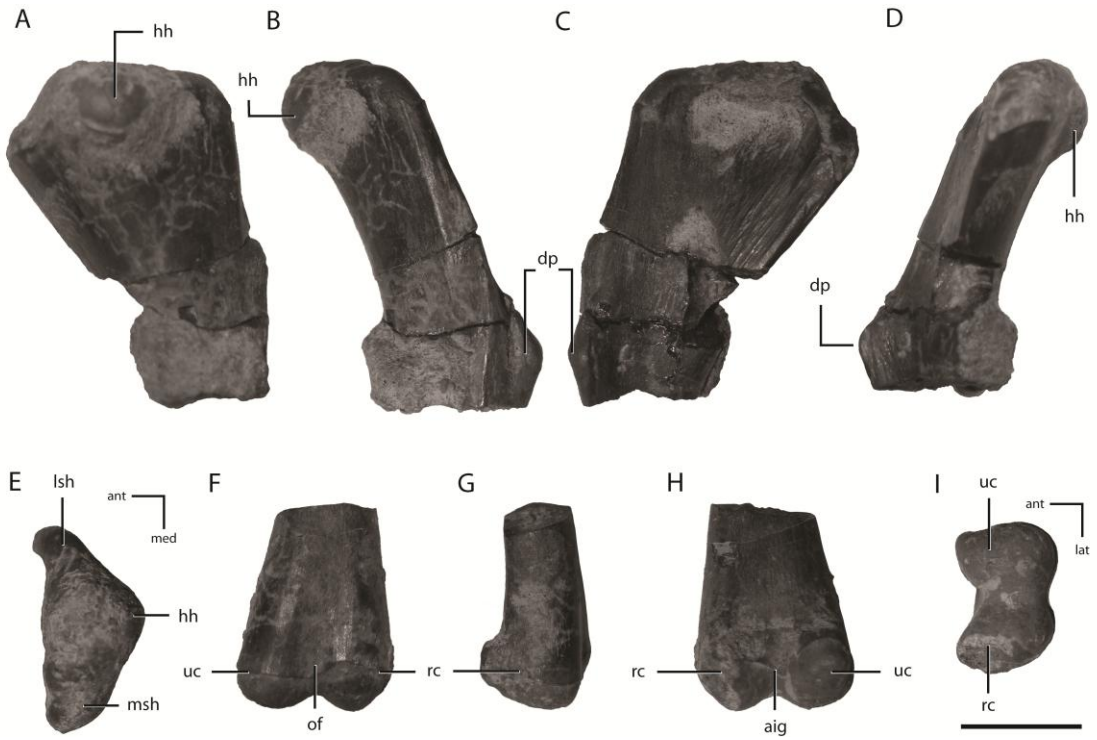

Figure 3.9: Proximal and distal portions of right humeri referred to *Skaladromeus*. Proximal portion of the humerus (UMNH VP 21105) figured in posterior (**A**), lateral (**B**), anterior (**C**), medial (**D**), and proximal (**E**) views. Distal portion of the humerus (UMNH VP 21101) figured in posterior (**F**), lateral (**G**), anterior (**H**), and distal (**I**) views. Scale bar equals 1 cm. See Appendix 2 for anatomical abbreviations.

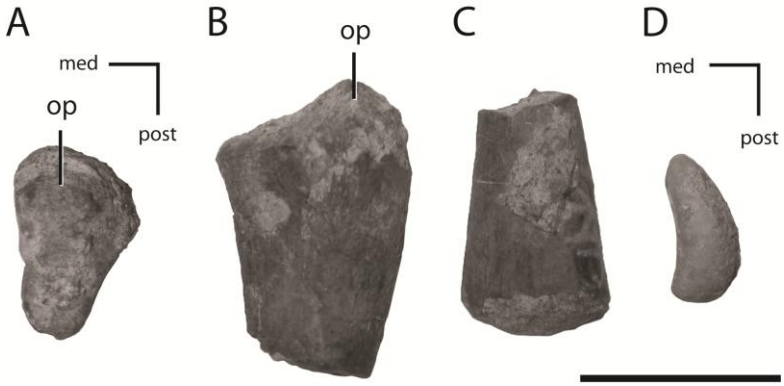

Figure 3.10: Proximal and distal portions of left ulnae referred to *Skaladromeus*. Proximal portion of the ulna (UMNH VP 21102) figured in proximal (**A**) and lateral (**B**) views. Distal portion of ulna (UMNH VP 21103) figured in lateral (**C**) and distal (**D**) views. Scale bar equals 1 cm. See Appendix 2 for anatomical abbreviations.

3.11; dc1), which sits snugly over all of metacarpal IV and the lateral portion of metacarpal III. The intermedium is positioned over the medial portion of metacarpal III and the lateral half of metacarpal II (Fig. 3.11; pc2). The original positions of two other carpals are uncertain as they were displaced during preparation.

An articulated manus is preserved and visible in plantar view in UMNH VP 12677 (Fig. 3.11). Digits I through IV are present, but digit V is either not present or was not preserved. The metacarpals are blocky on the distal and proximal ends, but narrow at midshaft. Metacarpal II is the longest, while metacarpal I is the shortest. The first phalanx of digit four is trapezoidal in shape, lacking a well-developed distal condyle. All other phalanges possess well-formed distal condyles and are concave ventrally. The unguals are longer than wide, distinctly pointed at the distal end, and concave in plantar view. Digit four is slightly splayed laterally from digit three, as evidenced by a medially oriented facet on the proximal end that rests against the proximolateral surface of metacarpal III (Fig. 3.11). A similar morphology is seen in *Thescelosaurus*, except that the facet is present on metacarpal II where it contacts metacarpal I. The phalangeal formula is 2-3-(4?)-2-?.

The phalangeal formula of *Hexinlusaurus multidens* (He and Cai 1983) is reported as 2-3-4-2?-2 (He and Cai, 1984). However, He and Cai (1984) state that digit four is poorly preserved and the number of phalanges is questionable. Thus, the reported presence of two phalanges in digit four of *H. multidens* is here considered dubious until additional evidence is provided to support this claim. In contrast, the proximal half of the

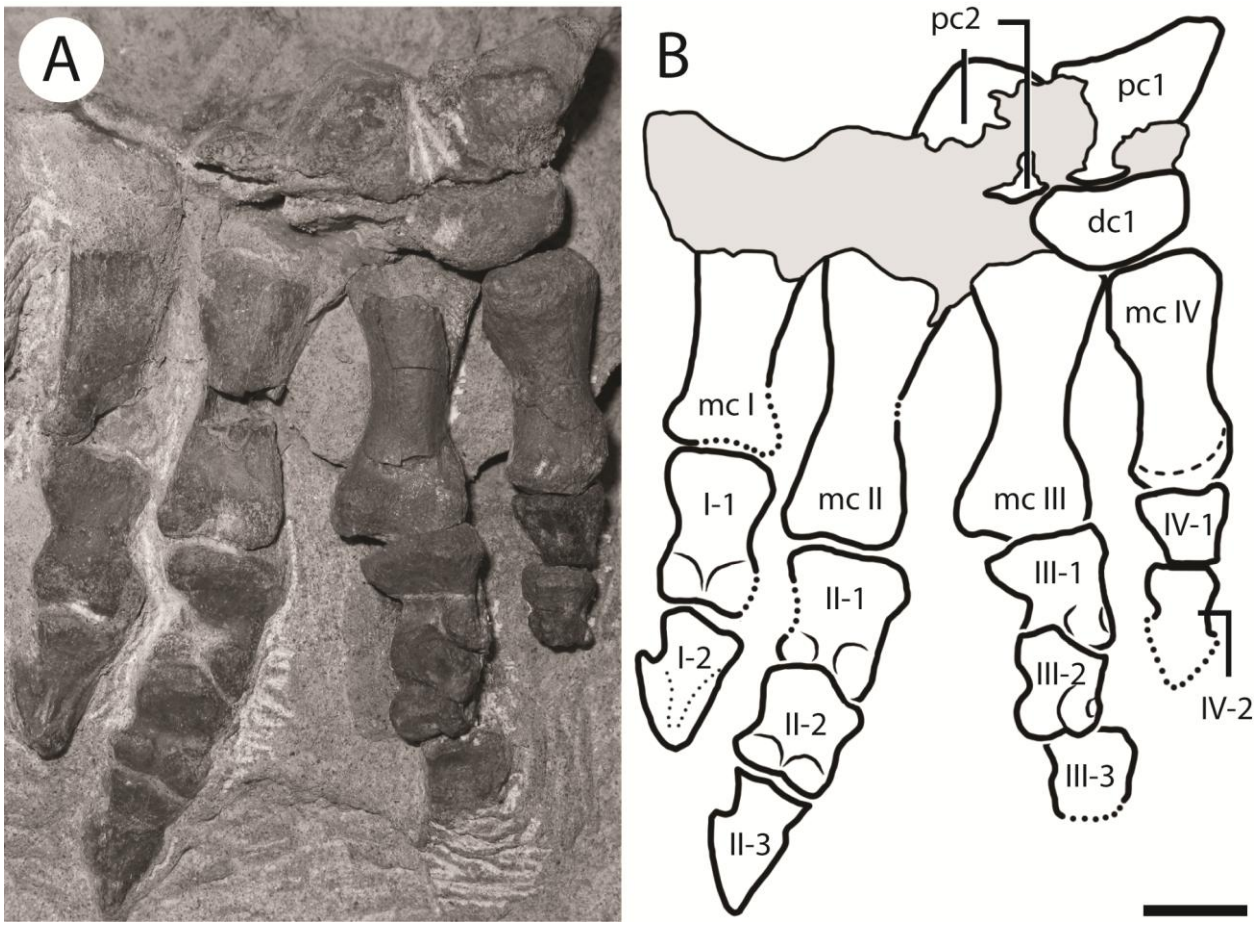

Figure 3.11: Partial right manus referred to *Skaladromeus*. Specimen UMNH VP 12667 photographed (left) and illustrated (right) in plantar view. In the illustration, matrix obscuring bone is shaded grey and dotted lines indicate reconstructed portions of incompletely preserved bones. Two additional carpals are preserved, but were not included as their exact positions are uncertain. Digit five was either not present or not preserved. Phalanges are labeled as follows: digit number in Roman numerals-number in the series in Arabic numerals. Scale bar equals 1 cm. See Appendix 2 for anatomical abbreviations.

ungual from digit four is present in *S. goldenii* and it displays the bases of the tendon grooves, confirming the presence of only two phalanges. This condition appears convergently in the heterodontosaurid *Abrictosaurus consors* Thulborn 1974 among basal ornithischians and in some derived members of the Iguanodontia and Thyreophora (Galton and Upchurch, 2004; Norman, 2004; Norman et al., 2004b; Vickaryous et al., 2004).

Polymorphism in the manual phalangeal formula was previously reported within a population of an undescribed basal neornithischian taxon (i.e., the 'Proctor Lake ornithopod') from the Twin Mountains Formation of Texas (Winkler, 1989). Specifically, the number of phalanges in digit III varies from four to three (D.A. Winkler, pers. com. 2009). The potential presence of polymorphism is difficult to assess in other basal neornithischians as the manus is only known from a single specimen in most taxa (Norman et al., 2004c). This polymorphism in the manus of the 'Proctor Lake ornithopod' could shed doubt on the taxonomic utility of the presence of only two phalanges in digit IV of the manus in *S. goldenii*. However, until evidence to the contrary is discovered, the presence of two phalanges in digit four of the manus is considered an apomorphic trait of *S. goldenii*.

A fragmentary piece of the postacetabular portion of the ilium is preserved in UMNH VP 12677. It is thin, concave medially, and bears a distinct lateral ridge that demarcates the border between the lateral postacetabular surface and the ventromedially oriented brevis shelf. The remainder of the ilium is not preserved.

The description of the femur is based upon a proximal portion of a femur (UMNH VP 21106; Figs. 3.12G, H, and I) and a distal portion of a femur (UMNH VP 21107; Figs.3.12 J, K, and L). The femur is straight in anterior view and bowed in lateral view. The head of the femur is

globular and separated from the greater trochanter by a distinct neck. The greater trochanter is laterally flattened and extends dorsally to the same height as the femoral head. The lesser trochanter is located anterior and lateral to the greater trochanter and is not separated from the greater trochanter by an intertrochanteric notch. The flexor intercondylar groove is prominent and deep, but no extensor intercondylar groove is present. The medial distal condyle (tibial) is slightly larger than the lateral condyle (fibular).

The description of the tibia is based on a proximal portion of a tibia (UMNH VP 21096; Figs. 3.12A, B, and C) and a distal portion of a tibia (UMNH VP 21097; Figs. 3.12D, E, and F). The lateral and posterior condyles on the proximal end of the tibia are separated by a narrow groove (Fig. 3.12A). The lateral condyle consists of a single lobe (Fig. 3.12A; plc), unlike in the orodromine taxa *Orodromeus* and *Oryctodromeus* where the lateral condyle is divided into two lobes (Scheetz, 1999; Varricchio *et al*., 2007). The cnemial crest is rounded (Fig 3.12A; cc). The mid-shaft of the tibia is triangular in transverse section. Distally, a prominent facet is present on the anterolateral surface against which the fibula abutted the lateral malleolus (Fig. 3.12F; lm). The ratio of femur to tibia size is unknown as neither element is completely preserved within a single specimen.

A complete fibula is preserved in UMNH VP 16772. The proximal portion of the fibula is anteroposteriorly expanded and inclined posteriorly. The medial side of the shaft is flattened throughout its entire length, while the lateral surface is convex, giving it a ‘D-shaped’ cross-section. The shaft decreases in diameter distally, though the posterior end is slightly expanded.

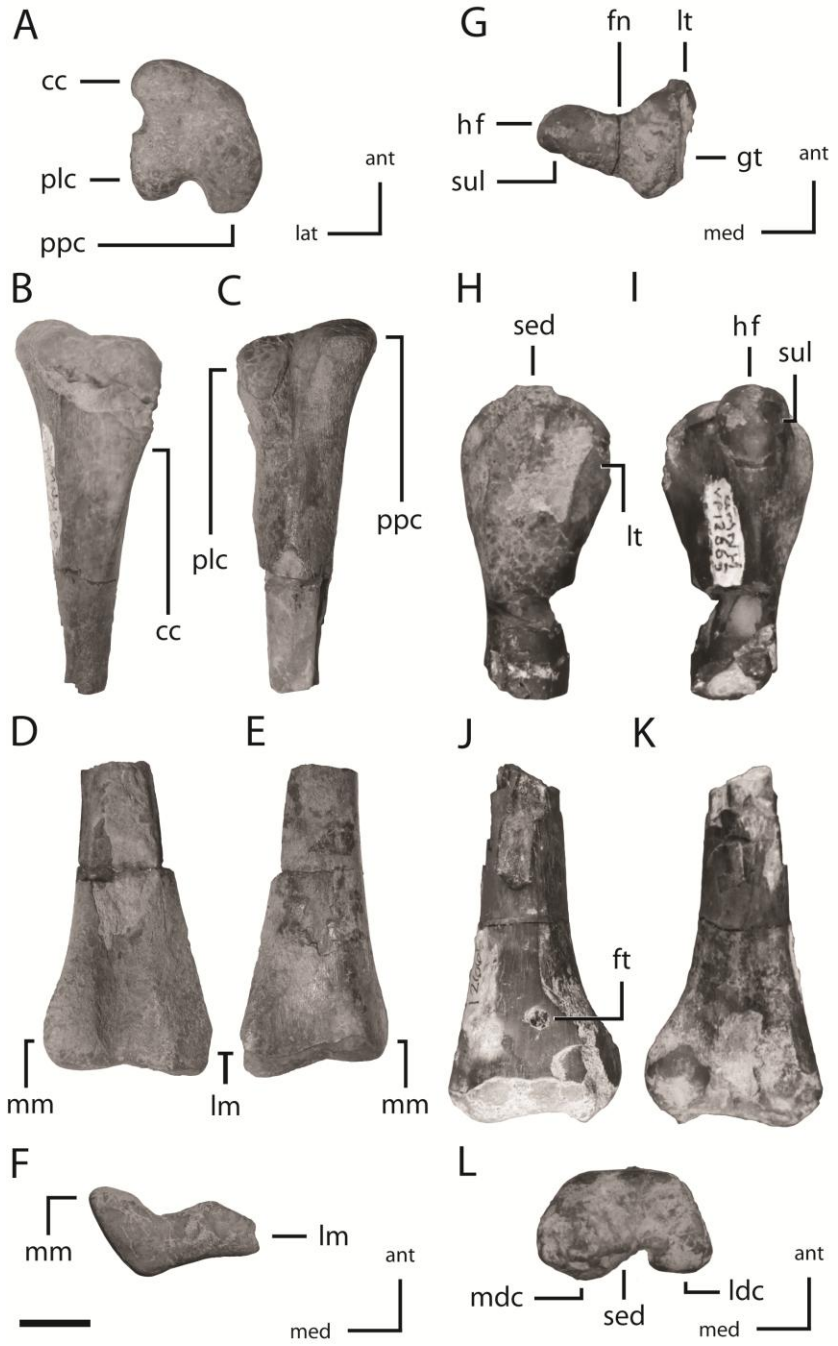

Figure 3.12: Partial femora and tibiae referred to *Skaladromeus*. Proximal portion of tibia (UMNH VP 211096) figured in proximal (**A**), anterior (**B**), and posterior (**C**) views. Distal portion of tibia (UMNH VP 21097) figured in anterior (**D**), posterior (**E**), and distal (**F**) views. Proximal portion of femur (UMNH VP 21106) figured in proximal (**G**), lateral (**H**), and medial (**G**) views. Distal portion of femur (UMNH VP 21107) figured in anterior (**J**), posterior (**K**), and distal (**L**) view. Scale bar equals 1 cm. See Appendix 2 for anatomical abbreviations.

A nearly complete, disarticulated calcaneum is preserved in UMNH VP 16281. The ventral and anterior margins of the lateral surface of the calcaneum are swollen. The dorsal articular surface for the fibula is concave. The majority of the articulation surface for the lateral malleolus of the tibia is damaged, but the angle between the articulation surfaces for the fibula and tibia is roughly 130 degrees. The articulation surface for the astragalus is not preserved.

Both the medial and lateral distal tarsals are preserved in contact with the metatarsals in UMNH VP 16281 (Fig. 3.13). The medial distal tarsal is 'L-shaped' in proximal view with the longer axis overlying all of metatarsal III and a shorter, dorsoventrally thin process extending medially over the posterior half of the dorsal end of metatarsal II. In proximal view the lateral edge is sinuous to fit against the lateral distal tarsal. The lateral distal tarsal overlies metatarsal IV, is weakly reniform in shape, concave dorsally, and the lateral surface is flattened.

Specimen UMNH VP 16281 preserves both the left and right pes. Metatarsal I bears a well-developed distal condyle (Fig. 3.13). Metatarsal I is less than half the size of metatarsal III. It is splint-like proximally and is closely appressed to the medial surface of metatarsal II. Its proximal end is even with the proximal end of metatarsal II as evidenced by the presence of a flattened facet on the medial side of metatarsal II. Metatarsal II is slightly longer than metatarsal IV, but does not extend as far distally because the proximal end is positioned higher than metatarsal IV (Fig. 3.13A). Laterally, metatarsal II is rounded distally and flattened proximally to articulate with metatarsal I, whereas medially it is flattened where it contacts metatarsal III. The proximal end of metatarsal II

is anteroposteriorly wider than the other metatarsals, wedge shaped in proximal view, and the posterior half is depressed for reception of the posteromedial process of the medial distal tarsal. Metatarsal III is the longest of the metatarsals. The shaft is flattened medially to accommodate metatarsal II, and rounded distolaterally below the contact with metatarsal IV. The proximal end of metatarsal III is rectangular in proximal view. The distal end bears two prominent condyles, the medial being larger than the lateral..

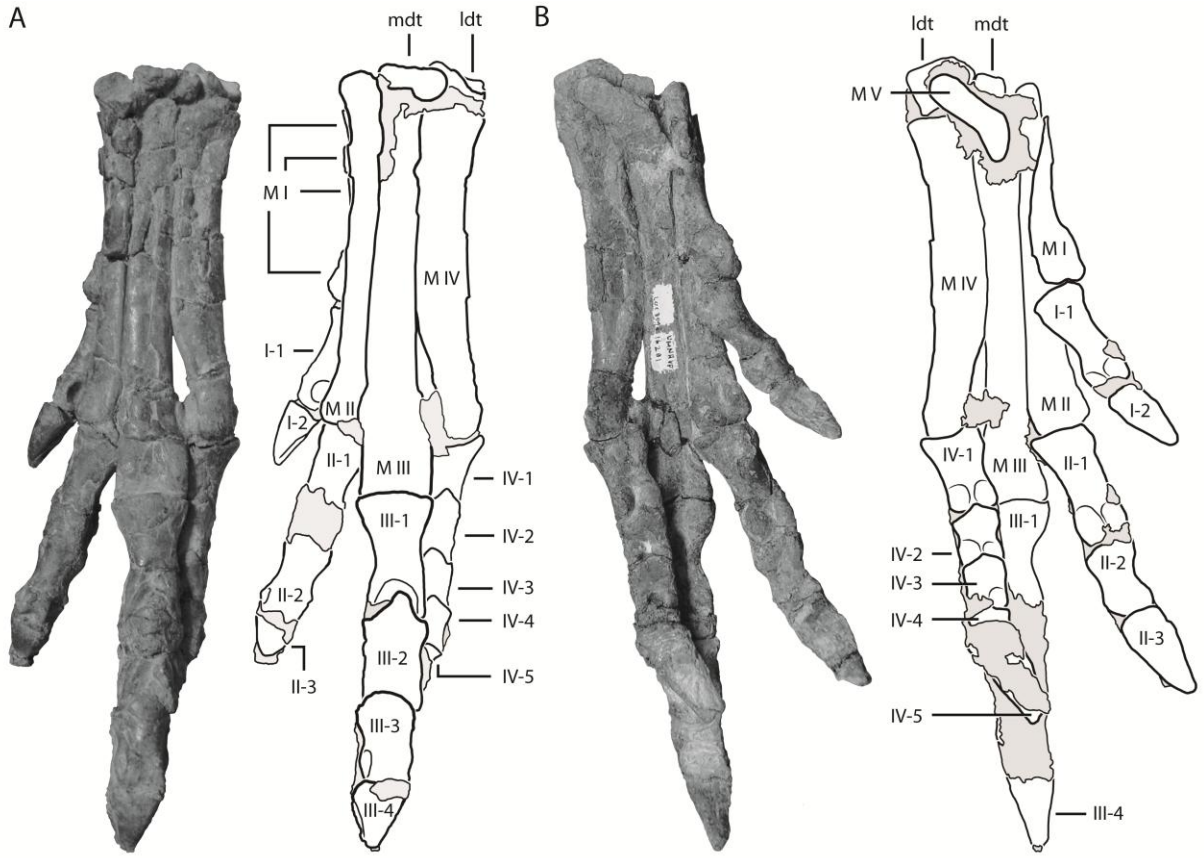

Figure 3.13: Left pes referred to *Skaladromeus*. Specimen UMNH VP 16281 figured in anterior (**A**) and posterior (**B**) views. In each view, the specimen is photographed (left) and illustrated (right). In the illustration, all sediment is shaded grey. Phalanges are labeled as follows: digit number in Roman numerals-number in the series in Arabic numerals. Scale bar equals 1 cm

Metatarsal IV is flattened medially to lie against metatarsal III for two-thirds of its length. The proximal end of metatarsal IV is 'D-shaped' in proximal view, being flattened medially to lie against metatarsal III. The distal third of metatarsal IV angles away from metatarsal III laterally and bears a single well-developed condyle. Metatarsal V is a flattened bone that is appressed to the posterior surface of the pes (Fig. 3.13B). It is about one-quarter the length of metatarsal III. The first phalanx on metatarsals I through III are elongate, but on metatarsal IV it is compact. In digits one and two the first phalanx is longer than the ungual, but in three and four the ungual is longer. The unguals are all at least two and a half times longer than wide and exhibit prominent grooves along their dorsolateral margins. The ratio of the combined width of the proximal ends of metatarsals II-IV to the length of metatarsal III is 0.34. The phalangeal formula of the pes is 2-3-4-5-0.

CLADISTIC METHODOLOGY

The systematic relationships of *S. goldenii* were analyzed using a modified version of the Boyd et al. (2009) dataset that originally contained 133 characters for 27 terminal taxa. That dataset was modified by adding one new outgroup terminal taxon (*Herrerasaurus* Reig 1963), one new ingroup taxon (*Koreanosaurus*) removing eight phylogenetically uninformative characters (characters 83, 125-127, 129, and 131-133 of Boyd et al. [2009]), splitting four characters (characters 96, 102, 104, and 110 from Boyd et al. [2009]) into nine characters (characters 95-97; 103-104; 106-107; and 113-114 in

Appendix 5), and adding an additional character state to three characters (characters 13, 41, and 60 in Appendix 5). Additionally, character data from the eight specimen-level terminals referred to *Thescelosaurus* by Boyd et al. (2009:fig. 3b) were combined to create the supraspecific terminal taxon *Thescelosaurus* (when character conflict is present all observed states are retained to reflect the presence of polymorphism [e.g., 0/1]). The terminal taxon *Skaladromeus* was then added using character data taken only from the holotype, though adding character data from all referred specimens does not change its phylogenetic position. The resulting dataset contains 130 characters for twenty-three terminal taxa. Two analyses of this dataset were conducted. In the first, all terminal taxa were included to assess the relationships of all five taxa here referred to the Orodrominae. In the second analysis, the terminal taxon *Koreanosaurus* was removed because it was acting as a wildcard taxon (sensu Nixon and Wheeler, 1992), and the relationships of the remaining terminal taxa were analyzed. Both analyses were conducted using the implicit enumeration search option in the program TNT version 1.1 (Goloboff et al., 2008). All characters were run unordered and the tree was rooted using the terminal taxon *Herrerasaurus*. Branches were collapsed if their minimum length equaled 0. Bootstrap (1000 replicates) and Bremer support values were calculated for the tree obtained during the second analysis using PAUP*v.4.0b10 (Swofford, 2002).

RESULTS

Analysis of the full dataset resulted in the recovery of three most parsimonious trees (MPTs) of length 363 (CI = 0.48, RI = 0.65). The resulting strict consensus tree (Fig. 3.14A) includes a polytomy containing the orodromine taxa *Koreanosaurus*, *Orodromeus*, *Skaladromeus*, and *Zephyrosaurus*. Examination of the three MPTs shows that this systematic uncertainty is caused by the unstable position of the terminal taxon *Koreanosaurus*, which is recovered as either the sister taxon to a clade containing *Orodromeus* and *Zephyrosaurus*, the sister taxon to *Zephyrosaurus*, or sister taxon to a clade containing *Orodromeus, Skaladromeus,* and *Zephyrosaurus*. Reanalysis of the dataset after the removal of *Koreanosaurus* resulted in the recovery of a single MPT of length 360 (CI = 0.48, RI = 0.66; Fig. 3.14B).

DISCUSSION

The interrelationships of orodromine taxa have never been robustly assessed, largely owing to the fact that three of the five taxa here referred to the clade have only recently been described (Varricchio et al., 2007; Huh et al., 2010; this study). Those analyses that have included orodromine taxa generally agree on their systematic relationships. *Orodromeus* and *Zephyrosaurus* traditionally are recovered as sister taxa in most cladistic analyses of basal neornithischian relationships (Weishampel and Heinrich, 1992; Scheetz, 1999; Buchholz, 2002; Varricchio et al., 2007; Boyd et al., 2009), except for in two analyses where they were placed in an unresolved position at the base of Ornithopoda (Butler et al., 2008a; Butler et al., 2011). In both analyses that included

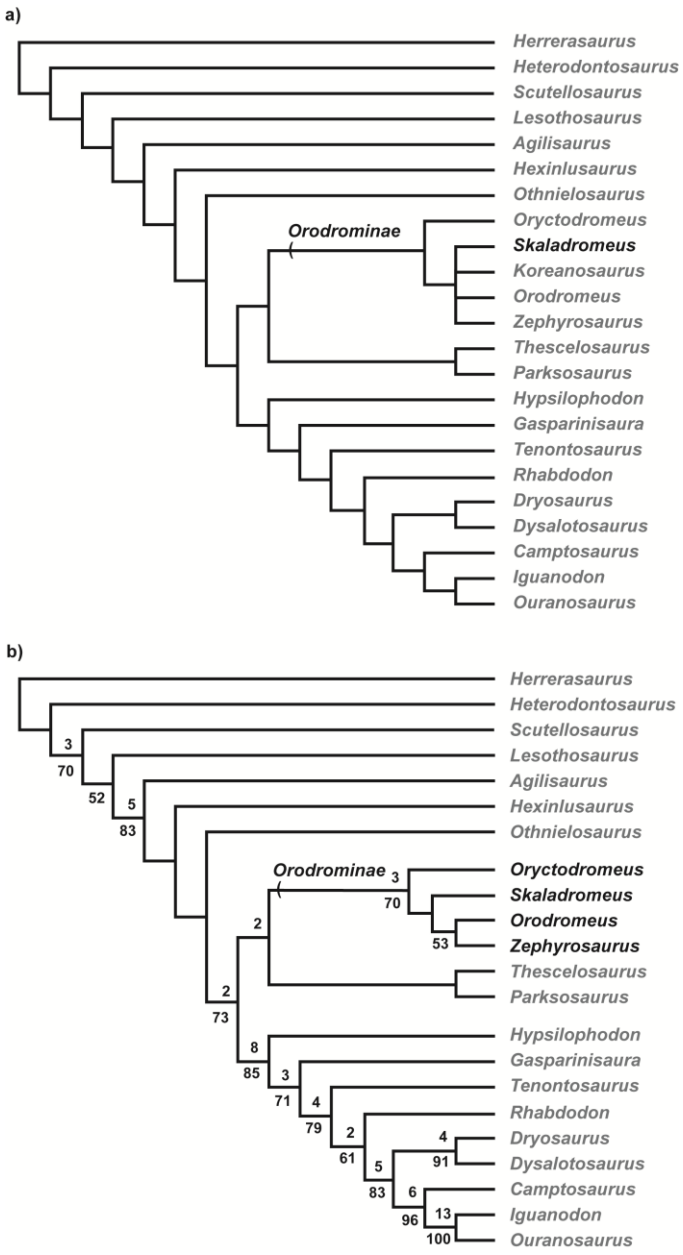

Figure 3.14: Results of the phylogenetic analyses conducted to evaluate the systematic position of *Skaladromeus* and to assess the interrelationships within Orodrominae. The strict consensus tree calculated from the three most parsimonious trees recovered via analysis of the full dataset is shown in (**A**). The polytomy present within Orodrominae is the result the terminal taxon *Koreanosaurus* acting as a 'wildcard taxon.' Therefore, a second analysis was run after the removal of *Koreanosaurus*, with the resulting single most parsimonious tree shown in (**B**). Bremer support numbers are reported in (**B**) when greater than 1 and are listed above each node in tree. Bootstrap values over 50% are reported in (**B**) below each node in tree.

Oryctodromeus, this taxon was recovered as the sister taxon to the *Orodromeus* + *Zephyrosaurus* clade (Varricchio et al., 2007; Boyd et al., 2009). The systematic relationships of *Koreanosaurus* have never been assessed in a cladistic analysis, though Huh et al. (2010) hand placed this taxon on a modified version of the Butler et al. (2008a) maximum agreement subtree as the sister taxon to *Orodromeus* (the only other orodromine taxon included) based on their interpretation of its morphology.

This study contains the most inclusive analysis of orodromine relationships yet conducted, which recovers *Koreanosaurus*, *Orodromeus*, *Oryctodromeus*, *Skaladromeus*, and *Zephyrosaurus* in a monophyletic group. The interrelationships presented here (Fig. 3.14) agree with those of the previously published analyses discussed above. The following is a brief discussion of the characters supporting the interrelationships of orodromine taxa based on this analysis. *Orodromeus* and *Zephyrosaurus* are united as sister taxa based upon the retention of the plesiomorphic shape of the anteroventral corner of the lateral temporal fenestra (oblique to right angle). This feature also occurs convergently in the ornithischian taxa *Dryosaurus*, *Dysalotosaurus* Virchow 1919, *Heterodontosaurus* Crompton and Charig 1962, and *Lesothosaurus* Galton 1978. *Skaladromeus* is placed as the sister taxon to the clade consisting of *Orodromeus* and *Zephyrosaurus* based on the presence in all three taxa of a pronounced jugal horn and the retention of the plesiomorphic shape of the cervical centra (plateocoelous or amphicoelous). Among taxa included in the analysis presented above, the presence of a jugal horn also occurs in *Heterodontosaurus*, whereas plateocoelous or amphicoelous cervical centra are present in *Camptosaurus* Marsh, 1885, *Hexinlusaurus* Barrett, Butler,

and Knoll, 2005, *Othnielosaurus* Galton, 2007, and *Rhabdodon*. *Oryctodromeus* is placed as the most basal taxon within Orodrominae based on the presence of a pronounced scapular spine, direct support of the pubis by the sacral centra, a fibular shaft that is 'D-shaped' in transverse section, and the lack of the three characters previously discussed above. When included in the analysis, *Koreanosaurus* is placed in a polytomy with all orodromine taxa except *Oryctodromeus* based on the presence in *Koreanosaurus* of a pronounced scapular spine, a fibular shaft that is 'D-shaped' in transverse section, and amphicoelous cervical centra (Huh et al., 2010).

Evaluating Proposed Osteological Correlates for Fossorial Behavior in Basal Neornithischians

The discovery of the type material of *Oryctodromeus cubicularis* within an infilled burrow (Varricchio et al., 2007) fundamentally changed our interpretation of basal neornithischian paleobiology. The co-occurrence of strong ichnological and body-fossil evidence reported by Varricchio et al. (2007) provides a rare opportunity to identify morphological traits that may correlate with fossorial behavior in basal neornithischian taxa. Seven such characters were identified in *Oryctodromeus* (Table 2), and the presence of several of these potential osteological correlates in *Orodromeus* and *Zephyrosaurus*, combined with additional sedimentological and taphonomic evidence, led Varricchio et al. (2007) to suggest these taxa may also have exhibited fossorial behavior. Additionally, fossorial behavior was recently inferred for the taxon *Koreanosaurus* (Huh et al., 2010) based on the presence of some of the osteological correlates proposed by Varricchio et al.

(2007). These examples highlight the importance of thoroughly investigating the distribution of proposed osteological correlates for fossorial behavior so that this behavior can be accurately inferred for taxa lacking ichnological evidence, clarifying the distribution of fossorial behavior within Neornithischia.

The recent discovery and description of *Koreanosaurus* and *Skaladromeus* combined with the recovery of new character data for members of the sister clade to Orodrominae (i.e., *Thescelosaurus* and *Parksosaurus*) facilitates a reevaluation of the distribution of those characters previously proposed to be correlated with fossorial behavior. The presence or absence of each character was reassessed for all taxa under study and ancestral state reconstruction was conducted on the tree shown in Figure 3.14B using the Parsimony Ancestral States reconstruction method in Mesquite v. 2.71 (Maddison and Maddison, 2009). For the purposes of this discussion, the term 'sister clade' is used to refer to the clade consisting of *Thescelosaurus* + *Parksosaurus*, which is the sister taxon to Orodrominae (Fig. 3.14B). Unless otherwise noted, the characters discussed below do not occur outside of Orodrominae and the sister clade among basal neornithischian taxa.

Character Evaluation

Other than the braincase, fusion of cranial elements in basal neornithischian taxa rarely occurs (Norman et al., 2004c), but in *Oryctodromeus* and *Zephyrosaurus* the premaxillae are fused into a single element. This condition was hypothesized to have stabilized the anterior portion of the skull for use in loosening and moving sediment

(Varricchio et al., 2007), as is seen in some extant fossorial vertebrates (Hildebrand, 1985). Fusion of the premaxillae is absent in *Orodromeus* (Scheetz, 1999), but the premaxillae are not preserved in any specimen of *Koreanosaurus* or *Skaladromeus*. Within the sister clade, fusion of the premaxillae is present in *Thescelosaurus* (NCSM

Table 3.2: Tracing the distribution of characters proposed to be osteological correlates for fossorial behavior in ornithischian dinosaurs by Varricchio et al., (2007). Characters 1, 2, and 3 are reconstructed to have evolved in the most recent common ancestor of Orodrominae and its sister clade. Characters 4 and 5 are thus far only known in *Oryctodromeus*, and are considered putative autapomorphies of that taxon. Character 6 is a local apomorphy of Orodrominae that is present convergently in *Rhabdodon,* negating its use as an osteological correlate for fossorial behavior. Character 7 is confirmed present in all orodromine taxa, making it a synapomorphy of the clade. This latter character may be an osteological correlate for fossorial behavior, assuming prior hypotheses concerning the distribution of fossorial behavior in this clade are correct (Varricchio *et al*., 2007). Abbreviations: **0**. character absent; **1**. character present; **-**. character state not preserved or unable to be scored.

	---------- Orodrominae ----------					-- Sister Clade --	
	Oryctodromeus	*Orodromeus*	*Zephyrosaurus*	*Koreanosaurus*	*Skaladromeus*	*Thescelosaurus*	*Parksosaurus*
1. Fused Premaxillae	1	0	1	-	-	1	-
2. Seven Sacral Vertebrae	1	1	-	-	-	1	-
3. Fused Scapula-Coracoid	1	0	-	-	-	1	-
4. Expanded Postacetabular Process	1	0	-	-	-	0	0
5. Recurved Scapular Blade	1	0	-	0	-	0	0
6. Sacral Centra Support Pubis	1	1	1	-	1	0	0
7. Prominent Scapular Spine	1	1	1	1	1	0	0

15728; C. Boyd, pers. obs.), but the premaxillae are unknown in *Parksosaurus*. As a result, this feature is unambiguously optimized to have evolved before the split of Orodrominae from the sister clade, and was secondarily lost in *Orodromeus*.

Fusion of the scapula and coracoid is only reported in *Koreanosaurus* and *Oryctodromeus* within Orodrominae (Varricchio et al., 2007; Huh et al., 2010). However, fusion of these two elements varies during ontogeny within *Oryctodromeus* (Varricchio et al., 2007), making the determination of its presence or absence in other orodromine taxa problematic. The majority of the material referred to *Skaladromeus* is from small, presumably immature specimens (based on observed patterns of neurocentral closure). Thus, the presence of unfused scapulae and coracoids in these specimens is not surprising or likely to be informative. Numerous specimens of disparate ontogenetic stages are known from *Orodromeus* and a detailed investigation of ontogenetic change within this taxon was conducted by Scheetz (1999); however, fusion between the scapula and coracoid was not reported from any specimen. In the sister clade, the scapula and coracoid are fused in the largest specimens of *Thescelosaurus* (e.g., NCSM 15728: C. Boyd pers. obs.), while the contact between the scapula and coracoid of the holotype and only known specimen of *Parksosaurus* (ROM 804) is too damaged to determine if the two were fused. Thus, the presence of a fused scapulocoracoid appears to be a feature that develops later in ontogeny that is common to at least Orodrominae and its sister clade among basal neornithischians.

The presence of at least six sacral vertebrae is a synapomorphy uniting all taxa more closely related to *Iguanodon* than to *Othnielosaurus* (Fig. 3.14B). *Oryctodromeus*

possesses a sacrum composed of seven vertebrae (Varricchio et al., 2007), which are here identified as follows: two sacrodorsals (SD1 and 2); three true sacrals (S1 through 3); and two sacrocaudals (SC1 and 2). These are arranged in the following order, from anterior to posterior: SD2-SD1-S1-S2-S3-SC1-SC2. While SD1 through SC2 all support portions of the sacral ribs in *Oryctodromeus*, SD2 supports the preacetabular process of the ilium via a dorsal rib that is fused to the neural arch. In taxa for which a growth series of sacra are known (e.g., *Thescelosaurus*) SD2 is the last sacral vertebra to fuse to the sacrum (based on examination of AMNH 117 and NCSM 15728: C. Boyd, pers. obs.). These characteristics make the presence or absence of SD2 difficult to identify in poorly preserved specimens, and in immature specimens where portions of the sacrum are disarticulated and/or unfused. The best preserved sacrum referred to *Orodromeus* is from the presumed juvenile holotype (MOR 294; Scheetz, 1999) that preserves six sacral vertebrae (SD1-SC2). Though SD2 is absent, the presence of irregular texturing on the posterior surfaces of unfused posterior-most dorsal vertebrae referred to this taxon suggest it would eventually fuse to the sacrum, resulting in the presence of seven sacral vertebrae in this taxon (Varricchio et al., 2007). Though no complete sacra are known for *Zephyrosaurus*, YPM 56695 preserves the disarticulated centrum from SD1 that exhibits an extremely roughened and irregular anterior surface that tightly interlocks with the preceding centrum (SD2?), providing strong evidence this taxon also had seven sacral vertebrae. The sacrum of *Skaladromeus* consists of at least six vertebrae (SD1-SC2), but the anterior portion of the articulated sacrum is unknown, and no disarticulated posterior dorsals are known, so it is uncertain whether this taxon possessed six or seven sacral

vertebrae. The morphology of the sacrum of *Koreanosaurus* is largely unknown. In the sister clade, the largest known specimen of *Thescelosaurus* for which the sacrum is visible displays seven fused sacral vertebrae (NCSM 15728; Boyd et al., 2009), whereas smaller specimens display either five (NMNH 7757) or six (AMNH 117) fused sacral vertebrae (Gilmore, 1915; Galton, 1974b). *Parksosaurus warreni* possesses at least six sacral vertebrae, though only SD1, S1, and S2 are fused, suggesting this specimen was immature (ROM 804: C. Brown pers. com.). The remaining posterior-most vertebrae (S3-SC2) are recognized based on their support of the posterior sacral ribs. Unfortunately, the sacrum of ROM 804 is not sufficiently prepared at this time to determine if a second sacrodorsal was present that supported the preacetabular portion of the ilium. Based on these observations, the number of sacral vertebrae was scored as follows: *Orodromeus*, *Oryctodromeus*, and *Thescelosaurus* scored for seven sacral vertebrae present (81:3); *Koreanosaurus*, *Parksosaurus*, *Skaladromeus*, and *Zephyrosaurus* scored as uncertain (81:?) owing to preservational issues. This results in the unambiguous optimization of seven sacral vertebrae present in the common ancestor of Orodrominae and its sister clade.

The presence of direct support of the medial protuberance of the pubis (*sensu* Scheetz, 1999) by the sacral centra (SD1 and S1) in *Orodromeus* (Scheetz, 1999), *Oryctodromeus* (Varricchio et al. 2007), *Zephyrosaurus* (Figs. 3.7D and H; mta), and now *Skaladromeus* (Figs.3. 7A, C, and G; mta) is unique among basal neornithischians and has long been recognized as an apomorphic trait uniting these taxa to the exclusion of all other basal neornithischians (Scheetz, 1999; Varricchio et al., 2007). This feature can

be traced in both mature (*Oryctodromeus*; MOR 1636a) and immature specimens (e.g., *Skaladromeus*; UMNH VP 21095). This condition is a marked departure from the plesiomorphic condition expressed in the sister clade where the first sacral rib supports the pubic peduncle of the ilium and sometimes also the iliac peduncle of the pubis, with no direct contact present between the pubis and the sacral centra (Galton, 1974a; C. Boyd, pers. obs.). However, this character is also present in the basal iguanodontian *Rhabdodon*, making it a local apomorphy of Orodrominae, but negating its use as an osteological correlate for inferring fossorial behavior.

A sharp and pronounced scapular spine is present in *Koreanosaurus, Orodromeus, Oryctodromeus*, and *Zephyrosaurus* (Varricchio et al., 2007; Huh et al., 2010). Though the known scapulae of *Skaladromeus* are incomplete, the base of the scapular spine is clearly visible (UMNH VP 21104: Fig. 3.8a; ss), confirming its presence in all orodromine taxa. Within the sister clade, well-preserved scapulae are known for both *Parksosaurus* and *Thescelosaurus*, neither of which display an enlarged scapular spine. Thus, this character is unambiguously optimized as a synapomorphy of Orodrominae.

The remaining two characters proposed as osteological correlates for fossorial behavior (Varricchio et al., 2007) are currently observed only in *Oryctodromeus*. However, evaluation of the presence or absence of a posteriorly recurved distal portion of the scapula and a highly elongate postacetabular portion of the ilium is complicated by a lack of comparable material from most other orodromine taxa. Both characters are confirmed absent in *Orodromeus* (Scheetz, 1999). In *Koreanosaurus*, the morphology of

the distal scapula more closely resembles *Thescelosaurus* than *Oryctodromeus*, but the morphology of the postacetabular portion of the ilium in unknown (Huh et al., 2010). In *Skaladromeus* and *Zephyrosaurus*, the morphology of these portions of the skeleton remains unknown. In the sister clade, both characters are confirmed absent in *Thescelosaurus* and *Parksosaurus*. Based on the observed distribution, these two characters remain putative autapomorphies of *Oryctodromeus*.

Implications

Accurately identifying potential osteological correlates for fossorial behavior is dependent on two factors. The first factor is an accurate reconstruction of the distribution of potential osteological correlates. As discussed above, ancestral state reconstruction of each of the seven previously proposed osteological correlates was conducted here using all available evidence. This reconstruction resulted in five of these characters being unambiguously optimized at specific nodes in the tree, while the remaining two are considered putative autapomorphies of *Oryctodromeus*. The second, and more difficult to determine factor is confidently inferring the distribution of fossorial behavior among known taxa. *Oryctodromeus* is the orodromine taxon with the strongest evidence for fossorial behavior, with taphonomic, sedimentological, and body-fossil evidence supporting the inference of this behavior. Two of the seven potential osteological correlates are only observed in *Oryctodromeus* (Table 2), though their presence or absence cannot be determined for *Koreanosaurus* or *Skaladromeus*. Thus, under this most conservative hypothesis, the presence of a posteriorly recurved distal portion of the

scapula and an extended postacetabular portion of the ilium could be osteological correlates for fossorial behavior.

Alternatively, there is some evidence to suggest that *Orodromeus* and/or *Zephyrosaurus* may have also exhibited fossorial behavior (Varricchio et al., 2007). Assuming a single origination of fossorial behavior within Neornithischia, this behavior would be primitive for Orodrominae. Only one of the seven characters examined here is unambiguously optimized as an autapomorphy of Orodrominae, the presence of a sharp scapular spine. This character is confirmed present in all five taxa here referred to Orodrominae, and confirmed absent in the sister clade. Therefore, this character is a possible osteological correlate for fossorial behavior, assuming this behavior is primitive to Orodrominae.

Three previously proposed osteological correlates for fossorial behavior are unambiguously optimized to have evolved in the most recent common ancestor of Orodrominae and its sister clade (Table 2). Thus, these characters cannot be used as osteological correlates for 'advanced' fossorial behavior (e.g., burrowing and denning). However, the presence of these characters in both orodromine taxa and the sister clade may indicate that the most recent common ancestor of these taxa exhibited fossorial behavior. Under this hypothesis, it is possible that the larger bodied *Parksosaurus* and/or *Thescelosaurus* retained a more conservative set of fossorial behaviors (e.g., rooting and digging, but not burrowing or denning), or retained these characters to serve other functions (e.g., expanded sacrum for larger body size).

Biogeographic Implications

Basal neornithischians were previously identified to species level only from more northern formations within the Western Interior Basin of North America (e.g., Black Leaf, Cloverly, Upper Two Medicine, Horseshoe Canyon, and Hell Creek Formations: Norman et al., 2004c; Varricchio et al., 2007, Boyd et al., 2009). *Skaladromeus* is the first described basal neornithischian taxon from North America found south of modern-day Wyoming, extending their known geographic range. The only taxon that is contemporaneous with *Skaladromeus* at approximately 75 Myr is *Orodromeus* from the Two Medicine Formation of Montana (Scheetz, 1999; Norman *et al*. 2004c). *Zephyrosaurus* and *Oryctodromeus* both occur earlier in time whereas the larger bodied taxa *Thescelosaurus* and *Parksosaurus* are found in overlying Maastrichtian sediments. Thus, given the range of orodromines over most of western North America and persisting throughout the Western Interior Basin for approximately 40 million years during the Cretaceous (Albian/Aptian through Campanian; Norman et al., 2004c), they comprised an important part of the North American dinosaur fauna. At the end of the Campanian (~71 Myr: Gradstein et al., 2005), orodromine taxa disappear from the fossil record and larger bodied basal neornithischian taxa (e.g., *Thescelosaurus*) appear within the Western Interior Basin. The co-presence of two orodromine taxa during the late Campanian (*Orodromeus* and *Skaladromeu*s) suggests that this faunal turnover was a relatively abrupt event in the Western Interior Basin, and not a gradual replacement of orodromine taxa by larger bodied basal neornithischians.

The pattern of higher-level taxonomic similarity throughout the Western Interior Basin has been documented by Lehman (1997; 2001), Sampson et al. (2004), and Gates et al. (2010). The discovery of the new orodromine *Skaladromeus goldenii*, a member of a clade whose distribution was previously restricted to the northern portion of the Western Interior Basin , links the dinosaurian assemblage of the Kaiparowits Formation to that of more northern Judithian formations that definitively contain taxa from this clade (e.g., Two Medicine Formation). Other dinosaurian taxa from the Kaiparowits Formation fall in line with this evidence, including the presence of the oviraptorosaurid *Hagryphus giganteus* and the hadrosaurid *Gryposaurus monumentensis*. However, the Kaiparowits Formation also contains taxa found in more southern formations (e.g., *Utahceratops*), suggesting this region of the Western Interior Basin may represent a transitional zone between the northern and southern 'faunas' defined by Lehman (1997; 2001) and further detailed as a latitudinal array of faunal distribution by Gates *et al*. (2010).

The global record of orodromine distribution was also recently expanded beyond North America with the discovery of *Koreanosaurus* from the Korean Peninsula (Huh et al., 2010). Additionally, relatively large burrows recently discovered within the Otway Group of Australia were shown to conform closely to the morphology of those attributed to *Oryctodromeus*, though no body-fossils were found within or associated with these burrows (Martin, 2009). If the referral of this taxon to a small-bodied ornithischian dinosaur is correct, two equally intriguing interpretations are possible. First, this evidence could indicate the presence of an orodromine taxon in the southern hemisphere during the

Early Cretaceous, though there is currently no evidence supporting a connection between Lauriasia and Australia during this time period. Alternatively, these burrows could indicate that fossorial behavior was more wide spread within Ornithischia than previously assumed. Unfortunately, the fragmentary nature of known basal neornithischian taxa from the Lower Cretaceous of Australia (e.g., *Leaellynasaura* Rich and Rich 1989) prevents examination of these taxa for either the synapomorphies of Orodrominae or the proposed osteological correlates for fossorial behavior outlined above and has precluded their inclusion in phylogenetic analyses of basal neornithischian relationships. Increasing our knowledge of the anatomy and systematic position of these taxa is critical to improving our understanding of the distribution of fossorial behavior in basal neornithischian dinosaurs and the geographic distribution of orodromine taxa. These recent discoveries combine to transform our understanding of orodromine taxa from a geographically restricted clade endemic to a small portion of the Western Interior Basin of North America to a potentially globally distributed clade of taxa that can provide important insights into ornithischian evolution, paleobiology, and patterns of geographic dispersal during the Cretaceous.

CHAPTER 4.

Exploring the Effects of Phylogenetic Uncertainty and Consensus Trees on Stratigraphic Consistency Scores: a New Program and a Standardized Method Proposed

INTRODUCTION

Stratigraphic consistency metrics estimate the congruence between the branching pattern of a cladogram and the stratigraphic order of the Oldest Known Records (OKRs sensu Walsh [1998]: = FADs of Pol and Norell [2006]) of those taxa with fossil histories. These metrics assume that as our understanding of the fossil record increases, phylogenetic hypotheses should become increasingly congruent with the stratigraphic record. Under this assumption, phylogenies close to the true tree should display a close fit to the fossil record. Over the past two decades, various stratigraphic consistency metrics were proposed (Gauthier et al., 1988; Norell and Novacek, 1992; Benton and Storrs, 1994; Huelsenbeck, 1994; Siddall, 1998; Wills, 1999; Marjanovic and Laurin, 2007), investigated for biases and limitations (Norell, 1993; Siddall, 1996; Hitchin and Benton, 1997a, 1997b; Siddall, 1997; Wills, 1999; Wagner and Sidor, 2000; Pol et al., 2004), and modified to improve their performance (Pol and Norell, 2001; Pol and Norell, 2006; Wills et al., 2008). Stratigraphic consistency scores have been used as descriptive statistics (Villier et al., 2004; Saucede et al., 2007; Tetlie and Poschmann, 2008), to compare alternative phylogenetic hypotheses (e.g., Pryer, 1999; O'Leary, 2001; Wilson, 2002; Marivaux et al., 2004; Brusatte and Sereno, 2008), to estimate the completeness of the fossil record for a particular clade (e.g., Kerr and Kim, 2001; Angielczyk and Kurkin, 2003; Jeffery and Emlet, 2003), to examine alternative positions of taxa within phylogenies (e.g., Brochu and Norell, 2000; Pol and Norell, 2006), and to calculate the

incongruence between molecular divergence dates and the fossil record of first appearances for a given topology (Clarke et al., 2007; Marjanovic and Laurin, 2007). These methods have been applied to a diverse array of taxa, including marsileaceous ferns (Pryer, 1999), harpid gastropods (Merle and Pacaud, 2003), arthropods (Wills, 2001), adelophthalmoid eurypterids (Tetlie and Poschmann, 2008), echinoids (Jeffery and Emlet, 2003; Villier et al., 2004; Saucede et al., 2007), holothuroids (Kerr and Kim, 2001), lissamphibians (Marjanovic and Laurin, 2007), amniotes (Gauthier et al., 1988), dicynodont therapsids (Angielczyk and Kurkin, 2003), cetaceans (O'Leary, 2001), rodents (Marivaux et al., 2004), and several dinosaurian clades (Brochu and Norell, 2000; Wilson, 2002; Rauhut, 2003; Pol and Norell, 2006; Brusatte and Sereno, 2008; Wills et al., 2008). Despite the widespread use of these metrics, a standardized method for treating polytomies when calculating stratigraphic consistency metrics has yet to emerge, though some authors have commented on this topic. One of the first proposals was to address polytomies by assigning the OKR of the oldest taxon within the polytomy to the uncertain node, effectively disregarding the stratigraphic data provided by the other taxa within the polytomy (Huelsenbeck, 1994). Alternatively, a command within the Manhattan Stratigraphic Measure script (MSM: Siddall, 1998) uses a heuristic search to optimize relationships within polytomies, maximizing stratigraphic congruence. That command was retained in the subsequent modification of the metric by Pol and Norell (2001), termed MSM*.

The most extensive discussion regarding how to calculate stratigraphic consistency metrics for polytomous phylogenies is found in Wills (1999), which

introduces the program Ghosts. Ghosts calculates the Relative Completeness Index (RCI; Benton and Storrs, 1994), the Stratigraphic Consistency Index (SCI; Huelsenbeck, 1994), and the Gap Excess Ratio (GER; Wills, 1999) metrics, and allows the user to rearrange taxa within a polytomy such that stratigraphic congruence is either maximized or minimized (i.e., the 'worst case' and 'best case' scenarios of Wills, 1999: supplementary documentation). In the instructions for that program the author suggests the 'worst case' scenario should be employed such that if a polytomous phylogeny is found to be more stratigraphically congruent than an alternative phylogeny it will be because of the order of the resolved nodes and not because of a hypothetical optimal arrangement of taxa within the polytomies.

All of these solutions are limited in that they either trim or rearrange the unresolved branches to produce a dichotomous branching pattern that may not accurately represent the total phylogenetic signal present in the set of most parsimonious trees (MPTs). The goals of this paper are to document how different approaches to resolving polytomies affect stratigraphic consistency metrics, to propose a standardized method for calculating stratigraphic consistency measures for polytomous phylogenies, to introduce a new program that simplifies the calculation of stratigraphic consistency metrics, to discuss how molecular divergence dates should be treated when estimating their incongruence with the stratigraphic record of first appearances for a given topology, and to demonstrate that scores calculated from consensus trees imperfectly describe the signal present in the source MPTs. The following discussion is limited to absolute temporal metrics (e.g., MSM* and GER), and their associated range metrics (e.g., MSM* range

and GER range; Pol and Norell, 2006), because it was previously demonstrated that these metrics are least influenced by variations in the size, shape, and scale of the tree(s) being analyzed (Pol et al., 2004).

EXAMINING METHODS FOR TREATING POLYTOMIES

Developing a standardized method for calculating stratigraphic consistency metrics from polytomous phylogenies (i.e., containing at least one polytomy) first requires understanding how different methods of treating polytomies affect stratigraphic consistency scores. Five distinct methods for treating polytomies are here recognized and classified as either reducing or restructuring based upon how they deal with taxa within a polytomy. Figure 4.1 contains a hypothetical pair of alternative phylogenies, one polytomous (Fig. 4.1A) and the other dichotomous (i.e., fully resolved; Fig. 4.1B). Both trees contain thirteen taxa, designated with the letters A through M, and the OKRs of these taxa were set precisely one million years apart starting with taxon A at 1 Myr and increasing in age according to alphabetical order. Examining how each of the five methods for treating polytomies affects the resulting stratigraphic consistency scores of both phylogenies illustrates that the choice of method can influence which tree is found to be more stratigraphically congruent. For all of the methods discussed below, higher-level taxa within polytomies are evaluated relative to each other based upon the oldest OKR present within each taxon, a rule that should be followed whenever calculating stratigraphic consistency metrics for polytomous phylogenies.

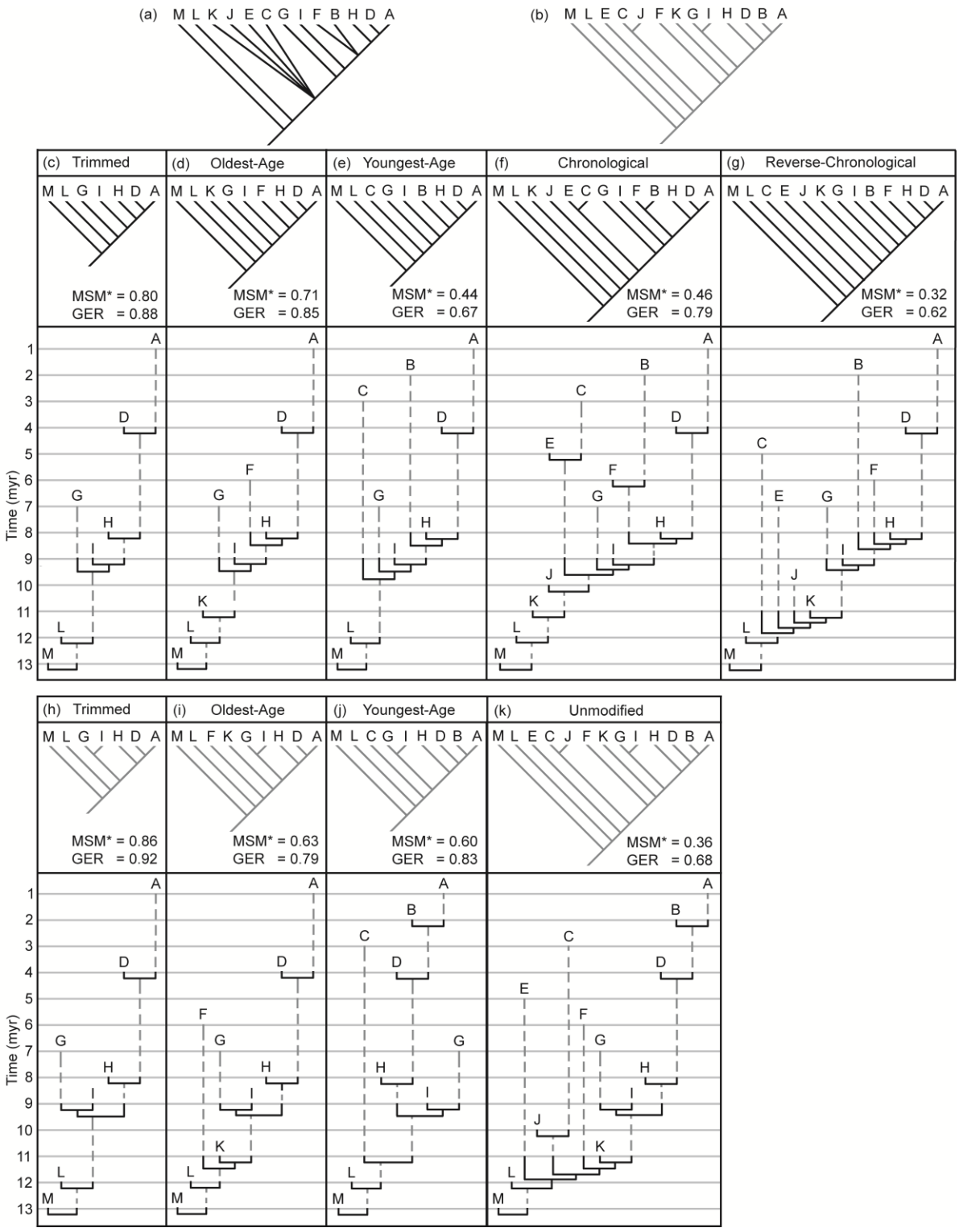
(a) M L K J E C G I F B H D A
(b) M L E C J F K G I H D B A
(c) Trimmed
M L G I H D A
MSM* = 0.80
GER = 0.88
(d) Oldest-Age
M L K G I F H D A
MSM* = 0.71
GER = 0.85
(e) Youngest-Age
M L C G I B H D A
MSM* = 0.44
GER = 0.67
(f) Chronological
M L K J E C G I F B H D A
MSM* = 0.46
GER = 0.79
(g) Reverse-Chronological
M L C E J K G I B F H D A
MSM* = 0.32
GER = 0.62
(h) Trimmed
M L G I H D A
MSM* = 0.86
GER = 0.92
(i) Oldest-Age
M L F K G I H D A
MSM* = 0.63
GER = 0.79
(j) Youngest-Age
M L C G I H D B A
MSM* = 0.60
GER = 0.83
(k) Unmodified
M L E C J F K G I H D B A
MSM* = 0.36
GER = 0.68
Time (myr)
1
2
3
4
5
6
7
8
9
10
11
12
13

Figure 4.1: The effects the five different methods for treating polytomies have on stratigraphic consistency metrics. Two hypothetical phylogenetic hypotheses are compared, one of which contains polytomies (**A**; drawn in black) while the other is dichotomous (**B**; drawn in grey). The polytomous phylogeny was modified using the five methods for resolving polytomies: **C**. the Trimmed method; **D**. the Oldest-Age method; **E**. the Youngest-Age method; **F**. the Chronological method; and **G**. the Reverse-Chronological method. To facilitate accurate comparison of stratigraphic consistency scores, corresponding taxa were trimmed from the dichotomous phylogeny as follows: **H**. for comparison with the Trimmed method; **I**. for comparison with the Oldest-Age method; **J**. for comparison with the Youngest-Age method; and **K**. the unmodified tree for comparison with both the Stratigraphic and the Reverse-Stratigraphic methods. The scores for both the MSM* and the GER metrics are provided below each cladogram. Modified from Boyd et al. (2011a).

Reducing Methods

The three reducing methods for treating polytomies are: 1) prune all taxa contained within a polytomy from the tree (e.g., the method employed by Marivaux et al. [2004]; hereafter, referred to as the Trimmed Method); 2) use only the taxon with the oldest OKR to represent all taxa within the polytomy (i.e., the method proposed by Huelsenbeck [1994]; hereafter, referred to as the Oldest-Age method); and 3) use only the taxon with the youngest OKR to represent all taxa within the polytomy (hereafter, referred to as the Youngest-Age method). All of these methods involve removing taxa from the polytomous tree and ignoring their associated age data (Figs. 4.1C, D, E). Therefore, the corresponding taxa must be removed from the dichotomous tree (Figs. 4.1H, I, J) prior to calculating stratigraphic consistency scores to facilitate accurate comparisons between these trees (Gauthier et al., 1988; Wills et al., 2008) due to the effect tree size (i.e., number of taxa) has on these metrics (Pol et al., 2004).

Restructuring Methods

The two restructuring methods for treating polytomies are: 1) situate taxa in a pectinate arrangement to maximize fit to stratigraphy (e.g., the method implemented by the MSM* script [Siddall, 1998; Pol and Norell, 2001]; hereafter referred to as the Chronological method); and 2) situate taxa in a pectinate arrangement in reverse-chronological order (e.g., the method suggested by Wills [1999]; hereafter referred to as the Reverse-Chronological method). No modifications to the dichotomous tree are necessary when these methods are employed because they do not ignore age data from any taxa, resulting in the retention of identical sets of taxa in each tree. Therefore, scores from both restructured polytomous topologies (Figs. 4.1F, G) are compared to those from the unmodified dichotomous tree (Fig. 4.1K).

RESULTS

The example in Figure 4.1 illustrates that recognition of the more stratigraphically congruent topology is dependent upon the reducing or restricting method chosen. The Trimmed (Fig. 4.1C versus 4.1H), Youngest-Age (Fig. 4.1E versus 4.1J), and Reverse-Chronological (Fig. 4.1G versus 4.1K) methods result in recovery of relatively lower stratigraphic consistency scores for the modified polytomous tree, while the Oldest-Age (Fig. 4.1D versus 4.1I) and Chronological (Fig. 4.1F versus 4.1K) methods result in relatively higher scores for the modified polytomous tree. The scores obtained for the restructured polytomous topologies using the Chronological (Fig. 4.1F) and Reverse-

chronological (Fig. 4.1G) methods mark the upper and lower bounds of the total variation that can be produced via restructuring the unresolved branches in the polytomous tree (Wills, 1999), reflecting the maximum amount of variation that could be present in the source MPTs. Both the Trimmed (Fig. 4.1C) and Oldest-Age (Fig. 4.1D) methods produce scores that fall outside of this range because they modify properties these metrics are sensitive to (e.g., tree size and number of OKRs; Pol and Norell, 2004). Similarly, trimming the dichotomous tree to facilitate comparison to the reduced polytomous topologies resulted in stratigraphic consistency scores that are higher than those obtained from the unmodified tree for the same reasons (Figs. 4.1H, I, J versus Fig. 4.1K). Based on these results, restructuring methods are preferred over reducing methods because they rearrange rather than prune taxa. This allows the full range of variation that phylogenetic uncertainty, indicated by polytomies, imparts on stratigraphic consistency scores to be understood, maximizes the amount of stratigraphic data available to compare alternative phylogenetic hypotheses, and prevents recovery of scores that fall outside of the range of possible variation present in the source MPTs.

COMPOLY AND THE ASCC PROGRAM SUITE

The manner in which the uncertainty in the age of the OKRs of taxa with fossil histories is handled has been shown to impact the resulting stratigraphic consistency scores (Pol and Norell, 2006). The MSM* range and GER range metrics were designed so that the effect this uncertainty has on stratigraphic consistency scores is taken into

consideration (Pol and Norell, 2006). We propose that the effects of phylogenetic uncertainty, reflected by the presence of polytomies, on these metrics be accounted for in a similar manner: by combining the scores obtained using the chronological and reverse-chronological methods to produce a range of scores that summarize this variation, here termed the Comprehensive Polytomy approach (ComPoly). When the ComPoly approach is employed when calculating stratigraphic consistency scores, a lower case p is added to the stratigraphic consistency metric acronym (e.g., MSMp* and GERp), just as the word range is added when the uncertainty in the age of OKRs of taxa with fossil histories is taken into consideration (e.g., MSM* range and GER range). If this is done for the polytomous tree from Figure 4.1A using the scores from Figures 4.1F and G, a range of 0.46 – 0.32 for MSMp* and 0.79 – 0.62 for GERp are obtained. The corresponding scores for the unmodified dichotomous tree (Fig. 4.1K) fall within that range, indicating that neither tree can be selected as more congruent with the stratigraphic record. Implementation of any other approach for treating polytomies would result in a different, inaccurate conclusion. Constructing a range score that accounts for both phylogenetic and age uncertainty requires that the highest score obtained for the Chronologically restructured topology is combined with the lowest score obtained from the Reverse-Chronologically restructured topology. The resulting range score effectively characterizes the full range of variation that age and phylogenetic uncertainty impart on these metrics.

To streamline the process of calculating an array of stratigraphic consistency metrics that account for age and/or phylogenetic uncertainty (e.g., MSM* range and MSMp* range), a collection of files was developed, collectively referred to as the Assistance with

Stratigraphic Consistency Calculations (ASCC) program suite (freely available at www.stratfit.org). A brief introduction to the files included in the program suite is provided below, and more detailed instructions are given in the readme file included in the suite.

Using the ASCC.pl Script to Construct Data Files

Previously published scripts that calculated stratigraphic consistency range metrics required manual construction of a set of data files that could be somewhat time-consuming to generate and to troubleshoot when constructed incorrectly. These issues may have discouraged some researchers from calculating these statistics despite their advantages over standard stratigraphic consistency metrics. The ASCC.pl script included in the ASCC program suite simplifies the construction of the agefile, treefile, and data.tnt files required to calculate stratigraphic consistency range metrics by guiding the user through a set of questions about the details of the tree(s) and taxa being analyzed. The script can be run in any Perl interpreter (see readme file for suggested programs). Taxa and trees can be read directly from files created by phylogenetic programs (e.g., NEXUS and tree files). Taxon names and trees can also be manually entered in the Newick notation format utilized by the phylogenetic program TNT (i.e., spaces separate terminal taxa, not commas; Goloboff et al., 2008), and terminal taxa should be numbered beginning with 1, because 0 is reserved for a hypothetical root taxon. When using the ComPoly approach, two topologies (Reverse-Chronologically and Chronologically restructured) are entered in that order for each polytomous tree analyzed. There is no

limit to the size or number of trees that can be entered and analyzed at one time, though all trees must include identical sets of taxa to facilitate accurate comparison of scores (Gauthier et al., 1988; Wills et al., 2008). The user assigns each terminal taxon to a specific age bin, which are user defined age ranges that encompass the uncertainty in the age of each taxon's OKR. When the program is finished, the agefile, treefile, and data.tnt files are created in the same location as the ASCC.pl script.

Using the stratfit.run Script to Calculate Scores

The stratfit.run script is a modified version of the ageuncert.run script created by Pol and Norell (2006) for the phylogenetic program TNT. While the former calculated only the MSM* range metric, the stratfit.run script facilitates the calculation of additional stratigraphic consistency metrics (i.e., GER range and MIG [Wills, 1999] range). Before running stratfit.run, ensure it is in the same folder as the files created by the ASCC.pl script and the program TNT. Next, run TNT and type in "stratfit.run" and press enter. For each replicate of the analysis (default = 1000), a score for MIG, MSM*, and GER is calculated using a set of OKRs randomly selected for each taxon from the age bins defined using the ASCC.pl script. Three output files are generated (MIG.out, msm.out, and ger.out) which contain a list of the scores calculated for the respective metric during each replicate.

Interpreting the Data

A set of Microsoft Excel macro files are included in the ASCC program suite. These files were developed to simplify processing the data generated by TNT. When the

scores stored in the output files are imported into these macros, the stratigraphic consistency range scores are automatically reported (see readme.pdf file for detailed instructions). These files also construct histograms of the pairwise differences between the MSM* and GER scores (or MSMp* and GERp scores when using the ComPoly approach) generated by each replicate of the analysis. Comparison of these output histograms is used to determine if one phylogeny is consistently more stratigraphically congruent (i.e., histogram plots entirely to one side of zero), or if the phylogenies are equally stratigraphically congruent (i.e., histogram crosses zero) when the resulting range scores overlap, as described in Pol and Norell (2006).

DISCUSSION

The restructuring methods used by the ComPoly approach rearrange, rather than trim, taxa placed at unresolved nodes in polytomous phylogenies, thereby maximizing the amount of stratigraphic data available to evaluate congruence between phylogeny and the fossil record. Previously proposed approaches do not describe the full effect phylogenetic uncertainty has on stratigraphic consistency scores. The ComPoly approach fully describes this variation and can be combined easily with existing stratigraphic consistency metrics (e.g., GER, MIG, and MSM*) using the new ASCC program suite. Here we discuss the benefits of using the ComPoly approach and the ASCC program suite for a new application of stratigraphic consistency metrics and highlight the

importance of carefully selecting the type of tree used to calculate stratigraphic consistency scores.

Stratigraphic consistency scores are often used to compare the stratigraphic congruence of alternative phylogenetic hypotheses for a given clade by holding the stratigraphic data (OKRs) constant while varying the tree topology. Two recent papers have expanded upon that methodology by exploring the ability of these metrics to evaluate the stratigraphic congruence of molecular divergence dates (Clarke et al., 2007; Marjanovic and Laurin, 2007). For example, in the Clarke et al. (2007) analysis, both the OKRs and the tree topology were held constant. Instead, the MIG value obtained by comparing the tree topology solely to the OKRs was contrasted with the value obtained for the same tree topology when molecular divergence dates for certain clades were enforced. Both studies had to account for uncertainty in the OKRs of taxa with fossil histories and the presence of polytomies within the trees analyzed. Despite the exhaustive nature of the study by Marjanovic and Laurin (2007), the calculation of stratigraphic consistency metrics was hampered by the fact that the investigation was completed before the publication, and without the benefit, of stratigraphic consistency range metrics (Pol and Norell, 2006), the ComPoly approach, and the ASCC program suite. The study by Clarke et al. (2007) used stratigraphic consistency range metrics (i.e., MIG range), the ComPoly approach, and an early version of the ASCC program suite to address age and phylogenetic uncertainty. Exploring the methodological differences between these studies, with regards to the calculation of stratigraphic consistency scores, clearly demonstrates the advantages of using both the ComPoly approach and the ASCC

program suite. It also highlights a few other important methodological details that should be taken into consideration when calculating these metrics.

Marjanovic and Laurin (2007) recognized the high level of uncertainty associated with designating a set date for the OKRs of taxa with fossil histories, specifically citing the difficulty of assessing the position of fossils relative to geochronologic boundaries and the uncertainty in the age of geochronologic unit boundaries themselves. They chose to address these issues by setting the OKR of each fossil taxon equal to the base of the oldest stage from which it was recovered and assumed that the taxon persisted through the entire stage. However, as demonstrated by Pol and Norell (2006:figs. 4.1 and 4.3) fixing the OKRs of taxa with fossil histories to a single age within the range of uncertainty can greatly influence the resulting stratigraphic consistency score. When dealing with topological uncertainty, Marjanovic and Laurin (2007) resolved polytomies using the chronological method, maximizing the fit between stratigraphy and phylogeny. As illustrated by Figure 4.1, failing to take into consideration the full range of phylogenetic uncertainty indicated by polytomies can bias the resulting stratigraphic consistency scores. Thus, despite their attempts to thoroughly calculate stratigraphic consistency scores, the resulting scores do not reflect the full range of age and phylogenetic uncertainty present in the trees analyzed. Additionally, both Clarke et al. (2007) and Marjanovic and Laurin (2007) treated molecular divergence estimates as fixed dates. However, because molecular divergence credibility intervals are analogous to the uncertainty in the age of OKRs of taxa with fossil histories when calculating stratigraphic consistency scores (i.e., both represent temporal uncertainty generated by different

methods of estimating the timing of cladogenesis), they can, and should, be accounted for using stratigraphic consistency range metrics to define a range of possible dates for the proposed origin of a clade rather than a single date. Despite these issues, which can now be accounted for using the ComPoly approach and the ASCC program suite, the use of stratigraphic consistency metrics to assess the congruence between molecular divergence data and the stratigraphic record of first appearances is a promising new application that deserves further investigation.

Restructuring polytomous strict consensus trees produces multiple dichotomous topologies, some of which may not represent the signal present in the primary trees (Swofford, 1991), resulting in the recovery of less accurate stratigraphic consistency range scores. For example, Figure 4.2 displays the two most parsimonious trees (MPTs) used to construct the strict consensus tree in Figure 4.1A The ranges calculated from these MPTs using the ASCC program suite (MSM* range = 0.34-0.32; GER range = 0.65-0.62) more accurately represent the signal present in the data than the ranges calculated from the strict consensus tree using the ComPoly approach and the ASCC program suite (MSMp* range = 0.46-0.32; GERp range = 0.79-0.62). Additionally, only the scores calculated from the source MPTs allow the dichotomous tree (Fig. 4.1K) to be recognized as more congruent with the stratigraphic record. This example clearly demonstrates that stratigraphic consistency scores should be calculated directly from the source MPTs whenever possible to insure the accuracy of the resulting scores. When more than two MPTs are recovered by a given analysis, these metrics are constructed using the ASCC program suite by computing scores for all the MPTs and then combining

the highest and lowest recovered scores (see readme file for further instructions). In situations where the topologies of the source MPTs were not reported, reanalysis of the original dataset and calculation of stratigraphic consistency scores from the resulting MPTs is recommended, as the resulting increase in accuracy vastly outweighs the extra time required.

Additionally, computing stratigraphic consistency scores from a less-than-strict consensus tree (e.g., majority-rule tree) is analogous to using the reducing methods for treating polytomies because they do not describe the total signal present in the source MPTs (Nixon and Carpenter, 1996). For example, comparison of two published polytomous phylogenies, the basal ornithischian phylogenetic hypotheses of Butler (2005) and Butler et al. (2008a), illustrates the pitfalls of comparing scores calculated from less-than-strict consensus trees. Comparison of the majority-rule consensus trees from these analyses (polytomies treated using the Reverse-Stratigraphic method) resulted in the phylogenetic hypothesis presented by Butler et al. (2008a) being identified as more congruent with the stratigraphic record by Wills et al. (2008). However, the results of our analysis of the strict consensus trees from both studies using the ComPoly approach and the ASCC program suite (1000 replicates) does not support this conclusion. Overlapping range scores are recovered for the two phylogenies (for the phylogeny proposed by Butler [2005]: MSMp* range = 0.55-0.38, GERp range = 0.87-0.64; for the phylogeny proposed by Butler et al. [2008a]: MSMp* range = 0.76-0.38, GERp range = 0.95-0.75), requiring that the pairwise differences between the scores obtained during each replicate to be

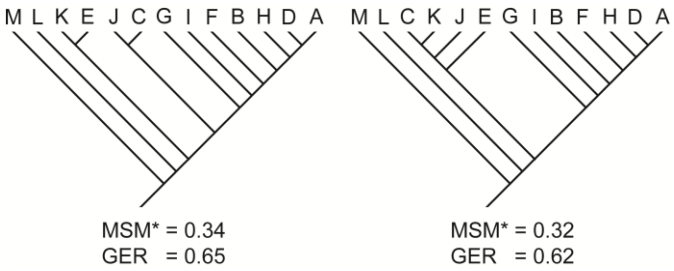

Figure 4.2: The two most-parsimonious trees (MPTs) used to construct the polytomous strict consensus tree illustrated in Fig. 4.1A. MSM* and GER scores for each tree are provided below and to the right of each tree. MSM* and GER range scores constructed by combining the scores from both trees (MSM* range = 0.34–0.32; GER range = 0.65–0.62) are more accurate than those obtained using the ComPoly approach on the polytomous strict consensus tree from Fig. 4.1A (MSM* range = 0.46–0.32; GER range = 0.79–0.62). Modified from Boyd et al. (2011a).

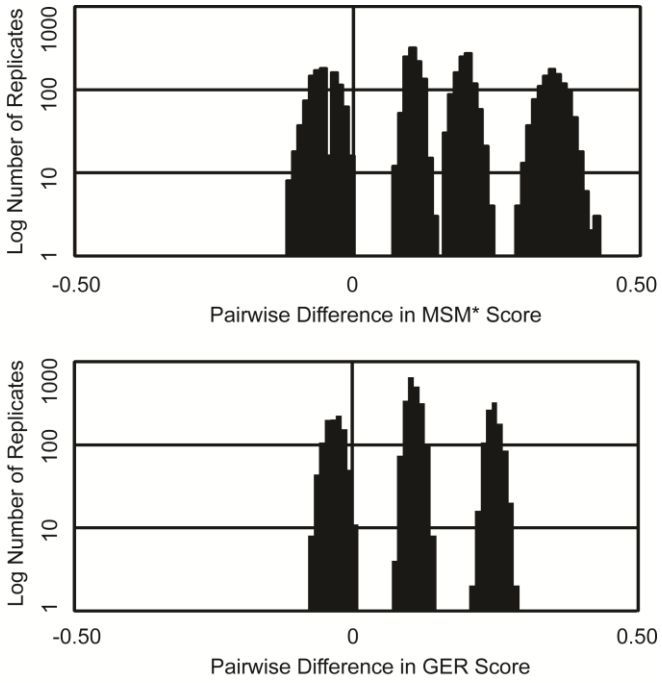

Figure 4.3: Histograms of pair-wise differences for the MSMp* and GERp metrics resulting from the comparison of stratigraphic congruence between the strict consensus trees proposed by Butler (2005) and Butler et al. (2008a). Because both histograms cross zero, these two phylogenetic hypotheses are considered equally congruent with the fossil record, contra Wills et al. (2008). Modified from Boyd et al. (2011a).

calculated and compiled into a frequency histogram to determine if either phylogeny consistently scores higher than the other regardless of what OKR is randomly assigned to each taxon (Pol and Norell, 2006). In this case, the frequency histograms for both MSM* and GER cross zero, indicating that neither phylogeny is consistently more congruent than the other (Fig. 4.3). Thus, both phylogenies are equally congruent with the fossil record. As was discussed above and illustrated in Figure 4.1, excluding data from the source MPTs when calculating stratigraphic consistency metrics can lead to scores that are artificially higher or lower than those calculated using the full signal present in the source MPTs. This potentially leads to erroneous conclusions regarding the stratigraphic congruence of a phylogeny or a set of alternative phylogenies. Therefore, if circumstances prevent calculation of scores directly from the source MPTs, calculating scores from the strict consensus tree using the ComPoly approach is the preferred solution because this method will always provide a conservative estimate of a phylogeny's stratigraphic congruence and never falsely identify a phylogenetic hypothesis as the most stratigraphically congruent based on spurious resolutions.

CONCLUSION

Previously, no standardized method existed for calculating stratigraphic consistency metrics for polytomous phylogenies. Researchers chose from a set of imperfect methods for treating polytomies, none of which took into consideration the full range of variation that polytomies impart on stratigraphic consistency scores. We demonstrate that the method by which polytomies are resolved impacts the resulting

stratigraphic consistency scores calculated for a given phylogeny. Therefore, it is imperative that the full effects of phylogenetic uncertainty be taken into consideration to ensure accuracy when comparing alternative phylogenies and to prevent erroneous conclusions. The Comprehensive Polytomy approach (ComPoly) defines the full range of possible variation polytomies impart on stratigraphic consistency measures. This allows all alternative phylogenies for a given set of taxa to be accurately compared to the stratigraphic record and prevents selection of a suboptimal phylogenetic hypothesis from a set of alternative hypotheses.

The new ASCC program suite (freely available at www.stratfit.org) simplifies the calculation of three stratigraphic consistency metrics (GER, MIG, MSM*) and their respective range scores (GER range, MIG range, MSM* range). These metrics can be used as descriptive statistics, or can be used to compare the stratigraphic fit of alternative phylogenetic hypotheses, estimate the completeness of the fossil record for a clade of interest, or examine the stratigraphic congruence of alternative placements of taxa within a phylogeny. Recently implemented methods that facilitate evaluation of the incongruence between the stratigraphic record of first appearances and molecular divergence estimates for a given tree topology illuminate a promising new application for these metrics that warrants further investigation (Clarke et al., 2007; Marjanovic and Laurin, 2007). When performing these calculations, the uncertainty in the age of the OKRs of taxa with fossil histories and the credibility intervals for molecular divergence dates should be treated analogously using stratigraphic consistency range metrics that allow these dates to be specified as ranges instead of set points because both represent

uncertainty in estimating the timing of cladogenesis. Further, stratigraphic consistency scores should be calculated from the original set of MPTs to ensure the accuracy of the resulting scores. When this is not possible, scores should be calculated from the resulting strict consensus tree so that the total signal present in the source MPTs is represented.

CHAPTER 5.

The Systematic Relationships and Biogeographic History of Ornithischian Dinosaurs

INTRODUCTION

In recent years, considerable controversy arose surrounding the systematic relationships of taxa traditionally considered to be basal members of Ornithopoda (i.e., heterodontosaurids and hypsilophodontids). Once considered to be a stable, well supported portion of the ornithischian evolutionary tree (e.g., Sereno, 1999), Ornithopoda (sensu Sereno, 1998) is now rarely recovered as a monophyletic group in phylogenetic analyses of ornithischian relationships owing to the recovery of heterodontosaurids near the base of Ornithischia (e.g., Spencer, 2007, Butler et al., 2008a). That situation prompted Butler et al. (2008a) to redefine Ornithopoda (see Appendix 7), removing heterodontosaurids as internal specifiers, and restricting the contents of Ornithopoda to only those taxa more closely related to Iguanodontia than to Marginocephalia. Despite this attempt to provide stability to use of the taxon name Ornithopoda, the exact contents of the clade remain poorly understood (Liu 2004; Butler, 2005; Butler et al., 2008a; Boyd et al., 2009).

The recognition of Hypsilophodontidae as a paraphyletic set of taxa (Scheetz, 1999; Butler et al., 2008a; Boyd et al., 2009, Brown et al., 2011) raised the question of whether all of these taxa belong within Ornithopoda (sensu Butler et al., 2008a), or if some represent non-cerapodan, basal neornithischian taxa. Efforts to address this question via phylogenetic analyses have proven extremely difficult, with the position of former 'hypsilophodontid' taxa remaining fluid between analyses, with little consensus reached (e.g., Scheetz, 1999; Weishampel et al., 2003; Butler, 2005). Given the high level of

confusion regarding their systematic position, some authors (i.e., Boyd et al., 2009) chose conservatively to refer to all non-marginocephalian, non-iguanodontian neornithischian taxa as 'basal neornithischians' until this question is adequately addressed. However, the majority of researchers continue to refer to these taxa as basal ornithopods or basal cerapodans, despite the fact that the use of those names implies resolved placement of the taxa relative to Marginocephalia lacking in most recently phylogenetic analyses of ornithischian relationships (e.g., Butler et al., 2008a, 2011; Makovicky et al., 2011).

Given the difficulties outlined above, phylogenetic analyses of basal ornithischian and/or neornithischian relationships tended to include few basal neornithischian taxa (e.g., Spencer, 2007), focusing on the most complete, well known taxa (e.g., *Hypsilophodon*) and ignoring less complete, but morphologically informative taxa (e.g., *Zephyrosaurus*). Moreover, smaller scale analyses of basal neornithischian relationships tended to include a noticeable level of geographic bias among the included taxa. For example, the dataset published by Scheetz (1999) and its subsequent modifications (e.g., Varricchio et al., 2007; Boyd et al., 2009; Brown et al., 2011) largely sample North American neornithischian taxa, with a few Asian taxa included. Along those same lines, analyses of South American taxa tend to heavily sample endemic taxa, while largely ignoring taxa from outside the continent (e.g., Coria, 1999; Novas et al., 2004; Calvo et al., 2007). Although these analyses may individually give the impression that the relationships of basal neornithischian taxa are well resolved, in truth the broader interrelationships of these taxa relative to each other and to the major ornithischian subclades (e.g., Marginocephalia) remain ambiguous.

The most extensive analysis of ornithischian relationships yet conducted sought to address, among other issues, the interrelationships of fifteen basal neornithischian taxa (Butler et al., 2008a). That analysis met with limited success, ultimately requiring the incorporation of a combination of less-than-strict consensus methods and the removal of six basal neornithischian taxa to resolve the relationships of the remaining taxa. Butler et al. (2008a) conclude their discussion of these 'hypsilophodontid' taxa (their usage) by commenting on the need for further work on the relationships of these important but enigmatic taxa.

During the past decade there was a sharp increase in the number of new basal neornithischian taxa described from across the globe, including new taxa from Asia (e.g., Zan et al., 2005, Huh et al., 2010; Zhang et al., 2012), North America (e.g., Varricchio et al., 2007; Brown et al., 2011), South America (Novas et al., 2004, Calvo et al., 2007), and Africa (Butler, 2005). Those new taxa provide a wealth of information regarding basal ornithischian evolutionary trends and patterns, though most have yet to be included in a large-scale analysis of basal ornithischian relationships. With this study I aim to robustly assess basal neornithischian dinosaur relationships using a newly constructed species-level dataset that is the largest yet assembled for this purpose both in the number of terminal taxa and characters. The goals of this study include assessment of the systematic relationships of Australian basal neornithischian, which were never before included in a broad analysis of basal ornithischian relationships, determination of the position of Marginocephalia within Neornithischia in order to clarify the contents of the clade Ornithopoda, clarification of the interrelationships of those taxa generally referred to as

'hypsilophodontids' and their placement relative to the major ornithischian subclades, and comparison of the results of this analysis to those of other recent phylogenetic analyses of basal ornithischian relationships (i.e., Buchholz, 2002; Spencer, 2007; Butler et al., 2008a: see Fig. 5.1). The results of this phylogenetic analysis provide new insight into the evolutionary and biogeographic history of basal ornithischian dinosaurs and broader relationships within the clade. See Appendix 7 for a list of phylogenetic definitions used in this chapter.

MATERIALS AND METHODS

Dataset Construction

The core of my dataset is composed of characters compiled from four prior analyses of neornithischian relationships (Weishampel and Heinrich, 1992; Scheetz, 1999; Weishampel et al., 2003; Butler, 2005). The characters from those analyses were first combined into a single dataset totaling 309 characters. Those characters were then analyzed and congruent characters were combined, character states were assessed and modified when required, and three characters were excluded (characters 53, 58, and 112 of Scheetz, 1999), reducing the dataset to 232 characters. Eleven additional characters were added from other published analyses (Xu et al., 2002; Varricchio et al., 2007; Butler et al., 2008a; McDonald et al., 2010; Nesbitt et al., 2010) largely to address relationships amongst outgroup taxa (e.g., Silesauridae) and within ornithischian subclades (e.g., Dryosauridae). Finally, twelve new characters were added based on personal observations. The final dataset consists of 255 characters. Appendix 8 provides the

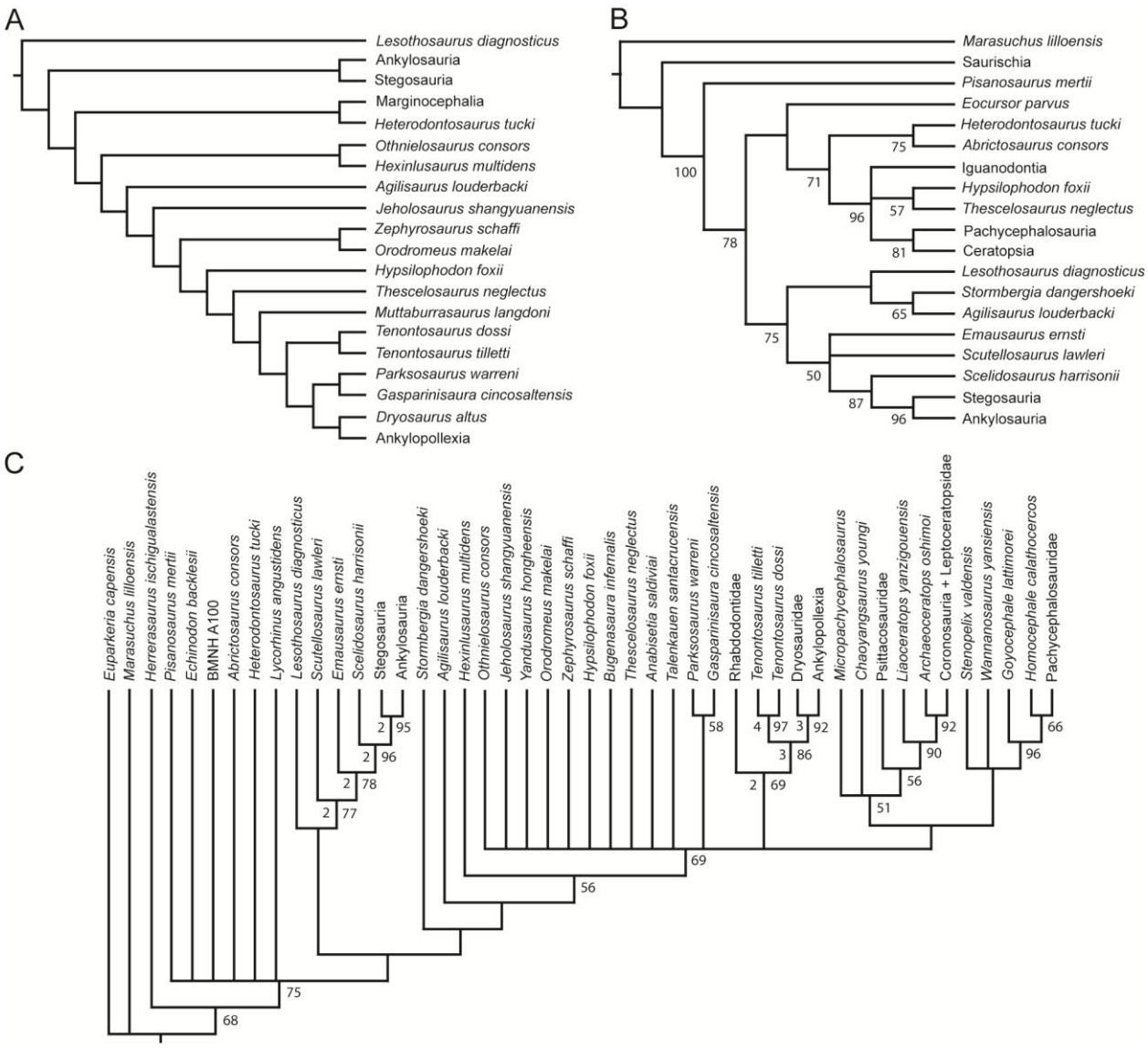

Figure 5.1: Recent phylogenetic hypotheses of basal ornithischian relationships. **A**. Tree topology reported by Buchholz (2002) based on analysis of 97 characters for 20 terminal taxa. **B**. Strict consensus of four most parsimonious trees recovered by Spencer (2007) based on analysis of 97 characters for 19 terminal taxa. **C**. Strict consensus of 756 most parsimonious trees recovered by Butler et al. (2008a) based on analysis of 221 characters for 46 terminal taxa. In **B** bootstrap values > 50% are listed below nodes. In **C**, Bremer support values > 1 are to the left of nodes while bootstrap values > 50% are to the right of nodes.

reference sources for each character, Appendix 9 provides the character descriptions, Appendix 10 contains the final data matrix, and Appendix 11 contains the list of specimens examined and references consulted for each taxon.

Taxon Selection

The purpose of this analysis is to assess the relationships of non-iguanodontian, non-marginocephalian neornithischian taxa (i.e., basal neornithischians). Specifically, all taxa previously included as members of the paraphyletic clades 'Fabrosauridae' and 'Hypsilophodontidae' were sampled, as were basal members of Iguanodontia whose relationships with 'hypsilophodontid' taxa remains ambiguous (e.g., *Gasparinisaura cincosaltensis*). To determine the position of these taxa relative to major ornithischian subclades, basal members of five additional ornithischian clades (see below) were included in the analysis. This approach was chosen rather than coding each clade as a supraspecific terminal taxon because use of species-level exemplars has been shown to increase the accuracy of phylogenetic analyses (Wiens, 1998; Prendini, 2001), ensuring that the results of this analysis are as accurate as possible. As a result, this study represents the first analysis of basal ornithischian relationships conducted entirely at the species level and analyzed using a single dataset. In addition to the ornithischian taxa included in this analysis, six non-ornithischian outgroup taxa, including three non-dinosaurian taxa, were included to root the tree. In total, sixty-five species level terminal taxa were included in this analysis. Each of these taxa is briefly discussed below.

Taxa of Interest

The twenty-seven basal neornithischian taxa discussed below constitute the focus of this investigation.

Agilisaurus louderbacki Peng 1990

The holotype of *Agilisaurus louderbacki* consists of a nearly complete skeleton from the Middle Jurassic lower Shaximiao Formation in Sichuan Province, China. This taxon was originally referred to the Fabrosauridae by Peng (1990, 1992), a clade now recognized as a paraphyletic assemblage of basal ornithischian taxa (Butler et al., 2008a). Phylogenetic analyses have recovered *Agilisaurus* as either a basal euornithopod (Buchholz, 2002; Weishampel et al., 2003), or as a basal neornithischian (e.g., Scheetz, 1999; Butler, 2005; Varricchio et al., 2007; Butler et al., 2008a; Boyd et al., 2009, Brown et al., 2011). Three other contemporaneous basal neornithischian taxa are also known from this formation: *Hexinlusaurus multidens*, *Xiaosaurus dashanpensis,* and *Yandusaurus hongheensis*. The former taxon was previously considered to represent a second species of *Agilisaurus* by Peng (1990, 1992) based on several shared characters, but a reassessment of this referral by Barrett et al. (2005) found this referral to be unwarranted.

Anabisetia saldiviai Coria and Calvo 2002

The South American taxon *Anabisetia saldiviai* is known from the Late Cretaceous Lisandro Formation of Argentina and is based upon a partial skull and

postcranial skeleton. It was first reported by Coria (1999), but was not formally named and described until 2002 by Coria and Calvo (2002). This taxon has been recovered as either an euiguanodontian (e.g., Coria, 1999; Coria and Calvo, 2002) or as a basal iguanodontian (e.g., Butler et al., 2008a).

Atlascopcosaurus loadsi Rich and Rich 1989

The Australian taxon *Atlascopcosaurus loadsi,* from the Early Cretaceous Otway Group, is based upon the holotype maxilla and a few referred specimens including isolated teeth, a maxilla, and dentaries (Rich and Rich, 1989). This taxon was originally referred to the Hypsilophodontidae, and subsequent treatments accepted that referral (e.g., Rich and Vickers-Rich, 1999).

Changchunsaurus parvus Zan et al. 2005

Changchunsaurus parvus is based on a single specimen consisting of a complete skull with partial postcranial skeleton recovered from the 'middle' Cretaceous Quantou Formation of Jilin Province, China. The anatomy of the holotype was recently redescribed and its systematic relationships were analyzed for the first time (Jin et al., 2010; Butler et al., 2011). Additionally, this taxon was included in an analysis of the systematic relationships of the new Asian taxon *Haya griva* (Makovicky et al., 2011). *Changchunsaurus parvus* was recovered by Butler et al. (2008a) and Makovicky et al. (2011) near the base of Ornithopoda as the sister taxon to *Jeholosaurus shangyuanensis*, another small-bodied taxon from the Early Cretaceous of China.

Gasparinisaura cincosaltensis Coria and Salgado 1996

The holotype of *Gasparinisaura cincosaltensis* is a nearly complete skull and partial postcranial skeleton from the Late Cretaceous Rio Colorado Formation of Argentina. Additional material that provided more information regarding the postcranial anatomy of this taxon was referred to this taxon by Salgado et al. (1997). Considerable controversy surrounds the phylogenetic position of this taxon, with various hypotheses placing it as a hypsilophodontid (e.g., Butler, 2005), a basal euornithopod (Weishampel et al., 2003), a basal iguanodontian (e.g., Scheetz, 1999; Varricchio et al., 2007; Boyd et al., 2009), or as an euiguanodontid (e.g., Coria and Salgado, 1996; Salgado et al., 1997).

Haya griva Makovicky et al. 2011

The holotype and referred specimens of *Haya griva* preserve representative portions of nearly the entire skeleton. This taxon was recovered from the Khugenetslavkant locality within the Late Cretaceous Javkhlant Formation of Mongolia. The phylogenetic analysis conducted by Makovicky et al. (2011), which used the dataset published by Butler et al. (2011), recovered *H. griva* as the sister taxon to a clade consisting of the Asian taxa *Jeholosaurus shangyuanensis* and *Changchunsaurus parvus*. In the strict consensus tree, the clade containing those three taxa was recovered in a polytomy at the base of Neornithischia.

Hexinlusaurus multidens (He and Cai 1983)

Hexinlusaurus multidens is known from the nearly complete holotype, lacking only the anterior-most portion of the skull, most of the mandibles, and the distal portion of the tail, as well as a second, disarticulated specimen (He and Cai, 1984). It was recovered from the Middle Jurassic lower Shaximiao Formation of Sichuan Province, China. The species was originally referred to the taxon *Yandusaurus* (He and Cai, 1983, 1984), but subsequent authors referred it to either *Othnielosaurus* (e.g., Paul, 1996) or the contemporaneous taxon *Agilisaurus* (e.g., Peng, 1990, 1992). A recent review of the morphology and taxonomy of the species by Barrett et al. (2005) led them to erect a new taxon for this species, *Hexinlusaurus*. *Hexinlusaurus multidens* was included in many prior cladistic analyses of ornithischian relationships, though it was usually labeled as *Yandusaurus* (e.g., Weishampel and Heinrich, 1992; Scheetz, 1999). Regardless of its designation, it is recovered as a basal member of either Hypsilophodontidae (e.g., Weishampel and Heinrich, 1992), Euornithopoda (e.g., Buchholz, 2002), or Neornithischia (e.g., Scheetz, 1999; Butler, 2005; Varricchio et al., 2007; Butler et al., 2008a; Boyd et al., 2009).'

Hypsilophodon foxii Huxley 1869

Hypsilophodon foxii was the first discovered and one of the best known taxa traditionally referred to the Hypsilophodontidae. Multiple specimens preserving representative portions of the entire skeleton are known from the Early Cretaceous Wessex Formation of England. Despite being the internal specifier for the clade Hypsilophodontidae (Sereno, 2005), its systematic position with respect to other taxa

traditionally referred to Hypsilophodontidae remains ambiguous, with some analyses recovering it as the sole member of the clade (e.g., Scheetz, 1999; Buchholz, 2002; Weishampel et al., 2003; Varricchio et al., 2007; Boyd et al., 2009), while others recover at least a reduced version of a monophyletic Hypsilophodontidae (e.g., Butler, 2005).

Jeholosaurus shangyuanensis Xu et al. 2000

Jeholosaurus shangyuanensis is a small-bodied taxon from the Early Cretaceous Yixian Formation of the Liaoning Province in China. The holotype and paratype specimens largely preserve only cranial material, and the cranial anatomy of this taxon was recently redescribed in detail based on the discovery of additional referred specimens (Barrett and Han, 2009). The postcranial anatomy of this taxon remains poorly known, aside from an incomplete hind limb preserved with the holotype. The systematic position of the taxon remains poorly resolved, with the most extensive analysis of ornithischian relationships placing it in an unresolved position at the base of Ornithopoda (Butler et al., 2008a). The analysis presented herein incorporates unpublished data from several undescribed specimens of *J. shangyuanensis* curated at Peking University in Beijing, China that consist of articulated cranial and postcranial skeletons that provide new insights into the phylogenetic position of *J. shangyuanensis*.

Koreanosaurus boseongensis Huh et al. 2011

Koreanosaurus boseongensis is based upon two partially articulated postcranial skeletons, designated as the holotype and paratype, and a third specimen consisting of a

fragmentary hind limb. All of these specimens were recovered from the Late Cretaceous Seonso Conglomerate of South Korea. *Koreanosaurus boseongensis* was tentatively referred to the Ornithopoda by Huh et al. (2011) as the sister taxon to *Orodromeus*; however, no phylogenetic analysis was conducted in the original publication (Huh et al., 2011).

Leaellynasaura amicagraphica Rich and Rich 1989

Leaellynasaura amicagraphica, from the Early Cretaceous of Australia, is known from a holotype specimen (partial left portion of a skull) and several referred specimens. Three of the referred specimens were found at the same locality as the holotype specimen, and it was argued repeatedly that all of these specimens belong to the holotype individual (Rich and Rich, 1989; Rich et al., 2010) based upon analysis of the original site map and the fact that several of the blocks containing these fossils interlock with each other. *Leaellynasaura amicagraphica* was originally assigned to the Hypsilophodontidae (Rich and Rich, 1989), but others argued that it is a non-dryomorphian iguanodontian (Herne and Salisbury, 2009). The most recent assessment of the anatomy of the taxon outlined character evidence supporting the latter taxonomic placement, though only referred the taxon to Ornithopoda (Rich et al., 2010).

Lesothosaurus diagnosticus Galton 1978

Lesothosaurus diagnosticus is a small-bodied taxon from the "Red Beds" of the Early Jurassic Upper Elliot Formation, southern Africa. Numerous specimens are referred

to this taxon (see Butler [2005] for a review) and together they preserve much of the cranial and postcranial skeleton. The systematic position of *Lesothosaurus* remains contentious; it is hypothesized as either a basal ornithischian (e.g., Norman et al., 2004a), a basal neornithischian (e.g., Scheetz, 1999; Varricchio et al., 2007; Butler, 2005; Boyd et al., 2009) or a basal thyreophoran (Spencer, 2007; Butler et al., 2008a). Clarifying the relationships of this taxon is a key step to understanding the evolutionary history of Ornithischia. Controversy also surrounds the taxonomic diversity of non-heterodontosaurid ornithischian taxa from the Upper Elliot Formation. Butler (2005) recognized the presence of two taxa, *L. diagnosticus* and *Stormbergia dangershoeki*. Other authors (e.g., Knoll, 2002a, 2002b) argued that the material referred to *S. dangershoeki* actually represents the adult form of *L. diagnosticus*, and histological evidence consistent with that interpretation was presented by Knoll et al. (2010). Neither of these taxa preserve distinct autapomorphies; rather, they are differentiated based upon unique combinations of character states, many of which are plesiomorphic for Ornithischia (Butler, 2005). However, because the synonymy of these taxa is not yet formally proposed, *L. diagnosticus* and *S. dangershoeki* are treated as distinct taxa in this study.

Macrogryphosaurus gondwanicus Calvo et al. 2007

Macrogryphosaurus gondwanicus is a large-bodied taxon from the Late Cretaceous Portezuelo Formation of Argentina. The holotype and only known specimen consists of an incomplete postcranial skeleton preserving almost the entire vertebral

column with associated cervical and dorsal ribs, both pelvic girdles, a sternal plate, and four intercostal plates (Calvo et al., 2007). *Macrogryphosaurus gondwanicus* was previously included in only a single phylogenetic analysis, where it was recovered as a basal euiguanodontian and the sister taxon to *Talenkauen santacrucensis* (Calvo et al., 2007). A new clade, Elasmaria Calvo et al. 2007, was erected by Calvo et al. (2007) to contain these two taxa.

Notohypsilophodon comodorensis Martinez 1998

Notohypsilophodon comodorensis is based on a partial postcranial skeleton from the Late Cretaceous Bajo Barreal Formation in Argentina. Described as the first hypsilophodontid recognized from South America, the only phylogenetic analysis of its relationships recovered it in an unresolved position at the base of Ornithopoda (Coria, 1999).

Orodromeus makelai Horner and Weishampel 1988

Orodromeus makelai was briefly described by Horner and Weishampel (1988) based on a nearly complete skull and postcranial skeleton from the Late Cretaceous upper Two Medicine Formation of Montana. Numerous specimens from that formation are referred to this taxon, and its anatomy is relatively well known. However, the most extensive descriptive work on this taxon completed to date is an unpublished dissertation (Scheetz, 1999), though additional accounts of the long bone histology of this taxon were published (Horner et al., 2009). In phylogenetic analyses, *O. makelai* is consistently

recovered as the sister taxon of *Zephyrosaurus schaffi* (e.g., Scheetz, 1999; Buchholz, 2002; Varricchio et al., 2007), though the placement of those two taxa within Neornithischia remains problematic.

Oryctodromeus cubicularis Varricchio et al. 2007

Oryctodromeus cubicularis was originally described based on a presumed adult holotype (premaxillae, partial braincase, and postcranial elements) and a paratype consisting of disarticulated cranial and postcranial elements from at least two immature individuals, all recovered from a single locality within the early Late Cretaceous Blackleaf Formation of Montana. Subsequently, additional material referable to this taxon was described from the contemporaneous Wayan Formation of Idaho (Krumenacker, 2010), which extends the geographical range of *Oryctodromeus* and adds to our knowledge of its anatomy. The only phylogenetic analysis to include *O. cubicularis*, which used a modified version of the Scheetz (1999) dataset, recovered this taxon as the sister taxon to a clade consisting of *Orodromeus makelai* + *Zephyrosaurus schaffi* (Varricchio et al., 2007).

Othnielosaurus consors (Marsh 1894)

The holotype of *Othnielia rex* (Marsh 1877b) is a left femur that preserves no autapomorphies; thus, it was declared a *nomen dubium* by Galton (2007). A partial, articulated skeleton previously referred to this taxon, BYU ESM-163R from the Upper Jurassic Morrison Formation of North America, was erected as the holotype of a new

taxon, *Othnielosaurus consors*, and all material previously referred to *Othnielia rex* is now referred to *O. consors*. Galton (1973) originally referred BYU ESM-163R to the Hypsilophodontidae. Phylogenetic analyses recovered *O. consors* (or the conspecific *O. rex*) as closely related to the Asian basal neornithischian taxa *Agilisaurus louderbacki*, *Hexinlusaurus multidens*, and *Yandusaurus hongheensis* at the base of either Hypsilophodontidae (e.g., Weishampel and Heinrich, 1992), Euornithopoda (e.g., Buchholz, 2002), or Neornithischia (e.g., Scheetz, 1999; Varricchio et al., 2007; Butler et al., 2008a; Boyd et al., 2009).

Parksosaurus warreni (Park 1926)

An articulated specimen preserving a partial skull and relatively complete postcranial skeleton was discovered in the Late Cretaceous Edmonton Formation of Alberta, Canada and was recognized as the holotype of a new species of *Thescelosaurus, Thescelosaurus warreni* (Parks, 1926). Sternberg (1937, 1940) subsequently removed this species from *Thescelosaurus* and placed it in its own taxon, *Parksosaurus*. Recent analysis of all specimens previously referred to the taxon *Thescelosaurus* upheld the validity of *Parksosaurus*, finding it to be diagnostically distinct from all specimens previously referred to *Thescelosaurus* (Boyd et al., 2009). The systematic placement of *P. warreni* remains uncertain, with phylogenetic analyses hypothesizing it as either the sister taxon to *Gasparinisaura* (e.g., Buchholz, 2002; Butler et al., 2008a), *Thescelosaurus* (e.g., Weishampel et al., 2003; Boyd et al., 2009; Brown et al., 2011), or *Hypsilophodon* (e.g., Weishampel and Heinrich, 1992).

Qantassaurus intrepidus Rich and Vickers-Rich 1999

Qantassaurus intrepidus, from the Early Cretaceous Wonthaggi Formation of Australia, is known from the holotype dentary and two referred dentaries, which are diagnosed by their relatively short anteroposterior length compared to their dorsoventral thickness. *Qantassaurus intrepidus* originally was referred to the Hypsilophodontidae (Rich and Vickers-Rich, 1999), though its systematic relationships were never investigated in a phylogenetic analysis.

Skaladromeus goldenii (See Chapter 3)

Skaladromeus goldenii, a small-bodied taxon from the Late Cretaceous Kaiparowits Formation of Utah, is based upon fragmentary cranial and postcranial elements from an immature individual. Though the use of an immature specimen as a holotype is not ideal, all other known specimens of the taxon are presumably immature and the specimen designated as the holotype preserves autapomorphic traits that make it diagnosably distinct from all other known ornithischian taxa. Several other presumably juvenile specimens also were referred to this taxon, including an articulated manus, providing insight into the morphology of much of the postcranial skeleton.

Stormbergia dangershoeki Butler 2005

All specimens of *Stormbergia dangershoeki* are from the 'Red Beds' of the Lower Jurassic Upper Elliot Formation of southern Africa. The holotype and paratype are partial

postcranial skeletons. Although some authors considered these specimens to represent a valid taxon (e.g., Butler,2005; Butler et al., 2008a), others argue that the morphological differences noted between *Stormbergia dangershoeki* and the contemporaneous *Lesothosaurus diagnosticus* are a result of ontogenetic variation within a single taxon, with *L. diagnosticus* representing the smaller, presumably juvenile form and *S. dangershoeki* representing the larger, presumably adult form (Knoll, 2002a, 2002b; Knoll et al., 2010). There is some support for that hypothesis based on histological evidence (Knoll et al., 2010), but further study is needed before the question of the validity of *S. dangershoeki* is satisfactorily answered. Additionally, phylogenetic analyses that include both of these taxa consistently place them in disparate positions within the base of Ornithischia based on the presence of unique combinations of key ornithischian characters in each taxon (e.g., Butler et al., 2008a). Therefore, I retain both *L. diagnosticus* and *S. dangershoeki* as terminal taxa.

Talenkauen santacrucensis Novas et al. 2004

The holotype and only known specimen of *Talenkauen santacrucensis* consists of a fragmentary skull and partial postcranial skeleton from the Late Cretaceous Pari Aike Formation in the Santa Cruz Province of Argentina. Prior phylogenetic analyses recovered *Talenkauen* as either a basal euiguanodontian (e.g., Novas et al., 2004; Calvo et al., 2007) or as a basal iguanodontian (e.g., Butler et al., 2008a). In the only phylogenetic analysis that included both *Talenkauen* and the South American taxon *Macrogryphosaurus gondwanicus* (also from the Late Cretaceous of Argentina), these

two taxa were recovered as sister taxa and identified as part of a new clade, Elasmaria (Calvo et al., 2007).

Thescelosaurus assiniboiensis Brown et al. 2011

Thescelosaurus assiniboiensis is known from a single specimen consisting of a fragmentary skull and partial postcranial skeleton from the Late Cretaceous Frenchman Formation of Saskatchewan, Canada. Originally referred to the type species of *Thescelosaurus* (*T. neglectus*), the holotype of *T. assiniboiensis* preserves autapomorphic traits that make it diagnosably distinct from all other ornithischian taxa (Brown et al., 2011). Both prior phylogenetic analyses that included this taxon placed it within a *Thescelosaurus* clade as the sister taxon to *Parksosaurus warreni* (Boyd et al., 2009; Brown et al., 2011).

Thescelosaurus garbanii Morris 1976

The holotype of *Thescelosaurus garbanii* is a fragmentary postcranial skeleton consisting of a few vertebrae and a partial hind limb from the Hell Creek Formation of Montana. Despite the incomplete nature of this specimen, it preserves an apomorphic structure of the ankle that makes it diagnosably distinct from all other ornithischian taxa. Additionally, Boyd et al. (2009) confirmed the referral of this species to the taxon *Thescelosaurus* based upon the preservation of a diagnostic set of character states present in the hind limb, recovering it in a phylogenetic analysis as part of a *Thescelosaurus* clade.

Thescelosaurus neglectus Gilmore 1913

Thescelosaurus neglectus is a relatively large-bodied taxon from the Late Cretaceous of North America and is the type species for the taxon *Thescelosaurus*. This taxon is known from numerous specimens, one of which includes a well-preserved, complete skull (see Chapter 2). A recent review of specimens referred to *Thescelosaurus* and other closely related taxa resulted in the synonymization of the contemporaneous taxon *Bugenasaura* with *Thescelosaurus* and confirmed the separation of *Thescelosaurus* and *Parksosaurus* (Boyd et al., 2009). The systematic position of *T. neglectus* within Ornithischia remains hotly debated. It was originally thought to be closely related to basal ankylopollexians (i.e., *Camptosaurus dispar*) within Ornithopoda, based on a preliminary examination of the hypodigm material (Gilmore, 1913), but was soon after referred to the Hypsilophodontidae (Gilmore, 1915). That referral was upheld by most subsequent authors for more than sixty years (e.g., Parks, 1926; Swinton, 1936; Janensch, 1955; Romer, 1956, 1966; Thulborn, 1970, 1972), with a few notable exceptions. Sternberg (1940) placed *T. neglectus* in its own clade within Hypsilophodontidae, which he named Thescelosaurinae (=Thescelosauridae of Sternberg [1937]), a referral that was followed by some authors (e.g., Kuhn, 1966; Morris, 1976). Galton (1971a, b, 1972, 1973, 1974b) argued against the placement of *T. neglectus* within Thescelosaurinae and even Hypsilophodontidae, instead referring the taxon to Iguanodontidae. Galton (1995, 1997, and 1999) later reassessed that referral and instead assigned *T. neglectus* to the Hypsilophodontidae. Despite these taxonomic disagreements, the placement of *T.*

neglectus within Ornithopoda (sensu Butler et al., 2008) was uncontested by all these authors.

Inclusion of *T. neglectus* in recent phylogenetic analyses of ornithischian relationships brought into question its placement within Ornithopoda (sensu Butler et al., 2008a). Several analyses that included *T. neglectus* do not include marginocephalian taxa, making it impossible to determine if *T. neglectus* is placed within a monophyletic Ornithopoda because they do not offer a strong assessment of ornithopod monophyly (e.g., Weishampel and Heinrich, 1992; Scheetz, 1999; Varricchio et al., 2007; Boyd et al., 2009). Additionally, the strict consensus trees produced by Butler (2005), Spencer (2007), and Butler et al. (2008a) placed *T. neglectus* in a large polytomy at the base of Neornithischia, a position that precludes its definitive referral to Ornithopoda. Another published study (Buchholz, 2002) did not include the strict consensus tree of the recovered set of ten most parsimonious trees, presenting only one of the recovered most parsimonious trees, making it impossible to determine if *T. neglectus* was recovered within Ornithopoda in all ten of the most parsimonious trees. Finally, Weishampel et al. (2003) set their supraspecific terminal taxon Marginocephalia as an outgroup taxon, making the unambiguous recovery of *T. neglectus* within Ornithopoda a certainty. Thus, in no previous phylogenetic analysis of ornithischian relationships was the placement of *T. neglectus* within Ornithopoda thoroughly assessed (sensu Butler et al., 2008a).

Yandusaurus hongheensis He 1979

Yandusaurus hongheensis is based on a fragmentary skull and postcranial skeleton from the Middle Jurassic upper Shaximiao Formation of Sichuan, China. Though this taxon is listed as being included in several prior phylogenetic analyses of ornithischian relationships (e.g., Weishampel and Heinrich, 1992; Scheetz, 1999), in most of these cases the taxon included was the more complete species *'Yandusaurus' multidens*, which was subsequently removed from *Yandusaurus* and placed in a new taxon, *Hexinlusaurus* (Barrett et al., 2005). The most recent phylogenetic analysis that included *Y. hongheensis* as a terminal taxon recovered it in an unresolved position at the base of Ornithopoda (Butler et al., 2008a).

Yueosaurus tiantaiensis Zheng et al. 2012

This taxon is known from a single, fragmentary postcranial skeleton from the Late Cretaceous Liangtoutang Formation of Zhejiang Province, China. Despite the fragmentary nature of the specimen, the presence of three autapomorphies on the scapula confirms the validity of this taxon. The systematic relationships of *Y. tiantaiensis* have never been assessed in a phylogenetic analysis.

Zephyrosaurus schaffi Sues 1980

Zephyrosaurus schaffi, a North American taxon from the Early Cretaceous Cloverly Formation, is based upon an incomplete skull and extremely fragmentary postcranial skeleton. Additional material referable to this taxon is known, but remains either undescribed or described only in an unpublished thesis (Kutter, 2004), limiting our

understanding of the taxon. In phylogenetic analyses, it is frequently recovered as the sister taxon to *Orodromeus makelai* (e.g., Weishampel and Heinrich, 1992; Scheetz, 1999; Varricchio et al., 2007; Boyd et al., 2009).

Basal Ornithischian Taxa

Two basal ornithischian taxa that are not considered part of the ingroup and do not fall within any of the major ornithischian subclades, but are key for evaluating ornithischian relationships, were included. These two taxa provide important insights into the early evolution of ornithischian dinosaurs. *Pisanosaurus mertii* Casamiquela 1967 is traditionally considered the most basal ornithischian taxon yet discovered, a hypothesis supported by phylogenetic analyses of ornithischian relationships (e.g., Butler, 2005; Spencer, 2007; Butler et al., 2008a). *Eocursor parvus* Butler et al. 2007 is currently considered a non-genasaurian, ornithischian dinosaur, situated between the clades Heterodontosauridae and Thyreophora (e.g., Butler et al., 2007). Alternatively, Spencer (2007) recovered *Eocursor* as a basal neornithischian, but still basal to the Heterodontosauridae, which was also placed within Neornithischia.

Species Exemplars of Major Ornithischian Subclades

The following ornithischian taxa were included in this analysis to represent major subclades whose monophyly is supported by prior analyses of ornithischian relationships (e.g., Butler et al., 2008a). Inclusion of species-level exemplars from all four major ornithischian subclades is critical for accurately resolving the relationships of the twenty-

seven taxa under study in this analysis and obtaining a clear understanding of character evolution and patterns of biogeographic dispersal within Ornithischia.

Heterodontosauridae Kuhn 1966 (Sensu Sereno, 2005)

The phylogenetic position of Heterodontosauridae has been problematic over the past two decades (e.g., Sereno, 1999; Buchholz, 2002; Butler, 2005; Butler et al., 2008a), being hypothesized either within Ornithopoda (e.g., Sereno, 1999), as the sister-taxon to Marginocephalia (e.g., Buchholz, 2002), near the base of Neornithischia (e.g., Butler, 2005), or outside of Genasauria (e.g., Butler et al., 2008a). Regardless of the placement of this clade within Ornithischia, a monophyletic core was consistently recovered. Six taxa were selected to represent this clade: the African taxa *Abrictosaurus consors* (Thulborn 1974), *Heterodontosaurus tucki* Crompton and Charig 1962, and *Lycorhinus angustidens* Haughton 1924; the European taxon *Echinodon becklesii* Owen 1861; the North American taxon *Fruitadens haagarorum* Butler et al. 2010; and, the Asian taxon *Tianyulong confuciusi* Zheng et al. 2009. When combined these taxa represent the full temporal range of this clade.

Thyreophora Nopsca 1915 (Sensu Butler et al., 2008a)

The monophyly of Thyreophora is one of the most stable components within Ornithischia (e.g., Norman, 1984; Cooper, 1985; Sereno, 1986, 1999; Butler et al., 2008a). The European taxa *Emausaurus ernsti* Haubold 1991 and *Scelidosaurus harrisonii* Owen 1861 and the North American taxon *Scutellosaurus lawleri* Colbert

1981 were long recognized as the most basal members of the Thyreophora (e.g., Sereno, 1999; Butler 2005; Butler et al., 2008a), and are here included as its representatives. New character data for the *S. lawleri* was incorporated from study of additional referred specimens currently being studied by CAB (see Appendix 11).

Marginocephalia Sereno 1986 (Sensu Butler et al., 2008a)

The monophyly of Marginocephalia was questioned by some researchers (e.g., Dodson, 1990; Sullivan, 2006), but recent phylogenetic analyses of the Ornithischia all support the monophyly of this clade (e.g., Butler et al., 2008a). Six marginocephalian taxa whose position within Marginocephalia is confirmed by several recent studies (e.g., Butler et al., 2008a) were included in this analysis. These taxa include the ceratopsian dinosaurs *Archaeoceratops oshimai* Dong and Azuma 1997, *Liaoceratops yanzigouensis* Xu et al. 2002, and *Yinlong downsi* Xu et al. 2006, and the pachycephalosaurian dinosaur *Wannanosaurus yansiensis* Hou, 1997. Two additional taxa whose exact positions within Marginocephalia remain uncertain were also included: *Micropachycephalosaurus hongtuyanensis* Dong, 1978 and *Stenopelix valdensis* Meyer 1859. These six taxa were chosen based upon their presumed basal position within Marginocephalia and because their anatomy is more completely known than other basally positioned taxa (e.g., *Chaoyangsaurus* Zhao et al. 1999).

Iguanodontia Dollo 1888 (Sensu Sereno, 2005)

Iguanodontia is a subclade within Ornithopoda, making the inclusion of species-level exemplars from this clade crucial to elucidating the relationships of the taxa of interest in this analysis, some of which were previously proposed to be situated within Iguanodontia (e.g., *Gasparinisaura cincosaltensis*, *Talenkauen santacrucensis*). Therefore, fourteen iguanodontian species were included in this study. These species are divided into three groups. The Australian species *Muttaburrasaurus langdoni* Bartholomai and Molnar 1981, the European species *Rhabdodon priscus* Matheron 1869, *Zalmoxes robustus* (Nopsca 1900), and *Zalmoxes shqiperorum* Weishampel et al. 2003, and the North American species *Tenontosaurus dossi* Winkler et al. 1997 and *Tenontosaurus tilletti* Ostrom 1970 are included as non-dryomorph basal iguanodontian representatives. The European species *Callovosaurus leedsi* (Lydekker 1889) and *Valdosaurus canaliculatus* (Galton 1975), the North American species *Dryosaurus altus* (Marsh 1878), and the African species *Dysalotosaurus lettowvorbecki* Virchow 1919 and *Elrhazosaurus nigeriensis* (Galton and Taquet 1982) are included to represent the iguanodontian subclade Dryosauridae (sensu Sereno, 2005) based on the phylogenetic hypothesis published by McDonald et al. (2010). Finally, the North American species *Camptosaurus dispar* (Marsh 1879), the European species *Iguanodon bernissartensis* Boulenger 1881, and the African species *Ouranosaurus nigeriensis* Taquet 1976 are included as representatives of the clade Ankylopollexia.

Outgroup Taxa

The following taxa were included as outgroups to Ornithischia. Three of these taxa were included to represent basal Saurischia, the sister taxon to Ornithischia (Sereno, 1999). The remaining taxa were selected based upon the phylogenetic results presented by Nesbitt et al. (2010) because they represent successive sister taxa to Dinosauria.

Saurischia Seeley, 1887

The monophyly of Dinosauria is well-supported, with Saurischia recognized as the sister taxon to Ornithischia (e.g., Novas, 1996; Sereno, 1999; Nesbitt et al., 2009, 2010). Three basal theropod dinosaurs *Herrerasaurus ischigualastensis* Reig 1963, *Sanjuansaurus gordilloi* Alcober and Marinez 2010, and *Tawa hallae* Nesbitt et al. 2009, were selected to represent this clade based upon the phylogenetic results presented by Nesbitt et al. (2009) and Alcober and Martinez (2010).

Silesauridae Nesbitt et al., 2010

Based upon the phylogenetic analysis by Nesbitt et al. (2010), the clade Silesauridae is the sister taxon to Dinosauria, making it a preferred outgroup for analyses of basal ornithischian relationships. The two taxa selected for inclusion in this analysis, *Asilisaurus kongwe* Nesbitt et al. 2010; and, *Silesaurus opolensis* Dzik 2003, represent basal and derived members of this clade, respectively.

Marasuchus lilloensis (Romer 1972)

This species originally was referred to the taxon *Lagosuchus* (Romer 1972). Subsequent revision of this taxon led Sereno and Arcucci (1994) to refer it to the new taxon *Marasuchus*. *Marasuchus liloensis* was previously included as an outgroup taxon in analyses of ornithischian relationships (e.g., Spencer, 2007; Butler et al., 2008a), and the phylogenetic analysis of ornithodiran relationships by Nesbitt et al. (2010) confirms this species is the sister taxon to a clade composed of Silesauridae + Dinosauria. Therefore, this species was included in this analysis as a third successive outgroup to Ornithischia.

Taxa A Priori Excluded from Study

Several putative basal ornithischian taxa were excluded from this analysis. Many of these taxa are fragmentary and were referred to Ornithischia based upon dental characters, a practice that was recently shown to be unreliable for accurately referring fragmentary taxa to Ornithischia (e.g., Irmis et al., 2007b). A brief discussion of these taxa and the reason for their exclusion is given below. I note that none of the taxa discussed below were ever included in prior phylogenetic analyses of ornithischian relationships.

Drinker nisti Bakker et al. 1990

The holotype of *Drinker nisti* is a partial subadult individual preserving parts of the upper and lower jaws, vertebral centra, and partial fore and hind limbs (Bakker et al., 1990). Additional specimens referred to this taxon include isolated teeth and

disarticulated postcranial elements. All of this material is from the Late Jurassic Morrison Formation of Wyoming. These specimens were briefly described and partially figured (Bakker et al., 1990), but their current location is unknown, preventing further elucidation of their anatomy. As a result, this taxon was excluded from the present analysis owing to a lack of relevant morphological data, despite the fact that the taxon is considered valid by some authors (e.g., Norman et al., 2004c).

Fulgurotherium australe von Huene 1932

This poorly known taxon from the Early Cretaceous of Australia is based on a partial, opalised femur. Although several other femora were referred to this taxon (Rich and Rich, 1989; Rich and Vickers-Rich, 1999), those referrals are suspect considering that the holotype femur does not preserve any autapomorphic traits. Noting this problem, Rich and Vickers-Rich (1999) considered *F. australe* to be a "form taxon" that was useful for distinguishing between morphologically distinct subsets of femora recovered from Early Cretaceous sediments in Australia. Although Norman et al. (2004c) considered the taxon to be valid, Butler (2005) regarded it as a *nomen dubium* and I follow the latter opinion.

Geranosaurus atavus Broom 1911

This taxon is based upon a dentary and limb elements from the Jurassic Cave Sandstone of South Africa. This taxon is currently considered to represent a *nomen dubium* (Norman et al., 2004c).

Gongbusaurus shiyii Dong et al. 1983

This taxon is based solely on two isolated teeth. Given the recently demonstrated difficulty of accurately assigning taxa based on isolated teeth to Ornithischia (e.g., Irmis et al., 2007), this taxon is considered of dubious validity and is excluded from this study.

Gongbusaurus wucaiwanensis Dong 1989

The holotype of *Gongbusaurus wucaiwanensis* consists of a fragmentary left mandible, three caudal vertebrae, and an incomplete forelimb (Dong, 1989). The paratype consists of two sacral vertebrae, eight caudal vertebrae, and a pair of complete hind limbs. The location of the type material of this taxon is currently unknown (Butler et al., 2008a) and the original description is brief and poorly figured. Additional specimens were since discovered that may be referable to this taxon and remain under study by other authors (Xu, pers. comm., 2007), but they remain unpublished. I personally examined one of those specimens and it does represent a distinct species, but until it is published and demonstrated that this specimen is referable to *Gongbusaurus wucaiwanensis*, it is unwise to include it in this analysis. Therefore, this taxon is excluded from this study.

Hypsilophodon wielandi Galton and Jensen 1979

This taxon is based upon an isolated femur collected from the Early Cretaceous Lakota Sandstone of South Dakota. The specimen does not preserve any autapomorphies

or a unique combination of characters and is considered to be a *nomen dubium* (Norman et al., 2004c).

Nanosaurus agilis Marsh 1877b

The hypodigm of *Nanosaurus agilis* consists of a dentary, femur, and ilium from two specimens collected from the Late Jurassic Morrison Formation of Colorado. This taxon is generally considered a *nomen dubium* owing to the lack of autapomorphic features preserved on this material (Norman et al., 2004c); thus, it was excluded from this analysis.

"Proctor Lake Ornithopod" (Sensu Winkler and Murray 1989)

This taxon is known from multiple specimens from the Early Cretaceous Twin Mountain Formation of Texas. Despite the wealth of morphological information this taxon preserves, it has yet to be formally described. It is currently under study by other researchers (Winkler, pers. comm., 2010), precluding its inclusion in this study.

Xiaosaurus dashanpensis Dong and Tang 1983

Xiaosaurus dashanpensis is based upon a fragmentary skeleton from the Middle Jurassic lower Shaximiao Formation of Sichuan, China. As discussed by Barrett et al. (2005), all of the apomorphies proposed by Dong and Tang (1983) are actually symplesiomorphies of Ornithischia, causing many to consider this taxon a *nomen dubium* (e.g., Norman et al., 2004a). However, this taxon does possess a single autapomorphy of

the humerus that indicates it is a valid taxon (Barrett et al., 2005). Despite this, I concur with Butler et al. (2008a) in considering the hypodigm too fragmentary and poorly figured/described to be included in a phylogenetic analysis.

Analysis

The data matrix was compiled using the program Mesquite v.2.74 (Maddison and Maddison, 2009). The final dataset was then exported as a TNT file and opened in the program Tree analysis using New Technology (TNT: Goloboff et al., 2008). All characters were run unordered (non-additive setting in TNT). The dataset was then analyzed using the traditional search option, which is analogous to the heuristic search option in the phylogenetic program PAUP* (Swofford, 2002). The search was run using the tree bisection reconnection (TBR) swapping algorithm. Branches were collapsed if the minimum possible branch length was equal to zero. The search utilized 10,000 replicates with a maximum of 10,000 trees saved during each replicate. A standard bootstrap analysis was run using the program TNT for 1000 replicates (each using a heuristic search of 100 replicates). The results are shown in Figure 5.2.

Evaluation of Stratigraphic Congruence

The strict consensus phylogenetic hypothesis generated by this analysis was compared to the phylogenetic hypotheses of ornithischian relationships of Buchholz (2002), Spencer (2007) and Butler et al. (2008a) using stratigraphic consistency metrics. These metrics assume that as our understanding of the fossil record increases, phylogenetic hypotheses should become increasingly congruent with the stratigraphic

record (Pol et al., 2004). Under that assumption, the phylogenetic hypothesis that exhibits the closest fit to the fossil record best estimates the topology of the true tree. For this investigation I selected the stratigraphic consistency measures minimum implied gap (MIG: Benton, 1994; Wills, 1999), modified manhattan stratigraphic measure (MSM*: Pol and Norell, 2001) and the gap excess ratio (GER: Wills, 1999) because those metrics are least affected by variations in tree size and shape (Pol et al., 2004). Additionally, accurately comparing stratigraphic congruence values calculated from different tree topologies requires that each tree includes an identical set of terminal taxa (Gautier et al., 1988; Wills et al., 2008). Therefore, when conducting these comparisons each tree topology was trimmed to include only those taxa that are present in both trees.

Calculations were conducted using the program Assistance with Stratigraphic Consistency Calculations v. 4.0.0a (ASCC: Boyd et al., 2011a). That program provides the user with an interactive framework for designing an analysis and entering the required data (e.g., tree topology, taxon ages) and then calculates the final values. In situations where the tree topology being analyzed was incompletely resolved (i.e., polytomies were present), that systematic uncertainty was incorporated into the calculations using the ComPoly approach (Boyd et al., 2011a), which allows the full range of variation this uncertainty imparts in stratigraphic consistency values to be described. The presence of uncertainty in the age of the oldest known record for each taxon was addressed using the methods outlined by Pol and Norell (2006), which allow the full range of possible dates to be defined rather than having to select a single date for each terminal taxon.

Incorporating all of these methods into this analysis ensured that the conclusions drawn from comparing the resulting stratigraphic consistency values are as accurate as possible.

Six comparisons were conducted during this study. The strict consensus tree topology generated by this analysis was compared to the tree reported by Buchholz (2002), the strict consensus tree by Spencer (2007), and the strict consensus, majority rule consensus, maximum agreement, and derivative strict reduced consensus trees by Butler et al. (2008a). The topology of three of these trees can be seen in Figure 5.1. Values were also calculated for the unaltered strict consensus tree topology generated by this analysis. All of the resulting values are shown in Table 1.

Reconstructing Patterns of Historical Biogeography

Numerous researchers discussed and/or modeled patterns of historical biogeographic dispersal of ornithischian taxa (e.g., Sereno, 1997, 1999; Upchurch et al., 2002; Butler et al., 2006; Brusatte et al., 2010). However, patterns of biogeographic dispersal within basal Ornithischia were never reconstructed within an inclusive phylogenetic hypothesis of ornithischian relationships. Given that this study is the most comprehensive analysis of basal ornithischian relationships yet conducted, the phylogenetic hypothesis produced by this analysis provides a robust framework within which to reconstruct biogeographical patterns within basal Ornithischia.

A variety of methods and programs exist for reconstructing patterns of historical biogeography (Ronquist, 1996, 1997; Hausdorf, 1998; Ree et al., 2005; Ree and Smith, 2008). Here, I employ an approach that incorporates time calibrated branch lengths set

equal to the implied missing fossil record for each taxon when reconstructing the geographic distribution of ancestral taxa. This allows older taxa, which are positioned closer to the ancestral nodes and are more likely to have remained in or near the ancestral geographic region, to have a larger influence over what geographic region is optimized at each node.

Reconstruction of historical biogeography was conducted using the program Mesquite v.2.74 (Maddison and Maddison, 2009). Four separate analyses focused on reconstructing the ancestral geographic ranges of basal ornithischian taxa were conducted. Before conducting those analyses, a new character was added to the dataset to represent the geographic range(s) of the terminal taxa. This character had six possible states, one for each continent represented in the dataset (no taxa from Antarctica were included in this analysis). Each taxon was then assigned a single state based upon their known geographic ranges. Each of the species included in this analysis are known from a single continent, precluding the need for polymorphic codings.

For all four methods, the strict consensus topology recovered during the phylogenetic analysis was loaded into Mesquite and opened within a new tree window. In the first analysis, all branch lengths in the tree were set equal to one (Tree > Alter/Transform Branch Lengths > Assign All Branch Lengths). The trace character history option was then selected (Analysis > Trace Character History), the Stored Characters option was selected, and the Parsimony Ancestral States reconstruction method was chosen. The second analysis was similar to the first, except that in the last

step the Likelihood Ancestral States reconstruction method was selected (using the default probability models).

In the third analysis, the branch lengths in the tree were manually set equal to the missing fossil record inferred for each branch (in myr). Implied missing fossil records were calculated for each branch by hand using the oldest possible age for each terminal taxon included in the analysis (see Appendix 11 for ages used for each taxon) and these values were assigned to their respective branches by selecting the appropriate branch in the tree and then choosing the Assign Selected Branch Lengths option (Tree > Alter/Transform Branch Lengths > Assign Selected Branch Lengths). Branch lengths for branches with no implied missing fossil record were set equal to 1. Once these data were entered, the character history of the geographic character was traced using parsimony (Analysis > Trace Character History). The fourth analysis also set all branch lengths equal to their implied missing fossil records, but the Likelihood Ancestral States reconstruction method was selected (using the default probability models). The resulting character state optimizations for the geographic character was recorded for all nodes in the tree during all four analyses (see Appendix 13).

RESULTS OF PHYLOGENETIC ANALYSIS

Analysis of the dataset as outlined above resulted in the recovery of thirty-six most parsimonious trees of length 868 (CI = 0.37; RI = 0.65; RCI = 0.24). The strict consensus of these thirty-six trees and the resulting bootstrap support values are shown in

Figure 5.2. The details of the strict consensus tree topology are discussed in detail below. It should be noted that in the following discussion existing phylogenetic nomenclature was utilized whenever possible (see Appendix 7 for a list of phylogenetic definitions). Numbers given below in parentheses refer to the character number:character state being discussed. Descriptions of the characters cited below can be found in Appendix 9, and a list of unambiguous character state changes within the tree is given in Appendix 12. All characters discussed below are unambiguously optimized synapomorphies.

Ornithischia

The monophyly of Ornithischia is supported in this analysis by the unambiguous presence of at least a slight buccal emargination of the maxilla (19:1), the development of a distinct coronoid process of the mandible (82:1), and by the presence of a dentary contribution to the anterior portion of the coronoid process (80:1). *Pisanosaurus mertii* is recovered as the basal-most member of Ornithischia, consistent with previous analyses of the clade (e.g., Sereno, 1999; Butler et al., 2008a) and is plesiomorphic with respect to all other ornithischians in possessing a lateral extension of the tibia that extends posterior to the medial margin of the fibula, but fails to contact the entire posterior margin of the fibula and calcaneum (229:1). The fragmentary nature of the holotype and only known specimen of *P. mertii* complicates optimization of several previously proposed synapomorphies of Ornithischia that cannot be assessed in this taxon. Thus, it is uncertain whether the presence of a predentary bone (2:1), an edentulous region anterior to the first

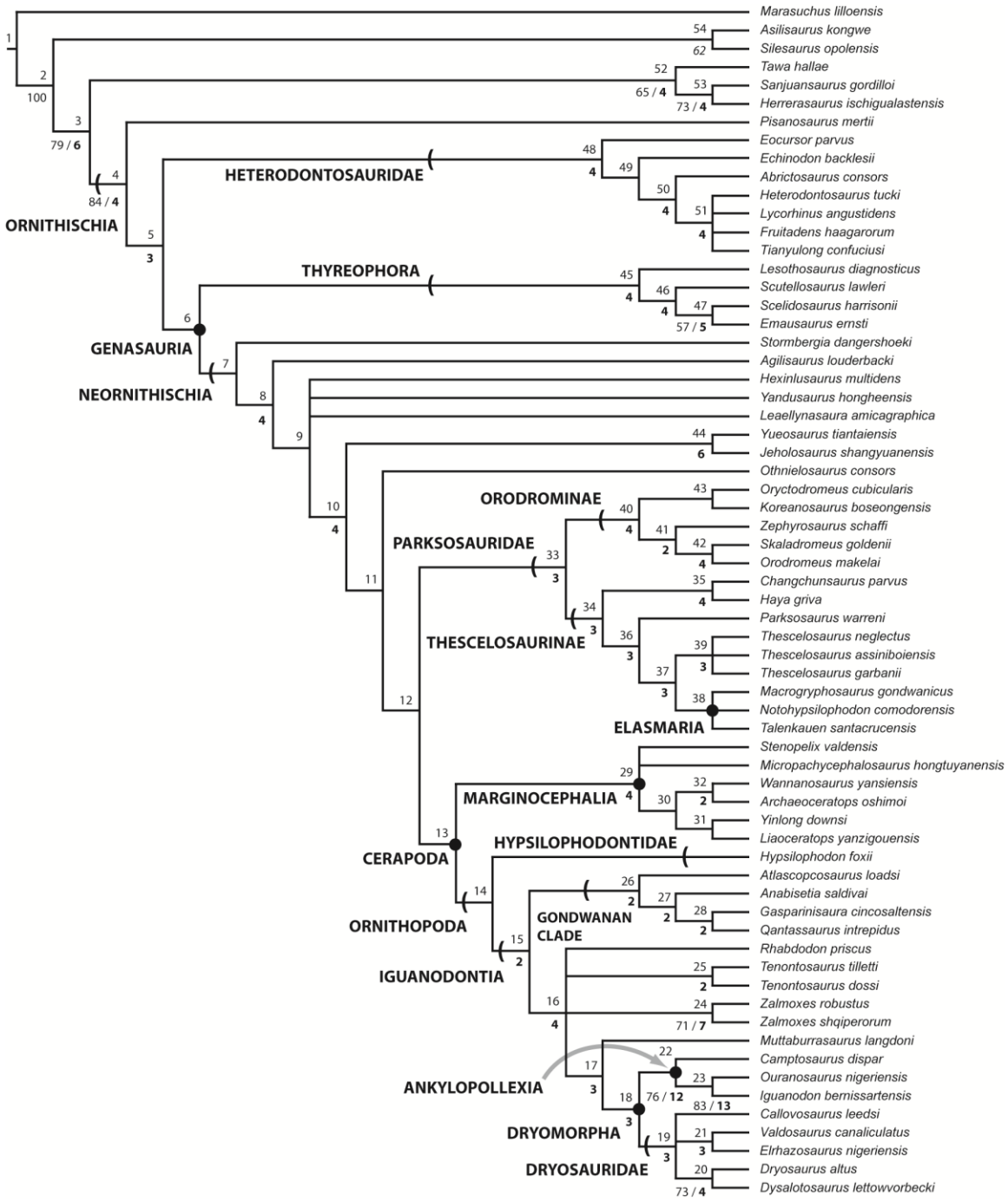

Figure 5.2: Strict consensus of the 36 most parsimonious trees recovered by this study. Major ornithischian subclades are labeled either along branches (stem-based definitions) or at nodes (node-based definitions). See Appendix 7 for phylogenetic definitions. Numbers above nodes refer to the list of unambiguous character changes for each node in Appendix 12. Bold numbers beneath nodes are Bremer support numbers > 1, while nonbold numbers beneath nodes are bootstrap support values > 50%.

premaxillary tooth (7:1), a preacetabular process of the ilium that extends anterior to the pubic peduncle (187:1), a posteroventrally oriented pubis (194:2), or a pendant fourth trochanter (219:2) represent synapomorphies of Ornithischia as a whole, or of all ornithischians excluding *Pisanosaurus*.

Heterodontosauridae

This analysis supports the findings of Butler et al. (2008a) in placing a monophyletic Heterodontosauridae (represented by *Abrictosaurus consors*, *Echinodon becklesii*; *Eocursor parvus*, *Fruitadens haagarorum*, *Heterodontosaurus tucki*, *Lycorhinus angustidens*, and *Tianyulong confuciusi*) outside of Genasauria, contra the findings of Sereno (1986, 1999), Buchholz (2002), Butler (2005), and Spencer (2007). This placement is supported by the presence of a lateral extension of the tibia that extends posterior to the entire fibula and calcaneum (229:2) in all ornithischian taxa except *Pisanosaurus*. Heterodontosauridae is placed outside of Genasauria based on the retention of a 'v-shaped' dentary symphysis (73:0) and the absence of a well-developed ventral process of the predentary (71:1). This study recovers *Eocursor parvus* as the basal-most member of Heterodontosauridae owing to the retention in this taxon of a 'V-shaped' dentary symphysis (71:1), the loss of the ventral acetabular flange of the ilium (183:1), and the presence of a horizontal brevis shelf of the ilium (189:1). Both of the latter states are present within Neornithischia in all taxa more closely related to Cerapoda than to *Agilisaurus louderbacki* (Fig. 5.2). *Eocursor* was previously recovered outside of Genasauria positioned between the clades Heterodontosauridae and Thyreophora (Butler

et al., 2007), or as a non-cerapodan basal neornithischian (Spencer, 2007). While no characters are unambiguously optimized as synapomorphies of Heterodontosauridae, all heterodontosaurids more closely related to *Heterodontosaurus* than to *Echinodon* are united in possessing maxillary and dentary teeth with denticles restricted to the apical third of the crown (134:1), as opposed to the condition in all other ornithischian taxa (except *Chaoyangsaurus youngi*) where denticles extend along the margin of most of the crown.

Genasauria

All ornithischians except *Pisanosaurus mertii* and the heterodontosaurids are recovered within the clade Genasauria based upon the presence of a well-developed ventral process of the predentary (71:1) and a 'spout-shaped' dentary symphysis (73:1). The contents of this node-based clade (sensu Butler et al., 2008a) are split between two less-inclusive clades, Thyreophora and Neornithischia.

Thyreophora

The presence of postcranial osteoderms (253:1) is traditionally considered to diagnose the clade Thyreophora; however, this analysis recovers *Lesothosaurus diagnosticus*, which lacks postcranial osteoderms, as the most basal member of Thyreophora. This placement is supported based on the presence of a horizontal ridge on the surangular (86:1). The position of *L. diagnosticus* varies in recent phylogenetic analyses, with some recovering this taxon as the sister taxon to Genasauria (Sereno, 1986, 1999; Buchholz, 2002), as a basal neornithischian (Butler, 2005), or as a basal

thyreophoran (Spencer, 2007; Butler et al., 2008a). The fluidity of the systematic position of *L. diagnosticus* was interpreted by Butler et al. (2008a) as evidence that the anatomy of this taxon closely resembles the basal genasaurian condition, making it a crucial taxon for evaluating the relationships of basal ornithischian taxa. Alternatively, if *L. diagnosticus* is the juvenile form of *Stormbergia dangershoeki,* as suggested by Knoll et al. (2010), the retention of an unusual suite of unique and derived features in the former taxon may be an artifact of its ontogenetic status rather than a true reflection of its systematic position. All thyreophorans to the exclusion of *L. diagnosticus* are united in possessing postcranial osteoderms (253:1) and an anterior process of the jugal that is mediolaterally broader than dorsoventrally deep (32:1). *Scelidosaurus harrisonii* and *Emausaurus ernsti* are united in possessing the apomorphic condition of a dentary tooth row that in sinuous in lateral view (78:1).

Neornithischia

Neornithischian taxa are united in possessing a tab shaped obturator process on the ischium (203:1) and an articulation between a sacral rib and the ischiadic peduncle of the ilium (190:1). The former character is lost Marginocephalia and Rhabdodontidae. Like Butler et al. (2008a) and Spencer (2007), this analysis places several taxa outside of the node-based clade Cerapoda as non-cerapodan basal neornithischians, though the set of taxa here included under this designation is larger than in any previous analysis. Twenty-two taxa in this study are recovered as non-cerapodan basal neornithischians (Fig. 5.2).

Stormbergia dangershoeki is placed below *Agilisaurus louderbacki* as the most-basal neornithischian taxon based upon the retention in *S. dangershoeki* of a pubic peduncle of the ilium that is larger than the ischiadic peduncle (192:0). Alternatively, the presence of a reduced pubic peduncle (192:1) is an unambiguously optimized synapomorphy of all neornithischian taxa more closely related to Cerapoda than to *S. dangershoeki*. All neornithischian taxa more closely related to Cerapoda than to *Agilisaurus louderbacki* lack a ventral acetabular flange of the ilium (183:1; present convergently in heterodontosaurids), possess a weakly developed or absent supra-acetabular rim on the ilium (184:1; reversed in *Zalmoxes* and present convergently in *L. diagnosticus*), and display a horizontal brevis shelf on the ilium (189:1; present convergently in heterodontosaurids).

Jeholosaurus shangyuanensis and *Yueosaurus tiantaiensis* both possess a relatively straight humerus that lacks a posterior flexure at the level of the deltopectoral crest (167:0), which is plesiomorphic for Ornithischia. The clade consisting of *J. shangyuanensis* + *Y. tiantaiensis* is unambiguously united with all other neornithischians in possessing a distinct 'trench' (i.e., *fossa trochanteris*) between the greater trochanter and the head of the femur (212:1). Other important characters that unite these taxa include the presence of six or more sacral vertebrae (148:2; convergently present in some heterodontosaurids), lateral swelling of the ischiadic peduncle of the ilium (191:1; apomorphically reversed in *Stenopelix valdensis* [Butler and Sullivan, 2009]), and a lesser trochanter of the femur that is anteroposteriorly narrow and closely appressed to the greater trochanter (217:2; also present in *Leaellynasaura amicagraphica* and some

heterodontosaurids and reversed in *Callovosaurus leedsi*) with its dorsal extent approximately level with the head of the femur (218:1; also present in some heterodontosaurids).

Othnielosaurus consors is positioned as more closely related to Cerapoda than to the clade consisting of *J. shangyuanensis* + *Y. tiantaiensis* based on the presence of neural spines on the caudal vertebrae that extend posteriorly beyond the caudal centra (152:1; reversed in *Orodromeus makelai*, *Parksosaurus warreni* and *Zalmoxes robustus*) and a tibia with a triangular cross-sectional shape (227:0; reversed in *Koreanosaurus boseongensis, Parksosaurus warreni*, and some iguanodontians, convergently present in *Stormbergia dangershoeki*). *Othnielosaurus consors* is placed below a clade consisting of Cerapoda + Parksosauridae (see Appendix 7 for definitions) based on the retention of a dentary with a dorsoventral height that is less than 20% of its length (77:0) and dentary teeth that lack a prominent primary ridge (139:0), though both of these characters display a relatively low CI (0.25 and 0.17, respectively).

Cerapoda

Cerapodan taxa differ from all other neornithischian taxa in possessing dorsomedially sloped or horizontal distal condyles of the quadrate (52:0; convergently present in Thyreophora), maxillary crowns that taper to the root (120:1; convergently present in *Jeholosaurus shangyuanensis* and *Heterodontosaurus tucki*, and reversed in *Yinlong downsi*), asymmetrically distributed enamel on the 'cheek' teeth (123:1; convergently present in *Abrictosaurus consors* and *Heterodontosaurus tucki*), and

dentary crowns with ridges restricted to the lingual surface (124:1; reversed in the clade of Gondwanan iguanodontians and convergently present in *Heterodontosaurus tucki*). This node-based clade (sensu Butler et al., 2008a) is subdivided into the stem-based clades Marginocephalia and Ornithopoda (see Appendix 7 for definitions).

Marginocephalia

A monophyletic Marginocephalia is recovered; however, because the cranial morphology of *Stenopelix valdensis* and *Micropachycephalosaurus hongtuyanensis* remain poorly understood, the presence of both a parietosquamosal shelf (58:1) and exclusion of the premaxillae from the internal nares (11:1) are not unambiguously optimized as synapomorphies of this clade. However, the presence of a dorsoventrally flattened anterior process of the pubis (197:3) is recovered as an unambiguous synapomorphy of the clade. Another proposed marginocephalian synapomorphy, a shortened postpubic process (Butler et al., 2008a), was not assessed in this study because it could only be scored for a single marginocephalian taxon (*Stenopelix valdensis*) included in this study (published data for *Yinlong downsi* does not sufficiently describe the anatomy of the ischium).

Ornithopoda

This study recovers a more restricted Ornithopoda than previously proposed (Fig. 5.2), consisting only of *Hypsilophodon foxii* + Iguanodontia. Ornithopod taxa are unambiguously united in possessing maxillary crowns that are shorter than wide (132:

states 0 or 1; reversed in *Qantassaurus intrepidus* and convergently present in *Pisanosaurus mertii*).

Hypsilophodontidae

The only member of this clade is *Hypsilophodon foxii*, supporting prior assertions that the traditional contents of this clade represent a paraphyletic assemblage of taxa and not a monophyletic grouping (e.g., Scheetz, 1999; Buchholz, 2002; Butler et al., 2008a), contra the findings of Sereno (1986, 1999), Butler (2005), and Spencer (2007).

Iguanodontia

Iguanodontians are unambiguously united in possessing a jugal wing of the quadrate that is positioned well dorsal to the distal condyles (49:1). They also display sacral neural spines that are at least twice the height of the sacral centra (149:1 or 2; state 1 convergently acquired in *Oryctodromeus cubicularis*). Four of the taxa of interest to this study are positioned at the base of Iguanodontia as part of a previously unrecognized clade: the South American taxa *Anabisetia saldiviai* and *Gasparinisaura cincosaltensis*, and, the Australian taxa *Atlascopcosaurus loadsi* and *Qantassaurus intrepidus*. The placement of *G. cincosaltensis* in a clade at the base of Iguanodontia makes the contents of the stem-based Iguanodontia (sensu Sereno, 2005) and the node-based Euiguanodontia (sensu Coria and Salgado, 1996) identical. As Iguanodontia has priority, the clade name Euiguanodontia is not used in the remainder of this discussion.

Unnamed Clade of Gondwanan Taxa

This study is the first to recover a clade composed entirely of Gondwanan basal iguanodontians. Character support is low for this clade, which is expected given that the Australian taxa are known only from disarticulated maxillae and dentaries. They are united in possessing mandibular teeth with vertical ridges present on both sides of the crown (124:0), which is the plesiomorphic ornithischian condition. These taxa are positioned basal to all other iguanodontians because they lack 'lozenge-shaped' dentary crowns (136:0), and robust (i.e., thickened) postorbitals (61:1), which are unambiguously optimized synapomorphies of more derived iguanodontians. The characters supporting the remainder of the iguanodontian taxa included in this study are not discussed as they were not a part of the taxa of interest.

Parksosauridae

The clade name Parksosauridae was first defined by Buchholz (2002), and was subsequently updated for use in this study (see Appendix 7 for exact definitions). This study supports the results of Boyd et al. (2009) and Brown et al. (2011) in recovering a clade of taxa traditionally recognized as 'hypsilophodontids' taxa, though *Hypsilophodon foxii* is not placed within this clade. These taxa are unambiguously united in possessing a posterolateral concavity within the posterior end of the premaxilla, near the lateral margin, for receipt of the anterolateral boss of the maxilla (14:1). They also possess a modestly flared oral margin of the premaxilla (5:1; reversed in *Haya griva* and *Orodromeus makelai* and convergently present in *Agilisaurus louderbacki*), fused

premaxillae (255:1; reversed in *Haya griva* and *Orodromeus makelai*), a flattened lateral surface of the greater trochanter (213:1; convergently evolved in *Gasparinisaura cincosaltensis* and *Zalmoxes*), and a braincase with an angle of less than 35 degrees between its base and the long axis (98:1; convergently present in *Hypsilophodon foxii*).

Orodrominae

The contents of Orodrominae recovered in this study exactly match that proposed in Chapter 3, consisting of four North American taxa (*Orodromeus makelai*, *Oryctodromeus cubicularis*, *Skaladromeus goldenii*, and *Zephyrosaurus schaffi*) and one Asian taxon (*Koreanosaurus boseongensis*). Two unambiguous synapomorphy unite these taxa: presence of a sharp and pronounced scapular spine (158:1); and, fibular shaft 'D-shaped' in cross-section throughout it length (233:1). Additionally, these taxa are united by the presence of a sharp ventral keel on the cervical vertebrae (143:1; convergently evolved in the dryosaurid *Valdosaurus canaliculatus*). Among the five taxa here referred to Orodrominae, *O. makelai*, *S. goldenii*, and *Z. schaffi* are united in displaying a tall, posterolaterally directed jugal horn (38:3; convergently present in *Heterodontosaurus tucki*).

Thescelosaurinae

The clade name Thescelosaurinae was first proposed by Sternberg (1940), but has never been phylogenetically defined until this study (see Appendix 7 for definition). The stem-based clade Thescelosaurinae is the sister-taxon to the stem-based clade Orodrominae, which together comprise the node-based clade Parksosauridae.

Thescelosaurines are united in possessing two supraorbital bones that are not fused to the orbital margin (23:2; convergently present in *Agilisaurus louderbacki*) and a dorsally projecting 'finger-like' process on the surangular anterior to the jaw joint (86:2; convergently present in the iguanodontian *Tenontosaurus tilletti*), though both of these characters suffer from missing data both within and outside the clade. *Haya griva* and *Changchunsaurus parvus* differ from all other thescelosaurines in possessing dentaries with parallel dorsal and ventral margins (75:1) and an anterior tip of the dentary positioned at approximately mid-height (74:1). The remaining seven thescelosaurines differ from most basal ornithischians in possessing a femur with the fourth trochanter extending onto the distal half of the shaft (221:1; convergently present in some iguanodontian taxa and other large-bodied ornithischian taxa not included in this analysis), partial ossification of the sternal segments of the cranial dorsal ribs (157:1; convergently present in *Othnielosaurus consors* and *Hypsilophodon foxii*), placement of the obturator process of the ischium along the distal 60% of the ischial shaft (204:1; convergently present in *Hypsilophodon foxii*), and a femoral shaft bowed in anterior view (209:1; convergently present in *Jeholosaurus shangyuanensis* and some basal iguanodontians). The three species of *Thescelosaurus* and Elasmaria are recovered as sister taxa to the exclusion of all other parksosaurids based on the presence of an ilium with a sinuous dorsal margin (185:1; straight in all other parksosaurids), a low olecranon process of the ulna (169:0), and the presence of a femur that is longer than the tibia (226:1; convergently present in most basal iguanodontians and *Scelidosaurus harrisonii*).

Elasmaria

This analysis recovers a slightly more inclusive Elasmaria clade than was originally proposed (see Calvo et al., 2007 and Appendix 7). In addition to *Talenkauen santacrucensis* and *Macrogryphosaurus gondwanicus*, the Patagonian taxon *Notohypsilophodon comodorensis* is placed within this clade. All three taxa possess an inconspicuous deltopectoral crest on the humerus (168:2; convergently present in basal iguanodontian *Anabisetia saldiviai*). *T. santacrucensis* and *M. gondwanicus* both retain the primitive condition of an epipophysis on cervical vertebra three (145:0; present in all ornithischians positioned below *Agilisaurus louderbacki*), which Calvo et al. (2007) used to diagnose this clade, and an ovoid, or subcylindrical, ischial shaft (205:1; convergently present in *Zephyrosaurus schaffi* and many iguanodontians). Because the presence or absence of both of these characters cannot be assessed in *Notohypsilophodon* due to preservational issues, it is unclear if they unite all elasmarians, or if they are diagnostic for a more restricted clade composed of *T. santacrucensis* and *M. gondwanicus*. The presence of thin mineralized plates on the anterior portion of the thoracic ribcage (= intercostal plates: Butler and Galton, 2008; Boyd et al., 2011b) was also proposed to diagnose this clade (Calvo et al., 2007). However, these structures are more widely distributed among basal neornithischian and basal ornithopod taxa (i.e., *Hypsilophodon foxii, Othnielosaurus consors, Parksosaurus warreni, and Thescelosaurus neglectus*: Butler and Galton, 2008; Boyd et al., 20011b) and do not diagnose this clade.

HISTORICAL BIOGEOGRAPHY OF ORNITHISCHIA

The results of the four analyses of basal ornithischian historical biogeography are presented in Figures 5.3 (parsimony) and 5.4 (likelihood). It should be noted that the results of both analyses that used parsimony are identical (Figs. 5.3A and B) because parsimony-based reconstruction in Mesquite do not take branch lengths into consideration. Therefore, only the results of the first parsimony-based analysis was reported in Appendix 13. To simplify comparisons between the remaining three sets of results, they will be referred to as follows: parsimony-based analysis (PB); likelihood-based analysis with equal branch lengths (LEB); and, likelihood-based analysis with time calibrated branch lengths set equal to implied missing fossil records (LFR). Additionally, a time-calibrated version of the strict consensus tree presented from Figure 5.2 is shown in Figure 5.5. By combining the temporal and geographic information presented in these figures, the biogeographic history of basal Ornithischia can be reconstructed and discussed in detail.

The LFR analysis reconstructs the ancestral area of the common ancestor of Dinosauria + Silesauridae (sensu Nesbitt et al., 2010) as Africa, while the other two analyses place the origin in South America. This difference reflects the fact that the African taxon *Asilisaurus kongwe* Sterling et al. 2010 is the oldest taxon included in this analysis, giving it more weight in the LFR analysis. All three analyses reconstruct the origin of Dinosauria and Ornithischia in South America, which is consistent with some prior proposals (e.g., Sereno, 1997). Considering two of the three basal theropods

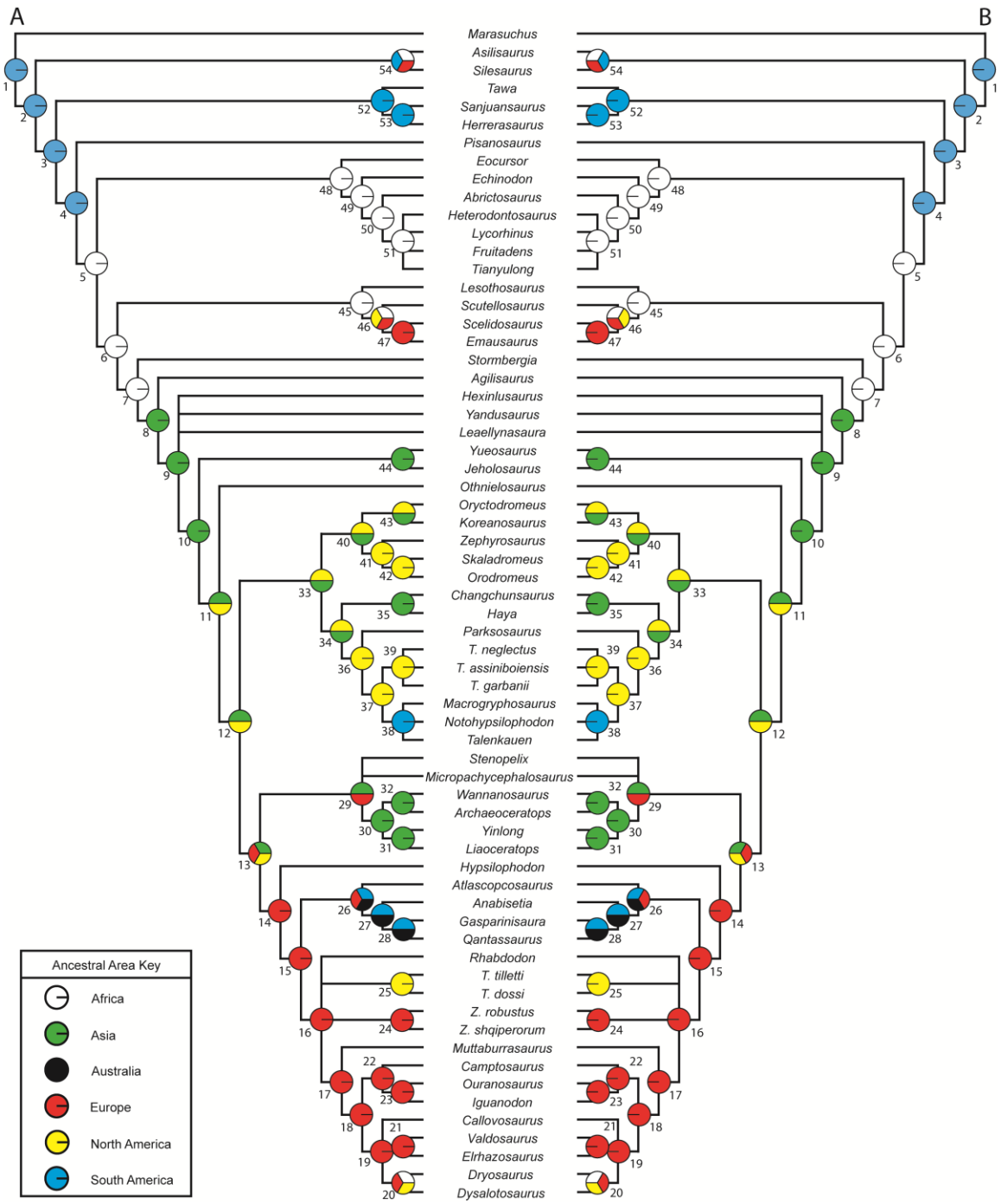

Figure 5.3: Parsimony-based reconstructions of ancestral geographic areas. **A**. results obtained when all branch lengths were equal. **B**. results obtained when branch lengths were set equal to inferred missing fossil records. Tree topology based on Figure 5.2. The pie charts at each node represent the level of support for each ancestral (See Appendix 13 for precise values). Each color represents a different geographic area (see key). Numbers next to nodes refer to those used in Appendix 13.

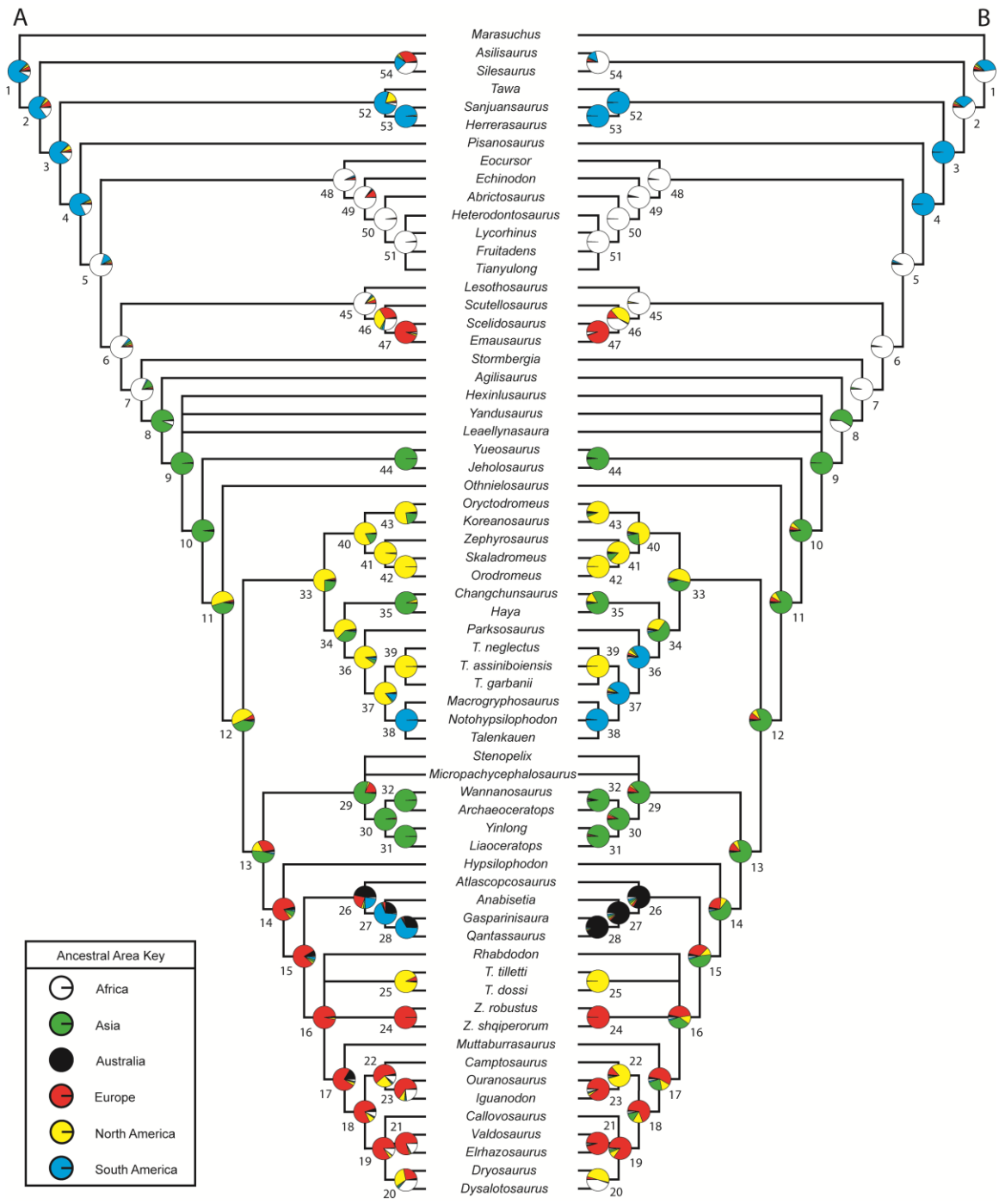

Figure 5.4: Likelihood-based reconstructions of ancestral geographic areas. **A**. results obtained when all branch lengths were equal. **B**. results obtained when time calibrated branch lengths were included and set equal to inferred missing fossil records. Tree topology based on Figure 5.2. The pie charts at each node represent the level of support for each ancestral (See Appendix 13 for values). Each color represents a different geographic area (see key). Numbers next to nodes refer to Appendix 13.

included in this study and the basal-most ornithischian taxon, *Pisanosaurus mertii*, are all from South America, this result is unsurprising. Ornithischia diverged from its sister taxon Saurischia by the early Late Triassic at the very latest (Fig. 5.5).

The ancestral area of the most recent common ancestor of the clade consisting of Heterodontosauridae + Genasauria is optimized as Africa by all three analyses, with this split likely taking place during the Late Triassic. Likewise, all three analyses reconstruct a period of rapid diversification of Heterodontosauridae to have occurred in Africa during either the Late Triassic or Early Jurassic (contra the results of Pol et al. [2011]), with the lineages leading to *Echinodon becklesii*, *Fruitadens haagarorum* and *Tianyulong confuciusi* later dispersing into Europe, North America, and Asia, respectively. These dispersals could have occurred anytime during the Jurassic (or even in the Early Cretaceous in the case of *T. confuciusi*).

The origin of Genasauria is hypothesized by all three analyses to have occurred in Africa during the Early Jurassic at the latest, and possibly during the Late Triassic, and the early diversification of Thyreophora also transpired in Africa, assuming the placement of *Lesothosaurus diagnosticus* at the base of this clade is accurate. There exists disagreement regarding the pattern of dispersal within Thyreophora. The LFR and LEB analyses slightly favor a scenario where basal thyreophorans dispersed from Africa into North America (giving rise to the *Scutellosaurus lawleri* lineage) and then migrating into Europe. The PB analysis is equivocal as to whether this is the case or if basal thyreophorans dispersed from Africa directly into Europe, with *Scutellosaurus lawleri* dispersing separately into North America. Either way, the diversification of these basal

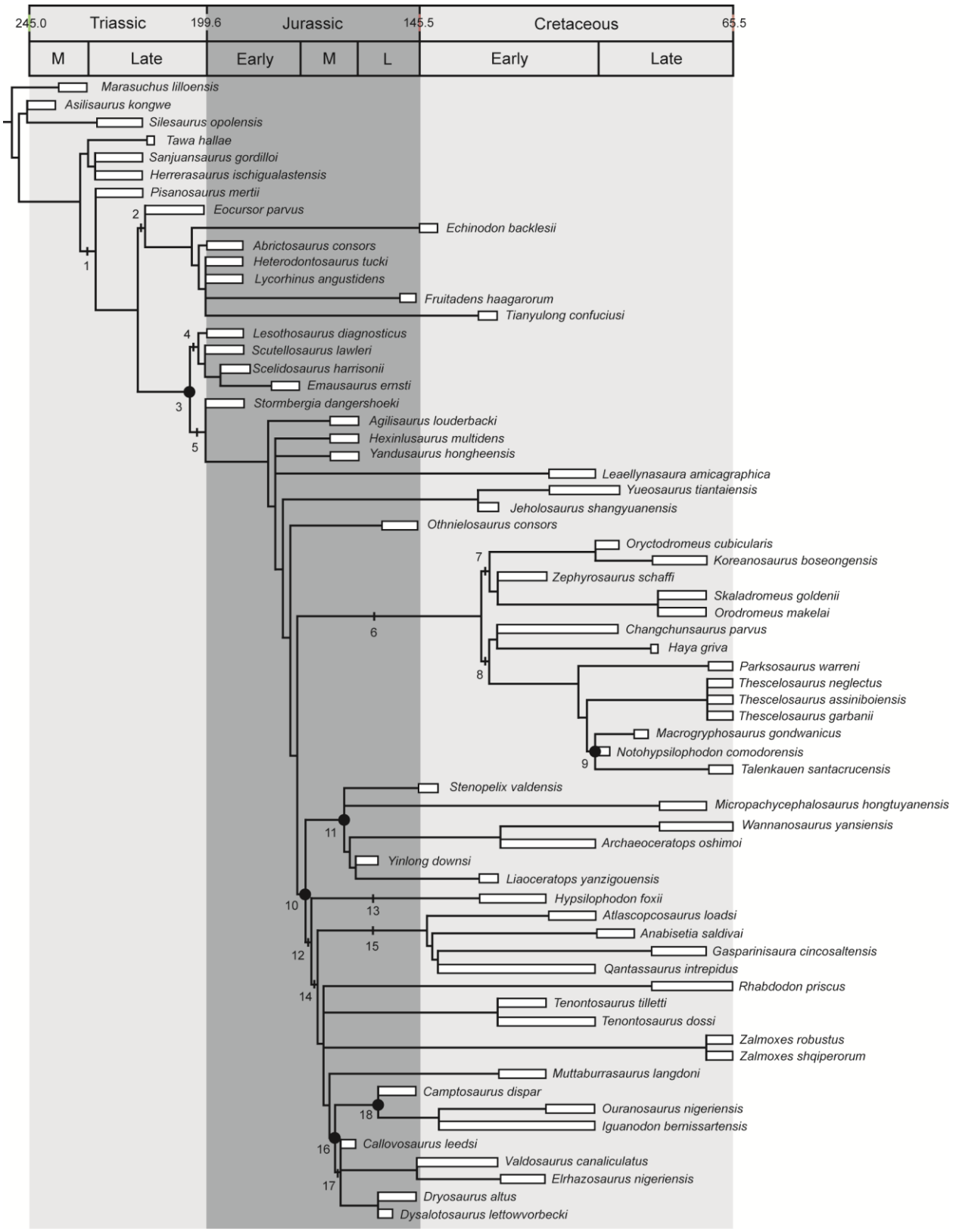
245.0
Triassic
199.6
Jurassic
145.5
Cretaceous
65.5
M
Late
Early
M
L
Early
Late
Marasuchus lilloensis
Asilisaurus kongwe
Silesaurus opolensis
Tawa hallae
Sanjuansaurus gordilloi
Herrerasaurus ischigualastensis
Pisanosaurus mertii
Eocursor parvus
Echinodon backlesii
Abrictosaurus consors
Heterodontosaurus tucki
Lycorhinus angustidens
Fruitadens haagarorum
Tianyulong confuciusi
Lesothosaurus diagnosticus
Scutellosaurus lawleri
Scelidosaurus harrisonii
Emausaurus ernsti
Stormbergia dangershoeki
Agilisaurus louderbacki
Hexinlusaurus multidens
Yandusaurus hongheensis
Leaellynasaura amicagraphica
Yueosaurus tiantaiensis
Jeholosaurus shangyuanensis
Othnielosaurus consors
Oryctodromeus cubicularis
Koreanosaurus boseongensis
Zephyrosaurus schaffi
Skaladromeus goldenii
Orodromeus makelai
Changchunsaurus parvus
Haya griva
Parksosaurus warreni
Thescelosaurus neglectus
Thescelosaurus assiniboiensis
Thescelosaurus garbanii
Macrogryphosaurus gondwanicus
Notohypsilophodon comodorensis
Talenkauen santacrucensis
Stenopelix valdensis
Micropachycephalosaurus hongtuyanensis
Wannanosaurus yansiensis
Archaeoceratops oshimoi
Yinlong downsi
Liaoceratops yanzigouensis
Hypsilophodon foxii
Atlascopcosaurus loadsi
Anabisetia saldivai
Gasparinisaura cincosaltensis
Qantassaurus intrepidus
Rhabdodon priscus
Tenontosaurus tilletti
Tenontosaurus dossi
Zalmoxes robustus
Zalmoxes shqiperorum
Muttaburrasaurus langdoni
Camptosaurus dispar
Ouranosaurus nigeriensis
Iguanodon bernissartensis
Callovosaurus leedsi
Valdosaurus canaliculatus
Elrhazosaurus nigeriensis
Dryosaurus altus
Dysalotosaurus lettowvorbecki
1
2
3
4
5
6
7
8
9
10
11
12
13
14
15
16
17
18

Figure 5.5: Time-calibrated phylogeny of Ornithischia. White boxes indicate the uncertainty around the age of first appearance for each terminal taxon (not the known occurrences), while black lines represent implied missing fossil records (i.e., ghost lineages). Note: some branches are necessarily drawn deeper in time due to drawing constraints. Numbers positioned along branches or at nodes indicate the position of major ornithischian subclades. **1**: Ornithischia; **2**: Heterodontosauridae; **3**: Genasauria; **4**: Thyreophora; **5**: Neornithischia; **6**: Parksosauridae; **7**: Orodrominae; **8**: Thescelosaurinae; **9**: Elasmaria; **10**: Cerapoda; **11**: Marginocephalia; **12**: Ornithopoda; **13**: Hypsilophodontidae; **14**: Iguanodontia; **15**: unnamed Gondwanan clade; **16**: Dryomorpha; **17**: Dryosauridae; **18**: Ankylopollexia.

members of Thyreophora was completed before the late Early Jurassic.

The species *Stormbergia dangershoeki* constrains the origin of the Neornithischia to the Early Jurassic at the latest, and all three analyses agree that this clade arose in Africa. Sometime before the late Middle Jurassic there is an extensive radiation of neornithischian taxa, though the poor fossil record of neornithischian taxa during the Early and early Middle Jurassic make it impossible to determine precisely how rapidly this radiation occurred. However, all three biogeographic analyses agree that this radiation occurred in Asia (Figs. 5.3 and 5.4). All three analyses remain in agreement regarding the diversification of Neornithischia occurring within Asia until the most recent common ancestor of the clade consisting of *Othnielosaurus consors* + (Parksosauridae + Cerapoda). At this node, the LEB analysis slightly favors North America as the ancestral area (50.7% versus 42.9% for Asia), while the LFR analysis strongly favors Asia (81.1% versus 8.8% for North America). The PB analysis is equivocal. The situation is similar for the most recent common ancestor of the clade consisting of Parksosauridae + Cerapoda.

The earliest known parksosaurid taxa, *Changchunsaurus parvus* and *Zephyrosaurus schaffi*, are present in the early Middle Jurassic (Fig. 5.5). However, a

long ghost lineage is present for Parksosauridae, stretching from at least the Bathonian until the Aptian, a time span of at least 40 myr. The LEB and LFR analyses agree that the basal split within Parksosauridae that gave rise to the clades Orodrominae and Thescelosaurinae occurred in North America by the Aptian (the PB analysis is undecided between North America and Asia). Both the LEB and LFR analyses also agree that the diversification of orodromine taxa occurred in North America during the Cretaceous, with the lineage leading to *Koreanosaurus boseongensis* splitting from *Oryctodromeus cubicularis* either during or prior to the Cenomanian, with the former taxon eventually dispersing into Asia by the Santonian (Figs 5.4 and 5.5). The PB analysis largely agrees with this interpretation, though it is equivocal as to whether at least some of the diversification of orodromine taxa occurred in Asia (Fig. 5.3).

Substantial disagreement exists between all three analyses regarding pattern of geographic dispersals present within Thescelosaurinae. In the PB analysis (Fig. 5.3), thescelosaurines originated in either North America or Asia. The most recent common ancestor of the clade composed of *Changchunsaurus parvus* and *Haya griva* was located in Asia, and this clade arose by the Aptian. The ancestral area for most of the remaining thescelosaurines was North America, though a single lineage dispersed to South America by the Cenomanian, giving rise to Elasmaria. The LEB analysis largely agrees with this interpretation (Fig. 5.4A), though it sets the origin of Thescelosaurinae within North America, with the clade consisting of *C. parvus* and *H. griva* dispersing into Asia by the Aptian. The results of the LRF analysis strongly contrast with both of the other analyses. The LRF analysis (Fig. 5.4B) places the basal split within Thescelosaurinae in Asia prior

to the Aptian. The sister taxon to the *C. parvus* + *H. griva* clade then migrates into South America (possibly by way of North America). Prior to the Cenomanian, two thescelosaurine lineages disperse into North America from South America. The first gives rise to *Parksosaurus warreni*, while the second gives rise to the *Thescelosaurus* clade.

The LFR and LEB analyses place the origin of Cerapoda within Asia prior to the late Middle Jurassic (Fig 5.4), though the PB analysis finds North America, Europe, and Asia equally likely areas (Fig. 5.3). The diversification of Marginocephalia occurred most likely in Asia by the Late Jurassic (the PB analysis is uncertain if this occurs in Asia or Europe owing to the basal position of *Stenopelix valdensis*).

Extensive disagreement exists between each of the three analyses concerning the biogeographic history of basal iguanodontians, and each set of results will be discussed separately. The PB analysis (Fig. 5.3) places the origin of Iguanodontia in Europe. The ancestral location of the newly recognized Gondwanan clade of iguanodontians was either in Europe, Australia, or South America. The pattern of geographic dispersals within the Gondwanan iguanodontian clade is not sufficiently resolved in this analysis to permit further comment. The majority of the remaining iguanodontian taxa were endemic to Europe, with a single lineage dispersing to North America by the Aptian that gave rise to *Tenontosaurus*. The pattern of geographic dispersals involving *Dryosaurus altus* and *Dysalotosaurus lettowvorbecki* are unresolved. The LEB analysis (Fig. 5.4A) also places the origin of Iguanodontia in Europe; however, the basal split within the Gondwanan iguanodontian clade is placed in Australia. After this split, the ancestral area of the

remaining members of the clade moves to South America, with *Qantassaurus intrepidus* dispersing back to Australia before the Valanginian. The remaining diversification follows that recovered by the PB analysis, though it recovers Africa as the ancestral area for the most recent common ancestor of *D. altus* and *D. lettowvorbecki*, with the former migrating into North America by the Late Jurassic.

The results of the LRF analysis contrast sharply with those of both the PB and LEB analyses (Fig. 5.4B). The LRF analysis places the origin of the Iguanodontia in Asia, requiring the lineage leading to *Hypsilophodon foxii* to disperse into Europe by the Aptian. The most recent common ancestor of the Gondwanan iguanodontian clade and Dryomorpha was also situated in Asia. The basal divergence within the Gondwanan iguanodontian clade occurred within Australia, as did all subsequent diversification within the clade, requiring two separate dispersals from Australia into South America. Above this clade, the ancestral area changes to Europe, with the lineage leading to the *Tenontosaurus* clade later migrating to North America and diversifying. The LFR analysis contradicts the LEB analysis in that the most recent common ancestor of the clade containing *D. altus* and *D. lettowvorbecki* migrates from Europe into North America, with the latter taxon then migrating to Africa (Fig. 5.4B versus 5.4A). One additional difference between the LFR analysis and the others is that the origin of Ankylopollexia is hypothesized to have occurred in North America and not Europe owing to the basal placement of the Jurassic taxon *Camptosaurus dispar*.

RESULTS OF STRATIGRAPHIC CONGRUENCE ANALYSIS

The results of the stratigraphic congruence analysis are shown in Table 1. Comparisons were limited in some cases by the necessity of trimming each tree topology to only include congruent sets of taxa. In the most extreme case, the strict consensus topology generated by this analysis was trimmed from sixty-five terminal taxa to sixteen to facilitate comparison with the strict consensus topology from Spencer (2007), limiting the amount of data available to compare these tree topologies (see Fig. 5.1B versus Fig. 5.2). An additional complicating factor was the high number of taxa placed within polytomies in each tree topology (e.g., 14 out of 35 taxa are placed in unresolved positions in the strict consensus tree of Butler et al. [2008a]). As a result, the minimum and maximum recovered values for each metric tend to be are highly disparate, lowering the chances of being able to select one tree topology as more congruent with the stratigraphic record of first appearances than another.

Despite these methodological difficulties, most of these comparisons resulted in the selection of one topology as more congruent with the stratigraphic record (Table 1). In five of the six comparisons made, the strict consensus tree produced by this analysis was found to be more stratigraphically congruent than the alternative topology, and in the sixth case the two trees were found to be equally congruent (Table 1). This latter result may be at least in part due to the small number of taxa shared between these two analyses (sixteen shared taxa); however, the topology from Buchholz (2002) only shares nineteen taxa in common with the strict consensus topology of this analysis, and in that case the

Table 5.1: Results of the stratigraphic congruence calculations comparing the ornithischian phylogenetic hypotheses of Buchholz (2002), Spencer (2007), and Butler et al. (2008a) with the results obtained in this study (Figs. 5.1 and 5.2). Values of MIG are reported in millions of years. Abbreviations: **DSRC** = derivative strict reduced consensus tree; **GER** = gap excess ratio; **MAS** = maximum agreement subtree; **MIG** = minimum implied gap; **MSM*** = modified manhattan stratigraphic measure; **MR** = majority-rule consensus tree; **SCC** = strict component consensus tree.

	# of Taxa	MIG	GER	MSM*	Result
Full Ornithischian Dataset	65	1908-1388	0.82-0.74	0.13-0.09	-
This Analysis	19	480-356	0.80-0.67	0.37-0.26	More Congruent
Buchholz (2002)	19	573-400	0.76-0.59	0.32-0.23	
This Analysis	16	289-212	0.92-0.80	0.76-0.57	Equally Congruent
Spencer (2007)	16	260-208	0.94-0.84	0.80-0.63	
This Analysis	35	852-611	0.86-0.76	0.28-0.19	More Congruent
Butler et al. (2008a) SCC	35	1582-844	0.77-0.49	0.20-0.10	
This Analysis	35	852-611	0.86-0.76	0.28-0.19	More Congruent
Butler et al. (2008a) MR	35	1170-877	0.77-0.65	0.19-0.14	
This Analysis	28	723-489	0.86-0.75	0.34-0.23	More Congruent
Butler et al. (2008a) MAS	28	816-620	0.81-0.70	0.27-0.20	
This Analysis	30	772-531	0.86-0.74	0.32-0.21	More Congruent
Butler et al. (2008a) DSRC	30	967-661	0.81-0.67	0.25-0.17	

topology from this analysis is clearly more congruent with the stratigraphic record of first appearances (Table 1). Most importantly, the strict consensus tree topology recovered in this study if found to be more congruent with the stratigraphic record of first appearances than any of the tree topologies put forth by Butler et al., (2008a), which was the most comprehensive analysis of basal ornithischian relationships prior to this study.

DISCUSSION

The strict consensus topology produced by this analysis (Fig. 5.2) is the most inclusive and well-resolved phylogenetic hypothesis of ornithischian relationships to date. This tree topology is equally congruent or more congruent with the stratigraphic record of first appearances than any other ornithischian phylogeny published in the last decade (Fig. 5.5; Table 1). Comparing the results of this study to those of other recently published ornithischian phylogenetic hypotheses (i.e., Buchholz, 2002; Spencer, 2007; and Butler, 2008a) provides important insights into those areas of the ornithischian evolutionary tree where our understanding is improving, where a consensus is beginning to be reached on contentious relationships, and where further improvement is needed.

Both this analysis and that of Butler et al. (2008a), recover a monophyletic Heterodontosauridae positioned outside of Genasauria at the base of Ornithischia, though more derived than *Pisanosaurus mertii*. This is in strong contrast to the traditional placement of Heterodontosauridae within Ornithopoda, a placement that has not been recovered since Sereno (1999). Thus, support is building for the removal of Heterodontosauridae from Genasauria. However, heterodontosaurids do convergently share some features with basal neornithischian taxa more closely related to Cerapoda than to *Agilisaurus louderbacki* (e.g., loss of a ventral acetabular flange on the ilium). This may account for the recovery of Heterodontosauridae at the base of Neornithischia outside of Cerapoda by the more restricted analysis conducted by Spencer (2007). Buchholz (2002) included only one heterodontosaurid, *Heterodontosaurus tucki*, in his

analysis of ornithischian relationships, recovering it as the sister taxon to a supraspecific terminal taxon representing Marginocephalia. The only other phylogenetic analysis to recover this set of relationships also included *H. tucki* as the only representative of Heterodontosauridae (Xu et al., 2006). These unconventional results are likely a result of the fact that *H. tucki* is a relatively derived member of Heterodontosauridae (Pol et al., 2011; this analysis), and is not an ideal exemplar species for representing Heterodontosauridae in phylogenetic analyses, at least not by itself.

This analysis recovers *Eocursor parvus* as a non-genasaurian ornithischian, as did Butler et al. (2007) and Pol et al. (2011), contrasting with its placement as a basal neornithischian by Spencer (2007). Unlike Butler et al. (2007) and Pol et al. (2011), this analysis identifies *E. parvus* as the basal-most heterodontosaurid. Butler (2010) provides a detailed list of features that separate *E. parvus* from heterodontosaurids, many of which are included as characters in this analysis (e.g., distribution of denticles on the tooth crowns and development of the coronoid process). Despite the inclusion of this evidence, *Eocursor* is positioned at the base of Heterodontosauridae based in part on the presence of some of the same features that are convergently shared between other heterodontosaurids and basal neornithischians more closely related to Cerapoda than to *Agilisaurus louderbacki* (e.g., presence of a ventral acetabular flange on the ilium). As such, it seems more plausible that *Eocursor* was a basal heterodontosaurid, which requires only two losses of these features within Ornithischia, as opposed to interpreting three independent losses near the base of Ornithischia.

This analysis recovers a very restricted Ornithopoda, which contains only *Hypsilophodon foxii* and Iguanodontia. Such a restricted Ornithopoda has never been recovered before in a published analysis, though the largely unpublished analysis of ornithischian relationships summarized in Liu (2004) recovered an even more restricted Ornithopoda that included an identical set of taxa as Iguanodontia. The reduced size of Ornithopoda in the study presented here is a result of the relatively high placement of Marginocephalia on the tree relative to other analyses (e.g., Sereno, 1999; Butler et al., 2008a). As a result, most taxa previously referred to the Hypsilophodontidae are now non-cerapodan basal neornithischians, with the exception of *H. foxii*. Despite not being strongly supported in the bootstrap analysis (Fig. 5.2), the placement of Marginocephalia on the tree is by far the most parsimonious placement given the character data analyzed. Moving Marginocephalia down the tree a single node to a position below Parksosauridae adds seven steps to the total tree length. Positioning Marginocephalia further down below *Jeholosaurus shangyuanensis* (the location recovered by Butler et al. [2008]) increases the tree length by nine steps. Thus, the recovered position of Marginocephalia is relatively well supported by the character data used in this study.

A clade composed solely of North American basal neornithischians was first recovered by Boyd et al. (2009) in their analysis of specimens previously referred to *Thescelosaurus*. This analysis recovers a similar clade, here termed Parksosauridae, though it now also contains Asian and South American taxa that were not included as terminal taxa by Boyd et al. (2009). The recovery of a monophyletic Parksosauridae significantly reduces the length of the inferred ghost lineages of many of its constituent

members. For example, *Thescelosaurus neglectus* was once inferred to possess one of the longest ghost lineages in all of Dinosauria (~105 myr: Weishampel and Heinrich, 1992). Based on its position in the strict consensus tree, the inferred ghost lineage for this taxon is reduced by more than two-thirds (Figure 5.5). Thus, not only is Parksosauridae well-supported by the character evidence, it also greatly improves the stratigraphic congruence of that subsection of the tree topology. However, a sizeable ghost lineage still exists at the base of Parksosauridae, extending ~40 myr from the Early Cretaceous back into the Middle Jurassic (Fig. 5.5). This implies that there is still much to learn regarding the early evolution and diversification of parksosaurids.

Recent analyses of the relationships of basal ornithischian taxa from Asia (e.g., *Changchunsaurus parvus*, *Haya griva*) have shown some support for a clade of basal ornithischian taxa endemic to Asia (Butler et al., 2011; Makovicky et al., 2011). In its most inclusive form (Makovicky et al., 2011) this clade consists of *Haya griva* as the sister taxon to a subclade composed of *Jeholosaurus shangyuanensis* + *Changchunsaurus parvus*. The exact position of this clade within Ornithischia is unresolved in the strict consensus trees of both Butler et al. (2011) and Makovicky et al. (2011), though the maximum agreement subtrees presented by both authors place this clade near the base of Ornithopoda. However, the latter authors cautioned that character support for these relationships was weak and that the large number of homoplastic characters displayed by these three taxa hinted at their possibly paraphyly (Makovicky et al., 2011). A different set of relationships is recovered for these taxa in this analysis. A clade consisting of *C. parvus* and *H. griva* is situated at the base of Thescelosaurinae within Parksosauridae

(Fig. 5.2), while *J. shangyuanensis* is positioned outside of Parksosauridae near the base of Neornithischia. Given the incongruence between the results presented here and those of prior studies (i.e., Butler et al., 2011 and Makovicky et al., 2011), a brief discussion of the characters supporting the placement of these taxa in the present analysis is warranted.

This study incorporates new character data for *J. shangyuanensis* based on personal examination of multiple articulated and nearly complete specimens in the collections at Peking University, allowing much of the postcranial skeleton to be analyzed for the first time and for a clearer understanding of the cranial anatomy to be achieved (see Appendix 11 for a list of specimens examined). As a result, a set of key differences between *J. shangyuanensis* and the Asian taxa *C. parvus* and *H. griva* were noted that are crucial to determining the position of these taxa within Neornithischia. The ventral process of the predentary of *J. shangyuanensis* is unilobate (72:0), while in *C. parvus* and *H. griva* it is bifurcate (72:1). Six premaxillary teeth are present in *J. shangyuanensis* (112:0) in contrast to *C. parvus* and *H. griva* that display five premaxillary teeth (112:1). The morphology of the dentary of *J. shangyuanensis* is distinctly different than that of *C. parvus* and *H. griva.* In *J. shangyuanensis*, the anterior tip of the dentary is positioned close to the ventral margin (74:2), the ventral and dorsal margins of the dentary converge anteriorly (75:0), and the dorsoventral height of the dentary just anterior to the coronoid process is less than 20% of the total length of the dentary (77:0). Alternatively, in *C. parvus* and *H. griva* the anterior tip of the dentary is positioned at midheight (74:1), the ventral and dorsal margins of the dentary are subparallel (75:1), and the dorsoventral height of the dentary just anterior to the rising

coronoid process is greater than 20% of the total length of the dentary (77:1). Additionally, the crowns of the dentary teeth in *J. shangyuanensis* lack a prominent primary ridge (139:0), while a primary ridge is present on the dentary crowns of both *C. parvus* and *H. griva* (139:1). In the postcranial skeleton, the lateral surface of the greater trochanter of the femur is convex in *J. shangyuanensis* (213:0), while the lateral surface of the greater trochanter of the femur is flattened in *C. parvus* and *H. griva* (213:1).That character is an unambiguous synapomorphy of Parksosauridae, clearly indicating *C. parvus* and *H. griva* are parksosaurids, while *J. shangyuanensis* is positioned outside of this clade. Overall, the character evidence outlined above strongly argues against a close relationship between *J. shangyuanensis* and either *C. parvus* or *H. griva.*

Previous investigations into the systematic relationships of South American taxa previously referred to either Hypsilophodontidae (e.g., *Notohypsilphodon comodorensis*) or Iguanodontia (e.g., *Anabisetia saldiviai*) tended to be relatively restricted in scope, focusing largely on South American taxa (e.g., Coria, 1999; Novas et al., 2004; Calvo et al., 2007). These investigations often recovered South American taxa in an endemic clade (Coria, 1999; Calvo et al., 2007), or closely situated to one another as part of a South American 'grade' of taxa (Novas et al., 2004). Several studies discussed tentative character support for some or all of these taxa forming a clade of strictly South American or Gondwanan taxa (Coria and Calvo, 2002; Novas et al., 2004; Calvo et al., 2007; Ibiricu et al., 2010). Thus, the recovery in this study of an iguanodontian clade comprised entirely of Gondwanan taxa is not unexpected. In fact, Coria (1999) previously recovered a clade composed of *Gasparinisaura cincosaltensis* + *Anabisetia saldiviai*, the same two

South American taxa recovered as a part of this Gondwanan clade. Coria (1999) also suggested that *G. cincosaltensis* and *A. saldiviai* had evolved from other Gondwanan taxa and likely dispersed into South America via Antarctica, possibly from Australia, prior to the Cretaceous (Coria, 1999:57). The structure of the strict consensus tree obtained by this study (Fig. 5.2), the results of the biogeographic reconstructions (Figs. 5.3 and 5.4), and the inferred distribution of ghost lineages for the taxa recovered within the Gondwanan clade (Fig. 5.5) all support this interpretation.

No prior analysis recovered a close relationship between any South American and Laurasian taxa, though some authors have suggested certain South American taxa more closely resembled Laurasian taxa than other Gondwanan taxa (e.g., *Talenkauen santacrucensis*; Novas et al., 2004). The placement of the South American taxa *Macrogryphosaurus gondwanicus*, *Notohypsilophodon comodorensis*, and *Talenkauen santacrucensis* within Thescelosaurinae amongst the North American taxa *Thescelosaurus* and *Parksosaurus warreni* provide insight into the evolution of the ornithischian fauna of South America. The South American ornithischian taxa treated in this study are supported as parts of two distinct radiations that dispersed into South America at different times via separate geographic paths. Based on the results presented in this study, basal iguanodontian taxa dispersed into South America from Australia (possibly via Antarctica) during the Late Jurassic or the beginning of the Early Cretaceous (Figs 5.4 and 5.5). Alternatively, thescelosaurine taxa most likely dispersed into South America from Asia (via North America) sometime during the latter portion of the Early Cretaceous, and then diversified, giving rise to Elasmaria (Figs. 5.4 and 5.5).

The close relationship between the South American members of Elasmaria and the North American taxa *Thescelosaurus* and *Parksosaurus warreni* may also answer some questions regarding the known stratigraphic distribution of parksosaurid taxa in North America during the Cretaceous. During most of the Cretaceous, orodromine taxa were the dominant basal neornithischian taxa present in North American faunas (Sues, 1980; Scheetz, 1999; Weishampel et al., 2004; Varricchio et al., 2007; Krumenacker, 2010). At the end of the Campanian, all orodromine taxa disappear from the North American fossil record. In the Maastrichtian the thescelosaurine taxa *Thescelosaurus* and *Parksosaurus warreni* appear in the North American fossil record, which may be an example of faunal replacement (Boyd et al., 2009; Brown et al., 2011). The results of the LFR biogeographic analysis suggest that the lineages leading to these latter two taxa may have originated in South America, and then dispersed into North America during the Maastrichtian. This observation strengthens the paleontological support for the presence of a land bridge and associated faunal interchange between North and South America during the latest Cretaceous (Brett-Surman and Paul, 1985; Rage, 1986; Hutchinson and Chiappe, 1998; Ezcurra and Agnolin, 2011).

APPENDIX 1

INSTITUTIONAL ABBREVIATIONS

AMNH: American Museum of Natural History, New York, New York, U.S.A.

CMN: Canadian Museum of Nature, Ottawa, Ontario, Canada

IVPP: Institute of Vertebrate Paleontology and Paleoanthropology, Beijing, People's Republic of China

KDRC: Korea Dinosaur Research Center, Chonnam National University, Gwangju, Republic of Korea

LACM: Los Angeles County Museum, Los Angeles, California, U.S.A.

MOR: Museum of the Rockies, Bozeman, Montana, U.S.A.

NCSM: North Carolina Museum of Natural Sciences, Raleigh, North Carolina, U.S.A.

NMV: National Museum of Victoria, Melbourne, Australia

PKUP: Peking University, Beijing, People's Republic of China

RSM: Royal Saskatchewan Museum, Regina, Saskatchewan, Canada

SDSM: South Dakota School of Mines and Technology, Rapid City, South Dakota, U.S.A.

UMNH VP: Utah Museum of Natural History, Salt Lake City, Utah, U.S.A.

USNM: Smithsonian Institution, National Museum of Natural History, Washington, D. C., U.S.A.

YPM: Yale Peabody Museum, New Haven, Connecticut, U.S.A.

APPENDIX 2

ANATOMICAL ABBREVIATIONS

aa: articulation surface for angular

ac: anterior concavity of laterosphenoid

ads: anterodorsal shelf of premaxilla

adp: anterodorsal process of palatine

aes: origin of m. adductor externus superficialis

afb: arched floor of braincase

aig: anterior intercondylar groove

aip: anterior inflation of postorbital

aj: articulation for jugal

almp: anterolateral maxillary process

alp: anterolateral processes of basisphenoid

am: articulation for maxilla

amt: anterior maxillary fossa

an: angular

ant: anterior

apa: articulation for palatine

apmf: anterior premaxillary foramen

apo: articulation surface for postorbital

app: anterior process of postorbital

apt: articulation for pterygoid

aqj: articulation for quadratojugal

ar: anterior ramus of postorbital

aso: articulation for supraoccipital

asor: accessory supraorbital

asq: articulation surface for squamosal

avp: anteroventral tip of premaxilla

bk: basioccipital keel

bo: basioccipital

bt: basal tubera

bpa: basipterygoid articulation

bpp: basipterygoid process

bpro: boss for articulation with proatlas

c: concretion

ca: articulation surface for coronoid

cc: cnemial crest

cf: coracoid foramen

ci: crista interfenestralis

cn: cranial nerve

co: coronoid

cp: coronoid process

cpr: crista prootica

ct: crista tuberalis

cup: cutriform process

d: damage

da: articulation surface for dentary

dc: distal carpal

de: dentary

dp: deltopectoral crest

dpj: dorsal projection of posterior process of jugal

drmm: dorsal rim of the medial process of the maxilla

dsq: dorsal projection of the anterior process of squamosal

dt: dentary tooth/teeth

ea: ectopterygoid articulation

eaof: external antorbital fenestra

eo: exoccipital

et: ectopterygoid

f: frontal

fl: flange

fm: foramen metoticum

fn: neck of femur

fo: fenestra ovalis

fom: foramen magnum

fr: frontal

fs: fossa subarcuata

ft: feeding trace

gf: glenoid fossa

gt: greater trochanter

hf: head of femur

hh: head of humerus

hl: head of laterosphenoid

iaof: internal antorbital fenestra

ib: irregular bosses

jh: jugal horn

jr: jugal ramus of postorbital

ju: jugal

jw: jugal wing

la: lacrimal

laa: articulation surface for lacrimal

lat: lateral

ldc: lateral distal condyle

lds: lateral depression of surangular

ldt: lateral distal tarsal

lf: lacrimal foramen

lfpd: lateral foramen of predentary

lg: lateral groove of predentary

lm: lateral malleolus

lof: lateral opisthotic fossa

lp: lateral process of posterior process of postorbital

lpf: lateral process foramen

lpp: lateral process of prearticular

lpr: lateral pterygoid ridge

lps: lateral process of surangular

ls: laterosphenoidsp

lsc: lateral semicircular canal

lsh: lateral humeral shoulder

lss: laterosphenoid socket

lt: lesser trochanter

M: metatarsal

mc: metacarpal

med: medial

mdc: medial distal condyle

mdt: medial distal tarsal

mfa: medial frontal articulation

mg: Meckelian groove

mgj: medial groove on jugal

mm: medial malleolus

mor: medial orbital ridge

mp: medial projection of the posterior process of the postorbital

mpp: mandibular process of pterygoid

mps: medial process of surangular

msh: medial humeral shoulder

mt: maxillary tooth/teeth

mta: articulation for the medial tubercle of the pubis

mx: maxilla

naa: neural arch articulation

na: nasal

nc: neural canal

ob: orbitosphenoid boss on laterosphenoid

oc: occipital condyle

of: olecranon fossa

om: orbital margin

op: olecranon process

or: orbit

pa: parietal articulation

paa: prearticular articulation surface

par: parietal

pb: prootic boss

pd: predentary

puff: prefrontal

pfa: prefrontal articulation surface

puff: prefrontal foramen

pc: proximal carpal

pdp: posterodorsal process of the premaxilla

pfa: prefrontal articulation

pes: postorbital-frontal suture

pg: pterygoid groove

pl: palatine

plc: proximal lateral condyle

plop: posterolateral process of premaxilla

plpd: posterolateral process of predentary

pals: posterolateral sulcus in premaxilla

pm: premaxilla

pmf: premaxillary foramen

pmt: premaxillary tooth/teeth

pnp: premaxillary narial process

pod: postorbital

poa: postorbital articulation

pop: paroccipital process

poq: postquadratic process of squamosal vsq

pos: postorbital socket

post: posterior

pp: postorbital projection into orbit

pap: proximal posterior condyle

ppf: postpalatine fenestra

ppp: palatine process of pterygoid

ppv: posterior process of vomer

pr: posterior ramus of postorbital

par: prootic articulation

pro: prootic

prp: preotic pendant

prq: prequadratic process

pes: parasphenoid

pes: posterior semicircular canal

pass: postorbital-squamosal suture

pt: pterygoid

puff: posterior temporal opening for the vena capitis dorsalis

pw: pterygoid wing

pwf: pterygoid wing fossa

pwg: pterygoid wing ventral groove

a: quadrate articulation

qap: quadrate alar process

qf: quadrate foramen

job: quadratojugal

qja: quadratojugal articulation

up: quadratic process

quad: quadrate

ra: ridge for articulation with angular

arc: radial condyle

rp: retroarticular process

rpf: rostral palatal foramen

rso: rugose contact for supraorbital

rsq: ventral ridge on squamosal

s: true sacral vertebra

as: scapula articulation

sas: splenial articulations surface

sc: sacrocaudal vertebra

seed: sediment

sell: sella turcica

sf: surangular foramen

she: socket for head of quadrate

sly: splenial

soak: supraoccipital articulation

soaa: articulation surface for accessory supraorbital

sor: supraorbital

sp: sclerotic plate

sq: squamosal

sr1: first sacral rib articulation

ss: scapular spine

st: stapes

stf: supratemporal fenestra

su: surangular

sul: sulcus for ligamentum capitis femoris

uc: ulnar condyle

vd: ventral depression on jugal

ve: vestibule

vcd: groove for the vena capitis dorsalis

vcf: ventral coracoid foramen

vcms: groove for the vena cerebralis media secunda

vcp: foramen for the vena cerebralis posterior

vlg: ventral laterosphenoid groove

vmr: ventral midline ridge

vpj: ventral process of the posterior projection of the jugal

vppo: ventral process of the postorbital

vppd: ventral process of the predentary

vr: vertical ridge

vsc: vestibule-semicircular canal connection

vsq: ventral projection of the anterior process of the squamosal

APPENDIX 3:

MORPHOLOGICAL CHARACTERS FOR CHAPTER 1

Description of characters used for the phylogenetic analysis of basal neornithischian relationships. See Scheetz (1999) for a detailed discussion of the distribution of character states for characters 1 through 123.

1. Length of jugal wing on quadrate greater than 20% quadrate length (0), less than 20% (1).

2. Quadrate notch absent (0), present (1).

3. Length of the articulation between the quadrate and quadratojugal greater than or equal to 50% length of quadrate (0), between 50% and 25% (1), contact 25% or less (2).

4. Proximal head of the quadrate recurved posteriorly (0), straight (1).

5. Pterygoid wing on quadrate greater than 25% length of quadrate (0), less than 25% (1).

6. Jugal or quadratojugal meets the quadrate near the distal end (0), above distal end (1), well above distal end (2).

7. Distal end of quadrate dorsomedially sloped or horizontal (0), dorsolaterally sloped (1).

8. Pterygoid wing emerges at the dorsal head of the quadrate (0), below the dorsal head of the quadrate (1).

9. The ventral extent of the jugal wing ends at or near distal condyles of quadrate (0), above distal condyles (1), well above the distal condyles (2).

10. Groove on the base of the posterior side of the pterygoid wing of the quadrate absent (0), groove or fossa present (1).

11. Lateral pit in mid-quadrate shaft present (0), absent (1).

12. Ventral process on squamosal less than 30% length of the quadrate (0), greater than 30% (1).

13. Quadrate leans posteriorly (0), oriented vertically (1).

14. Jugal fails to articulate with quadrate (0), jugal articulates with quadrate (1).

15. Quadratojugal height normal to short (0), tall and narrow (1).

16. Quadratojugal foramen absent (0), present (1).

17. Exoccipital contributes to part of basioccipital (0), occipital condyle entirely composed of basioccipital (1).

18. Orbital edge of postorbital smooth (0), striated and rugose orbital edge (1).

19. Postorbital non-robust (0), robust postorbital (1).

20. Orbital margin of the postorbital arcuate (0), anteriorly directed inflation along upper half of the orbital margin of the postorbital (1).

21. Socket for the head of the laterosphenoid occurs along frontal-postorbital suture (0), only in postorbital (1), socket absent (2).

22. Combined width of frontals less than 150% frontal length (0), greater than 150%.

23. Frontals arched over the orbits (0), dorsally flattened frontals (1).

24. Frontal contacts orbit along more than 25% of total frontal length (0), less than 25% (1).

25. Ratio of frontal length to nasal length greater than 120% (0), between 120% and 60% (1), less than 60% (2).

26. Frontals positioned over all of orbit (0), frontals only over the posterior half of orbit (1).

27. Six premaxillary teeth (0), five premaxillary teeth (1), no premaxillary teeth (2).

28. Oral margin of the premaxilla non-flared (0), slightly flared or everted oral margin of the premaxilla (1), everted oral margin of the premaxilla (2).

29. Posterolateral recess in the posterior end of the premaxilla for receipt of the anterolateral boss of the maxilla absent (0), present (1).

30. Premaxilla does not contact lacrimal (0), premaxilla contacts lacrimal (1).

31. Non-packed maxillary teeth (0), lack of space between adjacent maxillary teeth up through the occlusional margin (1).

32. Maxillary and dentary teeth not inset (0), maxillary and dentary teeth at least modestly inset (1).

33. Maxillary tooth roots straight (0), curved (1).

34. Cingulum present on maxillary tooth crowns (0), no cingulum on maxillary teeth (1).

35. Distinct neck present below maxillary crown (0), crown tapers to root (1).

36. Maxillary teeth independently occlude (0), maxillary teeth form a continuous occlusional surface (1).

37. Maxillary teeth lingually concave (0), lingually convex (1).

38. Maxillary teeth with centrally placed apical ridge (0), posteriorly-set apical ridge (1).

39. Maxillary teeth equally enameled on both sides (0), enamel restricted to one side (1).

40. Anterior end of the maxilla exhibits a spike-like process that inserts into the posterior end of the premaxilla (0), anterior end of maxilla bears an anterodorsal sulcus to receive the posterior portion of the premaxilla (1).

41. Maxillary crowns relatively low spade-like, rectangular, or triangular (0), high diamond-shaped maxillary tooth crowns (1).

42. Jugal contacts antorbital fenestra (0), jugal excluded from bordering antorbital fenestra (1).

43. Greatest posterior expanse of the jugal greater than ¼ skull height (0), less than ¼ skull height (1).

44. Jugal horn or boss absent (0), present (1).

45. Anterior process of jugal straight (0), dorsally curved (1).

46. Maxillary process on the medial side of jugal medially projected and modestly arched (0), presence of a straight groove for insertion of the posterior flange of the jugal (1), anteromedially projected and arched (2).

47. Ectopterygoid articular facet on medial jugal consists of a deep groove (0), rounded scar (1).

48. In lateral view anterior end of jugal ends above maxilla (0), inserts within maxilla (1).

49. Jugal forms an oblique to right angle bordering the anteroventral corner of the infratemporal fenestra (0), acute angle (1).

50. Jugal barely touches lacrimal (0), jugal meets lacrimal with more contact (1), lacrimal-jugal butt joint (2).

51. Position of the anterior tip of dentary positioned high (0), mid height (1), near lower margin of dentary (2), below lower margin (3), well below lower margin (4).

52. Apical ridge on dentary teeth anteriorly or centrally positioned (0), posteriorly positioned (1).

53. Dentary tooth crowns possess primary and some secondary ridges (0), dentary crown possess primary, secondary, and tertiary ridges (1).

54. Dentary teeth possess ridges on both sides of crown (0), ridges on only one side (1).

55. Dentary teeth with enamel on both sides (0), enamel primarily on one side (1).

56. Dentary crowns possess denticles supported by ridges (0), not all denticles supported by ridges (1).

57. Dentary teeth possess a modest cingulum (0), no cingulum on dentary teeth (1).

58. Dentary tooth roots round in cross-section (0), oval (1), squared (2), squared and grooved (3).

59. Dentary tooth roots straight (0), curved (1).

60. Dentary crowns rectangular, triangular, or leaf-shaped (0), crowns lozenge-shaped (1).

61. Dentaries straight in dorsal view (0), dentaries arched medially (1).

62. Post-coronoid elements make up 35-40% of the total length of the lower jaw (0), 25-35% (1), less than 25% (2).

63. Ratio of dentary height (just anterior to the rising coronoid process) divided by length of dentary between 15-20% (0), 20-35% (1).

64. Predentary possesses a single posteroventral process (0), posteroventral process paired or bifurcate (1).

65. External mandibular fenestra present (0), absent (1).

66. Surangular foramen absent (0), present (1).

67. Dorsal margin of the surangular convex or diagonal (0), concave in lateral view (1).

68. Nuchal crest on supraoccipital present (0), absent (1).

69. Supraoccipital forms greater than 5% of the margin of the foramen magnum (0), less than 5% (1), does not contribute to dorsal margin (2).

70. Basioccipital ventral keel absent (0), present (1).

71. Foramen magnum occupies over 30% of the width of occipital condyle (0), 20-30% (1), less than 20% of occipital condyle (2).

72. Floor of braincase on basioccipital flat (0), arched (1).

73. Median ridge on floor of braincase on the basioccipital absent (0), present (1).

74. Basioccipital tubera lower basisphenoid (0), level (1).

75. Basisphenoid shorter than basioccipital (0), equal in size (1), longer than basioccipital (2).

76. Foramen for cranial nerve V notches the anteroventral edge of the prootic (0), foramen nearly, or completely, enclosed in prootic (1).

77. Cervical vertebrae plateocoelous to amphicoelous (0), opisthocoelous (1).

78. Neural spine anteriorly positioned or centered over the dorsal centrum (0), posteriorly positioned (1).

79. Transition in dorsal ribs between a near vertical orientation of the tuberculum and capitulum to a horizontal orientation occurs within ribs 2-4 (0), 5-6 (1), 6-8 (2).

80. Twelve dorsal vertebrae (0), 15 dorsal vertebrae (1), 16 dorsal vertebrae (2), 17 dorsal vertebrae (3).

81. Four sacral vertebrae (0), five sacral vertebrae (1), six sacral vertebrae (2), seven sacral vertebrae (3).

82. Sacral neural spines less than twice the height of the centrum (0), neural spines between two and two and a half times the height of the centrum (1), greater than two and a half times (2).

83. Sacral spines lean posteriorly (0), slightly anteriorly (1).

84. Pubis does not articulate with the sacrum (0), pubis supported by sacral rib (1), pubis supported by sacral centrum (2).

85. Caudal ribs borne on centrum (0), on neurocentral suture (1), on neural arch (2).

86. Ossified hypaxial tendons on the tail absent (0), present (1).

87. First caudal vertebrae bears longest rib (0), longest rib posterior to the first (1).

88. Caudal neural spines positioned over centrum (0), neural spines extend beyond own centrum (1).

89. Scapular spine low or broad (0), sharp and pronounced (1).

90. Ratio of coracoid width to length less than 60% (0), between 70 and 100% (1), greater than 100% (2).

91. Coracoid foramen enclosed within coracoid (0), open along coracoid-scapula suture (1).

92. Sternals crescent-shaped (0), hatchet-shaped (1).

93. Olecranon process on ulna low (0), moderately developed (1), relatively high (2).

94. Shaft of ulna triangular or oval in cross section (0), cylindrical (1).

95. Shaft of ulna straight (0), bowed (1).

96. Manual phalangeal formula 2-3-4-3-0 (0), 2-3-4-2[3]-1 (1), 2-3-4-3-2 (2), 2-3-4-2-2 (3), 2-3-4-2-1 (4), 2-3-3-2-1 (5), 2-3-3-2-4 (6).

97. Unfused carpus (0), fused carpus (1).

98. Acetabulum high to normal (0), vertically short and long (1).

99. Ischiac peduncle of ilium not supported by sacral rib (0), ischiac peduncle articulates with sacral rib (1).

100. Shaft on ischium flat and blade-like (0), bar-like (1).

101. Distal end of ischium lacks an expanded foot (0), distal foot present (1).

102. Ischium lacks an obturator process (0), obturator process present and placed 60% down the shaft of ischium (1), placed 50% down the shaft (2), placed 40% down the shaft (3), placed with the proximal 30% of the ischial shaft (4).

103. Pubic peduncle of ischium larger than iliac peduncle (0), iliac peduncle of ischium as large as or larger than pubic peduncle (1).

104. Anterior process of pubis absent (0), present and rod-like or sword like (1), dorsoventrally expanded prepubis (2).

105. Anterior process of pubis straight when present (0), upturned anterior process (1).

106. Femur lacks a neck-like constriction below the femoral head (0), constriction present (1).

107. Lesser trochanter of femur lower or equal to greater trochanter (0), higher than greater trochanter(1).

108. Lesser trochanter of femur anterior and medial of greater trochanter (0), anterior and somewhat lateral to lesser trochanter (1).

109. Greater trochanter of femur laterally convex (0), laterally flattened (1).

110. Anterior intercondylar groove on the distal femur absent (0), modest intercondylar groove present (1), well-developed intercondylar groove (2).

111. Ratio of lateral distal condyle width to medial distal condyle width on femur roughly equal (0), 80-60% (1), 59-50% (2), 49-40% (3), 39-30% (4), 29-20% (5).

112. Both proximal lateral condyles on the tibia equal in size (0), fibular condyle smaller (1), only one lateral condyle present (2).

113. Cnemial crest of tibia rounded (0), sharply defined (1).

114. Midshaft of tibia triangular in cross-section (0), round in cross-section (1).

115. Fibula shaft elliptical or round in cross-section (0), D-shaped in cross-section (1).

116. Astragalus bears a short ascending process (0), triangular and tooth-like (1), spike-like (2), relatively large (3).

117. Posterior side of astragalus low (0), high (1).

118. Anterior side of astragalus high (0), moderate (1), low (2).

119. Angle between the tibial and fibular articular facets on the calcaneum greater than 120 degrees (0), less than 120 degrees (1).

120. Medial distal tarsal blocky in dorsal view (0), thin and rectangular (1), round (2).

121. Medial distal tarsal does not articulate over the proximal end of metatarsal II (0), medial distal tarsal articulates over a least a portion of the proximal end of metatarsal II (1).

122. Lateral distal tarsal square in dorsal view (0), kidney-shaped (1).

123.Four functional digits in the pes (0), three functional digits in the pes (1).

124. Premaxillae unfused (0), fused (1).

125. Palpebral dorsoventrally flattened and rugose along the medial and distal edges: absent (0), present (1).

126. Frontals wider across posterior end than at midorbit level (0), wider at midorbital level (1).

127. Presence of a 'Y-shaped' indentation on the dorsal edge of opisthotics: absent (0), present (1).

128. Angle formed by a line drawn along the ventral edge of the braincase (occipital condyle, basal tubera, and basipterygoid processes) and a line drawn through center of the trigeminal foramen and posterodorsal hypoglossal foramen: greater than fifteen degrees (0), less than fifteen degrees (1).

129. Dorsolaterally directed process on the lateral surface of the surangular: absent (0), present (1).

130. Ratio of femur length to tibia length: less than one (0), greater than one (1).

131. Presence and structure of a horizontal ridge on the maxilla: absent or smooth when present (0), present with at least the posterior portion covered by a series of obliquely inclined ridges (1).

132. Posterior half of ventral edge of jugal offset ventrally and covered laterally with obliquely inclined ridges: absent (0), present (1).

133. Foramen in the prefrontal positioned dorsomedial to the articulation surface for the palpebral that opens into the orbit: absent (0), present (1).

APPENDIX 4:

CHARACTER DATA FOR CHAPTER 1

Character codings for the 27 terminal taxa used in the analysis of specimens previously referred to *Thescelosaurus*. Modified from Scheetz (1999) and Varricchio et al. (2007). Question marks indicate lack of information for that taxon.

Taxon	10	20	30	40
Scutellosaurus	??????????	??????0000	???????00?	00?0000000?
Heterodontosaurus	?00000??0?	000000?0?0	?000100?1	11??11?00?
Lesothosaurus	0000000000?	0000000000	0000000000	0000000100
Agilisaurus	?001??????	???000????	?000101???	01?000?10?
Yandusaurus	0?0000?00?	?01000???0	?00010????	1100000100
Othnielosaurus	??????????	??????0000	?00??0????	0100000010?
Zephyrosaurus	0?10001001	01?0??0101	0010?0101?	1100001?00
Orodromeus	0010001101	0100000101	1000?0111?	0100000000
Oryctodromeus	001???1000	??????????	??????111?	010000???0
Parksosaurus	001?01?010	1000000000	?01010???0	0110001107
Hypsilophodon	000002002?	?000010?0	0000101000	1100111110
Tenontosaurus	0000100?00	0011010??0	1010102??0	1111111110
Dryosaurus	0120020100	?011000??0	1000102200	1111111111
Dysalotosaurus	1120020121	1011000???	?000102201	??????????
Rhabdodon	?010?10000	1?????????	??????200?	11?1?11100
Iguanodon	1101120120	1010101?10	2111212201	1111111111
Ouranosaurus	110112002?	?010101010	1111212201	11?????1?1
Camptosaurus	01?0120120	1111?00010	1011102201	1111111111
Gasparinisaura	1000?2??2?	?00011?000	??00??????	11?111?1??
USNM 7757/7758	??????????	???????101	??????????	??????????
RSM P.1225.1	??????????	??????0?0?	??1??0????	??????????
LACM 33542	??????????	??????????	??????????	??????????
SDSM 7210	??????????	????????0?	????????2??	11?000??0?
NCSM 15728	1?1001??1?	0000010101	?010100210	110?00?1?0
MOR 979	??11?00???	?01000?000	?000?0???0	11??00??0?
CMN 8537	??????????	???????001	?00???????	????0??10?
LACM 33543	??????????	??????0???	??0???????	??????????

Taxon	50	60	70	80
Scutellosaurus	0?????????	0000000000	0?000?????	??????????
Heterodontosaurus	00010??001	0001101100	0010000000	????0??00
Lesothosaurus	00000??001	0000000000	0000000000	00??10????
Agilisaurus	01?01??110	??????????	????10????	?????????1
Yandusaurus	01101???10	100?0001?0	1?0?1?????	??????0001
Othnielosaurus	0???0???1?	1000000000	1?001????0	101???00?1
Zephyrosaurus	0?1110000?	?000000000	1?1????001	1101200000
Orodromeus	0111000002	2000000000	1010110101	1101110001
Oryctodromeus	0??001??1?	200????0?00	1?0????001	110??11121
Parksosaurus	01000???11	?000000000	011011??0?	01???0?0?2
Hypsilophodon	01000??111	2011110010	111011?001	01?010?001
Tenontosaurus	01000??111	2001111211	001111?121	20?0001112
Dryosaurus	1000010001	2111111111	1011101001	2000011111
Dysalotosaurus	???0010101	2111111111	1011111001	2100211?1
Rhabdodon	0?????????	1001101210	1?11111??1	?000??01??
Iguanodon	1100021112	4111111311	1201111020	2000201123
Ouranosaurus	?010021112	3111????11	1100111120	00002?1123
Camptosaurus	1100001111	3111111311	1111111000	2011000102
Gasparinisaura	11?00??1?1	3?????????	?01?110000	2?????????
USNM 7757/7758	??????????	??????????	??????????	???????0?2
RSM P.1225.1	??????????	??????????	???????101	0??1?0?0??
LACM 33542	??????????	??????????	??????????	??????????
SDSM 7210	01?00?00?2	?0?0000?10	?????10???	??????????
NCSM 15728	01100?0012	20?0000?1?0	0111110111	0??1?110??
MOR 979	01100???02	2???00???0	0????00?1?	??????????
CMN 8537	0?????????	20?000???0	0?1?110?1?	?????????2
LACM 33543	?1?00?????	2?????????	0?????0111	0??????1??

Taxon	90	100	110	120
Scutellosaurus	1????0??01	0?0??00??0	0?1??00001	0????0????
Heterodontosaurus	0???0000?1	??20020?0	100000?100	0?0???????0
Lesothosaurus	2?????0?0?1	0?00010000	0000000000	00???3?001
Agilisaurus	1???10??0?	0??????110	03?111010?	?????0????
Yandusaurus	1??01??100	??0?030010	0301010010?	2????20011
Othnielosaurus	100010?101	000?0?0010	0301010100	1?00?21011
Zephyrosaurus	???210?111	0?00???1?0	?????10111	1?00100201
Orodromeus	2002100111	00110?0110	0201010110	1000120001
Oryctodromeus	30022?1111	0?100??11?	???1010110	?100100???
Parksosaurus	2???12010?	00??????10	0111110110	??0??0?0?1
Hypsilophodon	2001121101	1010130010	0101010100	2100010011
Tenontosaurus	1100110101	0000150110	1312110102	3201000211
Dryosaurus	2100200100	10100?1111	1402111102	3100?31011
Dysalotosaurus	2?01201100	10101????1	1402111102	3????31?1?
Rhabdodon	210210?100	0?101??111	101??10102	2200?012?2
Iguanodon	2201101102	112?061111	1412110102	5211001202
Ouranosaurus	22??0??102	11210?1110	1412100102	4211001212
Camptosaurus	22101?1101	1010121111	1412110102	?20100120?
Gasparinisaura	1001110101	0???0??110	?311011110	1201000212
USNM 7757/7758	1?00?1?1??	??00?20010	0?11110111	??00??0???
RSM P.1225.1	?????1?1??	???????01?	???1110111	??00??0???
LACM 33542	??????????	??????????	?????????1	??00000?1
SDSM 7210	??????????	??????????	??????????	??????????
NCSM 15728	3000?11100	0000??0010	0301110111	2?????????
MOR 979	??0??11?00	0?00??00?0	0??1?101??	??00000?1
CMN 8537	2?0??11100	0??????010	0??111011?	??0????0??
LACM 33543	??????????	???????010	030?1?????	??????????

Taxon	1 3 0	1 3 3
Scutellosaurus	??00?????0	???
Heterodontosaurus	0000000000	000
Lesothosaurus	0?000000?0	000
Agilisaurus	??0000??00	000
Yandusaurus	110000???0	???
Othnielosaurus	1100?????0	???
Zephyrosaurus	10010000?0	000
Orodromeus	100000??00	000
Oryctodromeus	???1??0??0	?0?
Parksosaurus	??0??0??00	000
Hypsilophodon	1100000000	000
Tenontosaurus	1000000001	000
Dryosaurus	1110000000	000
Dysalotosaurus	0?10000000	000
Rhabdodon	0110??????	???
Iguanodon	0110000?1	???
Ouranosaurus	??10000001	000
Camptosaurus	0?10000101	000
Gasparinisaura	11100???00	00?
USNM 7757/7758	1?0??1???1	???
RSM P.1225.1	??0?1111?1	?1?
LACM 33542	1?0???????	???
SDSM 7210	???01?????	11?
NCSM 15728	???11111?	111
MOR 979	??0?1???11	111
CMN 8537	????111?11	???
LACM 33543	???????11?	?1?

APPENDIX 5

MORPHOLOGICAL CHARACTERS FOR CHAPTER 3

The following characters were used to evaluate the systematic relationships of *Skaladromeus goldenii*. Characters are slightly modified form Boyd *et al*. (2009). See Cladistic Methodology section for details of these modifications.

1. Length of jugal wing on quadrate greater than 20% quadrate length (0), less than 20% (1).

2. Quadrate notch absent (0), present (1).

3. Length of the articulation between the quadrate and quadratojugal greater than or equal to 50% length of quadrate (0), between 50% and 25% (1), contact 25% or less (2).

4. Dorsal head of the quadrate recurved posteriorly (0), straight (1).

5. Pterygoid wing on quadrate greater than 25% length of quadrate (0), less than 25% (1).

6. Jugal or quadratojugal meets the quadrate near the distal end (0), above distal end (1), well above distal end (2).

7. Ventral condyles of quadrate dorsomedially sloped or horizontal (0), dorsolaterally sloped (1).

8. Pterygoid wing emerges at the dorsal head of the quadrate (0), below the dorsal head of the quadrate (1).

9. The ventral extent of the jugal wing ends at or near distal condyles of quadrate (0), above distal condyles (1), well above the distal condyles (2).

10. Groove on the base of the posterior side of the pterygoid wing of the quadrate absent (0), groove or fossa present (1).

11. Lateral pit in mid-quadrate shaft present (0), absent (1).

12. Ventral process on squamosal less than 30% length of the quadrate (0), greater than 30% (1).

13. Quadrate leans posteriorly (0), oriented vertically (1), leans anteriorly (2).

14. Jugal fails to articulate with quadrate (0), jugal articulates with quadrate (1).

15. Quadratojugal height normal to short (0), tall and narrow (1).

16. Quadratojugal foramen absent (0), present (1).

17. Exoccipital contributes to part of occipital condyle (0), occipital condyle entirely composed of basioccipital (1).

18. Orbital edge of postorbital smooth (0), striated and rugose orbital edge (1).

19. Postorbital non-robust (0), robust postorbital (1).

20. Orbital margin of the postorbital arcuate (0), anteriorly directed inflation along upper half of the orbital margin of the postorbital (1).

21. Socket for the head of the laterosphenoid occurs along frontal-postorbital suture (0), only in postorbital (1), socket absent (2).

22. Combined width of frontals less than 150% frontal length (0), greater than 150%.

23. Frontals arched over the orbits (0), dorsally flattened frontals (1).

24. Frontal contacts orbit along more than 25% of total frontal length (0), less than 25% (1).

25. Ratio of frontal length to nasal length greater than 120% (0), between 120% and 60% (1), less than 60% (2).

26. Frontals positioned over all of orbit (0), frontals only over the posterior half of orbit (1).

27. Six premaxillary teeth (0), five premaxillary teeth (1), no premaxillary teeth (2).

28. Oral margin of the premaxilla non-flared (0), slightly flared oral margin of the premaxilla (1), everted oral margin of the premaxilla (2).

29. Posterolateral recess in the posterior end of the premaxilla for receipt of the anterolateral boss of the maxilla absent (0), present (1).

30. Premaxilla does not contact lacrimal (0), premaxilla contacts lacrimal (1).

31. Non-packed maxillary teeth (0), lack of space between adjacent maxillary teeth up through the occlusional margin (1).

32. Maxillary and dentary teeth not inset (0), maxillary and dentary teeth at least modestly inset (1).

33. Maxillary tooth roots straight (0), curved (1).

34. Cingulum present on maxillary tooth crowns (0), no cingulum on maxillary teeth (1).

35. Distinct neck present below maxillary crown (0), crown tapers to root (1).

36. Maxillary teeth independently occlude (0), maxillary teeth form a continuous occlusional surface (1).

37. Maxillary teeth lingually concave (0), lingually convex (1).

38. Maxillary teeth with centrally placed apical ridge (0), posteriorly-set apical ridge (1).

39. Maxillary teeth equally enameled on both sides (0), enamel restricted to one side (1).

40. Anterior end of the maxilla exhibits a spike-like process that inserts into the posterior end of the premaxilla (0), anterior end of maxilla bears an anterodorsal sulcus to receive the posterior portion of the premaxilla (1).

41. Maxillary crowns relatively low and spade-like, rectangular, or triangular (0), high diamond-shaped maxillary tooth crowns (1), maxillary tooth crowns laterally compressed and recurved posteriorly (2).

42. Jugal contacts antorbital fenestra (0), jugal excluded from bordering antorbital fenestra (1).

43. Greatest posterior expanse of the jugal greater than ¼ skull height (0), less than ¼ skull height (1).

44. Jugal horn or boss absent (0), present (1).

45. Anterior process of jugal straight (0), dorsally curved (1).

46. Maxillary process on the medial side of jugal medially projected and modestly arched (0), presence of a straight groove for insertion of the posterior flange of the jugal (1), anteromedially projected and arched (2).

47. Ectopterygoid articular facet on medial jugal consists of a deep groove (0), rounded scar (1).

48. In lateral view anterior end of jugal ends above maxilla (0), inserts within maxilla (1).

49. Jugal forms an oblique to right angle bordering the anteroventral corner of the infratemporal fenestra (0), acute angle (1).

50. Jugal barely touches lacrimal (0), jugal meets lacrimal with more contact (1), lacrimal-jugal butt joint (2).

51. Position of the anterior tip of dentary positioned high (0), mid height (1), near lower margin of dentary (2), below lower margin (3), well below lower margin (4).

52. Apical ridge on dentary teeth anteriorly or centrally positioned (0), posteriorly positioned (1).

53. Dentary tooth crowns possess primary and some secondary ridges (0), dentary crown possess primary, secondary, and tertiary ridges (1).

54. Dentary teeth possess ridges on both sides of crown (0), ridges on only one side (1).

55. Dentary teeth with enamel on both sides (0), enamel primarily on one side (1).

56. Dentary crowns possess denticles supported by ridges (0), not all denticles supported by ridges (1).

57. Dentary teeth possess a modest cingulum (0), no cingulum on dentary teeth (1).

58. Dentary tooth roots round in cross-section (0), oval (1), squared (2), squared and grooved (3).

59. Dentary tooth roots straight (0), curved (1).

60. Dentary tooth crowns rectangular, triangular, or leaf-shaped (0), dentary tooth crowns lozenge-shaped (1), dentary tooth crowns laterally compressed and recurved posteriorly (2).

61. Dentaries straight in dorsal view (0), dentaries arched medially (1).

62. Post-coronoid elements make up 35-40% of the total length of the lower jaw (0), 25-35% (1), less than 25% (2).

63. Ratio of dentary height (just anterior to the rising coronoid process) divided by length of dentary between 15-20% (0), 20-35% (1).

64. Predentary possesses a single posteroventral process (0), posteroventral process paired or bifurcate (1).

65. External mandibular fenestra present (0), absent (1).

66. Surangular foramen absent (0), present (1).

67. Dorsal margin of the surangular convex or diagonal (0), concave in lateral view (1).

68. Nuchal crest on supraoccipital present (0), absent (1).

69. Supraoccipital forms greater than 5% of the margin of the foramen magnum (0), less than 5% (1), does not contribute to dorsal margin (2).

70. Basioccipital ventral keel absent (0), present (1).

71. Foramen magnum occupies over 30% of the width of occipital condyle (0), 20-30% (1), less than 20% of occipital condyle (2).

72. Floor of braincase on basioccipital flat (0), arched (1).

73. Median ridge on floor of braincase on the basioccipital absent (0), present (1).

74. Basioccipital tubera extend further ventrally than the basisphenoid (0), level (1).

75. Basisphenoid shorter than basioccipital (0), equal in size (1), longer than basioccipital (2).

76. Foramen for cranial nerve V notches the anteroventral edge of the prootic (0), foramen nearly, or completely, enclosed in prootic (1).

77. Cervical vertebrae plateocoelous to amphicoelous (0), opisthocoelous (1).

78. Neural spine anteriorly positioned or centered over the dorsal centrum (0), posteriorly positioned (1).

79. Transition in dorsal ribs between a near vertical orientation of the tuberculum and capitulum to a horizontal orientation occurs within ribs 2-4 (0), 5-6 (1), 6-8 (2).

80. Twelve dorsal vertebrae (0), 15 dorsal vertebrae (1), 16 dorsal vertebrae (2), 17 dorsal vertebrae (3).

81. Four sacral vertebrae (0), five sacral vertebrae (1), six sacral vertebrae (2), seven sacral vertebrae (3).

82. Sacral neural spines less than twice the height of the centrum (0), neural spines between two and two and a half times the height of the centrum (1), greater than two and a half times (2).

83. Pubis does not articulate with the sacrum (0), pubis supported by sacral rib (1), pubis supported by sacral centrum (2).

84. Caudal ribs borne on centrum (0), on neurocentral suture (1), on neural arch (2).

85. Ossified hypaxial tendons on the tail absent (0), present (1).

86. First caudal vertebrae bears longest rib (0), longest rib posterior to the first (1).

87. Caudal neural spines positioned over centrum (0), neural spines extend beyond own centrum (1).

88. Scapular spine low or broad (0), sharp and pronounced (1).

89. Coracoid width divided by length less than 60% (0), between 70 and 100% (1), greater than 100% (2).

90. Coracoid foramen enclosed within coracoid (0), open along coracoid- scapula suture (1).

91. Sternals crescent-shaped (0), hatchet-shaped (1).

92. Olecranon process on ulna low (0), moderately developed (1), relatively high (2).

93. Shaft of ulna triangular or oval in cross section (0), cylindrical (1).

94. Shaft of ulna straight (0), bowed (1).

95. Four phalanges in manual digit III (0), three phalanges (1).

96. Three phalanges in manual digit IV (0), two phalanges (1).

97. Three or more phalanges in manual digit V (0), two phalanges (1), one phalanx (2), none (3).

98. Unfused carpus (0), fused carpus (1).

99. Acetabulum high to normal (0), vertically short and long (1).

100. Ischiac peduncle of ilium not supported by sacral rib (0), ischiac peduncle articulates with sacral rib (1).

101. Shaft on ischium flat and blade-like (0), bar-like (1).

102. Distal end of ischium lacks an expanded foot (0), distal foot present (1).

103. Ischium obturator process absent (0), present (1).

104. Obturator process on ischium placed 60% or further down shaft (0), 50% (1), 40% (2), 30% or closer

105. Pubic peduncle of ischium larger than iliac peduncle (0), iliac peduncle of ischium as large or larger than pubic peduncle (1).

106. Anterior process of pubis absent (0), present (1).

107. Anterior process of pubis rod-like or sword-like in lateral view (0), anterior process dorsoventrally expanded (1)

108. Anterior process of pubis straight when present (0), upturned anterior process (1).

109. Femur lacks a neck-like constriction below the femoral head (0), constriction present (1).

110. Lesser trochanter of femur lower or equal to greater trochanter (0), higher than greater trochanter(1).

111. Lesser trochanter of femur anterior and medial of greater trochanter (0), anterior and somewhat lateral to lesser trochanter (1).

112. Greater trochanter of femur laterally convex (0), laterally flattened (1).

113. Anterior intercondylar groove on the distal end of femur absent (0), present (1).

114. Anterior intercondylar groove on the distal end of femur modestly developed (0), anterior intercondylar groove well-developed (1).

115. Lateral distal condyle width divided by medial distal condyle width on femur approximately 100% (0), 80-60% (1), 59-50% (2), 49-40% (3), 39-30% (4), 29-20% (5).

116. Both proximal lateral condyles on the tibia equal in size (0), fibular condyle smaller (1), only one lateral condyle present (2).

117. Cnemial crest of tibia rounded (0), sharply defined (1).

118. Midshaft of tibia triangular in cross-section (0), round in cross-section (1).

119. Fibula shaft elliptical or round in cross-section (0), D-shaped in cross-section (1).

120. Astragalus bears a short ascending process (0), triangular and tooth-like (1), spike-like (2), relatively large (3).

121. Posterior side of astragalus low (0), high (1).

122. Anterior side of astragalus high (0), moderate (1), low (2).

123. Angle between the tibial and fibular articular facets on the calcaneum greater than 120 degrees (0), less than 120 degrees (1).

124. Medial distal tarsal blocky in dorsal view (0), thin and rectangular (1), round (2).

125. Medial distal tarsal does not articulate over the proximal end of metatarsal II (0), medial distal tarsal articulates over a least a portion of the proximal end of metatarsal II (1).

126. Lateral distal tarsal square in dorsal view (0), kidney-shaped (1).

127. Four functional digits (i.e., bear phalanges) in the pes (0), three functional digits in the pes (1).

128. Premaxillae unfused (0), fused (1).

129. Angle formed by a line drawn along the ventral edge of the braincase (occipital condyle, basal tubera, and basipterygoid processes) and a line drawn through center of the trigeminal foramen and posterodorsal hypoglossal foramen: greater than fifteen degrees (0), less than fifteen degrees (1).

130. Ratio of femur length to tibia length: less than one (0), greater than one (1).

APPENDIX 6

CHARACTER DATA FOR CHAPTER 3

Character codings for the 23 terminal taxa included in the analysis shown in Figure 5.2B. Data for specimen-level terminals used to evaluate selection of the holotype of *Skaladromeus* and to evaluate the referral of additional specimens to this taxon are not shown. The terminal taxon *Skaladromeus* was scored from specimens UMNHVP 12665 and 19470. Modified from Boyd *et al*., (2009). Polymorphic codings represent conflicting character state observations between specimens referred to a single taxon. Abbreviations: ? = uncertainty; a = 0/1.

Taxon	1 0	2 0	3 0	4 0
Herrerasaurus	?00000??20	?020000000	?010202000	00?1101-0?
Heterodontosaurus	?00000??0?	000000?0?0	?000100?1	11??11?00?
Scutellosaurus	??????????	??????0000	??????00??	00?000000?
Lesothosaurus	000000000?	0000000000	0000000000	0000000100
Agilisaurus	?001?0????	?000000?00	0000101?0	01?000?10?
Hexinlusaurus	0000??????	??10000001	?00010???0	?1?000?10?
Othnielosaurus	??????????	??????0000	?00??0????	0100000010?
Oryctodromeus	001???1000	??????????	??????111?	010000???0
Zephyrosaurus	0?10001001	01?0??0101	0010?0101?	1100001?00
Orodromeus	0010001101	0100000101	1000?0111?	0100000000
Parksosaurus	001?01?010	1000000000	?01010???0	01?000110?
Hypsilophodon	000002002?	?000010?0	0000101000	1100111110
Gasparinisaura	1000?2???2?	?00011?000	??00??????	11?111?1??
Tenontosaurus	0000100?00	0011010??0	1010102?0	1111111110
Rhabdodon	?010?10000	1?????????	??????200?	11?1?11100
Dryosaurus	0120020100	?011000??0	1000102200	1111111111
Dysalotosaurus	1120020121	1011000???	?000102201	??????????
Camptosaurus	01?0120120	1111?00010	1011102201	1111111111
Iguanodon	1101120120	1010101?10	2111212201	1111111111
Ouranosaurus	110112002?	?010101010	1111212201	11?????1?1
Thescelosaurus	1?1a0a1?1?	00a00a0a0a	?0a0100210	110000?100
Skaladromeus	??????????	??????????	00?0?0????	?1????????
Koreanosaurus	??????????	??????????	??????????	??????????

Taxon	50	60	70	80
Herrerasaurus	20?00???02	----0-1??2	?00-000000	??????00??
Heterodontosaurus	00010??001	0001101100	0010000000	????0?0??00
Scutellosaurus	0?????????	0000000000	0?000?????	??????????
Lesothosaurus	00000??001	0000000000	0000000000	00??10????
Agilisaurus	01?01??110	1???0????0	???010?0??	??????1??1
Hexinlusaurus	01100???11	1?0???????0	1?0????00?	0??????00?1
Othnielosaurus	0???0???1?	1000000000	1?001????0	101???00?1
Oryctodromeus	0??001??1?	200????0?00	0?0????001	110??11121
Zephyrosaurus	0?1110000?	?000000000	1?1????001	110120000?
Orodromeus	0111000002	2000000000	1010110101	1101110001
Parksosaurus	01000???11	?000000000	011011??0?	000?0010?2
Hypsilophodon	01000??111	2011110010	111011?001	01?010?001
Gasparinisaura	11?00??1?1	3?????????	?01?110000	2?????????
Tenontosaurus	01000??111	2001111211	001111?121	20?0001112
Rhabdodon	0?????????	1001101210	1?11111??1	?000??01??
Dryosaurus	1000010001	2111111111	1011101001	2000011111
Dysalotosaurus	???0010101	2111111111	1011111001	2100211?1?
Camptosaurus	1100001111	3111111311	1111111000	2011000102
Iguanodon	1100021112	4111111311	1201111020	2000201123
Ouranosaurus	?010021112	3111????11	1100111120	00002?1123
Thescelosaurus	01100?00a2	20?0000110	01111a01a1	0??1?a1a?2
Skaladromeus	???1????1?	?000001100	??????????	?????10???
Koreanosaurus	??????????	??????????	??????????	??????00??

Taxon	9 0	1 0 0	1 1 0	1 2 0
Herrerasaurus	000?0000?0	?2000?3000	00??00--00	00?-000101
Heterodontosaurus	0??0000?1?	?20000100?	010-00-00?	100-0?0???
Scutellosaurus	1???0??010	?0?????0??	00??1???00	00100????0
Lesothosaurus	1???0?0?10	?000??2000	000-00-000	000-00???3
Agilisaurus	10?10??0?0	?0?0????11	0012010000	100-?????0
Hexinlusaurus	1??1??1?10	?0000?10??	0012010000	100-??0?01
Othnielosaurus	10010?1010	00?0?01001	0012010010	100-1?00?2
Oryctodromeus	3021?11110	?200????11	?????10010	111-?10012
Zephyrosaurus	??210?1110	?00?????1?	0???????10	11101?0010
Orodromeus	3021001110	011000?011	0011010010	110-100012
Parksosaurus	??01201010	01?0?????1	0010110110	110-0?0000
Hypsilophodon	2011211011	0101002001	0010010010	100-210001
Gasparinisaura	2011101010	???0????11	0?12110011	110-120100
Tenontosaurus	2101101010	00011??011	0112111110	1011320100
Rhabdodon	21210?1000	?101????11	110-1???10	1011220?0
Dryosaurus	2102001001	0100???111	1113011111	1011310?3
Dysalotosaurus	2?12011001	0101??????	1113011111	10113????3
Camptosaurus	2201?11011	0101101111	1113111110	1011?20100
Iguanodon	2211011021	12?0110111	1113111110	1011521100
Ouranosaurus	22?0??1021	1210???111	0113111100	1011421100
Thescelosaurus	300?111000	000?001001	0012a10110	11102?0000
Skaladromeus	??????????	??????????	????????1?	11??????1?
Koreanosaurus	?0?????100	010???????	????????10	110-1?011?

Taxon	130
Herrerasaurus	0???0000?1
Heterodontosaurus	???0000000
Scutellosaurus	??????00?0
Lesothosaurus	?0010?0000
Agilisaurus	????0?00?0
Hexinlusaurus	???11?0??0
Othnielosaurus	1011110?0
Oryctodromeus	0??????1?0
Zephyrosaurus	0201100100
Orodromeus	00011000?0
Parksosaurus	0011100??0
Hypsilophodon	0011110000
Gasparinisaura	0212110?0
Tenontosaurus	0211100001
Rhabdodon	12?20110??
Dryosaurus	1011111000
Dysalotosaurus	1?1?0?1000
Camptosaurus	120?0?1011
Iguanodon	1202011011
Ouranosaurus	1212??1001
Thescelosaurus	00?11?0011
Skaladromeus	??????????
Koreanosaurus	?????????0

APPENDIX 7

PHYLOGENETIC DEFINITIONS USED IN CHAPTER 5

Clade Name	Phylogenetic Definition	Diagnosis Type	Original Author	Definition Used
Ankylopollexia	*Camptosaurus dispar* (Marsh 1879), *Parasaurolophus walkeri* Parks 1922, their most recent common ancestor and all descendents.	Node	Sereno, 1986	Sereno, 2005
Cerapoda	*Parasaurolophus walkeri* Parks 1922, *Triceratops horrid us* Marsh 1889, their most recent common ancestor and all descendents.	Node	Sereno, 1986	Butler et al., 2008a
Dinosauria	*Triceratops horrid us* Marsh 1889, *Passer domestics* (Linnaeus 1758), their most recent common ancestor and all descendents.	Node	Owen, 1942	Butler et al., 2008a
Dryomorpha	*Dryosaurus altus (Marsh 1878), Parasaurolophus walkeri* Parks 1922, their most recent common ancestor and all descendents.	Node	Sereno, 1986	This Study
Dryosauridae	All iguanodontians more closely related to *Dryosaurus altus* (Marsh 1878) than to *Parasaurolophus walkeri* Parks 1922.	Stem	Milner and Norman, 1984	Sereno, 2005
Elasmaria	*Talenkauen santacrucensis* Novas, Cambia so, and Ambrosia 2004 and *Macrogryphosaurus gondwanicus* Calvo, Porphyry, and Novas 2007, their most recent common ancestor and all descendents.	Node	Calvo et al., 2007	Calvo et al., 2007
Euiguanodontia	*Gasparinisaura cincosaltensis* Coria and Salgado 1996, Dryosauridae Milner and Norman 1984, Ankylopollexia Sereno 1986, their most recent common ancestor and all descendents.	Node	Coria and Salgado, 1996	Coria and Salgado, 1996
Euornithopoda	All ornithischians more closely related to *Parasaurolophus walkeri* Parks 1922 than to *Heterodontosaurus tucki* Crompton and Charig 1962, *Pachycephalosaurus wyomingensis* (Gilmore 1931), *Triceratops horridus* Marsh 1889, or *Ankylosaurus marginventris* Brown 1908.	Stem	Sereno, 1986	Sereno, 2005
Genasauria	*Ankylosaurus magniventris* Brown 1908, *Stegosaurus stenops* Marsh 1877a , *Parasaurolophus walkeri* Parks 1922, *Triceratops horridus* Marsh 1889, *Pachycephalosaurus wyomingensis* (Gilmore 1931), their most recent common ancestor and all descendents.	Node	Sereno, 1986	Butler et al., 2008a
Heterodontosauridae	All ornithischians more closely related to *Heterodontosaurus tucki* Crompton and Charig 1962 than to *Parasaurolophus walkeri* Parks 1922, *Pachycephalosaurus wyomingensis* (Gilmore 1931), *Triceratops horridus* Marsh 1889, or *Ankylosaurus marginventris* Brown 1908.	Stem	Romer, 1966	Sereno, 2005

Clade Name	Phylogenetic Definition	Diagnosis Type	Original Author	Definition Used
Hypsilophodontidae	All neornithischians more closely related to *Hypsilophodon foxii* Huxley 1869 than to *Parasaurolophus walkeri* Parks 1922.	Stem	Dollo, 1882	Sereno, 2005
Iguanodontia	All ornithopods more closely related to *Parasaurolophus walkeri* Parks 1922 than to *Hypsilophodon foxii* Huxley 1869 or *Thescelosaurus neglectus* Gilmore 1913.	Stem	Dollo, 1888	Sereno, 2005
Marginocephalia	*Triceratops horridus* Marsh 1889, *Pachycephalosaurus wyomingensis* (Gilmore 1931), their most recent common ancestor and all descendents.	Node	Sereno, 1986	Butler et al., 2008a
Neornithischia	All genasaurians more closely related to *Parasaurolophus walkeri* Parks 1922 than to *Ankylosaurus magniventris* Brown 1908 or *Stegosaurus stenops* Marsh 1877a.	Stem	Cooper, 1985	Butler et al., 2008a
Ornithischia	All dinosaurs more closely related to *Triceratops horridus* Marsh 1889 than to either *Passer domesticus* (Linnaeus 1758), or *Saltasaurus loricatus* Bonaparte and Powell 1980.	Stem	Seeley, 1887	Butler et al., 2008a
Ornithopoda	All genasaurians more closely related to *Parasaurolophus walkeri* Parks 1922, than to *Triceratops horridus* Marsh 1889.	Stem	Marsh, 1881	Butler et al., 2008a
Orodrominae	All neornithischians more closely related to *Orodromeus makelai* Horner and Weishampel 1988 than to *Thescelosaurus neglectus* Gilmore 1913 or *Parasaurolophus walkeri* Parks 1922.	Stem	This Study	This Study
Parksosauridae	All neornithischians more closely related to *Parksosaurus warreni* (Parks 1926) than to *Hypsilophodon foxii* Huxley 1869, *Dryosaurus altus* (Marsh 1878), or *Parasaurolophus walkeri* Parks 1922.	Stem	Buchholz, 2002	This Study
Rhabdodontidae	All iguanodontians more closely related to *Rhabdodon priscus* Matheron 1869 than to *Parasaurolophus walkeri* Parks 1922.	Stem	Weishampel et al., 2003	Sereno, 2005
Saurischia	All dinosaurs more closely related to *Passer domesticus* (Linnaeus 1758) than to *Triceratops horridus* Marsh 1889.	Stem	Seeley, 1887	Butler et al., 2008a
Thescelosaurinae	All neornithischians more closely related to *Thescelosaurus neglectus* Gilmore 1913 than to *Orodromeus makelai* Horner and Weishampel 1988 or *Parasaurolophus walkeri* Parks 1922.	Stem	Sternberg, 1937	This Study
Thyreophora	All genasaurians more closely related to *Ankylosaurus magniventris* Brown 1908 than to *Parasaurolophus walkeri* Parks 1922, *Triceratops horridus* Marsh 1889, or *Pachycephalosaurus wyomingensis* (Gilmore 1931).	Stem	Nopcsa, 1915	Butler et al., 2008a

APPENDIX 8

CHARACTER CITATIONS FOR CHAPTER 5

Citations for each character and descriptions of how each character was modified. Abbreviations: B = Butler (2005); Bea = Butler et al. (2008a); M = McDonald et al. (2010); N =Nesbitt et al. (2010); S = Scheetz (1999); W = Weishampel et al. (2003); WH = Weishampel and Heinrich (1992); X = Xu et al. (2006).

#	Citation	Details of Modifications
1	W(1)	
2	B(32)	
3	X(3)	
4	W(7)	
5	WH(1); S(28); W(6)	States of Scheetz (1999) used.
6	B(13)	
7	B(2)	
8	B(4)	
9	B(5)	Modified state 1.
10	B(14)	
11	B(31)	
12	New	New character based on personal observations
13	B(11)	
14	S(29)	
15	WH(3)	
16	WH(4); S(30); W(8); B(12)	The states of Weishampel and Heinrich (1992) were reversed to match those of the other analyses.
17	WH(5); S(40); W(9)	Scheetz (1999) uses different terminology, but describes the same character states.
18	B(10)	
19	B(17)	
20	NEW	New character based on comments in Irmis et al. (2007).
21	B(18)	
22	Bea(13)	
23	B(22)	Added state 2.
24	B(23)	
25	WH(9); B(24)	Butler (2005) set the cutoff at 70%, while Weishampel and Heinrich (1992) set it at 80%. The former convention was followed.

#	Citation	Details of Modifications
26	S(43)	
27	S(45)	
28	S(48)	
29	S(50)	
30	WH(8); S(42); W(5); B(19)	Butler (2005) used different terminology, but describes same character states.
31	WH(11)	
32	B(21)	
33	WH(14); W(11)	States of Weishampel and Heinrich (1992) used, while those of Weishampel et al. (2003) were reversed.
34	S(49)	
35	W(10)	
36	S(14)	
37	S(6); W(16)	The states of Weishampel et al. (2003) were used. States of Scheetz (1999) were transformed as follows: 0 = 0; 1 and 2 = 1.
38	WH(10); S(44); B(20)	The states of Weishampel and Heinrich (1992) were reversed and state 1 was added.
39	S(46)	
40	S(47)	
41	S(16); W(17); B(25)	
42	WH(15); B(26)	The states of Butler (2005) were used.
43	S(15)	
44	S(3); W(15)	New states defined for this character.
45	S(4)	
46	New	New character based on personal observations.
47	S(13)	State 2 was added.
48	S(1)	
49	S(9)	States 1 and 2 were combined into state 1.
50	S(11)	

#	Citation	Details of Modifications
51	S(2)	
52	S(7)	
53	S(8)	
54	S(5)	
55	S(10)	
56	S(12)	
57	W(13); B(30)	
58	B(29)	
59	S(20)	
60	S(18)	
61	S(19)	
62	S(21)	State 2 was added.
63	S(24)	
64	S(26)	
65	S(23)	
66	WH(12); S(22); W(12); B(28)	The states from Scheetz (1999) were discarded due to incompatibility.
67	S(25)	
68	B(33)	Modified the definitions of the states.
69	W(18)	
70	WH(17); W(19)	
71	B(34)	
72	WH(18); S(64); W(20)	
73	B(35)	
74	S(51)	Redefined states, reduced from 5 states to 4 states, then added a new fifth state.
75	WH(19); W(21)	

#	Citation	Details of Modifications
76	S(61)	
77	S(63)	Edited state definitions.
78	B(36)	
79	B(37)	
80	B(38)	
81	W(23)	
82	W(22)	States modified to account for different shapes.
83	S(62)	
84	S(67)	
85	S(66)	
86	Bea(106)	
87	B(27)	State 2 was added.
88	WH(2)	
89	W(2)	
90	New	New character added based on personal observations.
91	B(16)	
92	New	New character added based on personal observations.
93	WH(6)	
94	WH(7); W(3); B(15)	Followed the states of Butler (2005) by adding a state 2.
95	W(4)	
96	WH(13)	
97	S(65); B(39)	States 0 and 1 of Butler (2005) were combined to match those of Scheetz (1999).
98	WH(16)	
99	S(73)	
100	S(17)	

#	Citation	Details of Modifications
101	S(68)	
102	S(69); W(14)	State 1 was added.
103	New	New character added based on personal observations.
104	New	New character added based on personal observations.
105	S(70)	
106	S(72)	
107	S(74)	
108	S(71)	
109	S(75)	
110	S(76)	
111	WH(20)	
112	S(27); W(24); B(1)	The states of Butler (2005) were used and state 2 was modified.
113	New	New character added based on personal observations.
114	WH(21); S(56); W(33)	The states of Scheetz (1999) were discarded, state 1 of Weishampel and Heinrich (1992) and Weishampel et al. (2003) was modified.
115	WH(23); S(38)	Used the states of Scheetz (1999).
116	B(3)	
117	S(31)	States were expanded to be more detailed.
118	WH(25); S(52)	
119	S(33)	
120	S(35)	
121	S(36)	
122	S(37)	State 2 was added.
123	S(39,55); W(29, 35); B(7)	
124	S(54)	
125	S(41)	State 2 was added.

#	Citation	Details of Modifications
126	W(25); B(8)	The states were incongruent, so new states were defined for this character.
127	W(27)	
128	W(28)	
129	S(34)	
130	WH(24); S(57)	The states from Weishampel and Heinrich (1992) were used.
131	S(32)	
132	WH(22); W(26)	
133	W(31)	
134	B(6)	
135	S(59)	
136	S(60)	State 2 was added.
137	W(30)	
138	W(32)	
139	W(34)	
140	B(9)	
141	W(36)	
142	S(77)	
143	New	New character added based on personal observations.
144	New	New character added based on personal observations.
145	B(40)	
146	S(78)	
147	S(80); W(37); B(42)	States 0 and 1 of Scheetz (1999) were combined into state 0 and states 2 and 3 of Scheetz (1999) were combined into state 1. States 0 and 2 of Butler (2005) were combined into state 0.
148	S(81); W(38); B(43)	Used the states of Butler (2005) and added state 4 based on Varricchio et al. (2007).
149	S(82)	
150	S(83)	

#	Citation	Details of Modifications
151	W(39)	
152	S(88)	
153	S(85)	
154	S(87)	
155	B(41)	
156	S(79)	
157	WH(26); W(40); B(44)	
158	S(89)	
159	W(43); B(46)	Used the states of Weishampel et al. (2003).
160	S(90)	
161	S(91)	
162	W(44)	
163	New	New character added based on personal observations.
164	S(92)	State 2 was added.
165	WH(28); W(45); B(45)	The states of Butler (2005) were discarded.
166	B(47)	
167	WH(29)	
168	W(46)	State 2 from Novas et al., 2004 was added.
169	S(93)	
170	S(94)	
171	S(95)	
172	W(47)	
173	S(97); W(49)	
174	W(50)	
175	W(48)	States modified.

#	Citation	Details of Modifications
176	W(51)	State 2 was added.
177	W(52)	
178	W(54)	
179	WH(30); W(53)	
180	S(96) IN PAMT	States modified and split between two characters.
181	S(96) IN PAMT	States modified and split between two characters.
182	S(98)	
183	B(52)	
184	W(57); B(53)	
185	W(55)	
186	W(56)	
187	B(48)	
188	B(51)	
189	B(50)	
190	S(99)	
191	B(54)	
192	B(49)	
193	S(84)	
194	B(58)	State 1 was added.
195	WH(33); S(105)	Used the states of Weishampel and Heinrich (1992) and added state 2.
196	WH(32)	
197	WH(31); S(104); W(63); B(60)	Used the states of Weishampel et al. (2003) and added state 2 of Butler (2005) as state 3.
198	B(59)	
199	N(219)	State 0 was removed.
200	S(103)	

#	Citation	Details of Modifications
201	WH(34); W(60)	State 2 was added.
202	B(57)	
203	W(58); B(55)	
204	WH(35); S(102); W(59)	Used approximately the states of Weishampel and Heinrich (1992), but modified their definitions slightly.
205	S(100); W(61)	
206	B(56)	
207	S(101); W(62)	
208	W(64)	
209	W(65)	
210	WH(36)	
211	S(106)	
212	B(61)	
213	S(109)	
214	W(67); B(64)	
215	S(107)	
216	S(108)	
217	B(63)	
218	B(65)	
219	W(68)	Redefined states to take the full range of morphological variation in account.
220	M(125)	
221	W(69); B(62)	
222	WH(37); S(110); W(70)	States 1 and 2 of Scheetz (1999) were combined to form state 1.
223	M(127)	
224	W(71)	
225	N(244)	

#	Citation	Details of Modifications
226	W(66); B(66)	
227	S(115)	
228	S(113)	State 3 was added.
229	B(67)	State 3 was added.
230	N(248)	
231	S(114)	
232	S(111)	
233	S(116)	
234	S(117)	
235	S(118)	
236	S(119)	
237	N(279)	
238	S(120)	
239	New	States modified and split between two characters.
240	S(121)	
241	S(122)	
242	S(123)	
243	B(69)	States 0 and 1 were combined into state 0.
244	W(74)	
245	W(73); B(68)	Constructed new states by combining the states of both prior analyses.
246	N(295)	
247	S(124)	
248	W(72)	
249	W(75)	
250	WH(27); S(86); W(41); B(70)	For Scheetz (1999) state 2 = 1.
251	B(71)	
252	W(42)	
253	B(72)	
254	B(73)	
255	V(125)	

APPENDIX 9

MORHPOLOGICAL CHARACTERS FOR CHAPTER 5

Description of characters used in the phylogenetic analysis of basal ornithischian relationships.

1. Preorbital skull length less than or equal to 50% total skull length (0), greater than 50% (1).

2. Premaxillary bone absent (0), present (1).

3. Rostral bone absent (0), present (1).

4. Oral margin of the premaxilla smooth (0), denticulate (1).

5. Lateral surface of the oral margins of the premaxillae flat (0), everted (1).

6. Ventral margin of the premaxilla level with the maxillary tooth row (0), ventrally deflected (1).

7. Anterior-most premaxillary tooth positioned at the anterior margin of the premaxilla (0), inset at least the width of one tooth crown (1).

8. Diastema between premaxilla and maxilla absent (0), present (1).

9. Diastema between premaxilla and maxilla flat (0), arched (1).

10. Anterior premaxillary foramen absent (0), present (1).

11. Premaxillary border of internal nares present (0), absent (1).

12. Anterodorsal surface of the premaxilla smooth (0), highly rugose (1).

13. Premaxillary posterolateral process does not exclude maxilla from nasal margin (0), does exclude maxilla from nasal margin (1).

14. Concavity within the posterior end of the premaxilla, near lateral margin, for receipt of the anterolateral boss of the maxilla absent (0), present (1).

15. Overlap of the dorsal process of the premaxilla onto the rostral process of the nasal absent (0), present (1).

16. Contact between premaxilla and lacrimal absent (0), present (1).

17. Premaxillary sulcus on the anterior process of the maxilla absent (0), present (1).

18. 'Special foramina' medial to dentary and maxillary tooth rows absent (0), present (1).

19. Buccal emargination on the maxilla absent (0), present (1).

20. Buccal emargination of maxilla consists of a gradual and shallow beveling of the ventrolateral surface of the maxilla (0), consists of a prominent ridge on the lateral surface of the maxilla (1).

21. Notch in maxilla for the lacrimal absent (0), present (1).

22. Fossa situated low along the boundary between the premaxilla and the maxilla absent (0), present (1).

23. Supraorbital absent (0), one supraorbital present (1), two or more supraorbitals present (2).

24. Supraorbital free and projects into orbit from contact with lacrimal and prefrontal (0), supraorbital incorporated into the orbital margin (1).

25. Supraorbital(s) extend across at least 71% of the maximum anteroposterior length of the orbit (0), 70% or less (1).

26. Greatest posterior expanse of the jugal greater than 25% height of skull (0), less than 25% (1).

27. Anterior process of the jugal straight (0), curved (1).

28. Anterior process of jugal situated dorsal to the maxilla (0), anterior process of jugal inserts into the maxilla (1).

29. Jugal barely contacts lacrimal (0), jugal touches lacrimal with more contact (1), butt joint between jugal and lacrimal (2).

30. Jugal contributes to the antorbital fenestra (0), does not reach antorbital fenestra (1).

31. Contact between jugal and postorbital faces anteriorly (0), contact faces partially laterally (1), postorbital inserts into a socket in the jugal (2).

32. Jugal dorsoventrally deeper than mediolaterally broad (0), broader than deep (1).

33. Jugal forms part of the posterior margin the infratemporal fenestra (0), only forms the ventral margin (1).

34. The anteroventral corner of the infratemporal fenestra, formed by the jugal, consists of an oblique or right angle (0), anteroventral corner of the infratemporal fenestra consists of an acute angle (1).

35. Contact between the jugal and quadratojugal consists of a butt or high angle scarf joint (0), the jugal overlaps the lateral surface of the quadratojugal posterodorsally and the medial surface posteroventrally (1).

36. Jugal does not contact quadrate (0), jugal does contact quadrate (1).

37. Jugal or quadratojugal contacts the quadrate near or slightly above the distal end (0), contacts positioned well above the distal end (1).

38. No boss or ornamentation present on lateral surface of the jugal (0), lateral surface of jugal ornamented, but no boss present (1), presence of a low boss on the lateral surface of the jugal (2), presence of a tall, posteriorly projecting boss on the lateral surface of the jugal (3).

39. Maxillary process on the medial side of the jugal is medially projected and modestly arched (0), maxillary process on the medial side of the jugal is straight and grooved (1), maxillary process on the medial side of the jugal is anteromedially projected and arched (2).

40. Ectopterygoid facet on the medial surface of the jugal consists of an abbreviated, deep groove (0), ectopterygoid facet consists of a rounded scar (1).

41. Quadratojugal foramen absent (0), present (1).

42. Dorsal process of the quadratojugal contacts the descending process of the squamosal (0), dorsal process of the quadratojugal does not contact the descending process of the squamosal (1).

43. Quadratojugal anteroposteriorly long and dorsoventrally short (0), quadratojugal anteroposteriorly short and dorsoventrally tall (1).

44. Quadratojugal contacts the quadrate along greater than 50% the total length of the quadrate (0), quadratojugal contacts the quadrate along less than 50% the total length of quadrate (1).

45. Proximal head of the quadrate recurved posteriorly (0), proximal head of quadrate straight (1).

46. Ventral portion of the quadrate shaft oriented vertically or anteroventrally angled (0), ventral portion of the quadrate shaft posteroventrally angled (1).

47. Body of the quadrate leans posteriorly (0), body of quadrate oriented vertically (1), body of quadrate leans anteriorly (2).

48. Jugal wing of the quadrate moderately developed (0), jugal wing of the quadrate shortened (1).

49. Ventral extent of the jugal wing of the quadrate positioned at or near the distal end of the quadrate (0), ventral extent of the jugal wing of the quadrate positioned above the distal end of the quadrate (1).

50. Pit in lateral side of quadrate at the base of the jugal wing present (0), absent (1).

51. Quadrate notch (tiny foramen between jugal wing of quadrate and quadratojugal) absent (0), present (1).

52. Distal condyles of the quadrate dorsomedially sloped or horizontally oriented (0), distal condyles of the quadrate dorsolaterally sloped (1).

53. The pterygoid wing of the quadrate arises at the dorsal head of the quadrate (0), pterygoid wing of the quadrate arises below the dorsal head of the quadrate (1).

54. Pterygoid wing of quadrate consists of a large, anteromedially extending fan of bone (0), pterygoid wing of the quadrate small (1).

55. Groove on the base of the posterior side of the pterygoid wing of the quadrate absent (0), present (1).

56. Length of ventral process of the squamosal less than 30% the total length of the quadrate (0), length of the ventral process of the squamosal greater than 30% the total length of the quadrate (1).

57. Paroccipital process oriented horizontally and slightly widened distally (0), distal end of paroccipital process ‘pendant-shaped ‘(1).

58. Parietosquamosal shelf absent (0), present (1).

59. Orbital edge of postorbital forms a smooth, continuous arc (0), orbital edge of postorbital possesses an anteriorly directed inflation into orbit (1).

60. Orbital margin of postorbital smooth (0), orbital margin striated and rugose (1).

61. Postorbital non-robust (0), postorbital robust (1).

62. Synovial socket for the head of the laterosphenoid positioned along the frontal-postorbital contact (0), synovial socket for the head of the laterosphenoid positioned only in the postorbital (1), synovial socket for the head of the laterosphenoid positioned only in the frontal (2), no synovial joint for the laterosphenoid present (3).

63. Greater than 25% of the frontal length participates in the orbital margin (0), less than 25% of the frontal length participates in the orbital margin.

64. Frontals extend over the entire orbit (0), frontals positioned only over the posterior half of orbit (1).

65. Frontals arched over orbit (0), frontals dorsally flattened (1).

66. Combined width of frontals greater than the total length of the frontals (0), combined width of the frontals less than the total length of the frontals (1).

67. Total length of frontals between 120% and 60% the total length of the nasals (0), total length of frontal less than 60% the total length of the nasals (1).

68. Length of the oral margin of the predentary less than the length of the oral margin of the premaxilla (0), length of the oral margin of the predentary equal to or greater than the length of the oral margin of the premaxilla (1).

69. Anterior tip of predentary pointed (0), anterior tip rounded (1).

70. Oral margin of the predentary smooth (0), oral margin denticulate (1).

71. Ventral process of the predentary present (0), ventral process of the predentary very reduced or absent (1).

72. One ventral process of the predentary (0), two ventral processes of the predentary (1).

73. Dentary symphysis ‘v-shaped’ (0), dentary symphysis ‘spout-shaped’ (1).

74. Anterior-most tip of dentary positioned within the dorsal 1/3 of the dentary (0), anterior-most tip positioned near mid-height of the dentary (1), anterior-most tip positioned within the lower 1/3 of the dentary (2), anterior-most tip curves ventrally below ventral margin of the dentary (3), anterior-most tip anterodorsally curved and positioned higher than the base of the dentary tooth row (4).

75. Dorsal and ventral margins of the dentary converge rostrally (0), dorsal and ventral margins of the dentary parallel (1).

76. Medial surface of the dentary straight (0), medial surface of the dentary medially arched (1).

77. Dentary depth just anterior to the rising coronoid process 20% or less the total length of the dentary (0), dentary depth 21% or more the total length of the dentary (1).

78. Dentary tooth row straight in lateral view (0), dentary tooth row sinuous in lateral view (1).

79. Coronoid process absent or weakly developed (0), coronoid process present (1).

80. Dentary does not contribute to the coronoid process (0), dentary does contribute to the coronoid process (1).

81. The posterior end of tooth row ends anterior to coronoid process (0), the posterior end of tooth the row is shrouded by the coronoid process in lateral view (1).

82. Coronoid process inconspicuous (0), coronoid process subtriangular (1), coronoid process subrectangular (2), coronoid process dorsally elongated with a lobe-shaped distal expansion (3).

83. The length of the mandible posterior to the coronoid process is 36% or greater the total length of mandible (0), the post-coronoid length of the mandible is between 25 and 35% the total length of the mandible (1), the post-coronoid length of the mandible is less than 25% the total length of the mandible (2).

84. Dorsal margin of the surangular convex or diagonal (0), dorsal margin of the surangular concave (1).

85. Surangular foramen absent (0), present (1).

86. Ridge or process on lateral surface of surangular, anterior to the jaw suture absent (0), a strong, anteroposteriorly extending ridge present (1), a dorsally directed, finger-like process present (2).

87. Distal condyles of the quadrate subequal (0), medial distal condyle larger (1), lateral distal condyle larger (2).

88. Maximum length of external nares less than 15% basal skull length (0), maximum length of external nares greater than 15% basal skull length (1).

89. External nares positioned close to the buccal margin and below the level of the orbit (0), external nares positioned higher than the maxilla (1).

90. Antorbital fenestra present (0), absent (1).

91. Antorbital fossa rounds smoothly onto maxilla along some part of its margin (0), antorbital fossa sharply defined or extended as a secondary lateral wall enclosing the fossa (1).

92. Maxillary fenestra absent (0), present (1).

93. Antorbital fossa triangular (0), antorbital fossa ovate or circular (1).

94. External opening of the antorbital fossa present and greater than 10% basal skull length (0), external opening of the antorbital fossa present and less than 10% basal skull length (1), external opening of the antorbital fossa absent (2).

95. Lower margin of the orbit circular (0), lower margin of the orbit subrectangular (1).

96. Ventral edge of the infratemporal fenestra extends to or below the ventral margin of the orbit (0), ventral edge of the infratemporal fenestra positioned well above the ventral margin of the orbit (1).

97. External mandibular fenestra present (0), absent (1).

98. Angle between the base and long axis of the braincase greater than 35 degrees (0), angle less than 35 degrees (1).

99. Median ridge on floor of the braincase absent (0), present (1).

100. Basioccipital and exoccipital contribute to the occipital condyle (0), exoccipital excluded from occipital condyle (1).

101. Nuchal crest on the supraoccipital absent (0), present (1).

102. Supraoccipital contributes to greater than 5% of the margin of the foramen magnum (0), supraoccipital contributes to less than 5% of the margin of the foramen magnum (1), supraoccipital excluded from the margin of the foramen magnum (2).

103. Posttemporal foramen positioned at the boundary between the parietals and the paroccipital process (0), posttemporal foramen positioned entirely within the opisthotic (1), posttemporal foramen positioned entirely within the squamosal (2).

104. Posttemporal foramen consists of an enclosed foramen (0), posttemporal foramen consists of a dorsally open groove (1).

105. Ventral keel on basioccipital absent (0), present (1).

106. Floor of basioccipital flat (0), arched (1).

107. Basioccipital tubera lower than basisphenoid (0), basioccipital tubera level with basisphenoid (1).

108. Foramen magnum occupies over 30% of the dorsal margin of the occipital condyle (0), foramen magnum occupies between 30 and 20% of the dorsal margin of the occipital condyle (1), foramen magnum occupies less than 20% of the dorsal margin of the occipital condyle (2).

109. Length of basisphenoid (from base of the parasphenoid process to the posterior edge of the basisphenoid) less than the length of basioccipital (0), basisphenoid and basioccipital subequal in length (1), length of basisphenoid greater than the length of the basioccipital (2).

110. Foramen for cranial nerve V notches anteroventral edge of prootic (0), foramen for cranial nerve V completely enclosed within the prootic (1).

111. Premaxillary teeth present (0), absent (1).

112. Six teeth present in each premaxilla (0), between four and five teeth present in each premaxilla (1), one or less teeth present in each premaxilla (2).

113. Enlarged anterior canine tooth in dentary absent (0), present (1).

114. Ridges absent on dentary teeth, only simple denticles present (0), at least some denticles confluent with ridges that extend to base of crown on dentary teeth (1).

115. Apex of the maxillary teeth centrally placed (0), apex of maxillary teeth placed posterior of center (1).

116. Premaxillary teeth recurved, transversely flattened, constricted at the base (0), premaxillary teeth straight, subcylindrical, and unconstructed at the base. (1).

117. Space present between the roots and crowns of adjacent maxillary teeth (0), lack of space between crowns of adjacent maxillary teeth up through the occlusional margin (1), lack of space between roots and crowns of adjacent maxillary teeth (2), no space between crowns within each tooth position within the maxilla (3).

118. Apical ridge on the dentary teeth placed centrally or anterior of center (0), apical ridge of the dentary teeth placed posterior of center (1).

119. Maxillary tooth roots straight in anterior or posterior view (0), maxillary tooth roots curved in anterior or posterior view (1).

120. Distinct neck present below the crown of the maxillary teeth (0), maxillary crown tapers to root (1).

121. Maxillary teeth independently occlude (0), maxillary teeth share a continuous occlusional surface (1).

122. Lingual surface of maxillary teeth concave (0), lingual surface convex (1), lingual surface flat (2).

123. Distribution of enamel on maxillary and dentary teeth roughly equal on both sides (0), enamel primarily restricted to one side on maxillary and dentary teeth (1).

124. Ridges present on both sides of dentary crowns (0), ridges limited to one side of dentary crowns (1).

125. Maxillary crowns low and spade-like, rectangular, or triangular (0), maxillary crowns high and diamond-shaped (1), maxillary crowns laterally flattened and posteriorly recurved (2), maxillary crowns conical (3).

126. Twelve or less teeth present in each maxilla (0), between thirteen and nineteen teeth present in each maxilla (1), twenty or more teeth present in each maxilla (2).

127. Maxillary teeth possess a smooth face with simple denticles (0), maxillary teeth possess ridges confluent with denticles that extend to base of crown (1).

128. All ridges on maxillary teeth equally prominent (0), one ridge on maxillary teeth more prominent than the rest (1).

129. Cingulum on maxillary teeth present (0), cingulum on maxillary teeth absent (1).

130. Cingulum on dentary teeth absent (0), cingulum on dentary teeth present (1).

131. Maxillary teeth positioned near the lateral margin (0), maxillary teeth inset medially (1).

132. Maxillary crown height less than 50% length (0), maxillary crown height between 50 and 90% crown length (1), maxillary crown height subequal to the crown length (2), maxillary crown height between 110 and 150% crown length (3), maxillary crown height greater than 150% crown length (4).

133. Dentary crowns less than 50% higher than mesiodistally wide (0), dentary crowns greater than 50% higher than mesiodistally wide (1).

134. Denticles extend beyond apical third of maxillary and dentary tooth crowns (0), denticles restricted to apical third of maxillary and dentary tooth crowns (1).

135. Dentary tooth roots straight in anterior or posterior view (0), dentary tooth roots curved in anterior or posterior view (1).

136. Dentary crowns rectangular, triangular, or leaf-shaped (0), dentary teeth lozenge-shaped (1), dentary teeth laterally flattened, posteriorly recurved (2), dentary teeth conical (3).

137. Thirteen or less dentary teeth present (0), between fourteen and seventeen dentary teeth present (1), eighteen or more dentary teeth present (2).

138. Fewer than ten ridges present on dentary teeth (0), ten or more ridges present on dentary teeth (1).

139. All ridges on the dentary teeth equally prominent (0), one ridge more prominent than the rest on the dentary teeth (1).

140. Anterior two dentary teeth similar in morphology to more posterior dentary teeth (0), anterior two dentary teeth lack denticles, first tooth strongly reduced (1).

141. Less than ten cervical vertebrae (0), ten or more cervical vertebrae (1).

142. Cervical vertebrae plateocoelous or amphicoelous (0), opisthocoelous (1).

143. Ventral surface of the cervical vertebrae rounded (0), presence of a broad, flattened keel on the ventral surface of the cervical vertebrae (1), presence of a sharp ventral keel on the ventral surface of the cervical vertebrae (2).

144. Anterior cervical centra less than 1.5 times longer than tall (0), length of anterior cervical centra equal or greater than 1.5 times longer than tall (1).

145. Epipophyses on anterior cervical three present (0), absent (1).

146. Dorsal neural spines arise anteriorly or are centered over centrum (0), dorsal neural spines posteriorly positioned on centrum (1).

147. Fourteen or less dorsal vertebrae present (0), fifteen dorsal vertebrae present (1), sixteen dorsal vertebrae present (2), seventeen or more dorsal vertebrae present (3).

148. Sacrum composed of three or fewer fused vertebral centra (0), sacrum composed of between four and five fused vertebral centra (1), sacrum composed of six fused vertebral centra (2), sacrum composed of seven or more fused vertebra centra (3).

149. Sacral neural spines less than twice the height of the sacral centra (0), sacral neural spines between 2 and 2.5 times the height of the sacral centra (1), sacral neural spines greater than 2.5 times the height of the sacral centra (2).

150. Sacral neural spines lean posteriorly (0), sacral neural spines lean anteriorly (1).

151. Height of neural spine on proximal caudal vertebrae less than 1.5 times taller than the height of the centrum (0), height of neural spine greater than 1.5 times taller than the height of the centrum (1).

152. Caudal neural spines positioned entirely over their respective caudal centra (0), caudal neural spines extend beyond their own centrum (1).

153. Caudal ribs positioned entirely on caudal centra (0), caudal ribs positioned along neurocentral suture (1), caudal ribs positioned on neural arch (2).

154. First caudal vertebra bears the longest caudal rib (0), longest caudal rib positioned posterior to first caudal vertebra (1).

155. Axial epiphyses present at least vestigally (0), axial epiphyses absent (1).

156. Transition from tuberculum and capitulum of dorsal ribs from vertical to near horizontal occurs between dorsal vertebrae 2 and 4 (0), transition occurs between dorsal vertebrae 5 and 6 (1), transition occurs between dorsal vertebrae 6 and 8 (2).

157. Partial ossification of the sternal segments of the cranial dorsal ribs absent (0), present (1).

158. Scapular spine on the anterodorsal corner of the scapula low or broad (0), scapular spine sharp and pronounced (1).

159. Minimum thickness of scapular neck less than 20% maximum length of the scapula (0), minimum width of neck greater than 20% maximum length of the scapula (1).

160. Width of coracoid less than 60% the length of the coracoid (0), width of coracoids between 61-100% the length of the coracoid (1), width of the coracoid greater than the length of the coracoid (2).

161. Coracoid foramen enclosed within the coracoids (0), coracoid foramen open along coracoid-scapula articular contact surface (1).

162. Length of sternal process of the coracoids [measured from the tip of the sternal process of the coracoid to the base of the coracoid notch]less than 70% the width of the sternal process [measured at the level of the base of the coracoids notch] (0), length of sternal process greater than 70% the width of the sternal process (1).

163. Ovoid fossa positioned anteroventral to the glenoid fossa on the coracoid absent (0), present (1).

164. Sternal plates crescent-shaped (0), sterna plates hatchet-shaped (1), sterna plates expanded along the anterior and posterior ends and constricted in the middle (2).

165. Humerus longer than or subequal to scapula (0), scapula longer than humerus (1).

166. Total forelimb length [measured from the head of the humerus to tip of the manus] longer than 40% the total length of the hind limb [measured from the head of the femur to tip of the pes] (0), total forelimb length equal to or less than 40% the total length of the hind limb (1).

167. Shaft of the humerus straight (0), shaft of the humerus exhibits at least a modest caudal flexure at the level of the deltopectoral crest (1).

168. Deltopectoral crest rounded in lateral view (0), deltopectoral crest angular in lateral view (1), deltopectoral crest inconspicuous (2).

169. Olecranon process low (0), olecranon process moderately developed (1), olecranon process well-developed (2).

170. Cross-sectional shape of the ulna at midshafttriangular or oval (0), cross-sectional shape of the ulna at midshaft cylindrical (1).

171. Shaft of the ulna straight (0), shaft of the ulna bowed (1).

172. Minimal radial width less than 10% the length of the radius (0), minimal radial width greater than 10% the length of the radius (1).

173. Carpus unfused (0), carpus fused (1).

174. Metacarpal i greater than 50% the length of metacarpal ii (0), metacarpal i less than 50% the length of metacarpal ii (1).

175. Manual digit i oriented less than 25 degrees from digit iii (0), manual digit i oriented between 25 and 60 degrees from digit iii (1), manual digit i oriented at an angle greater than 60 degrees from digit iii (2).

176. Ungual of manual digit i claw-like (0), ungual subconical (1), ungual absent (2).

177. First phalanx of manual digits ii-iv less than twice the size of second phalanx (0), first phalanx greater than twice the size of second phalanx (1).

178. Unguals on manual digits ii and iii longer than wide (0), unguals on manual digits ii and iii wider than long (1).

179. Four phalanges present in manual digit iii (0), three phalanges present in manual digit iii (1).

180. Three phalanges present in manual digit iv (0), two phalanges present in manual digit iv (1), one phalanx present in manual digit iv (2).

181. Two phalanges present in manual digit v (0), one phalanx present in manual digit v (1), phalanges absent in manual digit v (2).

182. Acetabulum on ilium normal to high (0), acetabulum on ilium short to long (1).

183. Ventral acetabular flange on the ilium present (0), absent (1).

184. Supra-acetabular rim on the ilium weakly developed or absent (0), supra-acetabular rim on the ilium strongly developed (1).

185. Dorsal margin of the ilium straight to slightly convex in lateral view (0), dorsal margin of the ilium sinuous in lateral view (1).

186. External surface of the preacetabular process of the ilium laterally facing and roughly in the same plane as the body of the ilium (0), external surface of the preacetabular process of the ilium twisted about its long axis (1).

187. Anterior tip of the preacetabular process of the ilium situated posterior to the anterior tip of the pubic peduncle of the ilium (0), anterior tip of the preacetabular process of the ilium situated anterior to the anterior tip of the pubic peduncle of the ilium (1).

188. Length of the postacetabular process of the ilium between 40 and 21% the total length of the ilium (0), postacetabular process of the ilium less than 20% the total length of the ilium (1), postacetabular process of the ilium greater than 40% the total length of the ilium (2).

189. Brevis shelf on the ilium oriented vertically (0), brevis shelf on the ilium extends medially in a roughly horizontal plane (1).

190. Ischiac peduncle of the ilium is not supported by a sacral rib (0), ischiac peduncle of the ilium supported by a sacral rib (1).

191. Lateral swelling of the ischiac peduncle of the ilium absent (0), present (1).

192. Pubic peduncle of the ilium more robust than the ischial peduncle and expands in lateral view (0), pubic peduncle of the ilium tapers distally and is smaller than the ischial peduncle (1).

193. Pubis not secondarily supported (0), pubis supported only by sacral rib (1), pubis supported directly by at least one sacral centrum (2).

194. Pubis anteroventrally facing (0), pubis vertically oriented (1), pubis posteroventrally rotated (2).

195. Anterior process of the pubis present and straight (0), anterior process of the pubis present and dorsally curved (1), anterior process of the pubis absent (2).

196. Angle between prepubic process and pubic shaft greater than 150 degrees (0), angle less than 100 degrees (1).

197. Prepubic process of the pubis short and peg-shaped (0), prepubic process of the pubis mediolaterally flattened (1), prepubic process of the pubis rod-shaped (2), prepubic process of the pubis dorsoventrally flattened (3).

198. Length of the prepubic process of the pubis (measured from the obturator notch) less than 20% the total length of the ilium (0), prepubic process of the pubis greater than 20% the total length of the ilium (1).

199. Iliac and pubic peduncles of the ischium continuous, but separated by a fossa (0), iliac and pubic peduncles distinct and separated by a concave surface (1).

200. Pubic peduncle of ischium larger than iliac peduncle (0), peduncles subequal or iliac peduncle larger than pubic peduncle (1).

201. Dorsal margin of ischial shaft straight at mid-length in lateral view (0), caudodorsally convex at mid-length in lateral view (1), caudodorsally concave at mid-length in lateral view (2).

202. Groove on the dorsal edge of the ischium absent (0), present (1).

203. Tab-shaped obturator process absent (0), present (1).

204. Obturator process placed within the proximal 40% of the ischium (0), obturator process placed within the distal 60% (1).

205. Ischial shaft flat and blade-like (0), ischial shaft ovoid to subcylindrical (1).

206. Ischial symphysis present along at least 50% of the ischial shaft (0), ischial symphysis only present distally (1).

207. Enlarged 'foot' on the distal end of the ischial shaft absent (0), present (1).

208. Minimum diameter of the femur less than 15% of total femur length (0), minimum diameter of the femur greater than 15% of total femur length (1).

209. Femoral shaft straight in anterior view (0), femoral shaft distinctly bowed in anterior view (1).

210. Angle between the neck of the femoral head and the femoral shaft less than or equal to 100 degrees (0), angle greater than 100 degrees (1).

211. Neck-like constriction under the head of the femur absent (0), present (1).

212. Trench between the greater trochanter and the head of the femur absent (0), present (1).

213. Lateral surface of the greater trochanter of femur convex (0), lateral surface of the greater trochanter flattened (1).

214. Intertrochanteric notch between the lesser and greater trochanters on the femur present (0), absent (1).

215. Dorsal margin of the lesser trochanter of the femur lower than or equal to the height of the greater trochanter (0), dorsal margin of lesser trochanter higher than the height of the greater trochanter (1).

216. Lesser trochanter of femur positioned anterior and medial to greater trochanter (0), lesser trochanter positioned anterior and somewhat lateral to greater trochanter (1).

217. Lesser trochanter of femur consists of a prominent crest (0), lesser trochanter similar in width to the greater trochanter and separated from it by a wide cleft (1), lesser trochanter narrow and closely appressed to the greater trochanter (2).

218. Dorsal margin of the lesser trochanter substantially lower than the head of the femur (0), dorsal margin of the lesser trochanter approximately the same height as the head of the femur (1).

219. Fourth trochanter of the femur ‘mound-like’ (0), fourth trochanter a sharp ridge (1), fourth trochanter ‘pendant-shaped’ (2), fourth trochanter subtriangular (3), fourth trochanter vestigial, consisting of a rugosity or scar (4).

220. Insertion scar of m. Caudifemoralis longus on femur extends from fourth trochanter onto medial surface of femoral shaft (0), insertion scar of m. Caudifemoralis longus widely separated from fourth trochanter and restricted to the medial surface of the femoral shaft (1).

221. Fourth trochanter entirely on the proximal half of the femur (0), fourth trochanter placed at or below midshaft of the femur (1).

222. Anterior intercondylar groove on the distal femur absent (0), present (1).

223. Anterior intercondylar groove of the femur broad, shallow, and 'v-shaped’ with the edges of the groove meeting at an angle of greater than 90 degrees (0), anterior intercondylar groove tight, deep, and 'v-shaped’ with edges of the groove meeting at less than a 90 degree angle (1), anterior intercondylar groove deep, narrow, 'u-shaped,’ and partially enclosed by a slight expansion of the medial condyle (2), anterior intercondylar groove 'u-shaped’ and partially enclosed by expansions of both distal condyles (3), anterior intercondylar groove consists of a canal fully enclosed by fusion of lateral and medial condyles (4).

224. Posterior intercondylar groove on the femur fully open (0), medial condyle inflated and at least partially covering the intercondylar groove (1).

225. Posterior intercondylar groove extends less than ¼ the length of the femur (0), posterior intercondylar groove extends greater than ¼ the length of the femur (1).

226. Femur shorter than or equal to tibia in length (0), femur longer than tibia (1).

227. Tibia triangular in transverse section (0), tibia rounded in transverse section (1).

228. Lateral proximal condyles on the tibia equal in size (0), fibular condyle smaller (1), only one lateral proximal condyle present (2), fibular condyle larger (3).

229. Lateral extension of the tibial posterior flange does not reach fibula (0), lateral extension of the tibial posterior flange extends posterior to the medial margin of the fibula (1), lateral extension of the tibial posterior flange extends posterior to entire distal end of the fibula and calcaneum (2), lateral extension of the tibial posterior flange absent (3).

230. Cnemial crest of tibia straight (0), cnemial crest arcs anterolaterally (1).

231. Cnemial crest of tibia rounded (0), cnemial crest sharply defined (1).

232. Lateral distal condyle on the femur subequal to the medial distal condyle (0), lateral distal condyle 80-60% the size of the medial distal condyle (1), lateral distal condyle 59-50% the size of the medial distal condyle (2), lateral distal condyle 49-40% the size of the medial distal condyle (3), lateral distal condyle 39-30% the size of the medial distal condyle (4), lateral distal condyle 29-20% the size of the medial distal condyle (5).

233. Fibular shaft elliptical or rounded in transverse section at mid-length (0), fibular shaft 'd-shaped' in transverse section throughout its length (1).

234. Ascending process of astragalus short (0), ascending process triangular and 'tooth-like' (1), ascending process 'spike-like' (2), ascending process relatively large (3).

235. Posterior side of astragalus low (0), high (1).

236. Height of anterior side of astragalus high (0), extends moderately high (1), height of anterior side low (2).

237. Articular surface for fibula on the astragalus covers more than 30% of the proximal surface (0), articular surface covers less than 30% of proximal surface of astragalus (1).

238. Angle between the articular facets for the tibia and fibula on the calcaneum greater than 120 degrees (0), angle less than 120 degrees (1).

239. Three or more distal tarsals present (0), two or less distal tarsals present (1).

240. Medial distal tarsal blocky, thin, and rectangular in proximal view (0), medial distal tarsal round in proximal view (1).

241. Medial distal tarsal does not cover any part of the proximal surface of metatarsal II (0), medial distal tarsal covers at least a portion of the proximal surface of metatarsal II (1).

242. Lateral distal tarsal 'square-shaped' (0), 'kidney-shaped' (1).

243. Metatarsal I present (0), absent (1).

244. Metatarsal V present (0), absent (1).

245. Metatarsal V less than 25% the length of metatarsal III (0), between 25% and 50% (1), greater than 50% (2).

246. Diameter of the midshafts of metatarsals I and V subequal to or greater than metatarsals II-IV (0), diameter of the midshafts of metatarsals i and v less than metatarsals II-IV (1).

247. Four functional digits in the pes (0), three functional digits in the pes (1).

248. Phalanges in pedal digit I present (0), absent (1).

249. Unguals on pedal digits II-IV longer than wide (0), approximately as wide as or wider than long (1).

250. Ossified hypaxial tendons along the tail absent (0), present (1).

251. Epaxial ossified tendons absent (0), present (1).

252. Epaxial tendons longitudinally arranged into a single layer (0), arranged in a double-layered lattice (1).

253. Postcranial osteoderms absent (0), present (1).

254. Dermal sculpturing of the skull and/or mandible absent (0), present (1).

255. Premaxillae unfused (0), fused (1).

APPENDIX 10

CHARACTER DATA FOR CHAPTER 5

Character codings used to evaluate the systematic relationships of ornithischian dinosaurs. Abbreviations: **a** = 0/1; - = character not applicable to taxon.

Taxon	1 0	2 0	3 0	4 0	5 0
Marasuchus	??????????	??????????	??????????	??????????	??????????
Silesaurus	?0000000-0	0?1?1?000-	?00--??0??	?0?1??00??	????101???
Asilisaurus	?0????????	???????0??	??????????	?0????????	?????02???
Sanjuansaurus	??????????	???????00-	00?????0??	??????????	??????????
Herrerasaurus	10000000-0	0010?0000-	000--00020	?01010000??	0100102??0
Tawa	1000000??0	00???0000-	000--00020	0000000???	00000?????
Pisanosaurus	??????????	???????011	??????????	??????????	??????????
Heterodontosaurus	0100011110	001?010011	0010100010	000000003??	0000000000?
Fruitadens	????0?111?	???0??0111	??????????	??????????	??????????
Echinodon	?1??0?????	??????0011	??????????	??????????	??????????
Lycorhinus	???????11?	??????0011	?0????????	??????????	??????????
Tianyulong	0100011111?	001010??1?	???????0?20	?0???000??	??????????
Abrictosaurus	?10?011110	0?1????011	00101????0	?0????????	??????????
Eocursor	??????????	????????1?	??????????	??????????	??????????
Lesothosaurus	010??01101	?110??0110	1010?00010	?0?000????	000?0000??
Scutellosaurus	?1000??10?	0??????110	???????0??	0110??00??	?1??00?001
Scelidosaurus	?1???0?0??	0?1????111	0????????0	?1????????	0?????????
Emausaurus	?1???0?0?0	??1????111	0????????0	?1????????	0?????????
Stormbergia	??????????	??????????	??????????	??????????	??????????
Agilisaurus	01001010-?	0?1?100?11	0020011101	1?0100000??	0100100??1
Hexinlusaurus	01????????	?????0??11	??10110011	00?0?0?0??	01??000???
Yandusaurus	?1????????	????????11	??????????	??????????	????000???
Leaellynasaura	??????????	????????11	???????0??1	0001?000??	????000?0?
Jeholosaurus	0100001101	011?110111	0110010021	100100012?	1100000001
Yueosaurus	??????????	??????????	??????????	??????????	??????????
Othnielosaurus	??????????	??????????	???????0??	???1??????	??????????
Parksosaurus	???????10?	??1??0?111	0??????00??	101100?0??	1?0??00???
T. neglectus	1100101101	0111100111	0120010021	1000100?0	a100000001
T. assiniboiensis	??????????	??????????	???0??????	??????????	??????????
T. garbanii	??????????	??????????	??????????	??????????	??????????
Talenkauen	?1001?110?	0???100?11	?0????????	??????????	??????????
Notohypsilophodon	??????????	??????????	??????????	??????????	??????????
Macrogryphosaurus	??????????	??????????	??????????	??????????	??????????

Taxon	1 0	2 0	3 0	4 0	5 0
Haya	0100001101	0011102111	0120010?1	?001000??	1100000???
Changchunsaurus	0100101101	0111?00111	?1?0??00??	?001?002??	0101??0??1
Oryctodromeus	?1001?1??1	0111??01??	???????0??	?0?1???0??	????0000??
Zephyrosaurus	?10?0?1101	01?11?0111	11101?10?1	10?1?00300	???0000000
Orodromeus	0100111102	0011?00111	?110110021	0011?00300	a10?00000?
Skaladromeus	?1????????	??????????	??????????	2??1???3??	??????????
Koreanosaurus	??????????	??????????	??????????	??????????	??????????
Archaeoceratops	0110001100	101000?111	0010100020	1010000?1??	0111000?01
Liaoceratops	0110001100	1010?1?111	00???0002?	1010000?2??	0110000000
Yinlong	011?001100	1?1001?111	0010110020	1010000?1??	0101111?00
Stenopelix	??????????	??????????	??????????	??????????	??????????
Micropachycephalosaurus	??????????	??????????	??????????	???????0??	??????00??
Wannanosaurus	??????????	??????????	???21??0??	10?0???1?0	??????????
Hypsilophodon	0100011101	0110100111	0110100111	001100000?	1100000001
Atlascopcosaurus	??????????	????????11	??????????	??????????	??????????
Qantassaurus	??????????	??????????	??????????	??????????	??????????
Anabisetia	??????????	????????11	?0????????	??????????	??????????
Gasparinisaura	01????????	????????11	0?100?0111	?001001??	0100000111
Z. robustus	110001--01	0?1?0?0111	0????00021	?0?01?10??	0110001111
Z. shqiperorum	?1????????	??????????	??????00021	?00010?0??	????0??11?
T. dossi	11002?110?	0?1???11?11	?010?????1	0000100?0?	0100001?1?
T. tilletti	1??0??????	?????1?0???	?0????00111	0??1100???	1????0??0?
Rhabdodon	??????????	????0??0???	??????????	??????????	?????0????
Muttaburrasaurus	??????????	0?1??0??11	0?10?001?1	0000011?0?	0?0??01???
Elrhazosaurus	??????????	??????????	??????????	??????????	??????????
Dysalotosaurus	010020---0	0?10011111	0010100110	1000011010	0001001?0
Dryosaurus	010020---0	0?10011111	0010000010	1000011010	0001001?0
Callovosaurus	??????????	??????????	??????????	??????????	??????????
Valdosaurus	??????????	??????????	??????????	??????????	??????????
Camptosaurus	1101??????	????00?1???	??????00111	1??101??01	0????0??0?
Iguanodon	1101??????	????0??1???	???????0121	???100??21	0????1??1?
Ouranosaurus	110???????	????0??1???	???????0120	????1?0??21	0????1??1?

Taxon	60	70	80	90	100
Marasuchus	??????????	??????????	??????????	?????????0	??????????
Silesaurus	?100??00??	??00111---	--?40??000	00?0??1000	????0?0000?
Asilisaurus	??????????	??????????	???4??????	??????????	??????????
Sanjuansaurus	??????????	??????????	??????????	??????????	?0?????????
Herrerasaurus	??10000010	0000??2---	--010?0000	000010?010	0010000??0
Tawa	??00?10000	0??????---	--010?0000	0000???100	?010000??
Pisanosaurus	??????????	??????????	???????0011	?10000????	??????????
Heterodontosaurus	0?00?01000	0?00110?0	100?001011	0100000000	1000000?0
Fruitadens	??????????	??????????	??0?0??0??	0?????????	??????????
Echinodon	??????????	??????????	1?000?1011	0?????????	??????????
Lycorhinus	??????????	??????????	??????????	??????????	?00???????
Tianyulong	??????????	???????1?0	???01?1011	0110??200?	??000?0???
Abrictosaurus	??????????	????????10	1-0?0??011	01?0?????0	0??????0??
Eocursor	???????0??	??????????	??0???0001	01000?????	???????0??
Lesothosaurus	0000?00000	0000010???	0010?00001	??00010??0	0???000??0
Scutellosaurus	?000?00000	0?00?1????	???0000001	0????11?0?	??????0??0
Scelidosaurus	??????00??	??????????	??1????101	??????11??	0?????????
Emausaurus	???????0??	??????????	0?1????101	??????11??	0?????????
Stormbergia	??????????	??????????	??????????	??????????	??????????
Agilisaurus	0??0?00000	0000011???	001?0?1011	0110001000	1000001??0
Hexinlusaurus	?????0101?	0?0001????	??12010011	?????????0	?00?00????
Yandusaurus	??00??????	??????????	??????????	??????????	?00???????
Leaellynasaura	??00??????	??00?1????	??????????	??????????	??????????
Jeholosaurus	0100101010	0000011100	0012010011	1110100000	1000001??0
Yueosaurus	??????????	??????????	??????????	??????????	??????????
Othnielosaurus	????????00	0??00?????	?0?1?10?11	??????????	????????10
Parksosaurus	???01?????	0?????????	?????0?011	01?0?????0	1011001?00
T. neglectus	1110101011	0?10111000	0112011011	111012?000	1010001100
T. assiniboiensis	???????010	001011????	??????????	??????????	????????10
T. garbanii	??????????	??????????	??????????	??????????	??????????
Talenkauen	??????????	???????100	011?0?1?11	??????????	??????????
Notohypsilophodon	??????????	??????????	??????????	??????????	??????????
Macrogryphosaurus	??????????	??????????	??????????	??????????	??????????

Taxon	60	70	80	90	100
Haya	1??0?01011	0?00110000	0111111011	?1?00??000	?110001??0
Changchunsaurus	???000?000	0??????100	01111?1011	1100120000	?0??001??0
Oryctodromeus	01000?10??	??????????	??1??1??11	????1?????	??????0??00
Zephyrosaurus	0100111011	00001?????	????0???11	???0??1???	0???00?110
Orodromeus	0110111011	01000?????	??12111011	0100102?00	1000001100
Skaladromeus	???????1???	?000??????	??1?????11	??????????	??????0????
Koreanosaurus	??????????	??????????	??????????	??????????	??????????
Archaeoceratops	0010?0?101	0?00101110	0110?11011	1100002000	00?00010??
Liaoceratops	0000?01101	0?00001100	0110111011	0100?0?000	????0010?0
Yinlong	0?00?0?10?	0?00001100	0110011011	01001??000	1011000??0
Stenopelix	??????????	??????????	??????????	??????????	??????????
Micropachycephalosaurus	?0????????	??????????	??????????	???????2???	??????????
Wannanosaurus	??????0?10?	0?10??????	????0??011	01?000????	??????01???
Hypsilophodon	0000?00000	0000011110	0012011011	0110100000	1100011?0
Atlascopcosaurus	??????????	??????????	????1???11	??????????	??????????
Qantassaurus	??????????	??????????	??12011011	0?????????	??????????
Anabisetia	??????????	??????????	????1???11	??????????	??????????0
Gasparinisaura	0????00000	0?0?0?????	??120?1011	?100100??0	101?001??0
Z. robustus	0010?01001	1001102110	01101?1011	111010201?	?01?101??0
Z. shqiperorum	?011?0?00?	10?111??1?	??10101011	11?0102???	????10???0
T. dossi	0??1?010??	10?01??111	?0121?1011	11?01??010	1011101?0
T. tilletti	00?1001???	?1001?1?01	????101???	1?0?12?11?	??1?11?0?0
Rhabdodon	000?0?????	??????????	????111?11	1??110????	?????????0?
Muttaburrasaurus	1??0???0??	??1?10????	????????11	????1????1	?0????1??0
Elrhazosaurus	??????????	??????????	??????????	??????????	??????????
Dysalotosaurus	101010100?	??000?1111	0111011011	110110?110	1011001000
Dryosaurus	101000100?	?1000?1111	0112111011	110100?110	1011001000
Callovosaurus	??????????	??????????	??????????	??????????	??????????
Valdosaurus	??????????	??????????	??????????	??????????	??????????
Camptosaurus	1011011?00	11101?2?01	?1??111???	1?111??11?	??1?00?011
Iguanodon	1011001?0?	11111?2?01	?1??110???	1?211????1?	????0???11
Ouranosaurus	1001?0??00	11111?2???	?0???10???	??111?????	?????????11

Taxon	11 10	12 0	13 0	14 0	15 0
Marasuchus	?????????0	??????????	??????????	??????????	???1?0?0??
Silesaurus	?0??000?20	01001?0-00	01?-3?0-10	030003?---	0021002100
Asilisaurus	??????????	???0???-??	???-3????0	??0003?---	???100?00?
Sanjuansaurus	??????????	????-?0-?1	0?0?2?001?	04?0?????-	00??0?000?
Herrerasaurus	?0010?????	0100-10-?1	0?0-210010	0410?21---	00?10000??
Tawa	?0????????	0200-10-?1	0?0-200010	0410?2?---	???10??0??
Pisanosaurus	??????????	??????1??0	??????10??	100????1?00	?????0????
Heterodontosaurus	0?100?0?20	0211012021	1?11001110	1?11000?11	0?10000??
Fruitadens	??????????	0210?01??0	??0-0?0001	1?0??0?00?	?0??????2??
Echinodon	??????????	020??11-?0	??0?0?0001	1200?0??0?	??????????
Lycorhinus	??????????	??1?-?1??0	0???0?000?	13?1??????	??????????
Tianyulong	??????????	0211?11??0	????0?0001	1?????0??0?	??????????
Abrictosaurus	??????????	0200-11??0	??1?000001	13?1?01?01	???????1??
Eocursor	1?????????	??0???????	??0???????1	??0000?00?	???????1??
Lesothosaurus	1?1000?010	0000-01100	0000010?01	0??000?0?0	????0?????
Scutellosaurus	??????????	0000001020	000-0?0001	0200002000	0011?011??
Scelidosaurus	??????????	?????0????	??0????????	???0?????0	????0?????
Emausaurus	??????????	?????0????	??0????????	???0?????0	??????????
Stormbergia	??????????	??????????	??????????	??????????	?0??0?????
Agilisaurus	00??1?????	0100001020	0?0???1001	1200?02000	01??1?11??
Hexinlusaurus	??????????	???0-?1-?0	0?000?1001	1300?0200?	0010101??
Yandusaurus	??????????	????-?1-?0	0?00011002	13?0????0?	?0????????
Leaellynasaura	??????????	??????1???	11??0?110?	13?0??????	??????????
Jeholosaurus	?0001?1?00	0001-010?1	????011001	1200?01000	0010?11200
Yueosaurus	??????????	??????????	??????????	??????????	0010??????
Othnielosaurus	????00?1??	???1-??000	0?000?1001	?200001?0?	0010??120?
Parksosaurus	?????1???0	???1??10?0	????0?10?1	1?0?10?00?	?0?1?0????
T. neglectus	?1011??001	0001-01010	0100011001	1200002110	001110?3?0
T. assiniboiensis	0101111000	??????????	??????????	1?????????	?0????????
T. garbanii	??????????	??????????	??????????	??????????	??????????
Talenkauen	??????????	0?01??1???	????0?11??	1????????1?	00?10?2???
Notohypsilophodon	??????????	??????????	??????????	??????????	?01?????00
Macrogryphosaurus	??????????	??????????	??????????	??????????	10?1010?20

Taxon	1 1 0	1 2 0	1 3 0	1 4 0	1 5 0
Haya	00101?????	0101-010??	020?011001	1?00?01?10	00?0???2??
Changchunsaurus	????1???1?	0100-010?0	1?0?0?1001	1200?0?01?	0010??1???
Oryctodromeus	00??11?1??	0?00???000	0??????0?1	??00?0?01?	?021?11310
Zephyrosaurus	0?10111120	01???01000	010001100?	12?00?????	?020?0????
Orodromeus	101011111?	010??01000	00000???01	12?000????	0020101300
Skaladromeus	???0??????	??00??1000	00??0?0?01	1?0000?01?	?021??????
Koreanosaurus	??????????	??????????	??????????	??????????	?021?0??0?
Archaeoceratops	?0??1?????	0201?01??1	1?1?0??101	141??0??10	???0???2?0
Liaoceratops	?0101????1	0201?01??1	??110?1001	1?00?01?10	??????????
Yinlong	??101???21	020?001??0	0???010?0?	12?0??????	??????????
Stenopelix	??????????	??????????	??????????	??????????	????????2??
Micropachycephalosaurus	??????????	??????????	??????????	???0??????	?????????0
Wannanosaurus	??????????	???0???1??	?????????0	??00?00?0?	?0?0??????
Hypsilophodon	0010110010	0001-02001	1111001001	1000101010	0010101200
Atlascopcosaurus	??????????	??????2011	11?00?111?	1?0010?11?	??????????
Qantassaurus	??????????	???????0??	???0?????0	?400100010	??????????
Anabisetia	????0?????	???1-?1-?1	??1?0??11?	1??0????0?	??????????
Gasparinisaura	10100??2?0	??0???1??1	1?1?001111	10?0?000?0	??1????210
Z. robustus	00200??1?0	1-011-2011	11111?1000	1100110111	?010?0?320
Z. shqiperorum	?0200?????	??01-??0?1	1111?????0	1100110110	?0?0?0?32?
T. dossi	1???1????0	0201???011	1111?0001?	11?0110010	11?0?11210
T. tilletti	1???10020?	1?01???011	1111??001?	11?0110010	11?0?11210
Rhabdodon	????100???	???????0?1	1111??101?	11?01??11?	?0????1??10
Muttaburrasaurus	?0??1?????	???1??10?1	1???0?11??	1??0????1?	011??1?2??
Elrhazosaurus	??????????	??????????	??????????	??????????	??????????
Dysalotosaurus	0?11110221	1-0??-21??	??11?11110	11?0110010	011??112?0
Dryosaurus	0?11100201	1-011-2111	11111?1110	11?0111010	?111?1?210
Callovosaurus	??????????	??????????	??????????	??????????	??????????
Valdosaurus	??????????	??????????	??????????	??????????	?121??????
Camptosaurus	0???001200	1?0????111	1111??011?	11??1?100?	?0????1??21
Iguanodon	1???000220	??0????111	1111??011?	11??1?200?	?1????1??21
Ouranosaurus	1???00002?	??0????1??	???1??????	1???1?????	??????1????

Taxon	160	170	180	190	200
Marasuchus	???1????0?	????0?????	??????????	?0001002-?	00?02---01
Silesaurus	1?????000	0????0?020?	00????????	?000000?0	00002---01
Asilisaurus	00?????000	0????0????	??????????	?00000????	???02---0?
Sanjuansaurus	???????000	01???????2?	??????????	??11??????	???02---??
Herrerasaurus	?0?????00?	0????0??2?	0000?00002	2011000?0	00002---10
Tawa	???????00?	0?????01??	??00?0?011	?0010?02??	?0?02---11
Pisanosaurus	??????????	??????????	??????????	??0???????	0???????11
Heterodontosaurus	0000100001	????000120	0000000000	0011001017	00?2000010
Fruitadens	??????????	??????????	??????????	??????????	??????????
Echinodon	??????????	??????????	??????????	??????????	??????????
Lycorhinus	??????????	??????????	??????????	??????????	??????????
Tianyulong	??????????	??????102?	??????????	??????????	???2???????
Abrictosaurus	??????????	????0000??	???????0??	??11001017	00????????
Eocursor	???????00?	????0?00??	???????0??	?011001017	00?2000010
Lesothosaurus	?0??1????1	0????1??00	0?00?0????	1000001000	00?2000010
Scutellosaurus	0??????0?1	000??0000?	?00????00?0	??0100100?	00?200??11
Scelidosaurus	????0?0???	?????0????	??????????	?001??110?	00?????0??
Emausaurus	??????????	??????????	??????????	??????????	??????????
Stormbergia	00??1??001	000??1??1?	?1????????	?001001001	00?20000??
Agilisaurus	0?1?1?0001	000?01100?	0000??000?	?101001001	01?21?2110
Hexinlusaurus	002????001	0????0?1000	?000?0000?	?010001011	01?2002110
Yandusaurus	???????010	00??0?1???	??????????	??????????	??????????
Leaellynasaura	??????????	??????????	??????????	??????????	???2003?10
Jeholosaurus	001????00?	?0??010000	000???????	?010001011	1102002110
Yueosaurus	?0?????00?	????0?002?	??????????	??????????	??????????
Othnielosaurus	?11???1001	00??0?100?	0?00?00??0	0010001011	1102002110
Parksosaurus	001???100?	00000???1?	00????????	???001?011	1??2????11
T. neglectus	111??0100?	0??2001000	0000?00000	0010101011	1112002110
T. assiniboiensis	?1????2????	??????????	??????????	?010?11?11	11?21021??
T. garbanii	??????????	??????????	??????????	??????????	??????????
Talenkauen	??????????	????0??2??	??????????	?0?0101???	1??20?1???
Notohypsilophodon	???????0??	0?????120?	??????????	??????????	??????????
Macrogryphosaurus	??????1???	????????2??	??????????	?010101?11	1112001???

Taxon	160	170	180	190	200
Haya	0111??0001	01000?001?	???0??????	?010001?1?	1122002???
Changchunsaurus	??????000?	0?00??10??	??????????	??1???????	??????????
Oryctodromeus	?121??2101	001??01010	00????????	?110001?1?	1122002???
Zephyrosaurus	?11??0?1?1	00???????0	??????????	????001???	???????????
Orodromeus	0010?0?101	000???1111	000???0000	?010001211	1122002?10
Skaladromeus	????????1??	0?1???111?	??00000001	??????????	???????????
Koreanosaurus	??????0111	01000?1010	??????????	??1?????11	1???????11
Archaeoceratops	011???????	??????????	??????????	?010011011	11?20030??
Liaoceratops	??????????	??????????	??????????	??????????	??????????
Yinlong	??????????	??????????	??????????	?010111011	?1?20030??
Stenopelix	????????0?	??????????	??????????	?010001011	01?20?3?1?
Micropachycephalosaurus	??????????	??????????	??????????	??1??01???	?1????????
Wannanosaurus	??????????	??????10??	??????????	??1???1???	??????????
Hypsilophodon	0111101001	1000001010	100000000?	?010001011	1112012110
Atlascopcosaurus	??????????	??????????	??????????	??????????	??????????
Qantassaurus	??????????	??????????	??????????	??????????	??????????
Anabisetia	????????001	00??0?02??	?0????????	?010101011	?1?2001111
Gasparinisaura	?1101??0?1	00?????10?	00????????	?010101011	1102002111
Z. robustus	101????00?	0?????110?	1?????????	?111011???	1???????11
Z. shqiperorum	1?????000	010???110?	1?????????	?111011?1	11?2002111
T. dossi	11????0001	00001?1100	100???10??	?110101011	11?21?1111
T. tilletti	1110?10001	00001?1100	100000101?	?110101011	1102011111
Rhabdodon	111????0?0	00????1010	1?????????	?1??0????1	???????????1
Muttaburrasaurus	????????00?	0?????0?10	100???????0	?1101?1?1?	11?2??111?
Elrhazosaurus	??????????	??????????	??????????	??????????	??????????
Dysalotosaurus	1121??00?0	10?0???110	10????10??	?110101011	1112111110
Dryosaurus	1120?100?0	1?????0110	00?0??10??	?110101011	1102111110
Callovosaurus	??????????	??????????	??????????	??????????	??????????
Valdosaurus	??????????	??????????	??????????	????????1?	????12????
Camptosaurus	1111?000?1	10????0110	1111??101?	?1?000???1	??0??1???1
Iguanodon	1111?200?2	10?????121	0111??111?	?1?010???1	???1???????1
Ouranosaurus	??????2?0?2	1????????21	0?1???????	?1????????	?????????1

Taxon	210	220	230	240	250
Marasuchus	2?0-0?00??	000000001?	00-000?230	-0?0020-0?	??00200?0
Silesaurus	000-01001?	00-000001?	00-011?210	00?0020-??	??0011??00
Asilisaurus	??0-0110??	?0?000000?	0??01??210	0??0020-??	?????1???0
Sanjuansaurus	?????????0	10??????1?	00-001?20?	0??0021-??	?????????0
Herrerasaurus	0?0-100000	100000001?	00-0011201	00?0021-10	??00210000
Tawa	????1??000	10??00001?	0???0??211	0??0021-??	??00?10000
Pisanosaurus	?????0????	??????????	????????11	0???001???	????????0?
Heterodontosaurus	000-011000	0001012 12?	00-000??21	00??????00	000??10000
Fruitadens	???????0??	?0?101212?	00-00???21	0???0010??	??????????
Echinodon	??????????	??????????	??????????	??????????	??????????
Lycorhinus	??????????	??????????	??????????	??????????	??????????
Tianyulong	010?0?0???	??????????	?1000?????	??????????	??0??10001
Abrictosaurus	??0???????	???0?1112?	00-??0??2?	??????????	??0001?00?
Eocursor	010-00?000	00?0001020	00-0001121	000???????	??????????
Lesothosaurus	010?000000?	0000001020	0????0??2?	?0?3?01011	0??????0??
Scutellosaurus	?10?000000	0000001020	00-000??21	00?0??????	??0????00??
Scelidosaurus	?00??1????	?0?0?010??	0????1??2?	??????????	??????????
Emausaurus	??????????	??????????	??????????	??????????	??????????
Stormbergia	0110010000	000000 10??	00-0000321	0???001???	???0????0?
Agilisaurus	011000000?	100001102?	00-0001?2?	?000??????	??00010000
Hexinlusaurus	0010??0001	000000102?	00-0001221	0100001?11	1100110000
Yandusaurus	??????????	??????????	?0-00?????	?1????????	????????0?
Leaellynasaura	00100?0000	?0?101202?	0??000??21	0??00010??	??00010000?
Jeholosaurus	0?1?000010	110001212?	00-0001321	0?00001111	1100??000?
Yueosaurus	0?????? 00?	11??012120	0????????2?	??????????	??0????00?
Othnielosaurus	1?100?0001	110001212?	00-00?0?21	01?2101111	1100010000?
Parksosaurus	2011010010	1111012120	1???001?21	0100001??1	??00010001
T. neglectus	0011010010	111001212?	1100010221	0200001111	1000010001
T. assiniboiensis	???????010	1110012 1?0	1100010221	0?00001?11	?000010001
T. garbanii	??????????	??????????	?100??02?1	0?00001?11	1000010000?
Talenkauen	????1??0??	?????12??2?	1????1????	??????????	??0??1????
Notohypsilophodon	??????????	11?00121??	?0-00???21	0???0??????	????????0?
Macrogryphosaurus	?0??111???	??????????	??????????	??????????	??????????

Taxon	210	220	230	240	250
Haya	00100??000	1110012l2?	00-000????	????0?1?11	???0010000
Changchunsaurus	?????????0	11?00121??	???????3?1	0?????????	??0??1000?
Oryctodromeus	???????001	1110012l2?	0100000?21	0?100?????	??00010001
Zephyrosaurus	101?1????1	1?10012???	???00?0?2?	?110021011	100??1000?
Orodromeus	00100?0000	111?01212?	0100000?1	0112001011	1000010000
Skaladromeus	???????000	111?01212?	?0-00??2?1	001????011	1100010000?
Koreanosaurus	???????001	1110012l2?	00-00013?1	011???????	??????????
Archaeoceratops	??0??????1	110?0121??	????????2?	???0011011	1?0??1000?
Liaoceratops	??????????	??????????	??????????	??????????	??????????
Yinlong	????????0??	????01212?	0?????????	??????????	??0???000?
Stenopelix	110-010???	?1?????1??	????????2?	??????????	??000?0000
Micropachycephalosaurus	??????0001	110?0121?0	0??0???3?1	0?????????	??????????
Wannanosaurus	????????00?	?????1????	00???00???	??????????	??????????
Hypsilophodon	0011010001	1100012l?0	0??0000321	0201001111	1100110001
Atlascopcosaurus	??????????	??????????	??????????	??????????	??????????
Qantassaurus	??????????	??????????	??????????	??????????	??????????
Anabisetia	0010??100?	1101112l2?	010000????	??????????	??00010?1
Gasparinisaura	?01?01?00?	111111212?	00-0000221	0100021112	1101-1110?
Z. robustus	100-110110	1110012120	1101011?21	01?00210??	???1??????
Z. shqiperorum	100-111110	1110012120	1111011?21	0??0???0??	??????????
T. dossi	1010011100	1100012l2?	1111011221	030??????1	1?00110001
T. tilletti	0010000100	1100012120	1111010221	0300021111	100a010001
Rhabdodon	0?0?1?111?	110001???0	0??1?10???	01?012????2	01?1-?1???
Muttaburrasaurus	????????1?0	1100012120	110101??21	?1?0101?1?	??01-1??0?
Elrhazosaurus	???????000	1100012l?1	01200?????	?0?????????	??????????
Dysalotosaurus	10101?1010	1100112121	011101??21	03?31?11??	0?00?11101
Dryosaurus	a0101?1010	1100112121	0101010021	03?3101111	11?0011101
Callovosaurus	???????000	1100011121	01110?????	??????????	??????????
Valdosaurus	001?11?000	1100012121	0121000221	130???1011	?011--1-??
Camptosaurus	a?1?1?1100	1?0001???0	1111?11???	0?0012????	0??1??100?
Iguanodon	1?1?1?110?	1?0101???0	1131?11???	15?012????2	01?1??111?
Ouranosaurus	????1?1???	0?0?01???0	??????1???	140012????2	??????1???

Taxon	2 5 5
Marasuchus	0-0??
Silesaurus	0-000
Asilisaurus	0-0??
Sanjuansaurus	0-???
Herrerasaurus	0-000
Tawa	0-000
Pisanosaurus	??00?
Heterodontosaurus	1-00?
Fruitadens	?????
Echinodon	???0?
Lycorhinus	?????
Tianyulong	1000?
Abrictosaurus	??00?
Eocursor	??00?
Lesothosaurus	1?00?
Scutellosaurus	1?10?
Scelidosaurus	1?11?
Emausaurus	??10?
Stormbergia	1?0??
Agilisaurus	11000
Hexinlusaurus	0-00?
Yandusaurus	?????
Leaellynasaura	?????
Jeholosaurus	1100?
Yueosaurus	?????
Othnielosaurus	??00?
Parksosaurus	1000?
T. neglectus	10001
T. assiniboiensis	1?00?
T. garbanii	?????
Talenkauen	1????
Notohypsilophodon	?????
Macrogryphosaurus	?????

Taxon	255
Haya	11000
Changchunsaurus	1?001
Oryctodromeus	11001
Zephyrosaurus	??001
Orodromeus	??000
Skaladromeus	??0??
Koreanosaurus	??0??
Archaeoceratops	??000
Liaoceratops	?????
Yinlong	????0
Stenopelix	1000?
Micropachycephalosaurus	?????
Wannanosaurus	?????
Hypsilophodon	10000
Atlascopcosaurus	?????
Qantassaurus	?????
Anabisetia	?????
Gasparinisaura	1000?
Z. robustus	??000
Z. shqiperorum	1000?
T. dossi	1000?
T. tilletti	1000?
Rhabdodon	??00?
Muttaburrasaurus	??00?
Elrhazosaurus	?????
Dysalotosaurus	10000
Dryosaurus	10000
Callovosaurus	?????
Valdosaurus	?????
Camptosaurus	?1???
Iguanodon	?1???
Ouranosaurus	?????

APPENDIX 11

CHARACTER DATA SOURCES FOR CHAPTER 5

List of references consulted and specimens examined for this analysis. Specimen numbers in bold indicate casts of that specimen were examined. Specimen numbers in italics indicate specimens for which additional photographs were examined, but the specimen was not examined first hand.

Taxon	Age	References	Specimens Examined
Abrictosaurus	Hettangian-Sinemurian	Thulborn, 1974; Hopson, 1975	
Agilisaurus	Bathonian-Callovian	Peng, 1992; Barrett et al., 2005	
Anabisetia	Cenomanian-Turonian	Coria and Calvo, 2002; Ibiricu et al., 2010	
Archaeoceratops	Aptian-Albian	You and Dodson, 2003	IVPP V11114, V11115
Asilisaurus	Anisian	Nesbitt et al., 2010	
Atlascopcosaurus	Albian	Rich and Rich, 1989	**NMV P186153**
Callovosaurus	Callovian	Galton, 1980; Ruiz-Omenaca et al., 2006	
Camptosaurus	Kimmeridgian-Tithonian	Norman, 2004	
Changchunsaurus	Aptian-Cenomanian	Zan et al., 2005; Jin et al., 2010; Butler, et al., 2011	
Dryosaurus	Kimmeridgian-Tithonian	Galton, 1977, 1981, 1983	
Dysalotosaurus	Kimmeridgian	Galton, 1977, 1981, 1983	
Echinodon	Berriasian	Galton, 1978; Galton, 2007	
Elrhazosaurus	Aptian	Galton and Taquet, 1982; Galton, 2009	
Emausaurus	Toarcian	Norman et al., 2004b	
Eocursor	Norian-Rhaetian	Butler et al., 2007; Butler, 2010	*SAM-PK-8025*

Taxon	Age	References	Specimens Examined
Fruitadens	Tithonian	Butler et al., 2010	
Gasparinisaura	Santonian-Campanian	Coria and Salgado, 1996; Salgado et al., 1997; Coria, 1999; Coria and Calvo, 2002; Ibiricu et al., 2010	
Haya	Santonian	Makovicky et al., 2011	IGM 100/ 2017, 100/2014, 100/ 2016
Herrerasaurus	Carnian	Novas, 1993; Sereno, 1993; Sereno and Novas, 1993	
Heterodontosaurus	Hettangian-Sinemurian	Crompton and Charig, 1962; Santa Luca et al., 1976; Santa Luca, 1980; Butler et al., 2008b	*SAM-PK-K337, 1332*
Hexinlusaurus	Bathonian-Callovian	He and Cai, 1984; Barrett et al., 2005	
Hypsilophodon	Barremian-Aptian	Galton, 1974a	
Iguanodon	Valanginian-Albian	Norman, 2004	
Jeholosaurus	Barremian	Xu et al., 2000; Barrett and Han, 2009	IVVP V 12529, IVPP V 15718; PKUP V 1061, 1062, 1063, 1064.
Koreanosaurus	Santonian-Campanian	Huh et al., 2011	
Leaellynasaura	Albian	Rich and Rich, 1989; Rich et al., 2010	**NVM P186047**
Lesothosaurus	Hettangian-Sinemurian	Galton, 1978; Sereno, 1991; Knoll, 2002a, b; Butler, 2005	*SAM-PK-401, 1106*
Liaoceratops	Barremian	Xu et al., 2002; Xu et al., 2006	IVPP V12738; V12633
Lycorhinus	Hettangian-Sinemurian	Haughton, 1924; Gow, 1975; Hopson, 1975; Gow, 1990	
Macrogryphosaurus	Coniacian	Calvo et al., 2007; Ibiricu et al., 2010	

Taxon	Age	References	Specimens Examined
Marasuchus	Ladinian	Sereno and Arcucci, 1994	
Micropachycephalosaurus	Campanian	Dong, 1978, Butler and Zhao, 2009	
Muttaburrasaurus	Albian	Bartholomai and Molnar, 1981; Molnar, 1996	
Notohypsilophodon	Cenomanian-Coniacian	Martinez, 1998; Ibiricu et al., 2010	
Orodromeus	Campanian	Scheetz, 1999	MOR 294, 403, 473, 1136, 1141; PU 23246, 23442
Oryctodromeus	Cenomanian	Varricchio et al., 2007; Krumenacker, 2010	BYU 19342, 19347; MOR 1636a, 1636b.
Othnielosaurus	Kimmeridgian-Tithonian	Galton and Jensen, 1973; Galton, 1977; Galton, 1978; Galton, 1983; Galton, 2007	BYU ESM-163R; UW 24823
Ouranosaurus	Aptian	Norman et al., 2004b	
Parksosaurus	Maastrichtian	Parks, 1926; Galton, 1973	ROM 804
Pisanosaurus	Carnian	Casamiquela, 1967; Bonaparte, 1976; Gow, 1981; Irmis et al., 2007	
Qantassaurus	Albian	Rich and Vickers-Rich, 1999	**NMV P198962, P199075**
Rhabdodon p.	Santonian-Maastrichtian	Garcia et al., 1999; Pincemaille-Quillevere et al., 2006	
Sanjuansaurus	Carnian	Alcober and Martinez, 2010	
Scelidosaurus	Sinemurian	Norman et al., 2004b	
Scutellosaurus	Hettangian-Sinemurian	Colbert, 1981; Rosenbaum and Padian, 2000	TMM 43647.7, 43663.1, 43664.1, 43687.16

Taxon	Age	References	Specimens Examined
Silesaurus	Carnian	Dzik, 2003; Piechowski and Dzik, 2010	
Skaladromeus	Campanian	Chapter 3	UMNH VP 12665, 12677, 16281, 16772, 16773, 19470, 21091-21099, 21101-21107
Stenopelix	Berriasian	Butler and Sullivan, 2009	
Stormbergia	Hettangian-Sinemurian	Butler, 2005	*SAM-PK-1105*
Talenkauen	Maastrichtian	Novas et al., 2004; Ibiricu et al., 2010	
Tawa	213-215 myr	Nesbitt et al., 2009	
Tenontosaurus dossi	Aptian	Winkler et al., 1997	
Tenontosaurus tilletti	Aptian-Albian	Forster, 1990	
Thescelosaurus assiniboiensis	Maastrichtian	Galton, 1989; Galton, 1997; Brown et al., 2011	RSM P 1225.1
Thescelosaurus garbanii	Maastrichtian	Morris, 1976	
Thescelosaurus neglectus	Maastrichtian	Gilmore, 1913, 1915; Sternberg, 1940; Galton, 1974b, 1995, 1997, 1999; Morris, 1976; Boyd et al., 2009	NCSM 15728; USNM 7757, 7758.
Tianyulong	Barremian	Zeng et al., 2009	
Valdosaurus	Barriasian-Barremian	Barrett et al., 2011	
Wannanosaurus	Campanian-Maastrichtian	Hou, 1977; Butler and Zhao, 2009	
Yandusaurus	Bathonian-Callovian	He, 1979; He and Cai, 1984; Barrett et al., 2005	

Taxon	Age	References	Specimens Examined
Yinlong	Oxfordian	Xu et al., 2006	IVPP V14530
Yueosaurus	Albian-Cenomanian	Zheng et al., 2012	
Zalmoxes robustus	Maastrichtian	Weishampel et al., 2003	
Zalmoxes shqiperorum	Maastrichtian	Weishampel et al., 2003; Godefroit et al., 2009	
Zephyrosaurus	Aptian	Sues, 1980; Kutter, 2004	YPM 56695

APPENDIX 12

UNAMBIGUOUSLY OPTIMIZED CHARACTER STATE CHANGES FOR CHAPTER 5

A list of all unambiguously optimized character state changes for the phylogeny of basal ornithischian relationships presented in Chapter 5. Nodes listed below refer to those labeled in Figure 5.2. For each character change listed below, the character name is given followed by the CI for that character and the specific state change observed at that branch or internode.

Node 2→ Node 54
225 1.00 0 → 1
Node 53 →*Silesaurus opolensis*
47 0.50 2 → 1
148 0.43 0 → 1
151 0.33 0 → 1
Node 53 →*Asilisaurus kongwe*
207 0.17 0 → 1
219 1.00 1 → 0
Node 2 → Node 3
184 0.25 0 → 1
199 1.00 0 → 1
230 1.00 0 → 1
237 1.00 0 → 1
Node 3 →Node 52
120 0.20 0 → 1
133 0.33 0 → 1
205 0.20 0 → 1
211 0.25 0 → 1
Node 52 → Node 53
183 0.33 0 → 1
229 1.00 1 → 0
Node 52 →*Tawa hallae*
56 0.33 0 → 1
88 0.33 0 → 1
112 0.29 1 → 2
179 0.50 0 → 1
Node 3 → Node 4
19 1.00 0 → 1
80 1.00 0 → 1

82 1.00 0 → 1
117 0.40 0 → 1
131 0.50 0 → 1
236 0.33 2 → 0

Node 4 → *Pisanosaurus mertii*

127 0.14 0 → 1

Node 4 → Node 5

200 0.14 1 → 0
229 1.00 1 → 2

Node 5 → Node 48

183 0.33 0 → 1

Node 48 → Node 49

77 0.25 0 → 1

Node 49 → Node 50

134 1.00 0 → 1

Node 50 → Node 51

113 1.00 0 → 1
148 0.43 1 → 2
214 0.20 0 → 1
217 0.50 1 → 2

Node 51 → *Heterodontosaurus tucki*

15 0.33 1 → 0
16 0.20 0 → 1
38 0.50 0 → 3
68 0.33 1 → 0
117 0.40 1 → 2
120 0.20 0 → 1
121 0.20 0 → 1
127 0.14 0 → 1
128 0.17 0 → 1
129 0.25 0 → 1
130 0.25 1 → 0
133 0.33 0 → 1
139 0.17 0 → 1
168 0.25 0 → 1
202 0.20 1 → 0
207 0.17 0 → 1

Node 51 → *Fruitadens haagarorum*

18 0.50 0 → 1
116 0.50 1 → 0

Node 51 → *Tianyulong confuciusi*

75 0.14 0 → 1
83 0.25 0 → 1
167 0.17 0 → 1

222 0.17 0 → 1
250 0.25 0 → 1
Node 5 → Node 6
12 0.25 0 → 1
18 0.50 0 → 1
71 1.00 0 → 1
73 1.00 0 → 1
109 0.25 2 → 1
116 0.50 1 → 0
137 0.22 1 → 2
147 0.50 0 → 1
240 0.50 0 → 1
Node 6 → Node 45
52 0.50 1 → 0
86 0.67 0 → 1
112 0.29 1 → 0
122 0.67 1 → 0
131 0.50 1 → 0
Node 45 →*Lesothosaurus diagnosticus*
21 0.50 0 → 1
118 0.33 0 → 1
184 0.25 1 → 0
234 0.60 0 → 3
Node 45 → Node 46
32 1.00 0 → 1
253 1.00 0 → 1
Node 46 → Node 47
8 0.33 1 → 0
78 1.00 0 → 1
Node 46 →*Scelidosaurus harrisonii*
254 1.00 0 → 1
Node 6 → Node 7
190 1.00 0 → 1
203 0.33 0 → 1
Node 7 →*Stormbergia dangershoeki*
169 0.22 0 → 1
172 0.50 0 → 1
206 0.17 0 → 1
227 0.14 1 → 0
Node 7 → Node 8
145 0.50 0 → 1
192 1.00 0 → 1
197 0.43 0 → 2

198 0.50 0 → 1

Node 8 → *Agilisaurus louderbacki*

5 0.40 0 → 1
8 0.33 1 → 0
23 0.50 1 → 2
25 0.20 1 → 0
27 0.50 0 → 1
28 0.25 0 → 1
29 0.29 1 → 0
45 0.20 0 → 1
77 0.25 0 → 1
142 0.33 0 → 1
182 0.33 0 → 1
195 0.40 0 → 1

Node 8 → Node 9

57 0.25 0 → 1
183 0.33 0 → 1
184 0.25 1 → 0
189 0.50 0 → 1
202 0.20 1 → 0
232 0.56 0 → 1

Node 9 → *Hexinlusaurus multidens*

34 0.13 1 → 0
210 0.20 0 → 1
216 0.33 1 → 0
245 0.40 0 → 1

Node 9 → *Yandusaurus hongheensis*

159 0.50 0 → 1
160 0.40 1 → 0

Node 9 → *Leaellynasaura amicagraphica*

121 0.20 0 → 1
128 0.17 0 → 1
197 0.43 2 → 3
214 0.20 0 → 1

Node 9 → Node 10

114 0.20 0 → 1
137 0.22 2 → 1
148 0.43 1 → 2
191 0.50 0 → 1
212 1.00 0 → 1
218 0.50 0 → 1
238 0.20 0 → 1

Node 10 → Node 44

167 0.17 1 → 0
Node 44 → *Jeholosaurus shangyuanensis*
209 0.20 0 → 1
Node 44 → *Yueosaurus tiantaiensis*
169 0.22 0 → 2
Node 10 → Node 11
152 0.25 0 → 1
210 0.20 0 → 1
227 0.14 1 → 0
Node 11 → *Othnielosaurus consors*
74 0.38 2 → 1
99 0.25 0 → 1
105 0.20 1 → 0
108 0.40 0 → 1
157 0.33 0 → 1
201 0.40 0 → 1
234 0.60 0 → 2
235 0.50 0 → 1
Node 11 → Node 12
77 0.25 0 → 1
139 0.17 0 → 1
Node 12 → Node 33
5 0.40 0 → 1
14 1.00 0 → 1
98 0.50 0 → 1
213 0.33 0 → 1
242 0.20 1 → 0
255 0.33 0 → 1
Node 33 → Node 34
23 0.50 1 → 2
25 0.20 1 → 0
51 0.50 0 → 1
86 0.67 0 → 2
210 0.20 1 → 0
Node 34 → Node 36
55 0.25 0 → 1
144 0.17 0 → 1
157 0.33 0 → 1
204 0.50 0 → 1
209 0.20 0 → 1
221 0.33 0 → 1
250 0.25 0 → 1
252 0.25 1 → 0
Node 36 → New Parksosaurus

76 0.33 1 → 0
94 0.33 0 → 1
135 0.50 0 → 1
139 0.17 1 → 0
152 0.25 1 → 0
186 0.25 0 → 1
200 0.14 0 → 1
201 0.40 0 → 2
214 0.20 0 → 1
227 0.14 0 → 1

Node 36 → Node 37

169 0.22 1 → 0
185 0.17 0 → 1
226 0.17 0 → 1

Node 37 → Node 39

222 0.17 0 → 1

Node 39 →*Thescelosaurus neglectus*

110 0.33 0 → 1

Node 39 →*Thescelosaurus assiniboiensis*

99 0.25 0 → 1
156 0.40 0 → 2
186 0.25 0 → 1
195 0.40 0 → 1

Node 37 → Node 38

145 0.50 1 → 0
168 0.25 0 → 2
197 0.43 2 → 1
205 0.25 0 → 1

Node 79 →*Macrogryphosaurus gondwanicus*

141 0.50 0 → 1

Node 34 → Node 35

74 0.38 2 → 1
75 0.14 0 → 1

Node 35 →*Haya griva*

5 0.40 1 → 0
12 0.25 1 → 0
68 0.33 1 → 0
85 0.20 1 → 0
92 0.50 0 → 1
167 0.17 1 → 0
255 0.33 1 → 0

Node 35 →*Changchunsaurus parvus*

38 0.50 0 → 2
44 0.25 0 → 1

59 0.20 1 → 0
114 0.20 1 → 0
121 0.20 0 → 1
Node 33 → Node 40
108 0.40 0 → 1
114 0.20 1 → 0
143 0.33 1 → 2
148 0.43 2 → 3
158 1.00 0 → 1
233 1.00 0 → 1
Node 40 → Node 43
144 0.17 0 → 1
Node 43 →*Oryctodromeus cubicularis*
146 0.25 0 → 1
149 0.50 0 → 1
163 0.50 0 → 1
222 0.17 0 → 1
Node 43 →*Koreanosaurus boseongensis*
159 0.50 0 → 1
162 0.25 0 → 1
227 0.14 0 → 1
Node 40 → Node 41
38 0.50 0 → 3
55 0.25 0 → 1
Node 41 →*Zephyrosaurus schaffi*
5 0.40 1 → 0
27 0.50 0 → 1
91 0.25 1 → 0
99 0.25 0 → 1
109 0.25 1 → 2
201 0.40 0 → 1
205 0.25 0 → 1
236 0.33 0 → 2
Node 41 → Node 42
122 0.67 1 → 0
210 0.20 1 → 0
Node 42 →*Orodromeus makelai*
62 0.33 0 → 1
222 0.17 0 → 1
Node 42 →*Skaladromeus goldenii*
144 0.17 0 → 1
163 0.50 0 → 1
180 0.67 0 → 1
232 0.56 1 → 0

242 0.20 0 → 1

Node 12 → Node 13

26 0.33 1 → 0
52 0.50 1 → 0
112 0.29 1 → 2
120 0.20 0 → 1
123 0.33 0 → 1
124 0.33 0 → 1
252 0.25 1 → 0

Node 13 → Node 29

87 0.25 0 → 2
197 0.43 2 → 3
203 0.33 1 → 0

Node 29 → Node 30

186 0.25 0 → 1

Node 30 → Node 32

85 0.20 1 → 0

Node 32 → *Archaeoceratops oshimoi*

81 0.20 0 → 1
133 0.33 0 → 1

Node 30 → Node 31

16 0.20 0 → 1
50 0.25 1 → 0

Node 31 → *Liaoceratops yanzigouensis*

38 0.50 1 → 2
75 0.14 0 → 1

Node 31 → *Yinlong downsi*

26 0.33 0 → 1
45 0.20 0 → 1
46 1.00 0 → 1
47 0.50 0 → 1
97 0.50 1 → 0
120 0.20 1 → 0
127 0.14 1 → 0

Node 32 → *Wannanosaurus yansiensis*

23 0.50 1 → 2
24 1.00 0 → 1
63 0.25 0 → 1
114 0.20 1 → 0
130 0.25 1 → 0
139 0.17 1 → 0

Node 13 → Node 14

28 0.25 0 → 1
29 0.29 2 → 1

31 0.33 1 → 0
117 0.40 1 → 2
126 0.25 1 → 0
132 0.44 2 → 0
250 0.25 0 → 1

Node 14 → *Hypsilophodon foxii*

83 0.25 0 → 1
92 0.50 0 → 1
96 0.50 0 → 1
98 0.50 0 → 1
112 0.29 2 → 0
157 0.33 0 → 1
161 0.50 0 → 1
196 0.50 0 → 1
204 0.50 0 → 1
232 0.56 1 → 2
234 0.60 0 → 1
245 0.40 0 → 1

Node 14 → Node 15

49 1.00 0 → 1
75 0.14 0 → 1
108 0.40 0 → 2
119 0.50 0 → 1
130 0.25 1 → 0
149 0.50 0 → 1
200 0.14 0 → 1
207 0.17 0 → 1
228 0.38 3 → 2

Node 15 → Node 26

124 0.33 1 → 0

Node 26 → *Atlascoposaurus loadsi*

138 0.33 0 → 1

Node 26 → Node 27

117 0.40 2 → 1

Node 27 → Node 28

75 0.14 1 → 0

Node 28 → *Qantassaurus intrepidus*

132 0.44 0 → 4

Node 27 → *Anabisetia saldivai*

139 0.17 1 → 0
168 0.43 1 → 2

Node 15 → Node 16

34 0.13 1 → 0
47 0.50 0 → 1

61 1.00 0 → 1
65 0.17 0 → 1
81 0.20 0 → 1
132 0.44 0 → 1
136 1.00 0 → 1
182 0.33 0 → 1
208 0.50 0 → 1
221 0.25 0 → 1
224 0.50 0 → 1
226 0.17 0 → 1

Node 16 → Node 24

28 0.25 1 → 0
29 0.29 1 → 2
64 0.50 0 → 1
74 0.38 2 → 0
105 0.20 1 → 0
148 0.43 2 → 3
149 0.50 1 → 2
184 0.25 0 → 1
186 0.25 0 → 1
213 0.33 0 → 1
227 0.14 0 → 1
238 0.20 1 → 0

Node 24 → *Zalmoxes robustus*

207 0.17 1 → 0

Node 16 → Node 25

37 0.50 1 → 0
101 0.17 0 → 1
127 0.14 1 → 0
142 0.25 0 → 1
205 0.20 1 → 0
232 0.56 1 → 3

Node 25 → *Tenontosaurus dossi*

17 0.50 0 → 1
111 0.50 1 → 0
195 0.40 0 → 1
227 0.14 0 → 1
245 0.40 0 → 1

Node 25 → *Tenontosaurus tilletti*

34 0.13 0 → 1
41 0.43 0 → 1
62 0.33 0 → 1
69 0.20 1 → 0
88 0.33 0 → 1

96 0.50 0 → 1
206 0.17 1 → 0
207 0.17 1 → 0
Node 16 →*Rhabdodon priscus*
84 0.50 0 → 1
168 0.25 1 → 0
193 0.33 0 → 2
203 0.25 1 → 0
221 0.25 1 → 0
235 0.33 0 → 1
Node 16 → Node 17
36 0.50 0 → 1
51 0.50 0 → 1
142 0.25 0 → 1
235 0.33 0 → 1
Node 17 →*Muttaburrasaurus longdoni*
90 1.00 0 → 1
117 0.40 2 → 1
Node 17 → Node 18
31 0.33 0 → 1
118 0.33 0 → 1
161 0.50 0 → 1
Node 18 → Node 19
208 0.50 1 → 0
220 1.00 0 → 1
221 0.33 1 → 0
Node 19 → Node 21
223 0.50 1 → 2
Node 21 →*Elrhazosaurus nigeriensis*
224 0.50 1 → 0
232 0.56 3 → 0
Node 19 → Node 20
209 0.20 0 → 1
215 0.50 0 → 1
244 0.50 1 → 0
Node 20 →*Dysalotosaurus lettowvorbecki*
55 0.25 0 → 1
74 0.38 2 → 1
75 0.14 1 → 0
106 0.33 0 → 1
109 0.25 0 → 2
193 0.33 0 → 1
Node 20 →*Dryosaurus altus*

28 0.25 1 → 0
85 0.20 1 → 0
171 0.25 1 → 0
223 0.50 1 → 0
241 0.33 0 → 1

Node 19 →*Callovosaurus leedsi*

217 0.40 2 → 1

Node 18 → Node 22

4 1.00 0 → 1
34 0.13 0 → 1
40 1.00 0 → 1
54 0.33 0 → 1
69 0.20 1 → 0
99 0.25 0 → 1
100 1.00 0 → 1
105 0.20 1 → 0
127 0.14 1 → 0
139 0.17 1 → 0
150 1.00 0 → 1
172 0.50 0 → 1
174 1.00 0 → 1
252 0.25 0 → 1

Node 22 →*Camptosaurus dispar*

56 0.33 0 → 1
107 0.33 0 → 1
142 0.33 1 → 0
185 0.17 1 → 0

Node 22 → Node 23

29 0.29 1 → 2
36 0.50 1 → 0
39 1.00 0 → 2
45 0.20 0 → 1
64 0.50 0 → 1
77 0.25 1 → 0
101 0.17 0 → 1
109 0.25 0 → 2
169 0.22 1 → 2
170 0.50 0 → 1
171 0.25 1 → 0
231 0.50 0 → 1

Node 23 →*Iguanodon bernissartensis*

83 0.25 1 → 2

Node 23 →*Ouranosaurus nigeriensis*

30	0.25	$1 \rightarrow 0$
53	0.17	$1 \rightarrow 0$
72	0.25	$1 \rightarrow 0$
108	0.40	$2 \rightarrow 0$
211	0.25	$1 \rightarrow 0$

APPENDIX 13

BIOGEOGRAPHICAL ANCESTRAL STATE RECONSTRUCTION

Results from the biogeographical ancestral state reconstructions. Nodes correspond to those labeled in Figures 5.3 and 5.4. Under the 'Analysis' column, the label 'PB' refers to parsimony-based analysis, 'LEB' refers to the likelihood-based analysis where all branch lengths were set equal to each other, and 'LFR' refers to the likelihood-based analysis with branch lengths set equal to implied missing fossil records. In each row, the most-likely ancestral area(s) are highlighted in bold text.

Node	Analysis	Africa	South America	Asia	North America	Europe	Australia
1	PB	0.0	**100.0**	0.0	0.0	0.0	0.0
	LEB	7.5	**79.8**	2.3	3.1	5.0	2.3
	LFR	**52.5**	34.8	2.8	2.8	4.2	2.8
2	PB	0.0	**100.0**	0.0	0.0	0.0	0.0
	LEB	15.2	**68.0**	2.0	4.0	8.8	2.0
	LFR	**61.0**	29.0	2.1	2.1	3.7	2.1
3	PB	0.0	**100.0**	0.0	0.0	0.0	0.0
	LEB	12.0	**75.5**	1.4	6.3	3.4	1.4
	LFR	0.5	**99.0**	0.1	0.2	0.1	0.1
4	PB	0.0	**100.0**	0.0	0.0	0.0	0.0
	LEB	17.9	**74.5**	1.4	2.8	2.1	1.2
	LFR	0.5	**99.2**	<0.1	0.1	<0.1	<0.1
5	PB	**100.0**	0.0	0.0	0.0	0.0	0.0
	LEB	**80.0**	12.0	2.2	1.9	2.6	1.2
	LFR	**92.8**	3.4	1.0	1.0	0.9	0.9
6	PB	**100.0**	0.0	0.0	0.0	0.0	0.0
	LEB	**86.1**	3.9	4.1	2.3	2.5	1.0
	LFR	**97.7**	<0.1	1.1	0.8	0.3	<0.1
7	PB	**100.0**	0.0	0.0	0.0	0.0	0.0
	LEB	**82.2**	1.9	11.9	1.5	1.5	1.1
	LFR	**97.2**	<0.1	2.2	0.4	0.1	<0.1
8	PB	0.0	0.0	**100.0**	0.0	0.0	0.0
	LEB	6.4	0.7	**90.8**	0.7	0.6	0.7
	LFR	41.2	0.7	**55.8**	0.8	0.7	0.7
9	PB	0.0	0.0	**100.0**	0.0	0.0	0.0
	LEB	0.4	<0.1	**98.2**	0.4	<0.1	0.7
	LFR	<0.1	<0.1	**99.9**	<0.1	<0.1	<0.1
10	PB	0.0	0.0	**100.0**	0.0	0.0	0.0
	LEB	0.6	0.5	**93.2**	0.4	0.6	0.6
	LFR	1.0	1.0	**85.7**	6.3	5.0	1.1

Node	Analysis	Africa	South America	Asia	North America	Europe	Australia
11	PB	0.0	0.0	50.0	**50.0**	0.0	0.0
	LEB	1.2	1.2	42.9	**50.7**	2.8	1.2
	LFR	1.0	1.0	**81.1**	8.8	6.9	1.2
12	PB	0.0	0.0	50.0	**50.0**	0.0	0.0
	LEB	1.3	1.4	41.0	**48.1**	6.7	1.4
	LFR	1.1	1.1	**79.0**	8.1	9.4	1.3
13	PB	0.0	0.0	**33.3**	**33.3**	**33.3**	0.0
	LEB	1.9	2.1	**47.4**	15.8	30.1	2.5
	LFR	1.1	1.0	**77.2**	7.2	12.2	1.3
14	PB	0.0	0.0	0.0	0.0	**100.0**	0.0
	LEB	1.2	2.1	8.2	3.8	**81.2**	3.4
	LFR	2.1	1.9	**60.6**	9.1	23.7	2.6
15	PB	0.0	0.0	0.0	0.0	**100.0**	0.0
	LEB	1.3	4.2	3.5	2.9	**79.5**	8.5
	LFR	2.7	2.3	**47.0**	10.9	33.4	3.6
16	PB	0.0	0.0	0.0	0.0	**100.0**	0.0
	LEB	0.2	0.2	0.2	2.2	**95.9**	1.4
	LFR	3.0	2.4	34.6	12.6	**44.0**	3.4
17	PB	0.0	0.0	0.0	0.0	**100.0**	0.0
	LEB	3.0	1.2	1.2	4.1	**74.2**	16.2
	LFR	2.9	2.1	23.2	13.6	**55.3**	2.8
18	PB	0.0	0.0	0.0	0.0	**100.0**	0.0
	LEB	7.6	1.1	1.1	8.4	**76.9**	5.0
	LFR	2.4	1.4	12.5	14.5	**67.5**	1.8
19	PB	0.0	0.0	0.0	0.0	**100.0**	0.0
	LEB	10.7	0.4	0.4	4.4	**83.3**	0.9
	LFR	1.8	0.6	4.1	8.8	**84.0**	0.7
20	PB	**33.3**	0.0	**33.3**	**33.3**	0.0	0.0
	LEB	**36.3**	2.2	2.2	31.0	25.9	2.3
	LFR	44.7	0.7	0.9	**49.4**	3.5	0.7

Node	Analysis	Africa	South America	Asia	North America	Europe	Australia
21	PB	0.0	0.0	0.0	0.0	**100.0**	0.0
	LEB	17.3	0.8	0.8	1.9	**78.4**	0.9
	LFR	1.8	0.9	0.9	1.0	**94.6**	0.9
22	PB	0.0	0.0	0.0	0.0	**100.0**	0.0
	LEB	11.0	1.7	1.7	24.4	**58.3**	2.9
	LFR	1.4	1.2	1.9	**81.9**	12.3	1.3
23	PB	0.0	0.0	0.0	0.0	**100.0**	0.0
	LEB	23.6	1.6	1.6	8.1	**63.3**	1.9
	LFR	3.9	1.4	1.4	3.4	**88.6**	1.4
24	PB	0.0	0.0	0.0	0.0	**100.0**	0.0
	LEB	<0.1	<0.1	<0.1	<0.1	**99.4**	<0.1
	LFR	<0.1	<0.1	<0.1	<0.1	**99.9**	<0.1
25	PB	0.0	0.0	0.0	**100.0**	0.0	0.0
	LEB	0.5	0.5	0.5	**91.1**	6.7	0.6
	LFR	<0.1	<0.1	<0.1	**99.9**	<0.1	<0.1
26	PB	0.0	**33.3**	0.0	0.0	**33.3**	**33.3**
	LEB	2.3	22.4	2.9	2.7	22.9	**46.7**
	LFR	3.1	3.3	3.9	3.2	3.7	**82.8**
27	PB	0.0	**50.0**	0.0	0.0	0.0	**50.0**
	LEB	1.2	**67.6**	1.3	1.2	4.3	24.5
	LFR	2.2	2.5	2.7	2.2	2.5	**87.9**
28	PB	0.0	**50.0**	0.0	0.0	0.0	**50.0**
	LEB	1.0	**65.6**	1.0	1.0	1.9	29.4
	LFR	1.1	1.3	1.4	1.2	1.3	**93.6**
29	PB	0.0	0.0	**50.0**	0.0	**50.0**	50.0
	LEB	0.7	0.8	**78.0**	2.5	17.2	0.8
	LFR	1.0	1.0	**85.8**	3.1	8.1	1.1
30	PB	0.0	0.0	**100.0**	0.0	0.0	0.0
	LEB	0.2	0.2	**97.5**	0.4	1.5	0.2
	LFR	0.7	0.7	**91.0**	1.9	4.8	0.8

Node	Analysis	Africa	South America	Asia	North America	Europe	Australia
31	PB	0.0	0.0	**100.0**	0.0	0.0	0.0
	LEB	<0.1	<0.1	**99.6**	<0.1	<0.1	<0.1
	LFR	0.4	0.4	**95.8**	0.9	2.1	0.4
32	PB	0.0	0.0	**100.0**	0.0	0.0	0.0
	LEB	<0.1	<0.1	**99.6**	0.4	<0.1	<0.1
	LFR	1.2	1.2	**94.0**	1.2	1.2	1.2
33	PB	0.0	0.0	**50.0**	**50.0**	0.0	0.0
	LEB	0.8	1.0	20.8	**64.6**	1.9	0.9
	LFR	1.9	2.4	42.3	**49.5**	1.9	1.9
34	PB	0.0	0.0	**50.0**	**50.0**	0.0	0.0
	LEB	1.0	1.5	34.9	**60.2**	1.3	1.0
	LFR	1.8	2.6	**60.7**	31.3	1.8	1.8
35	PB	0.0	0.0	**100.0**	0.0	0.0	0.0
	LEB	0.4	0.5	**94.1**	4.2	0.4	0.4
	LFR	1.1	1.5	**80.9**	14.3	1.1	1.1
36	PB	0.0	0.0	0.0	**100.0**	0.0	0.0
	LEB	0.7	3.2	5.9	**88.7**	0.8	0.7
	LFR	3.0	**81.1**	4.0	5.9	3.0	3.0
37	PB	0.0	0.0	0.0	**100.0**	0.0	0.0
	LEB	0.9	11.5	2.4	**83.4**	0.9	0.9
	LFR	1.7	**88.9**	2.2	3.7	1.7	1.7
38	PB	0.0	**100.0**	0.0	0.0	0.0	0.0
	LEB	0.1	**99.3**	0.1	0.5	0.1	0.1
	LFR	0.3	**98.4**	0.3	0.5	0.3	0.3
39	PB	0.0	0.0	0.0	**100.0**	0.0	0.0
	LEB	<0.1	<0.1	<0.1	**99.9**	<0.1	<0.1
	LFR	<0.1	<0.1	<0.1	**99.9**	<0.1	<0.1
40	PB	0.0	0.0	**50.0**	**50.0**	0.0	0.0
	LEB	0.5	0.6	16.3	**81.3**	0.7	0.6
	LFR	1.5	1.8	23.3	**70.4**	1.5	1.5

Node	Analysis	Africa	South America	Asia	North America	Europe	Australia
41	PB	0.0	0.0	0.0	**100.0**	0.0	0.0
	LEB	0.7	0.7	21.2	**75.9**	0.8	0.8
	LFR	1.0	1.0	10.8	**85.4**	0.9	0.9
42	PB	0.0	0.0	0.0	**100.0**	0.0	0.0
	LEB	0.2	0.2	1.3	**98.0**	0.2	0.2
	LFR	<0.1	<0.1	<0.1	**99.9**	<0.1	<0.1
43	PB	0.0	0.0	**50.0**	**50.0**	0.0	0.0
	LEB	0.1	0.1	0.1	**99.6**	0.1	0.1
	LFR	1.1	1.1	4.1	**91.4**	1.1	1.1
44	PB	0.0	0.0	**100.0**	0.0	0.0	0.0
	LEB	0.1	0.1	**99.2**	0.3	0.1	0.1
	LFR	0.6	0.6	**97.0**	0.6	0.6	0.6
45	PB	**100.0**	0.0	0.0	0.0	0.0	0.0
	LEB	**85.2**	2.0	2.0	5.0	4.8	1.1
	LFR	**97.2**	<0.1	0.4	1.8	0.5	<0.1
46	PB	**33.3**	0.0	0.0	**33.3**	**33.3**	0.0
	LEB	27.3	2.8	2.8	**33.6**	30.9	2.5
	LFR	41.5	0.7	0.9	**43.5**	12.7	0.7
47	PB	0.0	0.0	0.0	0.0	**100.0**	0.0
	LEB	2.1	0.6	0.6	2.5	**93.7**	0.5
	LFR	3.9	0.5	0.5	0.4	**90.6**	0.5
48	PB	**100.0**	0.0	0.0	0.0	0.0	0.0
	LEB	**93.2**	2.2	0.7	0.6	2.8	0.5
	LFR	**97.7**	1.0	0.3	0.3	0.3	0.3
49	PB	**100.0**	0.0	0.0	0.0	0.0	0.0
	LEB	**85.1**	1.3	0.9	0.9	11.0	0.8
	LFR	**96.6**	0.7	0.7	0.7	0.7	0.7
50	PB	**100.0**	0.0	0.0	0.0	0.0	0.0
	LEB	**97.9**	-.2	0.3	0.3	1.0	0.2
	LFR	**99.9**	<0.1	<0.1	<0.1	<0.1	<0.1

Node	Analysis	Africa	South America	Asia	North America	Europe	Australia
51	PB	**100.0**	0.0	0.0	0.0	0.0	0.0
	LEB	**98.1**	0.1	0.8	0.8	0.1	0.1
	LFR	**99.9**	<0.1	<0.1	<0.1	<0.1	<0.1
52	PB	0.0	**100.0**	0.0	0.0	0.0	0.0
	LEB	4.4	**74.5**	1.3	16.7	1.8	1.3
	LFR	0.3	**99.2**	<0.1	0.3	<0.1	<0.1
53	PB	0.0	**100.0**	0.0	0.0	0.0	0.0
	LEB	0.4	**97.6**	0.2	1.2	0.3	0.2
	LFR	<0.1	**99.9**	<0.1	<0.1	<0.1	<0.1
54	PB	**33.3**	**33.3**	0.0	0.0	**33.3**	0.0
	LEB	**37.9**	21.7	2.5	3.0	32.5	2.4
	LFR	**78.8**	14.0	1.3	1.3	3.4	1.3

REFERENCES

Alcober, O. A., and R. N. Martinez. 2010. A new herrerasaurid (Dinosauria, Saurischia) from the Upper Triassic Ischigualasto Formation of northwestern Argentina. ZooKeys 63:55-81.

Angielczyk, K. D., and A. A. Kurkin. 2003. Phylogenetic analysis of Russian Permian dicynodonts (Therapsida: Anomodontia): implications for Permian biostratigraphy and Pangaean biogeography. Zoological Journal of the Linnean Society 139:157-212.

Bakker, R. T., P. M. Galton, J. Siegwarth, and J. Filla. 1990. A new latest Jurassic vertebrate fauna from the highest levels of the Morrison Formation at Como Bluff, Wyoming. Part 4. The dinosaurs: A new *Othnielia*-like hypsilophodontid. Hunteria 2:1-24.

Barrett, P. M., and F.-L. Han. 2009. Cranial anatomy of *Jeholosaurus shangyuanensis* (Dinosauria: Ornithischia) from the Early Cretaceous of China. Zootaxa 2072:31-55.

Barrett, P. M., R. J. Butler, and F. Knoll. 2005. Small-bodied ornithischian dinosaurs from the Middle Jurassic of Sichuan, China. Journal of Vertebrate Paleontology 25:823-834.

Barrett, P. M., R. J. Butler, R. J. Twitchett, and S. Hutt. 2011. New material of *Valdosaurus canaliculatus* (Ornithischia: Ornithopoda) from the Lower Cretaceous of southern England. Special Papers in Palaeontology 86:131-163.

Bartholomai, A., and R. E. Molnar. 1981. *Muttaburrasaurus*, a new iguanodontid (Ornithischia: Ornithopoda) dinosaur from the Lower Cretaceous of Queensland. Memoirs of the Queensland Museum 20:319-349.

Benton, M. J., and G. W. Storrs. 1994. Testing the quality of the fossil record: paleontological knowledge is improving. Geology 22:111-114.

Bonaparte, J. F. 1976. *Pisanosaurus mertii* Casamiquela and the origin of the Ornithischia. Journal of Paleontology 50:808-820.

Bonaparte, J. F., and J. E. Powell. 1980. A continental assemblage of tetrapods from the Upper Cretaceous bed of El Brete, northwestern Argentina (Sauropoda-Coelurosauria-Carnosauria-Aves). Memoires de la Societe Geologique, France 139:19-28.

Boulenger, G. A. 1881. Sur l'arc pelvien chez les dinosauriens de Bernissart. Bulletins de L'Académie royale de Belgique, 3eme série 1:600-608.

Boyd, C. A., C. M. Brown, R. D. Scheetz, and J. A. Clarke. 2009. Taxonomic revision of the basal neornithischian taxa *Thescelosaurus* and *Bugenasaura*. Journal of Vertebrate Paleontology 29:758-770.

Boyd, C. A., T. P. Cleland, N. L. Marrero, and J. A. Clarke. 2011a. Exploring the effects of phylogenetic uncertainty and consensus trees on stratigraphic consistency scores: a new program and a standardized method. Cladistics 26:1-9.

Boyd, C. A., T. P. Cleland, and F. E. Novas. 2011b. Osteogenesis, homology, and function of the intercostal plates in ornithischian dinosaurs (Tetrapoda, Sauropsida). Zoomorphology 130:305-313.

Brett-Surman, M. K., and G. S. Paul. 1985. A new family of bird-like dinosaurs linking Laurasia and Gondwanaland. Journal of Vertebrate Paleontology 5:133-138.

Brochu, C. A. 1996. Closure of neurocentral sutures during crocodilian ontogeny: implications for maturity assessment in fossil archosaurs. Journal of Vertebrate Paleontology 16:49-62.

Brochu, C. A., and M. A. Norell. 2000. Temporal congruence and the origin of birds. Journal of Vertebrate Paleontology 20:197-200.

Broom, R. 1911. On the dinosaurs of the Stormberg, South Africa. Annals of the South African Museum 7:291-308.

Brown, B. 1908. The Ankylosauridae, a new family of armored dinosaurs from the Upper Cretaceous. Bulletin of the American Museum of Natural History 24:187-201.

Brown, C. M., C. A. Boyd, and A. Russell. 2011. A new basal ornithopod dinosaur (Frenchman Formation, Saskatchewan, Canada), and implications for late Maastrichtian ornithischian diversity in North America. Zoological Journal of the Linnean Society 163:1157-1198.

Brusatte, S. L., and P. C. Sereno. 2008. Phylogeny of Allosauroidea (Dinosauria: Theropoda): comparative analysis and resolution. Journal of Systematic Paleontology 6:155-182.

Brusatte, S. L., R. J. Butler, T. Sulej, and G. Niedzwiedzki. 2009. The taxonomy and anatomy of rauisuchian archosaurs from the Late Triassic of Germany and Poland. Acta Palaeontologica Polonica 54:221-230.

Brusatte, S. L., S. J. Nesbitt, R. B. Irmis, R. J. Butler, M. J. Benton, and M. A. Norell. 2010. The origin and early radiation of dinosaurs. Earth-Science Reviews 101:68-100.

Buchholz, P. W. 2002. Phylogeny and biogeography of basal Ornithischia; pp. 18-34 in D. E. Brown (ed.), The Mesozoic in Wyoming. Tate Geological Museum, Casper.

Butler, R. J. 2005. The 'fabrosaurid' ornithischian dinosaurs of the Upper Elliot Formation (Lower Jurassic) of South Africa and Lesotho. Zoological Journal of the Linnean Society 145:175-218.

Butler, R. J. 2010. The anatomy of the basal ornithischian dinosaur *Eocursor parvus* from the lower Elliot Formation (Late Triassic) of South Africa. Zoological Journal of the Linnean Society 160:648-684.

Butler, R. J., and P. M. Galton. 2008. The 'dermal armour' of the ornithopod dinosaur *Hypsilophodon* from the Wealden (Early Cretaceous: Barremian) of the Isle of Wight: a reappraisal. Cretaceous Research 29:636-642.

Butler, R. J., and R. M. Sullivan. 2009. The phylogenetic position of the ornithischian dinosaur *Stenopelix valdensis* from the Lower Cretaceous of Germany and the early fossil record of Pachycephalosauria. Acta Palaeontologica Polonica 54:21-34.

Butler, R. J., and Q. Zhao. 2009. The small-bodied ornithischian dinosaurs *Micropachycephalosaurus hongtuyanensis* and *Wannanosaurus yansiensis* from the Late Cretaceous of China. Cretaceous Research 30:63-77.

Butler, R. J., P. Upchurch, D. B. Norman, and J. Parish. 2006. A biogeographical analysis of the ornithischian dinosaurs; pp. 13-16 in P. M. Barrett and S. E. Evans (eds.), Ninth Symposium on Mesozoic Terrestrial Ecosystems and Biota. The Natural History Museum, London.

Butler, R. J., R. M. H. Smith, and D. B. Norman. 2007. A primitive ornithischian dinosaur from the Late Triassic of South Africa, and the early evolution and diversification of Ornithischia. Proceedings of the Royal Society B 274:2041-2046.

Butler, R. J., P. Upchurch, and D. B. Norman. 2008a. The phylogeny of the ornithischian dinosaurs. Journal of Systematic Paleontology 6:1-40.

Butler, R. J., L. B. Porro, and D. B. Norman. 2008b. A juvenile skull of the primitive ornithischian dinosaur *Heterodontosaurus tucki* from the 'Stormberg' of southern Africa. Journal of Vertebrate Paleontology 28:702-711.

Butler, R. J., P. M. Galton, L. B. Porro, L. M. Chiappe, D. M. Henderson, and G. M. Erickson. 2010. Lower limits of ornithischian dinosaur body size inferred from a new Upper Jurassic heterodontosaurid from North America. Proceedings of the Royal Society B 277:375-381.

Butler, R. J., L. Y. Jin, J. Chen, and P. Godefroit. 2011. The postcranial osteology and phylogenetic position of the small ornithischian dinosaur *Changchunsaurus parvus* from the Quantou Formation (Cretaceous: Aptian-Cenomanian) of Jilin Province, northeastern China. Palaeontology 54:667-683.

Butler, R. J., L. B. Porro, P. M. Galton, and L. M. Chiappe. in press. Anatomy and cranial functional morphology of the small-bodied dinosaur *Fruitadens haagarorum* (Ornithischia: Heterodontosauridae) from the Upper Jurassic of the USA. PLoS ONE.

Calvo, J. O., J. D. Porfiri, and F. E. Novas. 2007. Discovery of a new ornithopod dinosaur from the Portezuelo Formation (Upper Cretaceous), Neuquen, Patagonia, Argentina. Arquivos do Museu Nacional 65:471-483.

Casamiquela, R. M. 1967. Un nuevo dinosaurio ornitischio Triásico (*Pisanosaurus mertii*: Ornithopoda) de la Formación Ischigualasto, Argentina. Ameghiniana 4:47-64.

Clarke, J. A., D. T. Ksepka, M. Stucchi, M. Urbina, N. Giannini, S. Bertelli, Y. Narvaez, and C. A. Boyd. 2007. Paleogene equatorial penguins challenge the proposed relationship between biogeography, diversity, and Cenozoic climate change. Proceedings of the National Academy of Sciences 104:11545-11550.

Cleland, T. P., M. K. Stoskopf, and M. H. Schweitzer. 2011. Histological, chemical, and morphological reexamination of the "heart" of a small Late Cretaceous *Thescelosaurus*. Naturwissenschaften 98:203-211.

Colbert, E. H. 1981. A primitive ornithischian dinosaur from the Kayenta Formation of Arizona. Bulletin of the Museum of Northern Arizona 53:1-61.

Cooper, M. R. 1985. A revision of the ornithischian dinosaur *Kangnasaurus coetzeei* Haughton with a classification of the Ornithischia. Annals of the South African Museum 95:281-317.

Coria, R. A. 1999. Ornithopod dinosaurs from the Neuquen Group, Patagonia, Argentina; pp. 47-60 in Y. Tomida, T. H. Rich, and P. Vickers-Rich (eds.), Proceedings of the Second Gondwana Dinosaur Museum. National Science Museum Monographs, Tokyo.

Coria, R. A., and J. O. Calvo. 2002. A new iguanodontian ornithopod from Neuquen Basin, Patagonia, Argentina. Journal of Vertebrate Paleontology 22:503-509.

Coria, R. A., and L. Salgado. 1996. A basal iguanodontian (Ornithischian: Ornithopoda) from the Late Cretaceous of South America. Journal of Vertebrate Paleontology 16:445-457.

Crompton, A. W., and A. J. Charig. 1962. A new ornithischian from the Upper Triassic of South Africa. Nature 196:1074-1077.

Currie, P. J. 1997. Braincase Anatomy; pp. 81-85 in P. J. Currie and K. Padian (eds.), Encyclopedia of Dinosaurs. Academic Press, San Diego.

Dodson, P. 1990. Marginocephalia; pp. 562-563 in D. B. Weishampel, P. Dodson, and H. Osmólska (eds.), The Dinosauria: First Edition. University of California Press, Berkeley.

Dollo, L. 1888. Iguanodontidae et Camptonotidae. Comptes Rendus de Académie des Sciences (Paris) 106:775-777.

Dong, Z. 1978. A new genus of Pachychepalosauria from Laiyang, Shantung. Vertebrata PalAsiatica 16:225-228.

Dong, Z. 1989. On a small ornithopod (*Gongbusaurus wucaiwanensis* sp. nov.) from Kelamaili Junggar Basin, Xinjiang, China. Vertebrata PalAsiatica 27:140-146.

Dong, Z., and Z. Tang. 1983. Note on the new mid-Jurassic ornithopod from the Sichuan Basin, China. Vertebrata PalAsiatica 21:168-172.

Dong, Z., and Y. Azuma. 1997. On a primitive neoceratopsian from the Early Cretaceous; pp. 68-89 in Z. M. Dong (ed.), Sino-Japanese Silk Road Dinosaur Expedition. China Ocean Press, Beijing.

Dong, Z., S. Zhou, and Z. Zhang. 1983. Dinosaurs from the Jurassic of Sichuan. Palaeontologica Sinica, New Series C 23:1-145.

Dzik, J. 2003. A beaked herbivorous archosaur with dinosaur affinities from the early Late Triassic of Poland. Journal of Vertebrate Paleontology 23:556-574.

Erickson, G. M., and T. Tumanova. 2000. Growth curve of *Psittacosaurus mongoliensis* Osborn (Ceratopsia: Psittacosauridae) inferred from long bone histology. Zoological Journal of the Linnean Society 130:551-566.

Erickson, G. M., P. J. Makovicky, P. J. Currie, M. A. Norell, S. A. Yerby, and C. A. Brochu. 2004. Gigantism and comparative life-history parameters of tyrannosaurid dinosaurs. Nature 430:772-775.

Erickson, G. M., P. J. Makovicky, B. D. Inouye, C.-F. Zhou, and K.-Q. Gao. 2009. A life table for *Psittacosaurus lujiatunensis*: initial insights into ornithischian dinosaur population biology. Paleobiology 292:1514-1521.

Ezcurra, M. D., and F. L. Agnolin. 2011. A new global palaeobiogeographical model for the Late Mesozoic and Early Tertiary. Systematic Biology.

Fisher, P. E., D. A. Russell, M. K. Stoskopf, R. E. Barrick, M. Hammer, and A. A. Kuzmitz. 2000. Cardiovascular evidence for an intermediate or higher metabolic rate in an ornithischian dinosaur. Science 288:503-505.

Forster, C. A. 1990. The postcranial skeleton of the ornithopod dinosaur *Tenontosaurus tilletti*. Journal of Vertebrate Paleontology 10:273-294.

Francillon-Vieillot, H., J. de Buffrenil, J. Castanet, J. Geraudie, F. J. Meunier, J. Y. Sire, L. Zylberberg, and A. J. de Ricqles. 1990. Microstructure and mineralization of vertebrate skeletal tissues; pp. 471-530 in J. G. Carter (ed.), Skeletal Biomineralization: Patterns, Processes and Evolutionary Trends. Van Nostrand Reinhold, New York.

Galton, P. M. 1971a. *Hypsilophodon* the cursorial non-arboreal dinosaur. Nature 231:159-161.

Galton, P. M. 1971b. The mode of life of *Hypsilophodon*, the supposedly arboreal ornithopod dinosaur. Lethaia 4:453-465.

Galton, P. M. 1972. Classification and evolution of ornithopod dinosaurs. Nature 239:464-466.

Galton, P. M. 1973. Redescription of the skull and mandible of *Parksosaurus* from the Late Cretaceous with comments on the family Hypsilophodontidae (Ornithischia). Life Science Contributions, Royal Ontario Museum 89:1-21.

Galton, P. M. 1974a. The ornithischian dinosaur *Hypsilophodon* from the Wealden of the Isle of Wight. Bulletin of the British Museum (Natural History) Geology 25:1-152.

Galton, P. M. 1974b. Notes on *Thescelosaurus*, a conservative ornithopod dinosaur from the Upper Cretaceous of North America, with comments on ornithopod classification. Journal of Paleontology 48:1048-1067.

Galton, P. M. 1975. English hypsilophodontid dinosaurs (Reptilia: Ornithischia). Palaeontology 18:741-752.

Galton, P. M. 1977. The ornithopod dinosaur *Dryosaurus* and a Laurasia-Gondwanaland connection in the Upper Jurassic. Nature 268:230-232.

Galton, P. M. 1978. Fabrosauridae, the basal family of ornithischian dinosaurs (Reptilia: Ornithopoda). Paläontologische Zeitschrift 52:138-159.

Galton, P. M. 1980. European Jurassic ornithopod dinosaurs of the families Hypsilophodontidae and Camptosauridae. Neues Jahrbuch für Geologie und Paläontologie, Abhandlungen 160:73-95.

Galton, P. M. 1981. *Dryosaurus*, a hypsilophodontid dinosaur from the Upper Jurassic of North America and Africa. Postcranial skeleton. Paläontologische Zeitschrift 55:271-312.

Galton, P. M. 1983. The cranial anatomy of *Dryosaurus*, a hypsilophodontid dinosaur from the Upper Jurassic of North America and east Africa, with a review of hypsilophodontids from the Upper Jurassic of North America. Geologica et Palaeontologica 17:207-243.

Galton, P. M. 1989. Crania and endocranial casts from ornithopod dinosaurs of the families Dryosauridae and Hypsilophodontidae (Reptilia: Ornithischia). Geologica et Palaeontologica 23:217-239.

Galton, P. M. 1995. The species of the basal hypsilophodontid dinosaur *Thescelosaurus* Gilmore (Ornithischia: Ornithopoda) from the Late Cretaceous of North America. Neues Jahrbuch für Geologie und Paläontologie Abhandlungen 198:291-311.

Galton, P. M. 1997. Cranial anatomy of the basal hypsilophodontid dinosaur *Thescelosaurus neglectus* GILMORE (Ornithischia: Ornithopoda) from the Upper Cretaceous of North America. Revue de Paleobiologie 16:231-258.

Galton, P. M. 1999. Cranial anatomy of the hypsilophodontid dinosaur *Bugenasaura infernalis* (Ornithischia: Ornithopoda) from the Upper Cretaceous of North America. Revue de Paleobiologie 18:517-534.

Galton, P. M. 2007. Teeth of ornithischian dinosaurs (mostly Ornithopoda) from the Morrison Formation (Upper Jurassic) of the western United States; pp. 17-47 in K. Carpenter (ed.), Horns and Beaks: Ceratopsian and Ornithopod Dinosaurs. Indiana University Press, Bloomington and Indianapolis.

Galton, P. M. 2009. Notes on Neocomian (Late Cretaceous) ornithopod dinosaurs from England - *Hypsilophodon*, *Valdosaurus*, "*Camptosaurus*", "*Iguanodon*" - and referred specimens from Romania and elsewhere. Revue de Paleobiologie 28:211-273.

Galton, P. M., and J. A. Jensen. 1973. Small bones of the hypsilophodontid dinosaur *Dryosaurus altus* from the Upper Jurassic of Colorado. Great Basin Naturalist 33:129-132.

Galton, P. M., and J. A. Jensen. 1979. Remains of ornithopod dinosaurs from the Lower Cretaceous of North America. Brigham Young University Geological Studies 25:1-10.

Galton, P. M., and P. Taquet. 1982. *Valdosaurus*, a hypsilophodontid dinosaur from the Lower Cretaceous of Europe and Africa. Geobios 15:147-159.

Galton, P. M., and P. Upchurch. 2004. Stegosauria; pp. 343-362 in D. B. Weishampel, P. Dodson, and H. Osmólska (eds.), The Dinosauria Second Edition. University of California Press, Berkley.

Gangloff, R. A., and A. R. Fiorillo. 2010. Taphonomy and paleoecology of a bonebed from the Prince Creek Formation, north slope, Alaska. Palaios 25:299-317.

Garcia, G., M. Pincemaille, M. Vianey-Liaud, B. Marandat, E. Lorenz, G. Cheylan, H. Cappetta, J. Michaux, and J. Sudre. 1999. Découverte du premier squelette preque complet de *Rhabdodon priscus* (Dinosauria, Ornithopoda) du Maastrichtien inférieur de Provence.

Comptes Rendus de l'Académie des Sciences à Paris, Sciences de la Terre et des Planètes. 328:415-421.

Gates, T. A., and S. D. Sampson. 2007. A new species of *Gryposaurus* (Dinosauria: Hadrosauridae) from the Late Campanian Kaiparowits Formation. Zoological Journal of the Linnean Society 151:351-376.

Gates, T. A., S. D. Sampson, L. E. Zanno, E. M. Roberts, J. G. Eaton, R. L. Nydam, J. H. Hutchinson, J. A. Smith, M. A. Loewen, and M. A. Getty. 2010. Biogeography of terrestrial and freshwater vertebrates from the Late Cretaceous (Campanian) western interior of North America. Palaeogeography, Palaeoclimatology, Palaeoecology 291:371-387.

Gauthier, J., A. G. Kluge, and T. Rowe. 1988. Amniote phylogeny and the importance of fossils. Cladistics 4:105-209.

Gilmore, C. W. 1913. A new dinosaur from the Lance Formation of Wyoming. Smithsonian Miscellaneous Collections 61:1-5.

Gilmore, C. W. 1915. Osteology of *Thescelosaurus*, an orthopodous dinosaur from the Lance Formation of Wyoming. Proceedings of the United States National Museum 49:591-616.

Gilmore, C. W. 1931. A new species of troodont dinosaur from the Lance Formation of Wyoming. Proceedings of the United States National Museum 79:1-6.

Godefroit, P., V. Codrea, and D. B. Weishampel. 2009. Osteology of *Zalmoxes shqiperorum* (Dinosauria, Ornithopoda), based on new specimens from the Upper Cretaceous of Nalat-Vad (Romania). Geodiversitas 31:525-553.

Goloboff, P. A., J. S. Farris, and K. C. Nixon. 2008. TNT, a free program for phylogenetic analysis. Cladistics 24:774-786.

Gow, C. E. 1975. A new heterodontosaurid from the Redbeds of South Africa showing clear evidence of tooth replacement. Zoological Journal of the Linnean Society 57:335-339.

Gow, C. E. 1981. Taxonomy of the Fabrosauridae (Reptilia, Ornithischia) and the *Lesothosaurus* myth. South African Journal of Science 77:43-43.

Gow, C. E. 1990. A tooth-bearing maxilla referable to *Lycorhinus angustidens* Haughton, 1924 (Dinosauria, Ornithischia). Annals of the South African Museum 99:367-380.

Gradstein, F. M., J. G. Ogg, and A. G. Smith. 2005. A geologic time scale 2004. Cambridge University Press, Cambridge, 589 pp.

Haubold, H. 1991. Ein neuer Dinosaurier (Ornithischia, Thyreophora) aus dem unteren Jura des nördlichen Mitteleuropa. Revue de Paléobiologie 9:149-177.

Haughton, S. H. 1924. The fauna and stratigraphy of the Stormberg Series. Annals of the South African Museum 12:323-497.

Hausdorf, B. 1998. Weighted ancestral area analysis and a solution of the redundant distribution problem. Systematic Biology 47:445-456.

He, X. 1979. A newly discovered ornithopod dinosaur-*Yandusaurus* from Zigong, China; pp. 116-123, Contribution to International Exchange of Geology. Part 2, Stratigraphy and Paleontology. Geological Publishing House, Beijing.

He, X. L., and K. J. Cai. 1983. A new species of *Yandusaurus* (hypsilophodont dinosaur) from the Middle Jurassic of Dashanpu, Zigong, Sichuan. Journal of Chengdu College of Geology, Supplement 1:5-14.

He, X. L., and K. J. Cai. 1984. The Middle Jurassic dinosaurian fauna from Dashanpu, Zigong, Sichuan., The Ornithopod Dinosaurs, Volume 1. Sichuan Scientific and Technological Publishing House, 1-71 pp.

Herne, M. C., and S. W. Salisbury. 2009. The status of *Leaellynasaura amicagraphica* (Dinosauria: Ornithischia) from the Early Cretaceous of southeastern Australia. Geological Society of Australia Abstracts 93:35.

Hildebrand, M. 1985. Digging in quadrupeds; pp. 89-109 in M. Hildebrand, D. M. Bramble, K. F. Liem, and D. B. Wake (eds.), Functional vertebrate morphology. Bellknap Press, Cambridge, MA.

Hitchin, R., and M. J. Benton. 1997a. Congruence between parsimony and stratigraphy: comparisons of three indices. Paleobiology 23:20-32.

Hitchin, R., and M. J. Benton. 1997b. Stratigraphic indices and tree balance. Systematic Biology 46:563-569.

Hopson, J. A. 1975. On the generic separation of the ornithischian dinosaurs *Lycorhinus* and *Heterodontosaurus* from the Stormberg Series (Upper Triassic) of South Africa. South African Journal of Science 71:302-305.

Horner, J. 2001. Dinosaurs under the big sky. Mountain Press Publishing Company, Missoula, 195 pp.

Horner, J. R., and K. Padian. 2004. Age and growth dynamics of *Tyrannosaurus rex*. Proceedings of the Royal Society of London B 271:1875-1880.

Horner, J., and D. B. Weishampel. 1988. A comparative embryological study of two ornithischian dinosaurs. Nature 332:256-257.

Horner, J. R., A. J. de Ricqles, and K. Padian. 2000. Long bone histology of the hadrosaurid dinosaur *Maiasaura peeblesorum*: growth dynamics and physiology based on an ontogenetic series of skeletal elements. Journal of Vertebrate Paleontology 20:115-129.

Horner, J. R., A. de Ricqles, K. Padian, and R. D. Scheetz. 2009. Comparative long bone histology and growth of the "hypsilophodontid" dinosaurs *Orodromeus makelai*, *Dryosaurus altus*, and *Tenontosaurus tillettii* (Ornithischia: Euornithopoda). Journal of Vertebrate Paleontology 29:734-747.

Hou, L.-H. 1977. A new primitive Pachycephalosauria from Anhui, China. Vertebrata PalAsiatica 15:198-202.

Huelsenbeck, J. P. 1994. Comparing the stratigraphic record to estimates of phylogeny. Paleobiology 20:470-483.

Huh, M., D.-G. Lee, J.-K. Kim, J.-D. Lim, and P. Godefroit. 2010. A new basal ornithopod dinosaur from the Upper Cretaceous of South Korea. Neues Jahrbuch für Geologie und Paläontologie Abhandlungen.

Hutchinson, J. R., and L. M. Chiappe. 1998. The first known alvarezsaurid (Theropoda: Aves) from North America. Journal of Vertebrate Paleontology 18:447-450.

Huxley, T. J. 1869. On *Hypsilophodon*, a new genus of Dinosauria. Abstracts of the Proceedings of the Geological Society of London 204:3-4.

Ibiricu, L. M., R. D. Martinez, M. C. Lamanna, G. A. Casal, M. Luna, J. D. Harris, and K. J. Lacovara. 2010. A medium-sized ornithopod (Dinosauria: Ornithischia) from the Upper Cretaceous Bajo Barreal Formation of Lago Colhue Huapi, southern Chubut Province, Argentina. Annals of Carnegie Museum 79:39-50.

Irmis, R. B. 2007. Axial skeleton ontogeny in the Parasuchia (Archosauria: Pseudosuchia) and its implications for ontogenetic determination in archosaurs. Journal of Vertebrate Paleontology 27:350-361.

Irmis, R. B., W. Parker, and S. J. Nesbitt. 2007. Early ornithischian dinosaurs: the Triassic record. Historical Biology 19:3-22.

Janensch, W. 1955. Der Ornithopode *Dysalotosaurus* der Tendaguruschichten. Palaeontographica (supplement 7) 3:105-176.

Jeffery, C. H., and R. B. Emlet. 2003. Macroevolutionary consequences of developmental mode in temnopleurid echinoids from the Tertiary of southern Australia. Evolution 57:1031-1048.

Jin, L. Y., J. Chen, S. Q. Zan, R. J. Butler, and P. Godefroit. 2010. Cranial anatomy of the small ornithischian dinosaur *Changchunsaurus parvus* from the Quantou Formation (Cretaceous: Aptian-Cenomanian) of Jilin Province, northeastern China. Journal of Vertebrate Paleontology 30:196-214.

Kerr, A. M., and J. Kim. 2001. Phylogeny of Holothuroidea (Echinodermata) inferred from morphology. Zoological Journal of the Linnean Society 133:63-81.

Kirkland, J. I., L. E. Zanno, S. D. Sampson, J. M. Clark, and D. D. DeBlieux. 2005. A primitive therizinosauroid dinosaur from the Early Cretaceous of Utah. Nature 435:84-87.

Klein, N., and M. Sander. 2008. Ontogenetic stages in the long bone histology of sauropod dinosaurs. Paleobiology 34:247-263.

Knoll, F. 2002a. Nearly complete skull of *Lesothosaurus* (Dinosauria: Ornithischia) from the Upper Elliot Formation (Lower Jurassic: Hettangian) of Lesotho. Journal of Vertebrate Paleontology 22:238-243.

Knoll, F. 2002b. New skull of *Lesothosaurus* (Dinosauria: Ornithischia) from the Upper Elliot Formation (Lower Jurassic) of southern Africa. Geobios 35:595-603.

Knoll, F., K. Padian, and A. de Ricqles. 2010. Ontogenetic change and adult body size of the early ornithischian dinosaur *Lesothosaurus diagnosticus*: Implications for basal ornithischian taxonomy. Gondwana Research 17:171-179.

Kobayaski, Y., and R. Barsbold. 2005. Reexamination of a primitive ornithomimosaur, *Garudimimus brevipes* Barsbold, 1981 (Dinosauria: Theropoda), from the Late Cretaceous of Mongolia. Canadian Journal of Earth Sciences 42:1501-1521.

Krumenacker, L. J. 2010. Chronostratigraphy and paleontology of the mid-Cretaceous Wayan Formation of eastern Idaho, with a description of the first *Oryctodromeus* specimens from Idaho. Department of Geological Sciences, Brigham Young University, Provo, Utah, 88 pp.

Kuhn, O. 1966. Die Reptilien, System und Stammesgeschichte. Oeben Verlag, Kraillingen bei München, Germany, 154 pp.

Kutter, M. M. 2004. New material of *Zephyrosaurus schaffi* (Dinosauria; Ornithischia) from the Cloverly Formation (Aptian-Albian) of Montana and the phylogeny of Hypsilophodontidae. Biological Sciences, University of the Pacific, Stockton, California, 75 pp.

Lehman, T. M. 1997. Late Campanian dinosaur biogeography in the western interior of North America; pp. 223-240 in D. L. Wolberg, E. Stump, and G. D. Rosenberg (eds.), Dinofest International. Academy of Natural Sciences, Philadelphia.

Lehman, T. M. 2001. Late Cretaceous dinosaur provinciality; pp. 310-328 in D. H. Tanke and K. Carpenter (eds.), Mesozoic Vertebrate Life. Indiana University Press, Bloomington.

Linnaeus, C. 1758. Systema Naturae per Raegna Tria Naturae. Volume 1. Regnum Animale. 10th Edition. Trustees, British Museum (Natural History), London, 823 pp.

Liu, J. 2004. Phylogeny of Ornithischia. Journal of Vertebrate Paleontology 24 (suppl.):84A.

Lydekker, R. 1889. On the remains and affinities of five genera of Mesozoic reptiles. Quarterly Journal of the Geological Society of London 45:41-59.

Maddison, W. P., and D. R. Maddison. 2009. Mesquite: a modular system for evolutionary analysis. 2.71.

Makovicky, P. J., B. M. Kilbourne, R. W. Sadleir, and M. A. Norell. 2011. A new basal ornithopod (Dinosauria, Ornithischia) from the Late Cretaceous of Mongolia. Journal of Vertebrate Paleontology 31:626-640.

Marivaux, L., M. Vianey-Liaud, and J.-J. Jaeger. 2004. High-level phylogeny of early Tertiary rodents: dental evidence. Zoological Journal of the Linnean Society 142:105-134.

Marjanovic, D., and M. Laurin. 2007. Fossils, molecules, divergence times, and the origin of lissamphibians. Systematic Biology 56:369-388.

Marsh, O. C. 1877a. New order of extinct Reptilia (Stegosauria) from the Jurassic of the Rocky Mountains. American Journal of Science, Series 3, 14:513-514.

Marsh, O. C. 1877b. Notice of some new vertebrate fossils. American Journal of Science, Series 3, 14:249-256.

Marsh, O. C. 1878. Principal characters of American Jurassic dinosaurs. American Journal of Science, Series 3, 16:411-416.

Marsh, O. C. 1879. Notice of new Jurassic reptiles. American Journal of Science, Series 3, 18:501-505.

Marsh, O. C. 1881. Principal characters of American Jurassic dinosaurs. Part V. American Journal of Science, Series 3, 21 417-423.

Marsh, O. C. 1885. Names of extinct reptiles. American Journal of Science, Series 3, 29:169.

Marsh, O. C. 1889. Notice of gigantic horned Dinosauria from the Cretaceous. American Journal of Science, Series 3, 38:173-175.

Marsh, O. C. 1894. The typical Ornithopoda of the American Jurassic. American Journal of Science, Series 3, 43:85-90.

Martin, A. J. 2009. Dinosaur burrows in the Otway Group (Albian) of Victoria, Australia, and their relation to Cretaceous polar environments. Cretaceous Research 30:1223-1237.

Martinez, R. D. 1998. *Notohypsilophodon comodorensis* gen. et sp. nov. un Hypsilophodontidae (Ornithischia: Ornithopoda) del Cretacico superior de Chubut, Patagonia central, Argentina. Acta Geologica Leopoldensia 21:119-135.

Maryańska, T., and H. Osmólska. 1985. On ornithischian phylogeny. Acta Palaeontologica Polonica 30:137-150.

Maryańska, T., R. E. Chapman, and D. B. Weishampel. 2004. Pachycephalosauria; pp. 464-477 in D. B. Weishampel, P. Dodson, and H. Osmólska (eds.), The Dinosaura: Second Edition. University of California Press, Berkeley.

Matheron, P. 1869. Notes sur les reptiles fossiles des dépôts fluvio-lucustres crétacés du bassin à lignite de Fuveau. Bulletin de la Société Géologique de France, ser. 2, 26:781-795.

McDonald, A. T., J. I. Kirkland, D. D. DeBlieux, S. K. Madsen, J. Cavin, A. R. C. Milner, and L. Panzarin. 2010. New iguanodonts from the Cedar Mountain Formation of Utah and the evolution of thumb-spiked dinosaurs. PLoS ONE 5:e14075.

Merle, D., and J.-M. Pacaud. 2003. New species of *Eocithara* Fisher, 1883 (Mollusca, Gastropoda, Harpidae) from the Early Paleogene with phylogenetic analysis of the Harpidae. Geodiversitas 26:61-87.

Meyer, H. v. 1857. Beiträge zur näheren Kenntis fossiler Reptilien. Neues Jahrbuch für Mineralogie, Geologie und Paläontologie 1857:532-543.

Milner, A. R., and D. B. Norman. 1984. The biogeography of advanced ornithopod dinosaurs (Archosauria: Ornithischia)-a cladistic vicariance model; pp. 145-150 in W. E. Reif and F. Westphal (eds.), Third Symposium on Mesozoic Terrestrial Ecosystems, Short Papers. Attempto Verlag, Tubingen.

Molnar, R. E. 1996. Observations on the Australian ornithopod dinosaur, *Muttaburrasaurus*. Memoirs of the Queensland Museum 39:639-652.

Morris, W. J. 1976. Hypsilophodont dinosaurs: a new species and comments on their systematics; pp. 93-113 in C. S. Churcher (ed.), Athlon: Essays on Palaeontology in Honour of Loris Shano Russell. Royal Ontario Museum, Toronto.

Nesbitt, S. J., N. D. Smith, R. B. Irmis, A. H. Turner, A. Downs, and M. A. Norell. 2009. A complete skeleton of a Late Triassic saurischian and the early evolution of dinosaurs. Science 326:1530-1533.

Nesbitt, S. J., C. A. Sidor, R. B. Irmis, K. D. Angielczyk, R. M. H. Smith, and L. A. Tsuji. 2010. Ecologically distinct dinosaurian sister group shows early diversification of Ornithodira. Nature 464:95-98.

Nixon, K. C., and J. M. Carpenter. 1996. On consensus, collapsibility, and clade concordance. Cladistics 12:305-322.

Nixon, K. C., and Q. D. Wheeler. 1992. Extinction and the origin of species; pp. 119-143 in M. J. Novacek and Q. D. Wheeler (eds.), Extinction and Phylogeny. Columbia University Press, New York.

Nopcsa, F. 1900. Dinosaurierreste aus Siebenbürgen (Schädel von *Limnosaurus transsylvanicus* nov. gen. et spec.). Denkschriften der Kaiserlichen Akademie der Wissenschaften. Mathematisch-Naturwissenschaftliche Classe 68:555-591.

Nopcsa, F. 1915. Die Dinosaurier der siebenbürgischen Landesteile. Mitteilungen aus dem Jahrbuche der Koniglich-Ungarischen Geologischen Reichsanstalt 23:1-26.

Norell, M. A. 1993. Tree-based approaches to understanding history: comments on ranks, rules, and the quality of the fossil record. American Journal of Science 293:407-417.

Norell, M. A., and M. J. Novacek. 1992. Congruence between superpositional and phylogenetic patterns: comparing cladistic patterns with fossil records. Cladistics 8:319-337.

Norman, D. B. 1984. A systematic reappraisal of the reptile order Ornithischia; pp. 157-162 in W. E. Reif and F. Westphal (eds.), Third Symposium on Mesozoic Terrestrial Ecosystems, Short Papers. Attempto Verlag, Tubingen.

Norman, D. B. 2004. Basal Iguanodontia; pp. 413-437 in D. B. Weishampel, P. Dodson, and H. Osmólska (eds.), The Dinosauria Second Edition. University of California Press, Berkeley.

Norman, D. B., L. M. Witmer, and D. B. Weishampel. 2004a. Basal Ornithischia; pp. 325-334 in D. B. Weishampel, P. Dodson, and H. Osmólska (eds.), The Dinosauria: Second Edition. University of California Press, Berkeley.

Norman, D. B., L. M. Witmer, and D. B. Weishampel. 2004b. Basal Thyreophora; pp. 335-342 in D. B. Weishampel, P. Dodson, and H. Osmólska (eds.), The Dinosauria: Second Edition. University of California Press, Berkeley.

Norman, D. B., H.-D. Sues, L. M. Witmer, and R. A. Coria. 2004c. Basal Ornithopoda; pp. 393-412 in D. B. Weishampel, P. Dodson, and H. Osmólska (eds.), The Dinosauria: Second Edition. University of California Press, Berkeley.

Novas, F. E. 1993. New information on the systematics and postcranial skeleton of *Herrerasaurus ischigualastensis*. Journal of Vertebrate Paleontology 13:400-423.

Novas, F. E. 1996. Dinosaur monophyly. Journal of Vertebrate Paleontology 16:723-741.

Novas, F. E., A. V. Cambiaso, and A. Ambrosio. 2004. A new basal iguanodontian (Dinosauria, Ornithischia) from the Upper Cretaceous of Patagonia. Ameghiniana 41:75-82.

O'Leary, M. A. 2001. The phylogenetic position of cetaceans: further combined data analyses, comparisons with the stratigraphic record and a discussion of character optimization. American Zoologist 41:487-506.

Osi, A., R. J. Butler, and D. B. Weishampel. 2010. A Late Cretaceous ceratopsian dinosaur from Europe with Asian affinities. Nature 465:466-468.

Ostrom, J. H. 1970. Stratigraphy and paleontology of the Cloverly Formation (Lower Cretaceous) of the Bighorn Basin area, Wyoming and Montana. Bulletin of the Yale Peabody Museum of Natural History 35:1-234.

Owen, R. 1842. Report on British fossil reptiles, part II. Report of the British Association for the Advancement of Science for 1841 9:60-204.

Owen, R. 1861. Monograph on the fossil Reptilia of the Wealden and Purbeck Formations. Part V. Lacertilia. Palaeontographical Society Monograph 12:31-39.

Parks, W. A. 1922. *Parasaurolophus walkeri*, a new genus and species of crested trachodont dinosaur. University of Toronto Studies, Geological Series 13:1-32.

Parks, W. A. 1926. *Thescelosaurus warreni*. A new species of orthopodous dinosaur from the Edmonton Formation of Alberta. University of Toronto Studies, Geological Series 21:1-42.

Paul, G. S. 1996. The complete illustrated guide to dinosaur skeletons. Gakken Mook, Tokyo, 98 pp.

Peng, G. 1990. A new small ornithopod (*Agilisaurus louderbacki* gen. et sp. nov.) from Zigong, China. Newsletter of the Zigong Dinosaur Museum 2:19-27.

Peng, G. 1992. Jurassic ornithopod *Agilisaurus louderbacki* (Ornithopoda: Fabrosauridae) from Zigong, Sichuan, China. Vertebrata PalAsiatica 30:39-51.

Piechowski, R., and J. Dzik. 2010. The axial skeleton of *Silesaurus opolensis*. Journal of Vertebrate Paleontology 30:1127-1141.

Pincemaille-Quillevere, M., E. Buffetaut, and F. Quillevere. 2006. Description ostéologique de l'arrière-crane de *Rhabdodon* (Dinosauria, Euornithopoda) et implications phylogénétiques. Bulletin de la Societe Geologique de France 177:97-104.

Pol, D., and M. A. Norell. 2001. Comments on the manhattan stratigraphic measure. Cladistics 17:285-289.

Pol, D., and M. A. Norell. 2006. Uncertainty in the age of fossils and the stratigraphic fit to phylogenies. Systematic Biology 55:512-521.

Pol, D., M. A. Norell, and M. E. Siddall. 2004. Measures of stratigraphic fit to phylogeny and their sensitivity to tree size, shape and scale. Cladistics 20:64-75.

Pol, D., O. W. M. Rauhut, and M. Becerra. 2011. A Middle Jurassic heterodontosaurid dinosaur from Patagonia and the evolution of heterodontosaurids. Naturwissenschaften 98:369-379.

Prendini, L. 2001. Species or supraspecific taxa as terminals in cladistic analyses? Groundplans versus exemplars revisited. Systematic Biology 50:290-300.

Pryer, K. M. 1999. Phylogeny of marsileaceous ferns and relationships of the fossil *Hydropteris pinnata* reconsidered. International Journal of Plant Sciences 160:931-954.

Rage, J. C. 1986. South American/North American terrestrial interchanges in the latest Cretaceous: short comments on Brett-Surman and Paul (1985) with additional data. Journal of Vertebrate Paleontology 6:382-383.

Rauhut, O. W. M. 2003. The interrelationships and evolution of basal theropod dinosaurs. Special Papers in Palaeontology 69:1-213.

Ree, R. H., and S. A. Smith. 2008. Maximum likelihood inference of geographic range evolution by dispersal, local extinction, and cladogenesis. Systematic Biology 57:4-14.

Ree, R. H., B. R. Moore, C. O. Webb, and M. J. Donoghue. 2005. A likelihood framework for inferring the evolution of geographic range on phylogenetic trees. Evolution 59:2299-2311.

Reig, O. A. 1963. La presencia de dinosaurios saurisquios en los "Estratos de Ischigualasto" (Mesotriásico Superior) de las provincias de San Juan y La Rioja (República Argentina). Ameghiniana 3:3-20.

Rich, T. H., and P. V. Rich. 1989. Polar dinosaurs and biotas of the Early Cretaceous of southeastern Australia. National Geographic Research 5:15-53.

Rich, T. H., and P. Vickers-Rich. 1999. The Hypsilophodontidae from southeastern Australia; pp. 167-180 in Y. Tomida, T. H. Rich, and P. Vickers-Rich (eds.), Proceedings of the Second Gondwanan Dinosaur Symposium. National Science Museum Monographs, Tokyo.

Rich, T. H., P. M. Galton, and P. Vickers-Rich. 2010. The holotype individual of the ornithopod dinosaur *Leaellynasaura amicagraphica* Rich and Rich, 1989 (late Early Cretaceous, Victoria, Australia). Alcheringa 34:385-396.

Roberts, E. M. 2007. Facies architecture and depositional environments of the Upper Cretaceous Kaiparowits Formation, southern Utah. Sedimentary Geology 197:207-233.

Roberts, E. M., A. L. Deino, and M. A. Chan. 2005. 40Ar/39Ar age of the Kaiparowits Formation, southern Utah, and correlation of contemporaneous Campanian strata and vertebrate faunas along the margin of the western interior basin Cretaceous Research 26:307-318.

Romer, A. S. 1956. Osteology of the Reptiles. University of Chicago Press, Chicago, 772 pp.

Romer, A. S. 1966. Vertebrate Paleontology. 3rd Edition. University of Chicago Press, Chicago, 468 pp.

Romer, A. S. 1972. The Chanares (Argentina) Triassic reptile fauna. XV. Further remains of the thecodonts *Lagerpeton* and *Lagosuchus*. Breviora 394:1-7.

Ronquist, F. 1996. DIVA. version 1.1. Computer program and manual available by anonymous FTP from Uppsala University Available from: ftp://ftp.uu.se/ or ftp://ftp.systbot.uu.se/.

Ronquist, F. 1997. Dispersal-Vicariance analysis: a new approach to the quantification of historical biogeography. Systematic Biology 46:195-203.

Rosenbaum, J. N., and K. Padian. 2000. New material of the basal thyreophoran *Scutellosaurus lawleri* from the Kayenta Formation (Lower Jurassic) of Arizona. PaleoBios 20:13-23.

Rowe, T., E. F. McBride, and P. C. Sereno. 2001. Technical comment: dinosaur with a heart of stone. Science 291:783a.

Ruiz-Omenaca, J. I., X. P. Suberbiola, and P. M. Galton. 2006. *Callovosaurus leedsi*, the earliest dryosaurid dinosaur (Ornithischia: Euornithopoda) from the Middle Jurassic of England pp. in K. Carpenter (ed.), Horns and Beaks: Ceratopsian and Ornithopod Dinosaurs. Indiana University Press, Bloomington.

Russell, D. A., P. E. Fisher, E. Reese, and M. K. Stoskopf. 2001. Reply: dinosaur with a heart of stone. Science 291:783a.

Salgado, L., R. A. Coria, and S. E. Heredia. 1997. New materials of *Gasparinisaura cincosaltensis* (Ornithischia, Ornithopoda) from the Upper Cretaceous of Argentina. Journal of Paleontology 71:933-940.

Sampson, S. D., M. A. Loewen, E. M. Roberts, A. J. Smith, L. E. Zanno, and T. A. Gates. 2004. Provincialism in Late Cretaceous terrestrial faunas: new evidence from the Campanian Kaiparowits Formation of Utah. Journal of Vertebrate Paleontology 24:108A.

Sampson, S. D., M. A. Loewen, A. A. Farke, E. M. Roberts, C. A. Forster, J. A. Smith, and A. L. Titus. 2010a. New horned dinosaurs from Utah provide evidence for intercontinental dinosaur endemism. PLoS ONE 5:1-12.

Sampson, S. D., T. A. Gates, E. M. Roberts, M. A. Getty, L. E. Zanno, M. A. Loewen, E. K. Lund, J. Sertich, and A. L. Titus. 2010b. Grand Staircase-Escalante National Monument: a new and critical window in the world of dinosaurs pp. in M. Eaton (ed.), Learning from the Land. Bureau of Land Management.

Santa Luca, A. P. 1980. The postcranial skeleton of *Heterodontosaurus tucki* (Reptilia, Ornithischia) from the Stormberg of South Africa. Annals of the South African Museum 79:159-211.

Santa Luca, A. P., A. W. Crompton, and A. J. Charig. 1976. A complete skeleton of the Late Triassic ornithischian *Heterodontosaurus tucki*. Nature 264:324-328.

Saucede, T., R. Mooi, and B. David. 2007. Phylogeny and origin of Jurassic irregular echinoids (Echinodermata: Echinoidea). Geological Magazine 144:333-359.

Scheetz, R. D. 1998. Phylogeny of basal ornithopod dinosaurs and the dissolution of the Hypsilophodontidae. Journal of Vertebrate Paleontology 18:75A.

Scheetz, R. D. 1999. Osteology of *Orodromeus makelai* and the phylogeny of basal ornithopod dinosaurs. Montana State University, Bozeman, 186 pp.

Seeley, H. G. 1887. On the classification of the fossil animals commonly named Dinosauria. Proceedings of the Royal Society of London 43:165-171.

Sereno, P. C. 1986. Phylogeny of the bird-hipped dinosaurs. National Geographic Research 2:234-256.

Sereno, P. C. 1987. The ornithischian dinosaur Psittacosaurus from the Lower Cretaceous of Asia and the relationships of the Ceratopsia. Columbia University, New York, 554 pp.

Sereno, P. C. 1991. *Lesothosaurus*, "fabrosaurids", and the early evolution of Ornithischia. Journal of Vertebrate Paleontology 11:168-197.

Sereno, P. C. 1993. The pectoral girdle and forelimb of the basal theropod *Herrerasaurus ischigualastensis*. Journal of Vertebrate Paleontology 13:425-450.

Sereno, P. C. 1997. The origin and evolution of dinosaurs. Annual Revue of Earth and Planetary Sciences 25:435-489.

Sereno, P. C. 1998. A rational for phylogenetic definitions, with application to the higher level taxonomy of Dinosauria. Neues Jahrbuch für Geologie und Paläontologie Abhandlungen 210:41-83.

Sereno, P. C. 1999. The evolution of dinosaurs. Science 284:2137-2147.

Sereno, P. C. 2005. The logical basis of phylogenetic taxonomy. Systematic Biology 54:595-619.

Sereno, P. C., and A. B. Arcucci. 1994. Dinosaurian precursors from the Middle Triassic of Argentina: *Marasuchus lilloensis*, gen. nov. Journal of Vertebrate Paleontology 14:53-73.

Sereno, P. C., and F. E. Novas. 1993. The skull and neck of the basal theropod *Herrerasaurus ischigualastensis*. Journal of Vertebrate Paleontology 13:451-476.

Siddall, M. E. 1996. Stratigraphic consistency and the shape of things. Systematic Biology Systematic Biology:111-115.

Siddall, M. E. 1997. Stratigraphic indicies in the balance: a reply to Hitchin and Benton. Systematic Biology 46:569-573.

Siddall, M. E. 1998. Stratigraphic fit to phylogenies: a proposed solution. Cladistics 14:201-208.

Spencer, M. R. 2007. A phylogenetic analysis of the basal Ornithischia (Reptilia, Dinosauria). Department of Geology, Bowling Green State University, Bowling Green, Ohio, 140 pp.

Sternberg, C. M. 1937. A classification of *Thescelosaurus*, with a description of a new species. Proceedings of the Geological Society of America 1936:375.

Sternberg, C. M. 1940. *Thescelosaurus edmontonensis*, n. sp., and classification of the Hypsilophodontidae. Journal of Paleontology 14:481-494.

Sues, H.-D. 1980. Anatomy and relationships of a new hypsilophodontid dinosaur from the Lower Cretaceous of North America. Palaeontographica Abteilung a Palaeozoologie-Stratigraphie 169:51-72.

Sues, H.-D., and P. M. Galton. 1987. Anatomy and calssification of the North American Pachycephalosauria (Dinosauria: Ornithischia). Palaeontographica, Abteilung A 198:1-40.

Sullivan, R. M. 2006. A taxonomic review of the Pachycephalosauridae (Dinosauria: Ornithischia). New Mexico Museum of Natural HIstory and Science Bulletin 35:347-365.

Swinton, W. E. 1936. The dinosaurs of the Isle of Wight. Proceedings of the Geologists' Association 47:204-220.

Swofford, D. L. 1991. When are phylogeny estimates from molecular and morphological data incongruent; pp. 295-333 in M. M. Miyamoto and J. Cracraft (eds.), Phylogenetic Analysis of DNA Sequences. Oxford University Press, New York.

Swofford, D. L. 2002. PAUP*. Phylogenetic analysis using parsimony (* and other methods). 4.0b10.

Taquet, P. 1976. Géologie et Paléontologie du Gisement de Gadoufaoua (Aptien du Niger). Cahiers de Paléontologie, Éditions du Centre National de la Recherche Scientifique, Paris, 191 pp.

Tetlie, O. E., and M. Poschmann. 2008. Phylogeny and Palaeoecology of the Adelophthalmoidea (Arthropoda; Chelicerata; Eurypterida). Journal of Systematic Paleontology 6:237-249.

Thulborn, R. A. 1970. The skull of *Fabrosaurus australis*, a Triassic ornithischian dinosaur. Palaeontology 13:414-432.

Thulborn, R. A. 1972. The postcranial skeleton of the Triassic ornithischian dinosaur *Fabrosaurus australis*. Palaeontology 15:29-60.

Thulborn, R. A. 1974. A new heterodontosaurid dinosaur (Reptilia: Ornithischia) from the Upper Triassic Red Beds of Lesotho. Zoological Journal of the Linnean Society 55:151-175.

Upchurch, P., C. A. Hunn, and D. B. Norman. 2002. An analysis of dinosaurian biogeography: evidence for the existence of vicariance and dispersal patterns caused by geological events. Proceedings of the Royal Society B 269:613-621.

Upchurch, P., P. M. Barrett, and P. Dodson. 2004. Sauropoda; pp. 259-324 in D. B. Weishampel, P. Dodson, and T. Maryańska (eds.), The Dinosauria: Second Edition. University of California Press, Berkeley.

Varricchio, D. J., A. J. Martin, and Y. Katsura. 2007. First trace and body evidence of a burrowing, denning dinosaur. Proceedings of the Royal Society B: Biological Sciences 274:1361-1368.

Vickaryous, M. K., T. Maryańska, and D. B. Weishampel. 2004. Ankylosauria; pp. 363-392 in D. B. Weishampel, P. Dodson, and H. Osmólska (eds.), The Dinosauria Second Edition. University of California Press, Berkeley.

Villier, L., D. Neraudeau, B. Clavel, C. Neumann, and B. David. 2004. Phylogeny of Early Cretaceous spatangoids (Echinodermata: Echinoidea) and taxonomic implications. Palaeontology 47:265-292.

Virchow, H. 1919. Atlas and Epistropheus bei den Schildkröten. Sitzungsberichte der Gesellschaft Naturforschender Freunde zu Berlin 1919:303-332.

von Huene, F. 1932. Die fossile Reptil-Ordnung Saurischia, ihre Entwicklung und Geschichte. Monographien zur Geologie und Palaeontologie, serie 1, 4:1-361.

Wagner, P. J., and C. A. Sidor. 2000. Age rank/clade rank metrics-sampling, taxonomy, and the meaning of "stratigraphic consistency". Systematic Biology 49:463-479.

Walsh, S. L. 1998. Fossil datum and paleobiological event terms, paleontostratigraphy, chronostratigraphy, and the definition of land mammal "age" boundaries. Journal of Vertebrate Paleontology 18:150-179.

Weishampel, D. B., and R. E. Heinrich. 1992. Systematics of Hypsilophodontidae and basal Iguanodontia (Dinosauria: Ornithopoda). Historical Biology 6:159-184.

Weishampel, D. B., C.-M. Juanu, Z. Csiki, and D. B. Norman. 2003. Osteology and phylogeny of *Zalmoxes* (N. G.), an unusual euornithopod dinosaur from the latest Cretaceous of Romania. Journal of Systematic Palaeontology 1:65-123.

Weishampel, D. B., P. M. Barrett, R. A. Coria, J. Le Loeuff, X. Xing, Z. Xijin, A. Sahni, E. M. P. Gomani, and C. R. Noto. 2004. Dinosaur Distribution; pp. 517-613 in D. B. Weishampel, P. Dodson, and H. Osmólska (eds.), The Dinosauria. University of California Press, Berkeley.

Wiens, J. J. 1998. The accuracy of methods for coding and sampling higher-level taxa for phylogenetic analysis: a simulation study. Systematic Biology 47:397-413.

Wills, M. A. 1999. Congruence between stratigraphy and phylogeny: randomization tests and the gap excess ratio. Systematic Biology 48:559-580.

Wills, M. A. 2001. How good is the fossil record of arthropods? An assessment using the stratigraphic congruence of cladograms. Geological Journal 36:187-210.

Wills, M. A., P. M. Barrett, and J. F. Heathcote. 2008. The modified gap excess ratio (GER*) and the stratigraphic congruence of dinosaur phylogenies. Systematic Biology 57:891-904.

Wilson, J. A. 2002. Sauropod dinosaur phylogeny: critique and cladistic analysis. Zoological Journal of the Linnean Society 136:217-276.

Winkler, D. A. 1989. Paleoecology and hypsilophodontid behavior at the Proctor Lake dinosaur locality (Early Cretaceous), Texas. Special Paper - Geological Society of America 238:55-61.

Winkler, D. A., and P. A. Murry. 1989. Paleoecology and hypsilophodontid behavior at the Proctor Lake dinosaur locality (Early Cretaceous), Texas; pp. 55-61 in J. O. Farlow (ed.), Paleobiology of Dinosaurs. Geological Society of America Special Paper 238.

Winkler, D. A., P. A. Murry, and L. L. Jacobs. 1997. A new species of *Tenontosaurus* (Dinosauria: Ornithopoda) from the Early Cretaceous of Texas. Journal of Vertebrate Paleontology 17:330-348.

Winkler, D. A., P. A. Murry, and L. L. Jacobs. 1998. The new ornithopod dinosaur from Proctor Lake, Texas, and the deconstruction of the family Hypsilophodontidae. Journal of Vertebrate Paleontology 18:87A.

Xu, X., X. L. Wang, and H. L. You. 2000. A primitive ornithopod from the Early Cretaceous Yixian Formation of Liaoning. Vertebrata PalAsiatica 38:318-325.

Xu, X., P. J. Makovicky, X. L. Wang, M. A. Norell, and H. L. You. 2002. A ceratopsian dinosaur from China and the early evolution of Ceratopsia. Nature 416:314-317.

Xu, X., C. A. Forster, J. M. Clark, and J. Mo. 2006. A basal ceratopsian with transitional features from the Late Jurassic of northwestern China. Proceedings of the Royal Society B 273:2135-2140.

You, H. L., and P. Dodson. 2003. Redescription of neoceratopsian dinosaur *Archaeoceratops* and earl evolution of Neoceratopsia. Acta Palaeontologica Polonica 48:261-272.

You, H. L., and P. Dodson. 2004. Basal Ceratopsia; pp. 478-493 in D. B. Weishampel, P. Dodson, and H. Osmólska (eds.), The Dinosauria: Second Edition. University of California Press, Berkeley.

Zan, S. Q., J. Chen, L. Y. Jin, and T. Li. 2005. A primitive ornithopod from the Early Cretaceous Quantou Formation of central Jilin, China. Vertebrata PalAsiatica 43:182-193.

Zanno, L. E. 2005. Dinosaur diversity and biogeographical implications of the Kaiparowits Formation (Early Cretaceous), Grand Staircase-Escalante National Monument, southern Utah. Geological Society of America Abstracts with Programs 37:115.

Zanno, L. E., and S. D. Sampson. 2005. A new oviraptorosaur (Theropoda, Maniraptora) from the Late Cretaceous (Campanian) of Utah. Journal of Vertebrate Paleontology 25:897-904.

Zheng, X.-T., H.-L. You, X. Xu, and Z.-M. Dong. 2009. An Early Cretaceous heterodontosaurid dinosaur with filamentous integumentary structures. Nature 458:333-336.

Zheng, W., X. Jin, M. Shibata, Y. Azuma, and F. Yu. 2012. A new ornithischian dinosaur from the Cretaceous Liangtoutang Formation of Tiantai, Zhejiang Province, China. Cretaceous Research 34:208-219.